The Role of Cortactin in Arp2/3-Dependent Processes and Actin Nucleation

Von der Fakultät für Lebenswissenschaften

der Technischen Universität Carolo-Wilhelmina

zu Braunschweig

zur Erlangung des Grades einer

Doktorin der Naturwissenschaften

(Dr. rer. nat.)

genehmigte

D i s s e r t a t i o n

von **Julia Margit Oelkers**

aus Osterholz-Scharmbeck

1. Referent: Prof. Dr. Martin Korte
2. Referent: Prof. Dr. Klemens Rottner
eingereicht am: 04.04.2011
mündliche Prüfung (Disputation) am: 23.05.2011

Druckjahr 2011

Vorveröffentlichungen der Dissertation

Teilergebnisse aus dieser Arbeit wurden mit Genehmigung der Fakultät für Lebenswissenschaften, vertreten durch den Mentor der Arbeit, in folgenden Beiträgen vorab veröffentlicht:

Publikationen

Lai FPL, Szczodrak M, **Oelkers JM**, Ladwein M, Acconcia F, Benesch S, Auinger S, Faix J, Small JV, Polo S, Stradal TEB, Rottner K (2009) Cortactin promotes migration and platelet-derived growth factor-induced actin reorganization by signaling to Rho-GTPases. *Molecular Biology of the Cell*, 20(14):3209-23.

Posterpräsentationen

Oelkers JM, Jacob S, Kerkhoff E, Wedlich-Söldner R, Small JV, Stradal TEB, Köstler SA, Rottner K (2010) From test tube to microtub(ul)e: Assaying actin nucleation *in vivo*. 33rd Annual Meeting of the German Society for Cell Biology and the "Frontiers in melanoma research" Meeting of the German Melanoma Research Network, Regensburg

Oelkers JM, Jacob S, Lai FPL, Block J, Szczodrak M, Kerkhoff E, Wedlich-Söldner R, Backert S, Schlüter K, Stradal TEB, Small JV, Koestler SA, Rottner K (2010) A novel *in vivo* actin polymerization assay: targeting nucleators to microtubules. International Meeting on “Actin Dynamics”, Jena

Oelkers JM, Jacob S, Lai FPL, Block J, Szczodrak M, Kerkhoff E, Backert S, Schlüter K, Stradal TEB, Small JV, Koestler SA, Rottner K (2011) A novel *in vivo* actin polymerization assay: targeting nucleators to microtubules. Jahrestagung des Bonner Forum Biomedizin, Bonn

Vorträge

The use of microtubules as platforms for assaying actin nucleation *in vivo*. (2010) Workshop “Cellular Morphogenesis”, Gif-sur-Yvette, Frankreich. Short talk

Table of contents

1 Introduction

1.1 The cytoskeleton of mammalian cells

Actin is one of the most abundant and highest conserved proteins and together with microtubules and intermediate filaments it constitutes the cytoskeleton of mammalian cells. The cytoskeleton does not solely stabilize the shape of cells, but is involved in processes as diverse as cell migration, endocytosis, intracellular transport, cell division and adhesion. In order to fulfill their manifold functions, all three cytoskeletal compounds polymerize into filaments, which assemble into three-dimensional arrays. In contrast to the rigid skeleton of vertebrates, the cytoskeleton is highly dynamic enabling rapid adjustments in response to extracellular or intracellular signals (Blain, 2009).

Intermediate filaments are encoded by 70 genes and share a common domain organization. In higher eukaryotes two distinct intermediate filament systems are found. In the cytoplasm vimentin filaments contribute to the maintenance of the mechanical integrity of the cell, whereas in the nucleus lamin filaments form the nuclear envelop beneath the nuclear membrane (Herrmann et al., 2007). In contrast to microtubules and actin filaments, intermediate filament proteins are filamentous and assemble into apolar and flexible filaments (Herrmann et al., 2009).

The microtubule network provides the tracks for intracellular cargo transport, plays an important role in cell migration and is crucial for the separation of chromosomes in cell division as the mitotic spindle is built by microtubules. Microtubules consist of 13 protofilaments which are composed of linear α/β-tubulin dimers associating head-to-tail. In eukaryotic cells microtubules are nucleated at the microtubule organizing center (MTOC) to which the minus end of the filaments stays attached (Etienne-Manneville, 2010).

The actin cytoskeleton is built of globular actin monomers, which polymerize into single, helical filaments that are arranged into various supramolecular structures such as lamellipodia, filopodia and stress fibers. These and other actin filament assemblies are essential for diverse biological functions including cell migration and adhesion, membrane trafficking, endocytosis, contractile ring formation and the entry and intracellular movement of pathogens (Blain, 2009; Disanza et al., 2005; Firat-Karalar and Welch, 2011).

1.2 Actin polymerization

Actin exists in two distinct forms: as monomeric actin (G-actin) or as polymerized filamentous actin (F-actin). *De novo* nucleation of actin filaments requires the formation of actin seeds. Though actin filaments form spontaneously under *in vitro* conditions, actin polymerization is largely inhibited in the cytoplasm of cells. The rate limiting step *in vivo* is the assembly of actin dimers and trimers, as these actin nuclei are highly unstable and the pool of actin monomers is sequestered by G-actin binding proteins such as profilin (Qualmann and Kessels, 2009).

Actin is an ATPase that is bound to ATP or the hydrolyzed form ADP+P_i. ATP-actin monomers are incorporated into growing filaments and eventually ATP is hydrolyzed by actin. Upon disassembly of the filament, actin-ADP is released into the cytoplasm, because ATP hydrolysis reduces the affinity of actin monomers for the filament. In the cytoplasm actin-ADP rapidly releases the nucleotide and is again loaded with ATP, thereby providing a constant pool of incorporable actin monomers (Carlsson, 2010).

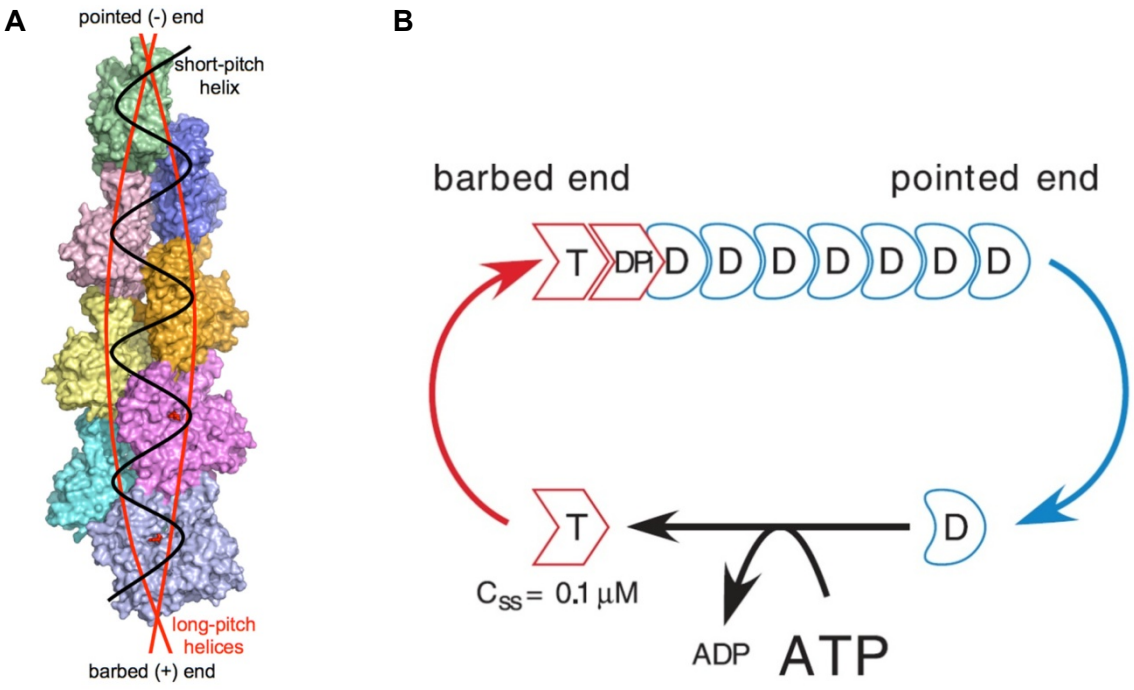

Figure 1-1: Actin filament structure and steady state actin treadmilling

(**A**) Structure of an actin filament. The actin filament can either be described as a single left-handed short-pitch helix (black line), or as a right-handed long-pitch helix (red lines) (Dominguez, 2009). (**B**) ATP-loaded actin monomers are incorporated at the barbed end of an actin filament. Near the pointed end, ATP is hydrolyzed and ADP-actin monomers dissociate from the actin filament at the pointed end (Pantaloni, Clainche, and Carlier, 2001).

In actin filaments, actin subunits are arranged into a double helix (Figure 1-1A), which allows an incoming actin monomer to connect to two subunits in the actin filament. Thus, in contrast to formation of actin dimers and trimers, the elongation of existing actin filaments can be strongly exothermic, which explains spontaneous filament

polymerization upon nucleation of an actin seed (Carlsson, 2010). Structurally, it is also possible to describe the actin filament as a single left handed short-pitch helix (Figure 1-1A), with consecutive lateral subunits staggered with respect to one another by half a monomer length (Dominguez, 2009).

Actin filaments are polar structures with a fast growing barbed end and a slow growing pointed end. This asymmetry is caused by the structure of G-actin molecules and by the distribution of ATP- versus ADP-loaded actin monomers (Bugyi and Carlier, 2010). The critical concentration, which is defined as the concentration of equal assembly and disassembly, is lower at the barbed end (0.1 µM) than at the pointed end (0.6 µM). Thus, newly incorporated ATP-actin is enriched at the barbed end and hydrolyzed ADP+P_i-actin accumulates at the pointed end (Pollard, Blanchoin, and Mullins, 2000). Polymerization at either end of the actin filament occurs when the G-actin concentration in solution is higher than the critical concentration. At steady-state, when the actin concentration equals or exceeds the critical concentration of the barbed end but at the same time is lower than the critical concentration at the pointed end, the disassembly at the pointed end is as fast as the assembly on the barbed end. Hence, the filament length stays constant but the filament moves in the direction of the barbed end due to addition of actin monomers at one end and their removal on the other end (see Figure 1-1B). This phenomenon is called “actin treadmilling” and is essential for forward movement e.g. in cell migration. In structures such as lamellipodia or filopodia, actin polymerization and depolymerization are tightly regulated and depend on various modifying and actin-binding proteins in order to fulfill their functions (Bugyi and Carlier, 2010) (see below).

1.3 Actin-dependent structures

Actin filament arrangements are crucial for many different cellular processes. One major role of actin is to form protrusive structures such as lamellipodia and filopodia, adhesive structures like focal adhesions and podosomes or providing contractile structures in concert with myosin such as stress fibers. Ultrastructures vary from lose to dense meshworks of actin filaments in the lamella or lamellipodia, respectively, to highly organized actin filament bundles in filopodia or stress fibers.

1.3.1 Lamellipodia

Cell migration was initially described as a three-step cycle. First, the protrusion of the membrane on the leading edge pushes the cell forward; second, the membrane adheres to the substratum; and third, the cell contracts by means of actomyosin structures, which pushes the cytoplasm to the front of the cell. All three steps occur in a

concerted and simultaneous fashion, thus all mechanisms engaged have to be tightly regulated (Abercrombie, 1980). The leading edge of a cell, called the lamellipodium, is on average an 0.1-0.2 µm thick and 1-5 µm wide layer of cytoplasm enclosed by the plasma membrane and filled with a dense meshwork of actin filaments that passes into the less dynamic lamella (Figure 1-2) (Ladwein and Rottner, 2008; Small et al., 2002). The fast growing barbed ends of actin filaments abut the plasma membrane at the tips of lamellipodia and constantly elongate providing the force for leading edge protrusion (Small, Isenberg, and Celis, 1978).

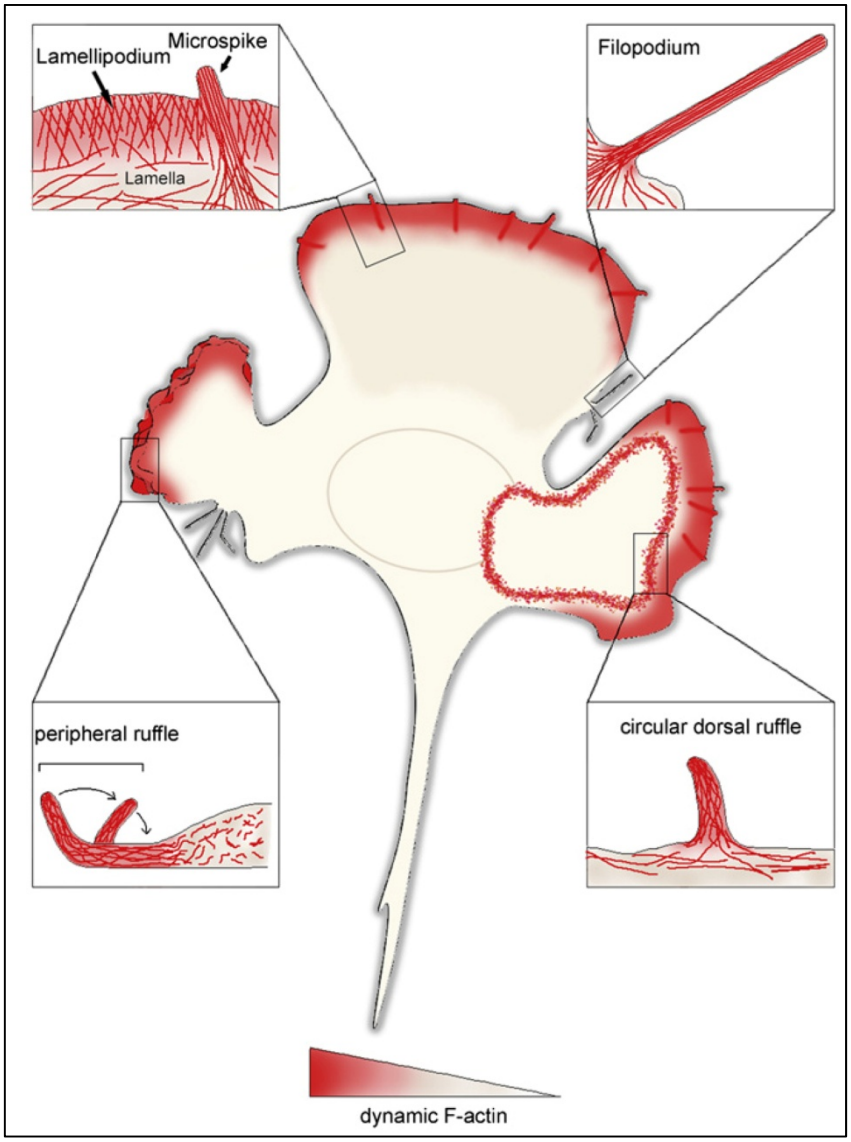

Figure 1-2: Dynamic actin structures in a migrating fibroblast cell.

In cells, the main membrane protrusions are lamellipodia, filopodia and ruffles. At the leading edge, criss-crossed actin filaments, which are continuously nucleated and elongated at the front, provide the force to push the cell forward. Bundled actin filaments are present in microspikes embedded into the lamellipodium and in filopodia. Both in the periphery and on the dorsal side of cells lamellipodia can fold upwards resulting dependent on the location in peripheral or circular dorsal ruffles. Dynamic F-actin is indicated as gradient in red (Ladwein and Rottner, 2008).

To keep the width of the lamellipodium constant, actin filaments are disassembled at the pointed ends, allowing the filaments to treadmill. This was, for instance, demonstrated using FRAP experiments, in which lamellipodia of EGFP-actin-expressing cells were bleached. The recovery of fluorescence was restricted to the tips of lamellipodia (Lai et al., 2008) demonstrating that actin incorporation takes place directly at the membrane, as was already described by Wang (Wang, 1985). A key regulator of lamellipodia formation and maintenance is the small Rho-GTPase Rac1. In its active, GTP-loaded state, it binds to and thus activates the WAVE-complex, a nucleation promoting factor (NPF) known to activate the actin nucleator Arp2/3 complex (see 5.1). It is well established that actin filaments in the lamellipodium are generated through nucleation via the Arp2/3 complex (Pollard and Borisy, 2003), still the exact mechanism and the resulting filament arrangements at the leading edge are discussed controversially. Supported by *in vitro* experiments, in which the Arp2/3 complex forms branched actin filaments with an angle of 70° (Blanchoin et al., 2000; Pantaloni, Clainche, and Carlier, 2001), and electron microscopy (EM) images of lamellipodia obtained after the critical point drying method (Svitkina and Borisy, 1999), the dendritic nucleation model was established. According to this model, the lamellipodial actin filaments are a highly branched and thereby interconnect the actin network (Pollard, 2007). Recent work has challenged this model with data generated using negative stain (Koestler et al., 2008) and Cryo-EM techniques in combination with electron tomography (Urban et al., 2010), in which no indications for branched actin filaments in lamellipodia were detected. The results from Svitkina and collaborators were mostly attributed to the sample preparation, thought prone to introduce distortions into actin networks such as fusion of crossing actin filaments into branching filaments. Additional studies are needed to resolve this controversy and shed light on the ultrastructural arrangements of lamellipodial actin filaments in three dimensions.

1.3.2 Circular dorsal ruffles

A second Arp2/3-dependent actin structure is the circular dorsal ruffle or dorsal wave (Figure 1-2). As the name implicates, this structure is formed on the dorsal plasma membrane of the cell and occurs spontaneously in cultured cells, but can also be induced, for instance, by stimulation with growth factors including platelet-derived growth factor (PDGF), epidermal growth factor (EGF) or hepatocyte growth factor (HGF) as well as bacterial compounds such as Internalin B (InlB) (Chinkers, McKanna, and Cohen, 1979; Dowrick et al., 1993; Mellstrom, 1983; Shen et al., 2000). The molecular machinery potentially participating in dorsal ruffle formation includes kinases such as receptor-tyrosine kinases and PAK1, the Rho-GTPases Rac and Cdc42, the

actin nucleator Arp2/3 complex and the NPFs N-WASP and cortactin (Buccione, Orth, and McNiven, 2004; Dharmawardhane et al., 1997; Krueger et al., 2003; Orth, Krueger, and McNiven, 2003). Dorsal ruffles form transiently for 5 to 20 min after stimulation, then the structure contracts and closes. Upon closure, macropinosomes are formed implicating a role for dorsal ruffles in rapid receptor internalization and uptake of extracellular fluids (Dowrick et al., 1993; Orth, Krueger, and McNiven, 2003).

1.3.3 Filopodia and microspikes

Besides lamellipodia, cells form an additional protrusive actin-dependent structure, called filopodium (Figure 1-2). These rod-like structures are rich of parallel actin filaments and vary in diameter between 100 and 300 nm (Faix et al., 2009). Filopodia can develop from microspikes, actin bundles that are embedded into but do not project beyond the lamellipodium, and are able to move laterally in the lamellipodium. Microspikes are thought to provide stability inside the lamellipodium, and in contrast to filopodia the existence of a lamellipodium is per definition a prerequisite for microspike formation.

As in lamellipodia, the protrusive force of filopodia is generated by actin polymerization at their tips. Filopodia participate in numerous physiological processes such as cell-cell adhesion, wound healing and embryonic development. In general, filopodia serve as “tentacles” sensing the environment. For instance, the filopodia of macrophages were shown to scan the environment for pathogens, and neuronal growth cones use filopodia for the recognition of and the guidance to chemoattractants (Faix and Rottner, 2006; Mattila and Lappalainen, 2008).

It is still controversial which components are essential for filopodia formation. Initial work implied a pathway, in which the small Rho-GTPase Cdc42, a trigger for filopodia formation, activates the NPF N-WASP leading to Arp2/3-dependent actin filament nucleation of filopodial filaments (Svitkina et al., 2003). However, knockdown of Arp2/3 complex refuted this connection and also demonstrated the formation of filopodia in the absence of lamellipodia (Nicholson-Dykstra and Higgs, 2008; Steffen et al., 2006). After the discovery of formin family proteins, actin nucleating and elongating proteins localizing to the tips of filopodia (see 1.1.7), more and more evidence accumulates that filopodia are established via *de novo* nucleation of actin filaments, although at least in some cell types actin filaments from lamellipodia seem to be able to converge into filopodia (Mattila and Lappalainen, 2008).

1.3.4 Stress fibers

Myosin II and actin filaments form a contractile structure found in non-muscle cells, called stress fibers. Stress fibers are composed of 10 to 30 actin filaments, which are bundled into cables e.g. by the crosslinking protein α-actinin (Cramer, Siebert, and Mitchison, 1997). α-actinin binds to stress fibers in a periodic fashion and alternates with bands containing non-muscle myosin II and tropomyosin, a pattern reminiscent of myofibrils in muscle cells. Stress fiber formation is induced by the Rho-GTPase RhoA (Paterson et al., 1990) and is antagonized by Rac1 (Rottner, Hall, and Small, 1999), the activation of which triggers the disassembly of actomyosin filaments and the formation of lamellipodia (Wildenberg et al., 2006). Additionally, Rac1 was also shown to induce the phosphorylation of myosin-II heavy chain, presumably by PAK kinases, which leads to loss of contractility and a release of actin filaments allowing reassembly into the lamellipodial actin network (van Leeuwen et al., 1999).

Stress fibers are either connected at both ends to focal adhesions or are attached to one focal adhesion and polymerize to the dorsal side of the cell. Additionally, also transverse arcs are found that keep in contact with the substratum via dorsal stress fibers (Small et al., 1998). The contractile force provided by the interplay between actin and myosin in stress fibers is crucial for retraction of the cell body during migration (Jay et al., 1995) and for the maintenance of cell tension and shape (Chrzanowska-Wodnicka and Burridge, 1996).

1.3.5 Focal adhesions and podosomes

In order to spread and move on a surface, cells have to connect to the substratum. In most cells focal adhesions are formed, which interact with the extracellular matrix via transmembrane adhesion receptors of the integrin family (Wiesner, Legate, and Fässler, 2005). Intracellular, a multiprotein complex is formed linking the extracellular matrix to the actin cytoskeleton (Figure 1-3). Examples for these actin-integrin linking proteins are talin (Horwitz et al., 1986), kindlin (Montanez et al., 2008), zyxin (Zaidel-Bar et al., 2003), vinculin (Humphries et al., 2007) and paxillin (Turner, Glenney, and Burridge, 1990), as well as actin bundling proteins like α-actinin (Pavalko and Burridge, 1991) or actin elongators such as VASP (Haffner et al., 1995). Another key player is focal adhesion kinase (FAK), a non-receptor tyrosine kinase shown to regulate focal adhesion disassembly by phosphorylation of target proteins (Gardel et al., 2010).

New focal contacts are constantly formed underneath lamellipodia and disassembled at the rear of moving cells (Giannone et al., 2007). The turnover of focal adhesions is crucial for migration as it allows the cells to dynamically attach to the substratum. A specialized adhesion structure, the podosome, is found in macrophages, osteoclasts

smooth muscle cells and v-Src transformed fibroblasts. In contrast to focal adhesions, which need up to 20 min for their formation (Gardel et al., 2010) podosomes have a life-span of only 2 to 4 min allowing faster cell migration and rapid attachment/ detachment cycles (Destaing et al., 2003). In osteoclasts, podosomes are involved in the formation of a sealing ring, which constitutes an isolated compartment in which bone is degraded. In some invasive cancer cells podosome-like structures are found, referred to as invadopodia according to their promotion of cancer invasion (Albiges-Rizo et al., 2009). Podosomes consist of an actin-rich core containing proteins of the actin nucleation machinery such as WASP and N-WASP, Arp2/3 complex and cortactin, surrounded by a ring of adhesion molecules found in focal adhesions e.g. integrin, talin, zyxin, vinculin and paxillin (Figure 1-3) (Gimona and Buccione, 2006).

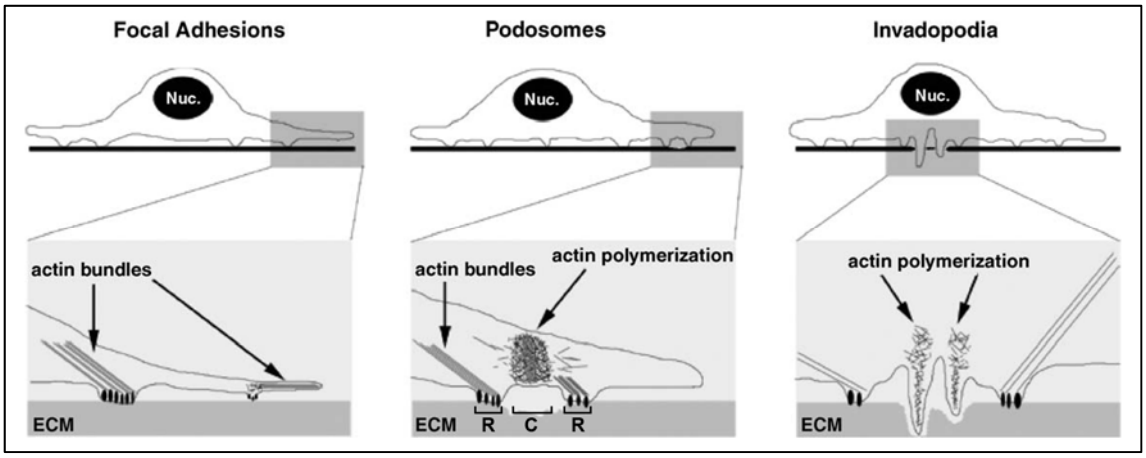

Figure 1-3: Actin distribution in focal adhesions, podosomes and invadopodia.

Focal adhesions, podosomes and invadopodia are anchored to the substratum via adhesion molecules (black spheres). Focal adhesions display prominent actin bundles expanding into the cell, whereas in podosomes an adhesive ring (R) surrounds a dynamic actin core (C). Invadopodia resemble podosome organization, although actin cores are less dense (Gimona and Buccione, 2006, adapted).

By secretion of metalloproteases that are delivered to the podosomes in vesicles transported through kinesins via the microtubule network (Wiesner et al., 2010), podosomes are able to degrade the extracellular matrix as exemplified by the bone resorption activity of osteoclasts.

1.4 Rho-GTPases

Rho-GTPases are small proteins with a molecular mass of approximately 20 to 25 kDa that cycle between an active, GTP-bound, and an inactive, GDP-bound state. The activity of Rho-GTPases is strictly controlled to ensure local and temporal stimulation of specific signaling pathways. Guanine nucleotide exchange factors (GEFs) catalyze the exchange of GDP for GTP and thereby activate Rho-GTPases. In this conformation Rho-GTPases are able to bind their effector proteins and, for instance, release the

autoinhibition of N-WASP or activate the WAVE complex (Rohatgi, Ho, and Kirschner, 2000; Steffen et al., 2004). GTPase-activating proteins (GAPs) bind active Rho-GTPases and enhance their intrinsic GTP hydrolyzing activity, thus promote their inactivation. This is necessary, as the Rho-GTPases only slowly hydrolyze GTP on their own, and their activity may has to be shut down quickly after the decline of an intracellular or extracellular signal (Ellenbroek and Collard, 2007; Ridley, 2006).

Rho-GTPases have a C-terminal CAAX motif, which is the target of posttranslational modifications such as farnesylation, geranylgeranylation or palmitoylation. With these membrane anchors, Rho-GTPases are able to integrate into membranes where they are thought to be activated by GEFs. In the inactive conformation, Rho-GTPases are bound by guanine nucleotide dissociation inhibitors (GDIs) that mask the lipid anchor and thereby prevent both binding to membranes as well as activation of the Rho-GTPases (Ellenbroek and Collard, 2007). Upon stimulation with a growth factor GDIs are phosphorylated, for instance, by PAK1 or PKC (DerMardirossian, Schnelzer, and Bokoch, 2004). Phosphorylation induces conformational changes of the GDIs and triggers the release of Rho-GTPases and subsequent activation and effector protein binding (DerMardirossian and Bokoch, 2005; Ellenbroek and Collard, 2007; Hoffman, Nassar, and Cerione, 2000).

In humans 20 genes encoding Rho-GTPases were found and those can be subdivided into eight subgroups (Gad and Aspenström, 2010). The classical Rho-GTPases from the subgroups Cdc42, Rac, Rho and Rif are regulated by their GTPase activity and play a role in actin cytoskeleton rearrangement and cell-matrix adhesion. Rac1 is known to induce lamellipodia by activating the WAVE complex, whereas RhoA antagonizes Rac and induces stress fiber formation. A possible pathway for RhoA-dependent Rac inhibition was described by Ohta et al., who found that FilGAP, a Rac GAP activated by Rho and ROCK decreases Rac activity in membrane protrusions and thereby suppresses lamellipodia maintenance (Ohta, Hartwig, and Stossel, 2006).

Cdc42-expression was shown to promote filopodia formation and Cdc42 can also cross-talk to Rac (Ellenbroek and Collard, 2007). One study claimed that activation of Rac downstream of Cdc42 depended on Cool-2, a GEF for Cdc42 and Rac. Upon binding of active Cdc42, the affinity for GDP-bound Rac was enhanced leading to an increase in GEF activity towards Rac (Baird, Feng, and Cerione, 2005). A different pathway was proposed in neurons, where the association of Cdc42 with PAR6 and PAR3 led to an activation of the Rac GEFs STEF/Tiam1, which was suggested to drive Cdc42-induced lamellipodia formation through Rac1 (Nishimura et al., 2005). Moreover, Cdc42 activates the NPF N-WASP during clathrin-mediated endocytosis and PIP_2-induced vesicle movement (Ridley, 2006).

1.5 Actin nucleation

The first steps in the nucleation of an actin filament are the association of two G-actin molecules and by subsequent binding of a third actin monomer the formation of an actin trimer. In living cells, the formation of these actin dimers and trimers is the rate limiting step in actin polymerization, as both structures are highly instable in the cytoplasm. To overcome this kinetic barrier, cells employ actin nucleators depicted in Figure 1-4. Nucleus formation is either accomplished by mimicking an actin dimer, as employed by the Arp2/3 complex, by stabilizing the actin seed like formins or binding three to four actin monomers and bringing them in close contact to facilitate nucleus formation such as in case of Spir and leiomodin.

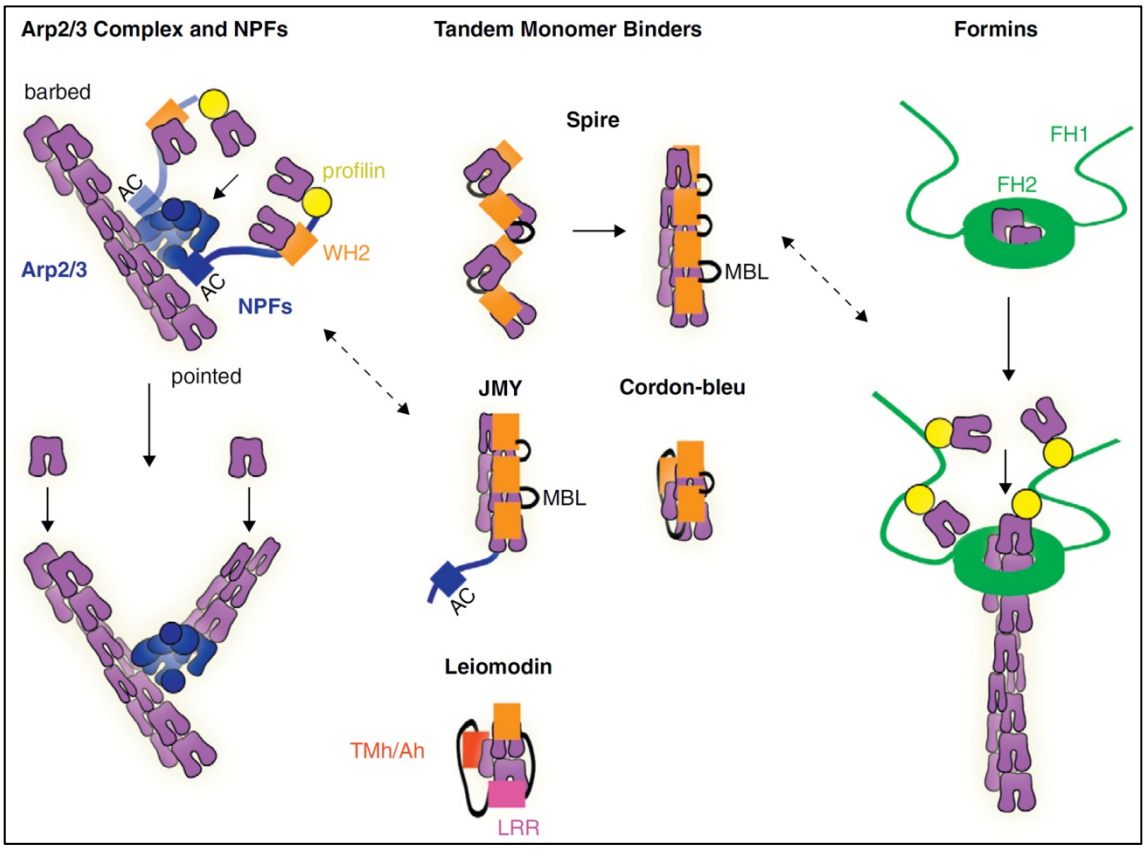

Figure 1-4: Different modes of actin nucleation.

Left: Branched actin filaments are generated through side-binding of the Arp2/3 complex to a mother filament and nucleation of a novel filament. The activity of the Arp2/3 complex is regulated by NPFs, which activate the Arp2/3 complex through binding with their CA domains and deliver G-actin for the nucleation via WH2 domains or profilin-actin via proline-rich domains, respectively. After the initiation step the actin filament assembles spontaneously. *Middle*: Spir, Cordon-bleu, leiomodin and JMY nucleate actin filaments by clustering three to four actin monomers. While Spir and JMY align G-actin with WH2 domains and a monomer-binding linker (MBL), Cordon-bleu and leiomodin form a short-pitch trimer with WH2 domains, tropomyosin and actin helices (TMh/Ah) and leucine-rich regions (LRR). *Right*: Two FH2 domains of formin proteins stabilize an actin dimer and stay attached to the growing barbed end. The elongation of the actin filament is enhanced by the binding of profilin-bound actin to the FH1 domains, which are incorporated at the barbed end (Firat-Karalar and Welch, 2011).

1.5.1 The Arp2/3 complex

The Arp2/3 complex was first purified in 1994 from *Acanthamoeba castellanii* (Machesky et al., 1994) and one year later identified as an actin nucleator (Kelleher, Atkinson, and Pollard, 1995). In the Arp2/3 complex, two actin related proteins named actin related protein 2 and 3 associate with five additional subunits ArpC1 (p40), ArpC2 (p34), ArpC3 (p21), ArpC4 (p20) and ArpC5 (p16), the numbers in brackets correspond to their size in kDa (Higgs and Pollard, 1999; Machesky et al., 1994). In the active conformation, Arp2 and 3 form an actin-like dimer that serves as nucleus for actin polymerization. *In vitro* the Arp2/3 complex nucleates branched actin filaments with an angle of 70° by first binding to the side of an existing mother filament followed by the nucleation and polymerization of a daughter filament (Figure 1-4) (Mullins, Heuser, and Pollard, 1998). Whether the Arp2/3 complex forms branched actin filaments also *in vivo* is controversial, as electron micrographs after gentle sample preparation revealed few actin branches (Koestler et al., 2008; Urban et al., 2010), in contradiction with earlier findings using alternative methods of sample preparation for electron microscopy (see also 1.1.1).

On its own the Arp2/3 complex has a very low intrinsic nucleation activity and thus requires nucleation promoting factors (NPFs) such as WASP or WAVE and related proteins for effective nucleation. These proteins bind and activate the Arp2/3 complex either through a VCA module in case of class I NPFs or through an acidic domain in case of class II NPFs. Additionally, threonine and tyrosine phosphorylation of Arp2 contribute to the activity of the complex and mediate its binding to pointed ends of actin filaments. However, phosphorylation is dispensable for both NPF recruitment and F-actin side binding (LeClaire et al., 2008). Like actin, also Arp2 and 3 bind ATP and the availability of the nucleotide is crucial for nucleation *in vitro* (Goley et al., 2004). Arp2 was shown to hydrolyze ATP, which probably contributes to debranching and recycling of the complex (Le Clainche, Pantaloni, and Carlier, 2003; Martin, Welch, and Drubin, 2006) though nucleotide hydrolysis was also implicated in promoting actin nucleation (Dayel and Mullins, 2004). During filament nucleation and elongation, the Arp2/3 complex stays attached to the pointed end of the filament leaving the barbed end free for polymerization. Both subunits ArpC2 and ArpC4 mediate the binding to pre-existing actin filaments, hence mutations of conserved residues in these subunits reduce the nucleation activity of the complex (Rouiller et al., 2008). By using *in vitro* reconstitution of the Arp2/3 complex, the implications of the different subunits in Arp2/3 functions could be defined. For the assembly of intact Arp2/3 complex, p20 and p34 were essential, which led to the assumption that both subunits constitute the structural core of the complex. In contrast, only p21 was shown to be non-essential for nucleation of

actin filaments by Arp2/3, whereas p41, p16 and p21 were dispensable for actin filament branching (Gournier et al., 2001).

1.5.1.1 Nucleation promoting factors

To enhance the nucleation activity of Arp2/3 complex, cells have developed several nucleation promoting factors (NPFs) that differ in their Arp2/3 activation mechanism as well as in upstream signals leading to their own activation. Two distinct classes of NPFs were described so far (Figure 1-5) (Campellone and Welch, 2010). Class I NPFs uniformly possess at least one WH2-domain providing an additional actin monomer for the Arp2/3 complex in order to form an actin trimer. In contrast, class II NPFs such as cortactin lack the actin monomer binding capacity and instead exhibit an F-actin binding domain assumed to be involved in stabilizing newly formed actin filaments.

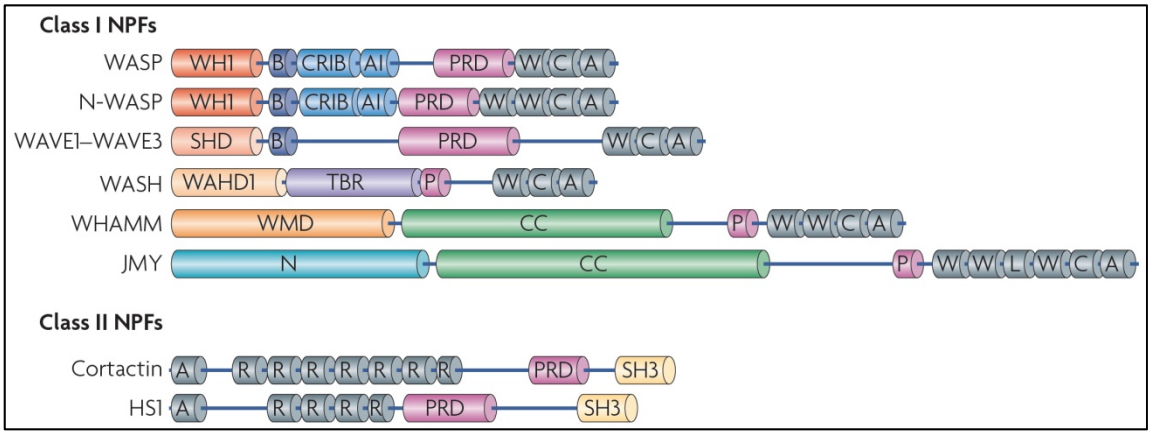

Figure 1-5: Domain organization of nucleation promoting factors.

Class I NPFs possess a C-terminal VCA domain for the activation of the Arp2/3 complex and regulatory domains at the N-terminus in varying number and length. Class II NPFs lack the VCA domain and instead harbor an N-terminal acidic domain and actin binding repeats both proposed to be essential for Arp2/3 activation. (A: acidic domain, AI: autoinhibitory domain, B: basic region, C: central domain, CC: coiled coil domain, CRIB: Cdc42-Rac-interactive-binding, L: linker, N: N-terminus, P: polyproline, PRD: proline-rich domain, R: F-actin-binding repeats, SH3: Src homology 3, SHD: SCAR homology domain, TBR: tubulin-binding region, W: WASP homology 2 domain, WAHD1: WASH homology domain 1, WH1: WASP homology 1 domain, WMD: WHAMM membrane interaction domain) (Campellone and Welch, 2010).

1.5.1.2 Class I NPFs

The output effector module present in all class I NPFs is the VCA domain (also known as WCA or WA domain) at the C-termini of the proteins, which constitutes the shortest peptide sufficient for activation of Arp2/3-dependent actin assembly (Machesky et al., 1999), and consists of three sub-elements (Figure 1-5). The verprolin (V) homology domain (more recently called WH2 domain) recruits monomeric actin, which is crucial for nucleus formation by Arp2/3, and is found in duplicate in N-WASP and as single domain in WASP and WAVE (Padrick and Rosen, 2010). Both the central (C) and the acidic (A) region mediate the association with Arp2/3 (Marchand et al., 2001; Zalevsky

et al., 2001), and the central domain was shown to associate with the nucleator via an amphipathic helix that induces conformational changes essential for its activation (Panchal et al., 2003). A conserved tryptophan residue was identified positioned within the acidic domain, the mutation of which was described to abolish Arp2/3 binding (Marchand et al., 2001). The regulatory domains at the N-termini of NPFs differ strongly between each other, which enables Arp2/3-dependent actin assembly at distinct compartments in the cell and upon diverse stimuli (Stradal and Scita, 2006).

The best characterized NPFs are the Wiskott-Aldrich syndrome protein (WASP) and its homologue neuronal WASP (N-WASP). The Wiskott-Aldrich syndrome, a severe immunodeficiency disorder, is caused by mutations in the *WAS* gene and was not curable until last year, when the Wiskott-Aldrich syndrome was successfully treated with genetically modified hematopoietic stem cells (Boztug et al., 2010). WASP expression is restricted to hematopoietic cells, whereas N-WASP is ubiquitously expressed. Deletion of the latter causes abnormalities in brain and heart and is embryonic lethal in mice (Lommel et al., 2001; Snapper et al., 2001). Both WASP and N-WASP are implicated in podosome formation, and although WASP-deficient macrophages were initially reported to be incapable of podosome formation (Mizutani et al., 2002), a recent study demonstrated that N-WASP could compensate the loss of WASP (Isaac et al., 2010). Additionally, N-WASP was shown to be part of the endocytic machinery, as EGF receptor internalization was impaired in N-WASP-deficient cells (Benesch et al., 2005). N-WASP was also shown to mediate PIP2-induced vesicle movement (Benesch et al., 2002) and is utilized by *Shigella* for the induction of intracellular movement (see 1.1.16).

Both WASP and N-WASP share the same domain organization with an N-terminal WASP homology 1 (WH1) domain, followed by a basic stretch, a GTPase-binding domain (GBD), a proline-rich domain (PRD) and the VCA domain. WASP-interacting protein (WIP) binds to the WH1 domain in WASP and N-WASP. While WIP-WASP interaction protects WASP from degradation (de la Fuente et al., 2007), association of WIP with N-WASP keeps the NPF in an inactive conformation (Martinez-Quiles et al., 2001). The proline-rich domain between the GBD and the VCA constitutes a docking platform for SH3 domain-containing proteins, which can also contribute to the activation of N-WASP. For instance, Nck, TOCA and Abi1 were found to promote N-WASP function (Ho et al., 2004; Innocenti et al., 2005; Tomasevic et al., 2007). Another important aspect of N-WASP activation is the interaction with phosphatidylinositol-4,5-bisphosphate (PIP_2), which is mediated by the basic region (Higgs and Pollard, 2000; Padrick et al., 2008).

In the inactive conformation of N-WASP, the basic region and the GBD are associated with the VCA domain and thereby inhibit NPF-Arp2/3 complex interactions. In order to release N-WASP from autoinhibition, GTP-loaded Cdc42 binds to the Cdc42-Rac-interactive-binding (CRIB) motif in the GBD, which induces conformational changes that free the VCA domain (Buck, Xu, and Rosen, 2004; Rohatgi, Ho, and Kirschner, 2000). This allosteric activation of N-WASP activity is further amplified by oligomerization, as was shown by Padrick et al. (Padrick et al., 2008). Oligomerization of VCA domains or N-WASP molecules could be mediated through chemical compounds, cellular adaptor proteins, such as Nck and Grb2 as well as clustering at PIP_2-rich membranes, which enhanced Arp2/3 activation up to 100-fold compared to the isolated NPF. In this study, a second VCA-binding domain of the Arp2/3 complex was identified and competition experiments suggested this domain to be identical with the cortactin-binding domain, implicating an inhibitory effect of cortactin on Arp2/3 activation (see also 1.1.6.3).

Shortly after the discovery of WASP and N-WASP, the WAVE/Scar (WASP-family verprolin-homologous protein/suppressor of cyclic AMP repressor) proteins were identified, which are expressed in three isoforms in mammals, WAVE1, 2 and 3. In contrast to WASP and N-WASP, WAVE proteins are not autoinhibited (Machesky et al., 1999), but instead are regulated by the incorporation into a heteropentameric complex. This WAVE complex consists of WAVE1/2/3, Abi1/2/3, HSPC300, Nap1 and Sra1 (Eden et al., 2002; Innocenti et al., 2004) and the lack of any of the WAVE complex components leads to the degradation of the whole complex (Innocenti et al., 2005; Kunda et al., 2003; Steffen et al., 2006). The Scar homology domain (SHD) of WAVE binds directly to Abi and HSPC300, which contributes to WAVE complex assembly (Gautreau et al., 2004). Carboxy-terminal to the SHD are a basic motive and a proline-rich region, the latter of which associates with IRSp53, a protein known to bind active Rac1 (Miki et al., 2000). Also another component of the WAVE complex, Sra1, is able to associate with Rac1 (Kobayashi et al., 1998). The WAVE complex itself is inhibited, until Rac binding activates the complex and stimulates Arp2/3-driven actin assembly (Chen et al., 2010; Ismail et al., 2009). In addition, phosphorylation (Ardern et al., 2006; Danson et al., 2007; Stuart et al., 2006) and apparently also oligomerization (Padrick et al., 2008) contribute to full activation of the WAVE complex. Many studies have demonstrated that the WAVE-complex is required for cell migration through induction of lamellipodia formation downstream of Rac (Kurisu and Takenawa, 2009; Pollitt and Insall, 2009; Stradal and Scita, 2006; Suetsugu et al., 2003). Furthermore, the WAVE complex was reported to contribute to cell spreading, cell polarization, T cell activation

and neuronal guidance (Billadeau, Nolz, and Gomez, 2007; Eden et al., 2002; Tahirovic et al., 2010).

Recently, three novel class I NPFs, WASH, WHAMM and JMY, were discovered. Like WAVE, WASH is assembled into a regulatory complex, but specifically activates the Arp2/3 complex on endosomes (Derivery et al., 2009; Duleh and Welch, 2010; Gomez and Billadeau, 2009) and together with its ability to bind microtubules WASH regulates the dynamics and trafficking of vesicles. Moreover, WASH was shown to trigger invasion of *Salmonella* in an Arp2/3-dependent manner, adding to NPFs that are exploited by pathogens (Hänisch et al., 2010; Rottner, Hänisch, and Campellone, 2010).

Besides interactions with the Arp2/3 complex and actin, WHAMM, an NPF with two WH2 domains in the VCA domain, can also bind to microtubules via a coiled-coil region. WHAMM localizes to *cis*-Golgi membranes and the ER-Golgi intermediate compartment (ERGIC), implicating a role in membrane transport between the secretory organelles (Campellone et al., 2008).

JMY harbors both a VCA domain activating the Arp2/3 complex and three tandem WH2 domains plus a monomer-binding linker known from Spire, which enables JMY to nucleate actin filaments both in an Arp2/3-dependent and -independent fashion (Zuchero et al., 2009). Although the biochemical properties have been studied in detail (Zuchero et al., 2009), the cellular role of JMY is still unclear. RNAi experiments indicated a role for JMY in cell migration, but JMY knockdown coincided with upregulation of E-cadherin, which stabilizes cell-cell adhesion and probably interfered with migration efficiency (Coutts, Weston, and La Thangue, 2009). Additional research is required in order to fully uncover the cellular roles of the three novel Arp2/3 complex activators (see e.g. (Rottner, Hänisch, and Campellone, 2010)).

1.5.1.3 Class II NPFs

Class II NPFs differ from those of class I in two important features. On one hand class II NPFs have an F-actin binding domain instead of an actin monomer-binding WH2-domain, and on the other hand they lack the VCA module and use just an acidic domain for Arp2/3 recruitment (Figure 1-5). So far, two class II NPFs were identified in *S. cerevisiae*, actin-binding protein-1 (Abp1) (Goode et al., 2001) and Pan1 (Duncan et al., 2001), whereas in mammals only cortactin and its hematopoietic homolog hematopoietic specific 1 (HS1) were assigned to this class (Schuuring et al., 1998; van Rossum et al., 2005b). Cortactin was first identified as a substrate of Src kinase (Huang et al., 1997; Wu et al., 1991), which displayed a characteristic double-band in SDS-PAGE at 80/85 kDa and was thus named according to the molecular masses as

p80/85 (Wu and Parsons, 1993). Cortactin and HS1 share the same domain organization. The N-terminus comprises an 84 aa-long region called NTA (N-terminal acidic domain), harboring a conserved tryptophan-containing DDW motif (aa 20-22), which is also found in class I NPFs. The NTA was shown to bind the Arp2/3 complex both *in vitro* and *in vivo* (Weaver et al., 2002; Weaver et al., 2001; Weed et al., 2000). The F-actin-binding domain located C-terminal to the NTA comprises tandem repeats of a 37 aa motif with 6.5 copies in cortactin and 3.5 copies in HS1 (Kitamura et al., 1989). The fourth repeat was identified to be crucial for actin filament binding of cortactin (Weed et al., 2000). At the C-terminus, both cortactin and HS1 contain a helical and a proline-rich domain, the latter of which is target for serine and tyrosine phosphatases. The SH3-domain at the C-terminus serves as platform for a plethora of proteins with proline-rich regions, including in the case of cortactin e.g. WIP, N-WASP and dynamin2 (Kinley et al., 2003; McNiven et al., 2000; Weaver et al., 2002).

In *in vitro* experiments, cortactin was able to weakly activate the Arp2/3 complex, which depended both on binding to the Arp2/3 complex via the NTA and the association with filamentous actin mediated by the repeat domain (Uruno et al., 2001; Weaver et al., 2001). The link between F-actin, the Arp2/3 complex and cortactin was further strengthened by the finding that cortactin promotes actin branching by the Arp2/3 complex and protects newly formed branches from disassembly (Weaver et al., 2001). Cortactin is able to bind the Arp2/3 complex simultaneously with N-WASP VCA. It was proposed that cortactin binding to activated Arp2/3 promotes the release of VCA and thereby enables the activation of a further Arp2/3 complex molecule (Uruno et al., 2003; Weaver et al., 2002). In other studies, the positive effect of cortactin regarding Arp2/3 complex activation was attributed to its ability to bind the NPF N-WASP via the SH3 domain and thus to act as a scaffold between Arp2/3 and N-WASP. Additionally, cortactin has been reported to recruit the Cdc42 GEF FGD1, which could contribute to the activation of N-WASP by Cdc42 (Kim et al., 2004). As opposed to these indications for a positive contribution of cortactin to Arp2/3-dependent actin assembly, findings concerning cortactin function in other results seem to challenge this view, at least in part. The discovery that N-WASP-mediated Arp2/3 complex activation is strongly amplified by dimerization of the NPF indicated an inhibitory role of cortactin binding to Arp2/3. This is due to the fact that the binding site for cortactin and one of the N-WASP molecules overlap, so upon cortactin binding hyperactivation induced by association of two VCA domains with Arp2/3 would not occur (Padrick et al., 2008). Similarly, the turnover of cortactin in the lamellipodium measured with FRAP differed strongly from the turnover of Arp2/3 or WAVE, in that fluorescence recovery did not occur from the tip of the lamellipodium but evenly throughout the lamellipodium. Assuming that Arp2/3

complex is activated at the lamellipodium tip, most cortactin molecules rapidly turning over throughout the lamellipodium would not be able to contribute to Arp2/3 activation (Lai et al., 2008).

The phosphorylation of cortactin was subject of many studies, which identified cortactin to be a substrate of tyrosine phosphorylation by Src (Huang et al., 1997), Fer (Craig et al., 2001) and c-Met (Crostella et al., 2001), whereas serine residues were shown to be phosphorylated by ERK (Martinez-Quiles et al., 2004), PAK (Webb et al., 2006) and PKD (Eiseler et al., 2010). Phosphorylation of cortactin did not appear to alter Arp2/3 complex activation, but modulated the affinity of the SH3 domain to different binding partners (Dudek et al., 2002; Lynch et al., 2003). Importantly, ERK-mediated serine phosphorylation enhanced binding of N-WASP to the SH3 domain of cortactin, which promoted Arp2/3 complex activation, whereas tyrosine phosphorylation by Src inhibited the interaction with N-WASP (Martinez-Quiles et al., 2004).

Cortactin has been implicated in a variety of different cellular functions, as cortactin localizes to virtually every site in the cell with active Arp2/3-dependent actin polymerization, such as lamellipodia, endocytic vesicles, cell-cell adhesions and podosomes (Cosen-Binker and Kapus, 2006). In resting cells, cortactin is mostly cytoplasmic, but relocates to the leading edge of the cell upon growth factor treatment, for instance after application of PDGF or EGF, which coincides with activation of Rac (Kempiak et al., 2005; Weed, Du, and Parsons, 1998). Both overexpression and RNAi experiments have established a positive role for cortactin in cell migration (Huang et al., 1998; Kowalski et al., 2005; Patel et al., 1998; van Rossum, Moolenaar, and Schuuring, 2006; Zhu et al., 2010) and cortactin was found to be crucial for the formation and persistence of lamellipodia (Bryce et al., 2005; Kelley et al., 2010). Additional to its role in lamellipodia dynamics, the reduced motility of cortactin-depleted cells was also attributed to decreased numbers of focal contacts seen in these cells (Bryce et al., 2005). However, in tumor cells with down-regulated cortactin, lamellipodia were formed more frequently towards EGF-coated beads (Kempiak et al., 2005), questioning the essential role for cortactin in lamellipodia formation. Cortactin has been reported to be overexpressed in a variety of human cancers, which correlated with enhanced tumor cell migration and metastasis (Cai et al., 2010; Croucher et al., 2010; Weaver, 2008). Cortactin was also found to be crucial for the formation of invadopodia (Oser et al., 2010) and podosomes, since knockdown of cortactin in vascular smooth muscle cells inhibited the assembly of podosomes (Webb, Eves, and Mak, 2006; Zhou et al., 2006). This was confirmed by RNAi studies in osteoclasts, where both podosome formation and bone resorption, which is regulated by podosomes, was abolished (Tehrani et al., 2006b). A potential role for cortactin in endocytosis was suggested by

its localization to clathrin-coated pits and its interaction with the vesicle scission mediator dynamin2 (Mooren et al., 2009). Knockdown of cortactin was reported to reduce transferrin uptake, which occurs in a clathrin-dependent fashion (Cao et al., 2010; Chen et al., 2006; Zhu et al., 2005). In addition, it interfered with clathrin-independent endocytosis of the γc cytokine receptor, which depended on the ability of cortactin to interact with Arp2/3 complex (Grassart et al., 2010; Sauvonnet, Dujeancourt, and Dautry-Varsat, 2005). However, overexpression of cortactin decreased the turnover of EGF receptor in carcinoma cells (van Rossum et al., 2005a) indicating that cortactin has to be present in the correct amount in order to fulfill its function in endocytosis. Moreover, cortactin is recruited to sites of pathogen adhesion, bacteria entry and intracellular movement, for instance, upon infection with EHEC and EPEC, *Listeria monocytogenes*, *Helicobacter pylori*, *Shigella flexneri*, *Vaccinia virus*, *Rickettsia conorii* and *Staphylococcus aureus* (Selbach and Backert, 2005). It was shown that EHEC and EPEC pedestal formation was suppressed using a dominant negative cortactin construct (Cantarelli et al., 2006; Cantarelli et al., 2002). *H. pylori* was identified to dephosphorylate and relocate cortactin in a CagA-dependent manner and was suspected to play a role in cell scattering induced by *H. pylori* (Selbach et al., 2003). RNAi experiments demonstrated that entry of *L. monocytogenes* was dependent on cortactin in both InlA- (Sousa et al., 2007) and InlB-mediated host cell invasion (Barroso et al., 2006). Knockdown of cortactin reduced the invasion of WT *Listeria* in HeLa and NIH cells (Barroso et al., 2006; Veiga and Cossart, 2005), although it did not affect the intracellular movement of the bacterium. In the nervous system, cortactin has been identified to be enriched in growth cones of developing neurons (Kurklinsky, Chen, and McNiven, 2011) and has been implicated in neuronal polarization and the morphogenesis of dendritic spines (Gray et al., 2005; Lee, 2005). Finally, cortactin has been reported to play a role in synaptic transmission (Iki et al., 2005; Madhavan et al., 2009) and to operate in processes as complex as learning and sleep (Davis et al., 2006; Meighan et al., 2006).

The generation and analysis of cortactin knockout MEF cells has challenged several findings obtained with dominant negative approaches and RNAi experiments concerning cortactin function in the cell (Lai et al., 2009). Electron microscopy revealed no differences in the lamellipodial ultrastructure of cortactin-deficient cells, and the turnover of actin and Arp2/3 complex in lamellipodia was not decreased but rather slightly enhanced as probed by FRAP experiments. Similarly, microinjection of active Rac into cortactin KO cells induced lamellipodia with dynamics indistinguishable to controls, proving that cortactin is not essential for lamellipodia formation. Likewise, the essential role for cortactin in endocytosis could not be confirmed, as both actin

recruitment to clathrin-coated pits and EGF internalization was normal in cortactin knockout cells. However, PDGF-induced membrane ruffling and focal adhesion disassembly was strongly impaired in cells lacking cortactin. These phenotypic observations could be correlated with reduced Rac activation upon PDGF stimulation, and also significantly lower levels of constitutively active Cdc42 were detected in cells lacking cortactin as compared to parental controls. The migration defect described using cortactin RNAi was also observed in cortactin KO cells, as both the migration speed and wound healing efficiency were reduced, although a similar study using independently generated cortactin KO cells reported contradictory results (Tanaka et al., 2009). In conclusion, the data from KO cells suggest a role for cortactin in signaling to Rho-GTPases rather than a direct impact on actin assembly downstream of Rho-GTPases.

1.5.2 Formins

Formins constitute another class of actin nucleators, which are expressed in all eukaryotes and were shown to be involved in filopodia formation in systems as diverse as *Dictyostelium* and mammalian cells (Block et al., 2008; Pellegrin and Mellor, 2005; Schirenbeck et al., 2005). Formins are able to nucleate actin filaments by stabilizing actin dimers, and in contrast to the Arp2/3 complex, they stay attached to the growing barbed ends (Paul and Pollard, 2009). By processive elongation of actin filaments and concomitant capping of the barbed end, formins promote actin polymerizing through actively adding actin monomers at the growing end and by preventing the termination of actin polymerization, for instance by capping protein (Harris, Li, and Higgs, 2004). Common features of all formins are the formin homology (FH) FH1 and FH2 domains. The active formin unit constitutes a homodimer that forms upon binding of two FH2 domains shaping into a “donut”-like structure (Xu et al., 2004), and also the dimerization domains contribute to the formation of the homodimer (Rose et al., 2005). While the FH2 domain is implicated in stabilizing actin seeds, thereby facilitating actin nucleus formation and associating with the barbed ends of actin filaments, the FH1 domain recruits profilin-bound actin and promotes the incorporation of actin monomers into the filament (Figure 1-4) resulting in unbranched filaments (Kovar et al., 2006; Paul and Pollard, 2008; Romero et al., 2004).

The diaphanous-related formins, such as mDia2/Drf3, are autoinhibited through intramolecular binding of the diaphanous inhibitory domain (DID) and diaphanous autoregulatory domain (DAD). Small Rho-GTPases like Cdc42, Rac or RhoA release formins from autoinhibition through binding to the GTPase-binding domain (Lammers et al., 2005; Pellegrin and Mellor, 2005; Peng et al., 2003). Constitutively active formins

can be generated by deletion of the DAD, which induces the formation of large numbers of filopodia in B16-F1 cells and *de novo* actin polymerization in the case of mDia2/Drf3 overexpression (Block et al., 2008). A novel study from Gould et al. indicates that the DAD of mDia1 binds profilin-unbound actin monomers and strongly promotes actin nucleation of the FH2 domain, so probably both the FH1 and DAD contribute to the delivery of actin monomers to the FH2 domain during nucleation (Gould et al., 2011).

1.5.3 WH2-domain containing nucleators

The third class of actin nucleators forms actin seeds by clustering three to four actin monomers, mostly with WH2 domains (Figure 1-4). Proteins belonging to this class of actin nucleators include Spir, leiomodin-2 and cordon-bleu (Cobl), but also the NPF JMY and bacterial factors like VopL (Dominguez, 2009).

The Spir domain organization includes an N-terminal kinase non-catalytic C-lobe domain (KIND), a central region with four WH2 domains including an additional actin monomer-binding linker, and a central FYVE domain, which mediates targeting to endosomal membranes (Quinlan et al., 2005). Data from *Drosophila* mutants and cellular studies suggest a role for Spir in vesicle transport processes and in the coordination of cortical microtubule and actin filaments (Kerkhoff et al., 2001; Rosales-Nieves et al., 2006). Spir has been shown to cooperate with the formin Cappuccino in *Drosophila* (Quinlan et al., 2005), and also in mammals an interaction between Spir1 and formin2 could be established (Pechlivanis, Samol, and Kerkhoff, 2009). Nevertheless, Spir was shown to nucleate actin filaments individually in *in vitro* experiments. It was postulated that the four WH2 domains each bind one actin monomer, which interconnect and thereby form longitudinal bonds found in the long-pitch helix of actin filaments, although this model is not consistent with the fact that the last two WH2 domains are sufficient for actin nucleation (Quinlan et al., 2005). A novel structural-based analysis, which is also able to explain the nucleation activity of only two Spir WH2 domains, proposed that actin binding of each WH2 domain and MBL leads to a loose actin/Spir configuration resembling a long-pitch helix (see Figure 1-1A). Further addition of actin monomers crosslinking two subunits already bound to Spir leads to the formation of a short-pitch nucleus, which is dependent on rotation of the WH2 domains (Ducka et al., 2010).

Leiomodin with its three isoforms is restricted to muscle cells and its domain organization closely resembles that of tropomodulins. At the N-terminus of leiomodin, a tropomyosin-binding domain is located, followed by an actin capping domain, a leucine-rich region and a second actin capping domain. The extended C-terminus of leiomodin

consists of a proline-rich region and a WH2-domain. It is known that tropomodulin binds to adjacent actin monomers at the pointed end, so the nucleation activity of leiomodin could be explained with recruitment of a third actin monomer via its WH2 domain, leading to a cross-filament actin trimer. Evidence for the actin nucleation activity of leiomodin *in vivo* was obtained by overexpression of a GFP-labeled truncated version, which induced abnormal actin bundles in the nucleus.

Cobl is mostly expressed in neuronal tissues, where it is essential for inducing the formation and branching of neurites (Ahuja et al., 2007), and recently Cobl was found to be involved in motile cilia formation in zebrafish (Ravanelli and Klingensmith, 2011). Its nucleation unit comprises three C-terminal WH2 domains, which are all crucial for nucleation, and an extended linker L2. The first two WH2 domains are in close proximity to each other, whereas the third is more distant due to the length of L2 (Ahuja et al., 2007). This WH2 domain arrangement suggests that the first two WH2 domains form a linear actin dimer and the third adds an actin monomer to the back of the actin dimer, resulting in a short-pitch filament trimer (see Figure 1-1A) ready for spontaneous actin polymerization (Ahuja et al., 2007; Dominguez, 2009).

1.6 Regulators of actin filaments and monomers

1.6.1 Ena/VASP

The Enabled/vasodilator-activated phosphoprotein (VASP), as well as the other members of the Ena/VASP family, Mena and EVL, is a key regulator of cell movement and cell shape changes. They are thought to drive the assembly of the actin filament network, for instance, in lamellipodia, filopodia or cell-substrate contacts, but also during intracellular movement of bacteria (Bear and Gertler, 2009). Genetic studies in mice revealed that VASP plays crucial roles in axon guidance, neuritogenesis and endothelial barrier formation (Furman et al., 2007; Kwiatkowski et al., 2007; Menzies et al., 2004). VASP consists of an N-terminal Ena/VASP homology 1 (EVH1) domain, followed by a proline rich domain and an EVH2-domain. The EVH1- and proline-rich domains act as protein interaction platforms and mediate binding to lamellipodin (Krause et al., 2004) and PREL-1 (Jenzora et al., 2005), Robo (Yu et al., 2002) and zyxin (Moody et al., 2009; Niebuhr et al., 1997), as well as SH3- and WW-domain-containing proteins. The EVH2-domain is able to interact both with monomeric and filamentous actin and additionally harbors a tetramerization domain. In contrast to formin-mediated actin filament elongation, VASP does not depend on profilin-bound actin in *in vitro* experiments (Breitsprecher et al., 2008). In *Dictyostelium discoideum*, the intimate connection of VASP and the formin dDia2 during filopodia formation was

demonstrated in knockout experiments, which showed that lack of either VASP or dDia2 abolished filopodia formation (Schirenbeck et al., 2005).

In vitro, VASP was shown to bundle actin filaments, which was suggested to be crucial for filopodia formation (Schirenbeck et al., 2006), and upon surface-immobilization VASP is able to capture growing actin barbed ends (Pasic, Kotova, and Schafer, 2008). The impact of VASP on heterodimeric capping protein activity is still controversial. Whereas some studies reported VASP to directly antagonize filament capping by capping protein and thereby promoting filament elongation (Barzik et al., 2005; Bear et al., 2002), others did not find a competition of VASP and capping protein for barbed ends, and showed that binding of VASP does not prevent actin filaments from disassembly (Samarin et al., 2003; Schirenbeck et al., 2006).

One important biochemical activity of VASP is its ability to processively elongate actin filaments, which was assayed using TIRF microscopy of single actin filaments (Breitsprecher et al., 2008). When VASP was clustered on polystyrene beads, it promoted actin filament growth by delivering actin monomers for filament elongation. Both the actin monomer- and F-actin-binding domain contributed to this process but the tetramerization domain was shown to be dispensable. A recent study demonstrated that although VASP can bind both to sides and barbed ends of actin filaments, actin monomers inhibit side-binding and promote association with the barbed ends (Hansen and Mullins, 2010).

1.6.2 ADF/Cofilin

All eukaryotes express members of the actin depolymerizing factor (ADF)/cofilin family. ADF and cofilin-1 are present in non-muscle tissue, whereas cofilin-2 is the major isoform of muscle cells. On cellular level, either protein seems to be able to rescue the loss of one ADF/cofilin member in RNAi experiments (Hotulainen et al., 2005), but the knockout of cofilin-1 in mice leads to embryonic lethality demonstrating the importance of the individual ADF/cofilin isoforms in the context of organism development (Gurniak, Perlas, and Witke, 2005). Depletion of cofilin in fibroblast cells reduced migration speed, decreased lamellipodia width and FRAP experiments using cofilin knockdown cells demonstrated that actin turnover in stress fibers as well as in lamellipodia was reduced (Hotulainen et al., 2005). The turnover dynamics of cofilin itself in the lamellipodium strongly differed from actin and Arp2/3, as cofilin recovers throughout the whole lamellipodium (Lai et al., 2008) contradicting earlier findings implicating cofilin to actively promote Arp2/3-dependent actin nucleation (Ghosh et al., 2004).

Cofilin-1 is a key protein in the regulation of actin dynamics in cell migration (Nagata-Ohashi et al., 2004; Sidani et al., 2007) and is one of the crucial components for

reconstituted actin based motility (Le Clainche and Carlier, 2001; Loisel et al., 1999). Cofilin1 is implicated in the depolymerization of actin filaments in order to provide the pool of monomeric actin for actin polymerization at steady state, but was also proposed to increase the number of free barbed ends for actin polymerization by filament severing (Bamburg, Harris, and Weeds, 1980; Ichetovkin, Grant, and Condeelis, 2002; Maciver, Zot, and Pollard, 1991). Which of the two activities predominates might depend on the cofilin/actin ratio as well as the concentration of other actin binding proteins such as tropomyosin (Bryce et al., 2003), cortactin (Oser et al., 2009) or coronins (Gandhi et al., 2009). *In vitro* experiments have demonstrated that severing occurs upon low cofilin/actin concentration and higher cofilin/actin ratios induce cofilin-mediated actin nucleation (Andrianantoandro and Pollard, 2006). The depolymerizing activity of cofilin is caused by its high affinity for ADP-loaded actin monomers. Upon binding of cofilin, ADP-actin dissociates from actin filaments. Cofilin is regulated by its pH sensitivity and PIP_2 binding (Bernstein and Bamburg, 2010) as well as by phosphorylation on Ser3, which inhibits its binding to G- and F-actin (Arber et al., 1998).

1.6.3 Capping protein

Another regulator of the actin cytoskeleton, capping protein, binds to barbed ends of actin filaments, which serves as a “cap” and inhibits further elongation but also prevents depolymerization of the filament. Capping protein is an α/β heterodimer that is very stable as compared to the individual subunits (Cooper and Sept, 2008). Although the two subunits lack any sequence similarities, they form strikingly similar secondary structures and as heterodimer they adopt a mushroom-like shape (Yamashita, Maeda, and Maeda, 2003). Together with ADF/cofilin, capping protein is required for the reconstitution of actin-based motility (Loisel et al., 1999). Capping protein plays an important role in Arp2/3-dependent structures, as e.g. lamellipodia formation is abolished upon capping protein knockdown (Mejillano et al., 2004). Although capping protein terminates filament elongation by capping growing barbed ends, it was proposed to promote actin assembly and to accelerate actin-based motility. The actin funneling hypothesis for capping protein function suggests that capping protein binds most of the growing barbed ends, thereby increasing the actin monomer concentration at steady state. This leads to higher polymerization rates of the small number of uncapped filaments, which in turn allows faster migration (Carlier and Pantaloni, 1997). More recently, Akin and Mullins coined the so-called “monomer gating” model (Akin and Mullins, 2008), in which they proposed that growing barbed ends and WH2-domains of NPFs compete for actin monomers in actin filament arrays. If capping protein is missing, all barbed ends are able to polymerize. This leads to a decrease in

actin nucleation by the Arp2/3 complex due to the reduction of available actin monomers, which results in the loss of Arp2/3-dependent actin networks such as the lamellipodium. By capping protein binding to barbed ends, the concentration of actin monomers available for nucleation is increased promoting Arp2/3-dependent actin assembly. To find out which of these hypotheses proves correct or whether capping protein mode of action differs from both models, further research is required.

1.6.4 Profilin

Profilin, a highly abundant and small protein is able to bind and sequester actin monomers in a 1:1 complex. After initial description as an inhibitor of actin polymerization (Carlson et al., 1976), it was identified to catalyze the exchange of ADP for ATP in G-actin (Mockrin and Korn, 1980), thereby continuously refilling the pool of ATP-actin ready for polymerization. Profilin binds ATP-actin at its barbed face, which prevents the incorporation of actin at pointed ends but allows barbed end assembly (Schutt et al., 1993). Upon addition of the actin monomer to the barbed end, profilin is released and ready for a new round of nucleotide exchange in actin molecules (Pollard and Cooper, 1984). Profilin is able to simultaneously bind actin and proline-rich regions of different actin regulators such as Ena/VASP, drebrin and formins as well as lipids like PIP_2 (Ahern-Djamali et al., 1999; Lassing and Lindberg, 1988; Mammoto et al., 1998; Watanabe et al., 1997). Formin-mediated actin filament elongation depends on profilin-bound actin, which is bound first by the FH1-domain and then transferred to the FH2-domain for incorporation into an actin filament. However, high concentrations of profilin inhibit elongation by formins, as free and actin-bound profilin competes for the FH1-domain, which decreases incorporation of actin monomers (Kovar et al., 2006; Vavylonis et al., 2006). *In vivo* profilin was found to be essential in early embryogenesis (Witke et al., 2001) as well as for late cytokinesis (Bottcher et al., 2009). In the brain, knockdown of profilin2a, which is neuron-specific, reduced the dendrite complexity and spine numbers of hippocampal neurons. Additionally, profilins were found to act in regulating actin dynamics downstream of the pan-neutrophin receptor (Michaelsen et al., 2010).

1.6.5 Fascin

The 55 kDa, globular protein fascin arranges actin filaments into parallel bundles with a distance of 8 nm between filaments. In vertebrates, three forms of fascin are expressed. Fascin-1 is present in mesenchymal tissues and the nervous system, fascin-2 is restricted to retinal photoreceptor cells and fascin-3 is testis-specific (De Arcangelis, Georges-Labouesse, and Adams, 2004; Tubb et al., 2002; Wada et al., 2001). In order to bundle actin filaments, fascin contains two actin binding sites.

Phosphorylation of the N-terminal actin binding domain on Ser39 by protein kinase C (PKC) inhibits the bundling activity, since it abolishes its actin binding capacity (Yamakita et al., 1996). Fascin localizes to filopodia, dendrites, cell-cell contacts and microspikes in the lamellipodium and stabilizes actin bundles in these structures. Depletion of fascin in B16-F1 cells reduced the number of filopodia, and the remaining filopodia showed an abnormal morphology, which suggested that fascin is required for intact filopodia maintenance (Vignjevic et al., 2006). In addition, knockdown of fascin suggested a role in the regulation of focal contacts in spite of its absence in these structures (Hashimoto, Parsons, and Adams, 2007). Nevertheless, fascin localizes to two other adhesive structures, podosomes and invadopodia (Li et al., 2010; Quintavalle et al., 2010). In many different cancer types, fascin is highly upregulated and correlates with aggressive tumors, which might be due to a role in promoting motility (Hashimoto, Skacel, and Adams, 2005).

1.6.6 α-actinin

Another actin cross-linker is the 100 kDa protein α-actinin, which belongs to the highly conserved spectrin superfamily of actin-binding proteins (Blanchard, Ohanian, and Critchley, 1989). In total, four isoforms of α-actinin are expressed in mammalian cells. The muscle isoforms 2 and 3 are present in the Z-disc, where α-actinin anchors actin filaments from neighboring sarcomeres at the Z-disc and thereby stabilizes the contractile apparatus (Luther, 2009). Non-muscle forms 1 and 4 localize to focal contacts, periodically label stress fibers alternating with myosins and are found in circular dorsal ruffles (Araki et al., 2000; Edlund, Lotano, and Otey, 2001). Beside its actin-bundling activity, α-actinin is an important link between the cytoskeleton and transmembrane proteins e.g. in focal adhesions, but it also works as a scaffold for cytoskeletal signaling pathways (Otey and Carpen, 2004).

In contrast to fascin, α-actinin molecules possess only one actin-binding domain, thus they have to dimerize in order to bundle filaments. The dimerization domain in the middle of the protein consists of four spectrin repeats, which form a rod-like structure and allow anti-parallel assembly of two α-actinin molecules (Virel and Backman, 2007). The spectrin repeats also serve as membrane targeting domains due to their ability to bind phospholipids and the cytoplasmic domains of transmembrane receptors, such as $mGlu_{5b}$ receptor (Cabello et al., 2007) or NMDA receptor (Bouhamdan et al., 2006) . At the N-terminus α-actinin harbors the actin-binding domain (ABD), a tandem pair of calponin homology (CH) domains. Although both CH domains are in principle able to associate with actin, only the CH1 domain was able to bind actin on its own in *in vitro* experiments, and the highest actin binding activity is achieved with both CH domains

(Gimona et al., 2002). The calmodulin-like domain (CaM) at the C-terminus serves as calcium sensor and calcium-loaded α-actinin is inhibited in its interaction with actin (Witke et al., 1993). α-actinin function is also regulated by processing with proteases (Christerson, Vanderbilt, and Cobb, 1999; Cuevas et al., 2003) and by tyrosine phosphorylation (Egerton et al., 1996; Izaguirre et al., 2001).

Especially α-actinin 4 has additionally been reported to be involved in cell migration, for instance, of cells participating in the immune response (Evans et al., 1999) as well as in cancer cell progression and metastasis (Kikuchi et al., 2008; Yamamoto et al., 2009), and in the reorganization of dynamic actin structures such as dorsal ruffles (Lanzetti et al., 2004).

1.7 Manipulation of the actin cytoskeleton by pathogenic bacteria

1.7.1 *Listeria monocytogenes*

L. monocytogenes is a Gram-positive and facultative intracellular bacterium, which causes a severe disease through contaminated food and leads to gastroenteritis, meningitis, septicemia and miscarriage. *Listeria* is able to cross the intestinal, blood-brain and fetoplacental barrier and also spreads from cell to cell in an actin-dependent process. For the latter, the bacterial NPF ActA is expressed, which induces the formation of actin filament tails (Domann et al., 1992; Kocks et al., 1992). The research on *Listeria* also provided insight into actin nucleation in mammals, as the human Arp2/3 complex was first characterized as actin nucleator by employment of *Listeria* (Welch, Iwamatsu, and Mitchison, 1997; Welch et al., 1998). The polymerization of actin filaments provides the force to propel the pathogen through the cytoplasm and to protrude the membrane of neighboring cells during cell-cell spreading. *Listeria* can reach intracellular velocities of 1.46 µm/s (Dabiri et al., 1990).

In order to enter host cells, *Listeria* expresses two virulence factors, Internalin A and B, which mediate close proximity of the host plasma membrane and the bacterium, referred to as “zipper mechanism”. In contrast to the “trigger mechanism” employed by other pathogens such as *Salmonella* or *Shigella*, which is characterized by the injection of bacterial factors into the host cells to induce their uptake, InlA and B are surface ligands and stay attached to the bacterium during invasion (Pizarro-Cerdá and Cossart, 2006). InlA binds to the transmembrane glycoprotein E-cadherin required for cell-cell adhesion, which is restricted to epithelial cells (Mengaud et al., 1996). Upon binding of InlA and E-cadherin, α- and β-catenin and as secondary component the Rho-GAP ARHGAP10 are recruited to the bacterial entry site. This results in the enrichment of vezatin and the unconventional myosin VIIA, and both drive the internalization of the

pathogen (Sousa et al., 2005; Sousa et al., 2004). Furthermore, the non-receptor tyrosine kinase Src is activated through the E-cadherin pathway, which in turn recruits cortactin and the clathrin machinery thought to facilitate the invasion process (Sousa et al., 2007).

In contrast to InlA, InlB is able to bind three different host receptors: gC1qR, glycosaminoglycans, and the hepatocyte growth factor (HGF) receptor c-Met (Braun, Ghebrehiwet, and Cossart, 2000; Lang Hrtska et al., 2007; Shen et al., 2000). c-Met belongs to the group of tyrosine kinase receptors and forms heterodimers after extracellular ligand-receptor binding, which induces the autophosphorylation of the intracellular domains of the receptor (Bardelli, Ponzetto, and Comoglio, 1994). Although no sequence similarity between HGF and InlB exist, both proteins are able to activate the c-Met signaling cascade. Co-crystallization of InlB and c-Met revealed that the binding sites of HGF and InlB do not overlap, which is consistent with the lack of a competitive binding of HGF and InlB for c-Met, and could explain the different cellular responses of the two ligands (Niemann et al., 2007; Shen et al., 2000). After activation of c-Met with InlB, several adaptor proteins accumulate at the invasion site including Gab1, Cbl and Shc, which recruit the PI3 kinase known to be responsible for the activation of Rac and Cdc42 (Bosse et al., 2007; Ireton et al., 1996). Active Rho-GTPases are crucial for the invasion process, as they induce actin polymerization through WAVE and Arp2/3 complex required for the internalization of *Listeria*, but also cofilin and LIM kinase contribute to the actin rearrangements downstream of Rac (Bierne et al., 2001). InlB-mediated invasion experiments in HeLa cells indicated that *Listeria* also uses clathrin-mediated endocytosis for invasion, although clathrin coated pits formed e.g. in the course of receptor internalization normally endocytose a much smaller volume than would be needed for the engulfment of a bacterium (Pizarro-Cerdá, Bonazzi, and Cossart, 2010).

1.7.2 *Shigella flexneri*

Shigella flexneri, a Gram-negative bacterium, causes acute gastroenteritis in humans and like listeriosis is a foodborne illness. *Shigella* utilizes a type-III-secretion system to invade epithelial cells, which delivers effector proteins into the cytoplasm capable to interact with host components to induce the uptake of the bacterium. *Shigella* is released into the cytoplasm through lysis of the phagosomal membrane enclosing the pathogen after invading the host cell (Sansonetti et al., 1986). In the cytoplasm, actin tail formation is triggered by IcsA that localizes to the outer membrane of the bacterium and concentrates on one pole, from which actin filaments polymerize (Bernardini et al., 1989). In contrast to ActA from *Listeria*, IcsA does not activate the Arp2/3 complex itself

but instead recruits the NPF N-WASP to the bacterial surface. IscA is both essential and sufficient to induce comet tails in cell extracts and in infected cells (Goldberg and Theriot, 1995; Goldberg, Theriot, and Sansonetti, 1994). It binds to the N-WASP N-terminal autoregulatory domain via its glycine rich region (Suzuki et al., 1998) and is thought to cause the release of N-WASP autoinhibition comparable to binding of active Cdc42 (Egile et al., 1999). Activated N-WASP then initiates actin polymerization by activating the Arp2/3 complex. *Shigella* intracellular motility relies on N-WASP as Arp2/3 activator and cannot be reconstituted with other NPFs of the WASP/WAVE protein family. This was demonstrated using N-WASP-deficient cells, in which actin tail formation is abrogated, but can be rescued by expression of N-WASP constructs (Lommel et al., 2001) but not WASP (Snapper et al., 2001). A set of actin regulatory proteins localizes to actin comet tails such as VASP, profilin, vinculin, capping protein and α-actinin, which possibly contribute to actin tail formation, maintenance and depolymerization (Goldberg, 2001).

1.8 Aims of the thesis

Considering the discrepancies between results from RNAi and dominant negative approaches and those obtained in cortactin KO cells, the precise role of cortactin in Arp2/3 complex-dependent processes in general and its implication in the activation of Arp2/3 was studied in this thesis. The effect of reduced Rho-GTPase levels in cortactin KO cells on cell migration, the impact on cortactin loss-of-function in *Listeria* uptake as well as the examination of primary macrophages from cortactin and HS1/cortactin KO mice regarding podosome formation was of particular interest. Moreover, an experimental setup had to be designed, in which the ability of cortactin to activate the Arp2/3 complex could be analyzed *in vivo*. For this purpose, a novel microtubule-based actin polymerization assay was established. A microtubule binding domain fused to EGFP served as targeting module to direct actin nucleators or NPFs to the surface of microtubules. This allowed probing the capability of these proteins to, directly or indirectly, mediate actin filament nucleation *in vivo*.

2 Materials and Methods

2.1 Chemicals, media and buffers

If not stated otherwise, all chemicals were purchased from the following companies: Amersham, Bioscience, BioRad, Boehringer Mannheim, Fermentas, Fluka, GE Healthcare, Invitrogen, Life Technologies, Merck, Macherey-Nagel, Millipore, New England Biolabs, PAA, Promega, Qiagen, Riedel de Haen, Roche, Roth, Sigma-Aldrich, Serva and TaKaRa. The quality standard was p.a. (*per analysis*). All buffers were prepared in deionised water, which had been purified by a milli-Q-system (Millipore).

2.2 Cell culture reagents and plasticware

Cell culture media and additives were from Gibco, Invitrogen, PAA or Sigma unless stated otherwise. Plasticware was obtained from Corning, Falcon, Nunc and PAA.

2.3 Enzymes and reagents for molecular biology

Enzymes were from New England Biolabs, MBI Fermentas or Roche. T4-DNA Ligase and alkaline phosphatase were obtained from Roche. Pfu and GoTaq DNA polymerase were purchased from Promega. Oligonucleotides were from Biosprings or MWG-Eurofins. DNA-standards were from Eurogentec and protein markers from MBI Fermentas.

2.4 Vectors

For generation of EGFP-fusion constructs, pEGFP-C1, -C2, -C3 and -N1, -N2, -N3 vectors from Clontech were used.

2.5 Bacterial cultures

For amplification of plasmids, *Escherichia coli* strain TG2 (Stratagene) with the following genotype was used: *supE hsd*Δ5 *thi* Δ(*lac-proAB*) Δ(*srl-recA*)306::Tn*10(tet^r)* F[*tra*D36 *proAB*$^+$ *lacI*^{q} *lacZ*ΔM15].

Invasion experiments were performed with *Listeria monocytogenes*, either EGD, serotype 1/2a as wild type (WT) or ΔInlA/B-mutant.

For actin tail formation experiments, *Shigella flexneri* serotype 5 was used.

2.6 Media for bacterial culture

LB-medium (**L**uria **B**ertain broth):	bacto-tryptone	10 g/l
	bacto-yeast extract	5 g/l
	NaCl	20 mM
SOB-medium (**S**uper **O**ptimal **B**roth):	bacto-tryptone	20 g/l
	bacto-yeast extract	5 g/l
	NaCl	0.6 g/l
	KCl	0.1 g/l
SOC-medium (**S**uper **O**ptimal broth with **C**atabolite repression):	SOB-Medium	
	$MgCl_2$	10 mM
	$MgSO_4$	10 mM
	Glucose	2 mM
BHI-medium (**B**rain-**H**eart **I**nfusion):	Brain-Heart Infusion	37 g/l
TSB-medium (**T**ryptic **S**oy **B**roth)	Tryptic Soy Broth	30 g/l

2.7 Conditions for bacterial culture

Escherichia coli:	LB-medium
Listeria monocytogenes:	BHI-medium
Shigella flexneri:	TSB-medium

Bacteria were inoculated into the respective medium and incubated at 37 °C at 180 rpm overnight.

2.8 Molecular biological standard techniques

2.8.1 Plasmids

Table 2-1: Constructs used in this thesis

plasmid	origin	source
EGFP-Rac1L61	human	Markus Ladwein, HZI, Germany
EGFP-Cdc42L61	human	Frank Lai, HZI, Germany
HS1-EGFP	human	Frank Lai, HZI, Germany
EGFP-cortactin	mouse	Steffen Backert, University College Dublin, Ireland
EGFP-cortactin (aa 1-146)	human	Frank Lai, HZI, Germany
EGFP-cortactin (aa 1-84)	mouse	this thesis
EGFP-MBD	human	this thesis
EGFP-MBD-VVCA (aa 392-501 of N-WASP)	mouse	Stefan Köstler, IMBA, Austria
mCherry-p16B	human	Jennifer Block, HZI, Germany
mCherry-actin	human	Malgorzata Sczcodrak, HZI, Germany
EGFP-MBD-fascin	human	this thesis
EGFP-MBD-ABD (aa 1-246 of α-actinin)	human	this thesis
EGFP-actin	human	Clontech, Mountain View, U. S. A.
mCherry-MBD-VVCA (aa 392-501 of N-WASP)	mouse	this thesis
EGFP-MBD-cortactin	mouse	this thesis
EGFP-MBD-cortactin (aa 1-84)	mouse	this thesis
EGFP-MBD-Drf3ΔDAD	human	this thesis
EGFP-MBD-Spir-NT	human	this thesis
EGFP-MBD-Lifeact	yeast	this thesis
EGFP-MBD-actin	human	this thesis
EGFP-MBD-VVC (aa 392-483 of N-WASP)	mouse	this thesis
EGFP-MBD-Spir-CD (aa 334-388)	human	this thesis
EGFP-MBD-VV (aa 392-460 of N-WASP)	mouse	this thesis
EGFP-N-WASP	mouse	Silvia Lommel, HZI, Germany
EGFP-N-WASPΔA (aa 1-483)	mouse	this thesis
EGFP-capping protein β2	human	Dorothy Schafer, Charlottesville, USA
mCherry-MBD-Spir-NT	human	this thesis
EGFP-MBD-capping protein β2	human	this thesis
mCherry-capping protein α1	human	J. Faix, MHH, Germany

2.8.2 Oligonucleotide primers

Table 2-2: List of primers for amplifying used in this thesis.

no.	name	sequence 5´to 3´	purpose
1	Fwd oligo start EcoR	gagagaattcatggaccattatgattctc	Cloning of ABD (α-actinin aa 1-246)
2	Rev oligo CH2 SalI	gagagtcgactgctgtctccgccttctgg	Cloning of ABD (α-actinin aa 1-246)
3	Cttn 1-84 EcoRI for	gagagaattcatgtggaaagcctctgc	Cloning of cortactin (aa 1-84)
4	Cttn 1-84 SalI rev	gagagtcgacatagccgtgggaagcctt	Cloning of cortactin (aa 1-84)
5	huSpir1WH2CDf	gagagaattcaaaaagagtgctcatgaaa	Cloning of Spir-CD (aa 334-388)
6	huSpir1WH2CDr	gagagtcgactggtgatacaggccgcag	Cloning of Spir-CD (aa 334-388)
7	VV EcoRI for	gagagaattccatcaagttccagctcct	Cloning of N-WASP VV (aa 392-460)
8	VV SalI rev	gagagtcgacagtgggtgcgggtgttgg	Cloning of N-WASP VV (aa 392-460)
9	N-WASPΔAf	gagagaattcatgagctcgggccagcag	Cloning of N-WASPΔA (aa 1-483)
10	N-WASPΔAr	gagagtcgacttattcatctgaggaatga	Cloning of N-WASPΔA (aa 1-483)

Oligonucleotides used in this thesis were designed with Vector NTI Suite 8 and 10 (Invitrogen) and were synthesized by MWG Eurofins.

2.8.3 Generation of DNA constructs

EGFP-fusion constructs were generated by polymerase chain reaction (PCR) introducing the respective restriction sites at the C- and N-termini of the respective fragment. *Pfu* DNA polymerase was used according to the manufacturer´s protocol. Annealing temperature and extension time were adapted according to the primers used and the size of the expected product, respectively. For subcloning DNA fragments from existing plasmids into different vectors, cutting sites of the multiple cloning sites were used. Both donor and acceptor vector were cut with the same enzymes or enzymes producing compatible ends and subsequently ligated using T4-DNA-ligase. All constructs were verified by restriction digests, sequencing and expression tests.

2.8.4 DNA sequencing

Plasmid DNA samples were sent to MWG Operon (Martinsried, Germany) for sequencing. Sequence files were downloaded from the website and aligned using

Multalin interface page (http://multalin.toulouse.inra.fr/multalin/multalin.html) or Vector NTI Suite 8 and 10 to verify correct DNA sequence.

2.8.5 Restriction digest and dephosphorylation

5 µg of plasmid DNA were digested in a total volume of 15-30 µl in the appropriate restriction buffer containing 10 U restriction enzyme for 1-2 h at 37 °C or 55 °C, dependent on the enzyme's optimal operation temperature. To prevent religation of cut DNA vectors in cases where only one restriction enzyme was employed, vectors were dephosphorylated with 1 U alkaline phosphatase (Roche) for 5 min at 37 °C. Restricted fragments were run on a preparative agarose gel to verify correct size.

2.8.6 DNA extraction from agarose gels

DNA fragments for subcloning were extracted from agarose gels using the NucleoSpin Extract II Kit from Macherey&Nagel (Macherey-Nagel, Düren, Germany) according to manufacturer's instructions.

2.8.7 Ligation

T4-DNA ligase (Roche) was used to covalently link DNA fragments with required vectors as recommended by the manufacturer. 10 to 100 ng of the vector was mixed with three times molar excess of the fragment and incubated overnight at 16 °C. Afterwards, the reaction was transformed into $CaCl_2$-competent TG2 *E. coli.*

2.8.8 Generation of $CaCl_2$-competent *E. coli*

To prepare competent *E. coli* that are highly efficient in taking up plasmid DNA, an overnight culture of TG2 was diluted 1:100 into SOB medium and incubated at 180 rpm at 37 °C until the optical density at 600 nm reached 0.5. The bacteria were harvested by centrifugation (5000 x g, 10 min, 4 °C). The pellet was resuspended in 1/5 of the culture volume of ice-cold 0.1 M $CaCl_2$ and incubated for 20 min on ice. After centrifugation (5000 x g, 10 min, 4 °C), bacteria were resuspended in 1/100 to 1/200 of the culture volume of ice-cold 0.1 M $CaCl_2$ and incubated for 3 h on ice. The bacteria were supplemented with glycerin to a final concentration of 10% (v/v), snap-frozen in liquid nitrogen and stored at -80 °C.

2.8.9 Transformation of *E. coli*

50 to 100 µl aliquots of competent *E. coli* were thawed on ice, mixed gently with 100 ng Plasmid-DNA or 10 to 20 µl of a ligation reaction and incubated on ice for 15 min. Bacteria were then heat-shocked at 42 °C for 1.25 min, incubated on ice for 2 min and resuspended in 250 µl of SOC-Medium. Bacteria were gently shaken at 37 °C for

30 min when a construct with ampicillin resistance was transformed, or for 1 h at 37 °C when the plasmid transformed harbored a kanamycin resistance to allow the bacteria to express the respective resistance gene. The bacterial suspension was plated on agar plates containing the appropriate antibiotic and incubated at 37 °C for 16 h.

2.8.10 Preparation of plasmids from *E. coli*

Mini, midi and maxi plasmid preparations were performed using the respective Nucleo-Bond plasmid purification kit from Macherey&Nagel.

Briefly, bacteria were inoculated into LB-medium containing the appropriate antibiotic and incubated at 37 °C and 180 rpm overnight. Bacteria were harvested by centrifugation and resuspended in buffer containing RNase A. After lysis of the bacteria and a neutralizing step, the lysate was cleared by centrifugation. Cleared lysates were subjected to columns binding the DNA, followed by a washing step. The DNA was eluted and precipitated with isopropanol or ethanol to enhance purity. The DNA pellet was re-dissolved in an appropriate volume of H_2O.

2.8.11 Quantification of DNA

The photometric absorption of DNA in solution has a maximum at a wavelength of 260 nm. To determine the concentration of nucleic acid, an aliquot of the DNA solution was diluted to OD_{260} values between 0.1 and 1.0, which corresponds to a concentration range, in which the absorption is still linear. The concentration of the DNA can be calculated by including the molar extinction coefficient of DNA ε = 50 µg/µl as follows: c DNA [µg/µl] = OD_{260} · dilution factor · ε [µg/µl].

2.9 Protein biochemistry

2.9.1 Sodium dodecyl sulfate polyacrylamide gel electrophoresis

Sodium dodecyl sulfate polyacrylamide gel electrophoresis (SDS-PAGE) was performed essentially according to Laemmli (Laemmli, 1970). SDS-PAGE gels were run in Minigel apparatures (Biometra) with 1 mm spacers.

2.9.2 Coomassie Blue staining

Proteins in SDS gels or blotted onto PVDF membranes were stained with a 0.1% Coomassie R-250 solution in 10% acetic acid and 25% isopropanol for 30 to 60 min followed by destaining of the gel or membrane in 10% acetic acid and 40% methanol.

2.9.3 Preparation of protein extracts from cultured cells

Extracts from adherent tissue culture cells were obtained by one of the following method after washing the cells with 1x PBS. For standard extracts, 4x reducing SDS-sample buffer was added directly to the cells (500 µl on a 10 cm diameter dish), then the cell lysate was removed from the dish using a cell scraper, boiled at 95 °C for 5 min and stored at -20 °C. If the determination of protein concentration in cell lysates was necessary, cells were lysed in ice cold IP-buffer (15 mM KCl, 50 mM NaCl, 8 mM Tris base, 12 mM Hepes, 5 mM $MgCl_2$, pH 7.5 containing 1% Triton X-100 and supplemented with one Roche complete Protease inhibitor pill per 10 ml) and cell debris was removed by centrifugation of the lysate for 3 min at 13000 rpm.

2.9.4 Measurement of protein concentration

Protein concentration was determined using the Precision Red Advance protein assay (Cytoskeleton) according to the manufacturer´s manual or using Bradford assay.

2.10 Immunobiological methods

2.10.1 Primary antibodies

Primary antibodies used in this study are listed in Table 2-3.

Table 2-3: Primary antibodies

antigen	name	mc/pc	application	source
GFP	101G4B2	mc	WB	B. Behrendt, HZI, Braunschweig, Germany
α-actinin4	–	pc	WB, IF	Immunoglobe, Himmelstadt, Germany
Cortactin	289H10	mc	WB, IF, IP	Christian Erck/Frank Lai, HZI, Braunschweig, Germany
Vinculin	V9131	mc	WB, IF	Sigma Aldrich, Hamburg, Germany
ArpC5	323H3	mc	IF	Christian Erck/Kerstin Schilling, HZI, Braunschweig
HS1	–	pc	WB	Cell Signaling, Danvers, U. S. A.
Shigella	–	pc	IF	Abcam, Cambridge, U. K.
α-Tubulin	3A2	mc	WB, IF	Synaptic Systems, Göttingen, Germany

2.10.2 Secondary reagents

Secondary reagents used in this study are listed in Table 2-4.

Table 2-4: Secondary reagents

name	species antibody	species antigen	conjugation	source
A4a	Goat	Mouse	Peroxidase (PO)	Dianova, Hamburg, Germany
B4c	Goat	Rabbit	Peroxidase (PO)	Dianova, Hamburg, Germany
B12c	Goat	Rabbit	Alexa Fluor™ 488	Invitrogen, Darmstadt, Germany
B13c	Goat	Rabbit	Alexa Fluor™ 594	Invitrogen, Darmstadt, Germany
B16c	Goat	Rabbit	Alexa Fluor™ 350	Invitrogen, Darmstadt, Germany
A12c	Goat	Mouse	Alexa Fluor™ 488	Invitrogen, Darmstadt, Germany
A13c	Goat	Mouse	Alexa Fluor™ 594	Invitrogen, Darmstadt, Germany
Ph12 (Phalloidin)			Alexa Fluor™ 488	Invitrogen, Darmstadt, Germany
Ph13 (Phalloidin)			Alexa Fluor™ 594	Invitrogen, Darmstadt, Germany
Ph16 (Phalloidin)			Alexa Fluor™ 350	Invitrogen, Darmstadt, Germany

2.10.3 Western blotting

Western blots were performed as follows: after separation on SDS-PAGE gels, proteins were transferred onto PVDF-membranes (Immobilon P, Millipore) using a semidry blotting system (Pegasus, Phase, Germany) and a glycine methanol SDS blotting buffer [50 mM Tris, 39 mM glycine, 0.037% (w/v) SDS, 20% (v/v) methanol] at a constant current of 2 mA per cm^2 of gel area for 90 to 120 min. Transfer efficiency was monitored by staining of the membranes with Ponceau S solution (0.5% Ponceau S (Sigma), 40% methanol, 15% acetic acid). Membranes were blocked for 30 min at room temperature or at 4 °C overnight in blocking buffer (10% dry-milk in TBS-T buffer (20 mM Tris-HCl pH 7.6; 137 mM NaCl; 0.1% Tween20)). Afterwards, membranes were incubated for 1 h at room temperature or overnight at 4 °C in 1% dry-milk in TBS-T buffer containing the primary antibody typically at a concentration of 1 µg/ml. Membranes were washed three times in TBS-T buffer for 5 min and then incubated for 1 h at room temperature with 1% dry-milk in TBS-T buffer containing the secondary antibody. Membranes were again washed three times with TBS-T buffer and additionally with TBS-T containing 0.1% Triton X-100 and incubated for up to 4 min with the chemiluminescence substrate Lumilight (Roche) and exposed to Hyperfilm ECL (Amersham Biosciences).

2.11 Tissue culture, transfections and treatments

2.11.1 Media and solvents

Growth medium 1:	DMEM high (Dulbecco´s Modified Eagle Medium, Gibco), 4.5 g/l glucose	
	FCS PAA Clone (PAA)	10%
	L-glutamine (Gibco)	2 mM
Growth medium 2:	DMEM low (Dulbecco´s Modified Eagle Medium, Gibco), 1 g/l glucose	
	FCS Lot: 047K3395 (Sigma)	10%
	L-glutamine (Gibco)	2 mM
Growth medium 3:	RPMI 1640 (Roswell Park Memorial Institute, Gibco)	
	FCS Lot: 047K3395 (Sigma)	10%
	L-glutamine (Gibco)	2 mM
Microscopy Medium:	F12-HAM Medium Hepes Modification (Sigma)	
	FCS PAA Clone (PAA)	10%
	L-glutamine (Gibco)	2 mM
	Penicillium (Gibco)	25000 U
	Streptomycin (Gibco)	25000 µg

2.11.2 Cell lines

All cell lines were cultured at 37 °C and 7.5% (v/v) CO_2.

Table 2-5: Cell lines employed in this work.

name	species	type	growth medium	source
B16-F1	*Mus musculus*	Melanoma, skin	1	ATCC (CRL-6323)
$Cttn^{fl/fl}$	*Mus musculus*	ES cell-derived $Cortactin^{fl/fl}$ fibroblastoid cells harboring puromycin and neomycin resistance	2	Frank Lai, HZI (Lai et al., 2009)
$Cttn^{del/del}$	*Mus musculus*	Cortactin KO fibroblastoid cells obtained by Cre recombinase-mediated removal of cortactin gene *in vitro*	2	Frank Lai, HZI (Lai et al., 2009)
$Cttn^{fl/fl\ Flpe}$	*Mus musculus*	$Cortactin^{fl/fl\ Flpe}$ fibroblasts isolated from mice after excision of neomycin cassette	2	Frank Lai, HZI
$Cttn^{del/del\ Flpe}$	*Mus musculus*	Cortactin KO fibroblasts derived from $Cttn^{fl/fl\ Flpe}$ cells upon cortactin gene deletion *in vitro*	2	Frank Lai, HZI
Raw 264.7	*Mus musculus*	macrophage cell line	3	ATCC (TIB-71)
Klon 1	*Mus musculus*	$N\text{-}WASP^{fl/fl}$ fibroblast	2	(Lommel et al., 2001)
Klon 1H51	*Mus musculus*	N-WASP KO fibroblast	2	(Lommel et al., 2001)

$Cttn^{fl/fl}$ and $Cttn^{del/del}$ cells were as described in Lai et al. (Lai et al., 2009). $Cttn^{fl/fl\ Flpe}$ and $Cttn^{del/del\ Flpe}$ cells were also kindly provided by Frank Lai. Briefly, primary fibroblasts from mice carrying the cortactin floxed allele (see Figure 3-1) were prepared from embryos in E14.5 and immortalized by retroviral transduction of SV40 LargeT antigen. For deletion of exon 7, cells were treated with Adenovirus Cre.

All experiments in chapter 23.1 were performed with the $Cttn^{fl/fl}$ and $Cttn^{del/del}$ cells, which were published in Lai et al., 2009, except for the repetition of *Listeria* invasion, in which $Cttn^{fl/fl\ Flpe}$ and $Cttn^{del/del\ Flpe}$ were used.

2.11.3 Cell culture prior to microscopic analysis

For microscopic analysis, either untransfected cells or cells transiently transfected with respective constructs were seeded subconfluently on glass coverslips coated with 25 µg/ml laminin (Roche) or 25 µg/ml fibronectin (Roche). Cells seeded on laminin were allowed to spread for at least 3 h, cells seeded on Fibronectin were allowed to spread overnight.

Coverslips were pretreated by incubation in a solution of 60% ethanol and 40% concentrated HCl for 1 to 3 h under agitation followed by extensive washing with deionized water. Coverslips were air-dried on Whatman filter paper overnight and autoclaved.

2.11.4 Transfections

Transfections were carried out using SuperFect (Qiagen, Germany, for B16-F1), FuGene HD (Roche, Germany, for $Cttn^{fl/fl}$ and KO cells) or FuGene 6 (Roche, Germany, for N-$WASP^{fl/fl}$ and KO cells) according to manufacturer´s protocols.

Briefly, 50 µl Optimem were mixed with 3 µl FuGene (6 or HD), incubated for 5 min before 1 µg DNA was added and the mixture was again incubated for 20 min at room temperature. Transfection mixture was added directly to the growth medium of cells in a 3 cm diameter dish and incubated for 16 to 40 h.

For B16-F1 transfections, 1 µg DNA was mixed with 50 µl Optimem and 6 µl SuperFect, incubated for 15 to 30 min at room temperature and added to cells in a 3 cm diameter dish. Cells were cultivated with the transfection medium for 16 h. For transfections of cells in larger or smaller dishes, the volumes of each component were scaled up or down accordingly.

2.11.5 Gentamicin protection assay

Invasiveness assays with *L. monocytogenes* EGD WT and the isogenic negative control strain *L. monocytogenes* ΔInlA/B were performed in 24-well tissue culture plates. Before infection, bacteria were washed once in PBS and diluted in tissue culture medium to a concentration of 10^9 colony forming units per ml. Growth medium of the cells was exchanged for the bacterial suspensions (1 ml per well) and bacteria were centrifuged onto the cells at 1900 rpm for 4 min. After 1 h incubation at 37 °C and 7.5% CO_2, cells were washed twice with PBS, and medium containing gentamicin (50 µg/ml) was added. The antibiotic gentamicin hardly crosses the plasma membrane of mammalian cells, leading to selective killing of extracellular bacteria but protection of bacteria inside the host cells. After 1.5 h incubation at 37 °C and 7.5% CO_2, cells were washed three times with pre-warmed PBS and lysed by adding 500 µl of 0.2% Triton X-100. The number of viable bacteria released from the cells was assessed by plating the cell lysates on BHI agar plates in triplicates and counting bacterial colonies after incubation of the plates at 37 °C overnight. Data from three independent experiments were normalized to an invasion of 1 (100%) in respective control populations as indicated.

2.11.6 Cells treatments

For stimulation of cells with HGF or InlB, cells were seeded onto glass coverslips coated with fibronectin and starved overnight for 16 to 18 h in minimal medium (DMEM without supplements). Cells were stimulated for 7.5 min with DMEM containing 20 ng/µl HGF (human recombinant, Sigma, Germany) or 55 ng/µl InlB (purified, full length InlB (Bosse et al., 2007) kindly provided by Dr. Hartmut Niemann, University of Bielefeld, Germany), respectively.

2.12 Immunofluorescence microscopy and live-cell imaging

2.12.1 Labeling of the actin cytoskeleton

Phalloidin, a component derived from the mushroom *Amanita phalloides*, specifically binds to actin filaments and stabilizes them against depolymerization (Cooper, 1987). 3 U/ml of fluorescent phalloidin derivatives coupled with Alexa Fluor™ 488, Alexa Fluor™ 594 or Alexa Fluor™ 350 (Molecular Probes) were diluted in PBS to label actin filaments in fixed and permeabilized cells.

2.12.2 Fixation procedures, stainings and analysis

Prior to stainings with antibodies or phalloidin, cells were fixed with 4% formaldehyde (PFA) in PBS for 20 min and extracted with a mixture of 0.1% Triton X-100 and 4% PFA in PBS for 1 min. Afterwards, cells were washed three times with PBS and blocked with 5% horse serum in 1% BSA for 1 h at room temperature.

For immunofluorescence stainings, primary antibodies were diluted in 1% BSA and incubated for 1 h at room temperature. After washing the coverslips extensively with PBS, the samples were incubated with secondary antibodies coupled with Alexa Fluor™ 350, Alexa Fluor™ 488 or Alexa Fluor™ 594 for 45 min at room temperature. The samples were mounted in 5 µl Mowiol 4-88 (Calbiochem) supplemented with n-propylgallate (2.5 µg/ml), dried and stored in the dark at 4 °C until analysis.

Immunofluorescence stainings were analyzed on an inverted microscope (Axiovert 100TV, Zeiss, Jena, Germany) using 63x/1.4 NA or 100x/1.4 NA plan apochromatic objective. For triple stainings, analysis was performed using 63x/1.25 NA or 100X/1.3 NA Plan-Neofluar objectives. The microscope was equipped for epifluorescence with electronic shutters (i.e. Uniblitz Electronic 35 mm shutter including driver Model VMMD-1, BFI Optilas) to allow for computer-controlled opening of the light paths, filter wheel (e.g. LUDL Electronic Products LTD, SN: 102691 and driver SN: 1029595) to enable two-color live cell imaging in combination with appropriate dichroic beam splitters and emission filters (Chroma Technology Corp., Rockingham, USA), tungsten lamp (Osram, HLX64625, FCR 12V, 100W) for phase contrast optics and mercury lamp

(HBO 100W/2, Osram) for epifluorescence and immersion oil (refraction index of 1.518, Zeiss). Images were acquired with a back-illuminated, cooled charge-coupled-device (CCD) camera (TE-CCD 800PB, CoolSnap K4 or CoolSnap HQ_2, Princeton Scientific Instruments, Princeton, USA) driven by IPLab software (Scanalytics Inc., Fairfax, USA) or MetaMorph software (Molecular Devices, Sunnydale, USA). Data and images were processed using ImageJ and Adobe Photoshop 7.0 or CS4 software.

2.12.3 Electron microscopy

Electron microscopy images were performed by Vic Small, Marlene Vinzenz, Maria Nemethova and Sonja Jakob at the Austrian Academy of Science, Vienna, Austria. For negative stain electron microscopy, cells were grown on formvar films and processed essentially as described (Auinger and Small, 2008).

2.12.4 Live cell imaging and data analysis

Cells were observed in an open chamber (Warner Instruments, Hamden, USA) with a heater controller (model TC-324B, SN:1176) at 37 °C. Microscopy medium with complete supplements of the regular growth medium (see 2.1.19) was used for imaging of B16-F1 cells.

Wound healing assays were performed by using an AxioCam MRm camera (Carl Zeiss Jena) on an Axiovert 200 automatic microscope equipped with closed heating and CO_2 perfusion devices. Cells were transfected with Fugene HD, sorted after 24 h with a FACS sorter to enrich EGFP-positive cells and seeded in a 12-well cell culture dish. After 48 h, a wound was scratched in the confluent layer of cells using a pipette tip and wound closure recorded for 24 h with a time interval of 15 min between frames. Wound closure rates were calculated by dividing the cell-free area at the beginning of the movie by the time the cells needed to cover the entire wound. Wound area was determined using ImageJ (http://rsb.info.nih.gov/ij/), and statistics were carried out using Sigma Plot 10.

2.12.5 Fluorescence recovery after photobleaching (FRAP) microscopy

Cells were maintained on the microscope as described in 2.1.28. FRAP experiments were performed using a double-scanheaded confocal microscope (Fluoview1000, Olympus) equipped with a 100x/1.45NA PlanApo TIRF objective (Olympus Inc.), allowing simultaneous imaging of EGFP- and mCherry-tagged probes (with 30 mW 488 nm multiline argon and 20 mW 561 nm solid-state lasers, respectively) and photobleaching using a 20 mW 405 nm diode laser. Circular regions were bleached in the tornado mode. Image analysis was carried out on a PC using FV10-ASW 1.6 viewer (Olympus Inc., Olympus, Hamburg, Germany) and Metamorph (Molecular

Devices Corp.). FRAP data were analyzed using SigmaPlot 10.0 (Scientific Solutions SA, Pully-Lausanne, Switzerland) and Microsoft Excel 2000.

2.12.6 FRAP data analysis

FRAP data were analyzed essentially as described (Rabut and Ellenberg, 2005). Best linear fits were calculated using SigmaPlot 10.0 (Scientific Solutions SA, Pully-Lausanne, Switzerland). Background fluorescence intensities taken from a region outside the cell were subtracted from each individual region and frame. Acquisition photobleaching was subtracted as recommended (Rabut and Ellenberg, 2005) and determined using a single microtubule largely unaffected by experimental bleaching. The average fluorescence intensity of the microtubule in the last frame before photobleaching was defined as maximum and normalized to 1. Exponential curves in Figure 3-25 corresponded to best fits of means. Fitted data followed equation $y(t) = a\cdot(1-\exp(-b\cdot t)) + c\cdot(1-\exp(-d\cdot t))$, with $a = 0.5628$, $b = 0.1583$, $c = 0.3708$ and $d = 0.0253$ for MBD-VVCA and $a = 0.2743$, $b = 0.3601$, $c = 0.6246$ and $d = 0.0164$ for actin. Half times of recovery ($t_{1/2}$) were calculated by solving the corresponding equations at 50% of the maximal recovery value derived from each fitted curve.

2.13 Transgenic mouse strains and genotyping of mice

2.13.1 Transgenic mouse strains

HS1-deficient mice (Taniuchi et al., 1995) were provided by Takeshi Watanabe (Kyushu University, Japan) and Daisuke Kitamura (University of Tokyo, Japan). Transgenic cortactin mice used in this thesis were generated by Frank Lai (HZI) and maintained under specific-pathogen-free (SPF) conditions in an animal facility. Cortactin-deficient mice were produced using a conditional knockout approach. Two different mouse strains were available. In the first approach, mice carrying the targeted allele were mated with Cre-deletor mice resulting in mice with deleted Neo alleles, whereas in the second approach first the neomycin cassette was deleted using Flpe recombinase resulting in the floxed allele and subsequent crossings with mice carrying the Cre recombinase gene gave the deleted allele Figure 3-1. For Cortactin/HS1 double mutant mice HS1 null mice were crossed with cortactin KO mice carrying the deleted Neo allele to obtain animals heterozygous for both genes.

2.13.2 DNA preparation of tail biopsies

To determine the genotypes of transgenic mice, DNA from tail biopsies was extracted by incubating the tails in 300 µl DNA lysis buffer (100 mM Tris-Base, 5 mM EDTA pH 8.0, 0.2% SDS, 200 mM NaCl, pH 8.5, 500 µg/ml Proteinase K) for 2 h at 55 °C

under agitation. Un-dissolved particles were pelleted by centrifugation at 13000 rpm for 1 min and removed from the supernatant. DNA was precipitated by addition of 700 µl pure ethanol, pelleted for 10 min at 4000 rpm and washed with 70% ethanol. The DNA was dried for 10 min at room temperature, dissolved in 100 to 200 µl sterile H_20 and stored at 4 °C.

2.13.3 Genotyping PCR

Genomic DNA from mouse biopsies was used to determine the genotype of transgenic mice in genotyping PCRs. See table Table 2-6 for the primer sets employed in this thesis. The genotyping PCR was performed in 10 µl standard reaction buffer (1x GoTaq buffer green, 2 mM $MgCl_2$, 0.2 mM dNTPs, 0.4 mM forward primer(s), 0.4 mM reverse primer, 0.25 U GoTaq polymerase) supplemented with 1.5 µl DNA.

The following PCR program was used:

95 °C for 2 min
95 °C for 20 s
58 °C for 30 s
72 °C for 30 to 45 s
} x 34 cycles
72 °C for 3 min

PCR products were separated in 2% agarose gels.

Table 2-6: Primer pairs used for cortactin and HS1 genotyping

genotype	primer names	primer sequences
Cttn WT allele (150 bp) targeted allele (250 bp)	Cttn-allele-loxPL fw Cttn-allele-loxPR rv	5'-agggtctgaccatcatgtcc-3' 5'-gacttattccaggcacagca-3'
Cttn Exon 7 allele (650 bp)	Cttn exon7 del fw Cttn exon7 del rv	5'-cctggaataagtcagccaagc-3' 5'-atggccctagaggtcaaagc-3'
Cttn WT allele (150 bp) floxed allele (370 bp)	Frt-det Fw Frt-det Rv	5'-ctctgctctgtgctttgacc-3' 5'-gtgctgttcatccacaatgc-3'
Cttn WT allele (200 bp) deleted Neo allele (400 bp)	Cttn-allele-loxPL fw Cttn-allele-loxPR rv PPNT-seq Rv	5'-agggtctgaccatcatgtcc-3' 5'-gacttattccaggcacagca-3' 5'-ggtggatgtggaatgtgtg-3'
Cttn WT allele (900 bp) deleted allele (400 bp)	Cttn-allele-loxPL fw Frt-det Rv	5'-agggtctgaccatcatgtcc-3' 5'-gtgctgttcatccacaatgc-3'
HS1 WT allele (350 bp) KO allele (250 bp)	HS1-KO-end-3' LacZ 3' HS1 Ex10 seq Fw	5'- ggcatggatggctgctggac-3' 5'-catgcttggaacaacgagcgc-3' 5'-ccttcgtcacatggaatatg-3'

2.14 Isolation and culture of peritoneal macrophages

Peritoneal macrophages were isolated from cortactin control and KO mice as well as Cortactin/HS1 control and KO mice. After gasing the mice with CO_2 and sterilizing them in 70% ethanol, the fur on the abdomen was removed and 5 ml ice cold PBS was carefully injected into the abdominal cavity. The abdomen was gently massaged to detach macrophages inside the peritoneum. PBS containing macrophages was harvested from the peritoneum using a Pasteur pipette and collected in a 15 ml tube. The cells were pelleted for 4 min at 1000 rpm, resuspended in Growth medium 3 (see 2.1.19) and seeded in 4-well plates. After 24 h, the cells were gently washed 5 times with PBS to remove non-adherent cells. Prior to immunofluorescence stainings, macrophages were washed with PBS and detached from the cell culture dish with Alfazyme (PAA) for 45 min at 37 °C. Macrophages were seeded onto coverslips coated with fibronectin (25 µg/ml), allowed to spread for 16 to 24 h and subjected to immunofluorescence procedure as described above (2.1.26).

3 Results

3.1 Characterization of cortactin knockout in fibroblast cells and primary macrophages

Cortactin is a multidomain protein implicated in a variety of different cellular functions. It harbors an N-terminal acidic domain that was shown to bind the Arp2/3 complex, six and a half F-actin binding repeats, a helix motif with so far unknown function, a proline-rich domain with various phosphorylation sites and a SH3 domain at the very C-terminus. In pyrene assays cortactin was shown to weakly activate the Arp2/3 complex (Weed et al., 2000), and RNAi studies implicated cortactin to play crucial roles in cell migration, endocytosis and invasion of pathogens (see 1.1.6.3). To define the precise function of cortactin in the aforementioned processes, a conditional knock out (KO) in mice as well as cortactin knockout mouse embryonic fibroblasts (MEF cells) were generated and provided by Frank Lai.

Characterization of cortactin-deficient MEF cells revealed that there was no alteration in the ability of these cells to form lamellipodia upon microinjection of constitutively active Rac1 (Lai et al., 2009). Similarly, the ultrastructure of lamellipodia was normal, as shown by electron microscopy and the retrograde flow of actin and Arp2/3 complex was even slightly enhanced in the absence of cortactin (Lai et al., 2009). In contradiction to results obtained using RNAi approaches, the assembly of clathrin-coated pits and the uptake of EGF-receptor was not impaired upon KO of cortactin. Instead, evidence was provided that the signaling cascade induced by PDGF was abrogated upon cortactin KO (Lai et al., 2009). Moreover, in agreement with results obtained from knockdown experiments (van Rossum, Moolenaar, and Schuuring, 2006; Zhu et al., 2010), the wound healing rate in cortactin-deficient cells was reduced to 70% of control cells (Lai et al., 2009).

In Figure 3-1, a schematic overview is given of the targeting strategy as well as the allele composition after Cre- and Flpe-mediated recombination, respectively, that led to the generation of cortactin KO cells and mice. In the first approach, Cre recombinase in cells or mice carrying the cortactin targeted allele resulted in a deleted allele that still harbored the neomycin-cassette, referred to as deleted Neo allele. In the second approach, the neomycin-cassette was deleted by Flpe recombinase giving the floxed allele and subsequently Cre-mediated excision of exon 7 generated the deleted allele.

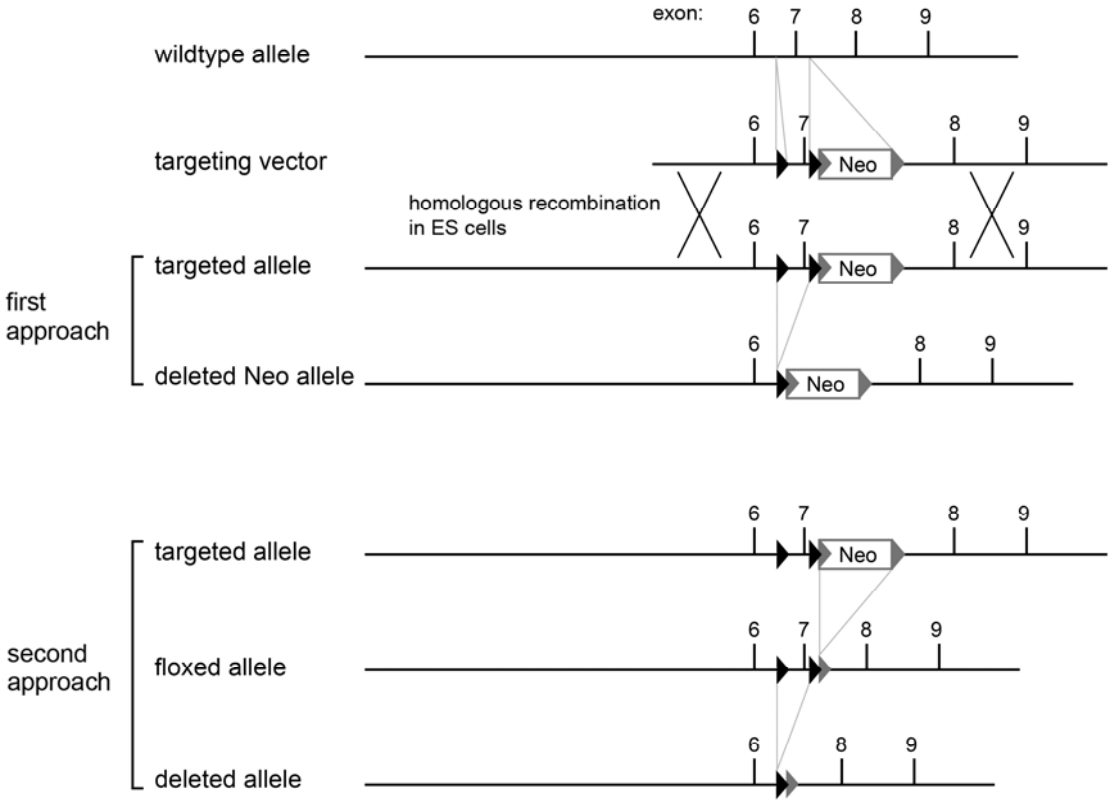

Figure 3-1: Targeting strategy and allele composition after recombination via Cre and Flpe recombinase for the generation of cortactin KO cells and mice.

Through homologous recombination of the targeting vector and the wildtype allele in ES cells, a targeted cortactin allele was generated. In the targeted allele exon 7 is flanked by loxP-sites (black arrowheads) and a neomycin-cassette (Neo) adjacent to the second loxP-site is present that contains frt-sites at the beginning and the end of the sequence. The deleted Neo allele was obtained by Cre-mediated excision of exon7, whereas Flpe recombination transformed the targeted allele into the floxed allele and subsequent Cre recombination resulted in the deleted allele.

3.1.1 Rescue of the wound healing defect in cortactin-deficient cells with constitutively active Rho-GTPases

In cortactin KO cells of the first KO approach (Figure 3-1), the levels of active Rho-GTPases were altered and wound closure was less efficient as compared to control cells (Lai et al., 2009). To investigate if there was a link between both observations, EGFP-tagged, constitutively active forms of the Rho-GTPases Rac and Cdc42 were transfected into cortactin control and deficient cells, which were subsequently subjected to wound healing assays. As controls, both parental, cortactin-expressing and cortactin KO cell lines were transfected with EGFP. Wound healing experiments of EGFP-transfected cells confirmed a significant reduction in wound closure efficiency to 75% in the KO cells compared to cortactin-expressing control cells (Figure 3-2). However, when cortactin KO cells were transfected with active Rac1, they displayed an increased wound closure rate of approximately 85%. The opposite effect was observed in the control cells, where Rac1 overexpression decreased wound healing efficiency

significantly by 8%. In addition, expression of constitutively active Cdc42 in cortactin KO cells restored wound healing rates to almost 95% of control cell rates. Active Rho-GTPases were thus able, at least in part, to rescue the wound healing defect in cortactin-deficient cells. These data indicate that the impaired migration rates in cortactin-depleted cells are not due to altered architecture in the actin cytoskeleton or lower levels of active Arp2/3 complex, but instead the result of a signaling defect leading to lower levels of active Rac1 and Cdc42.

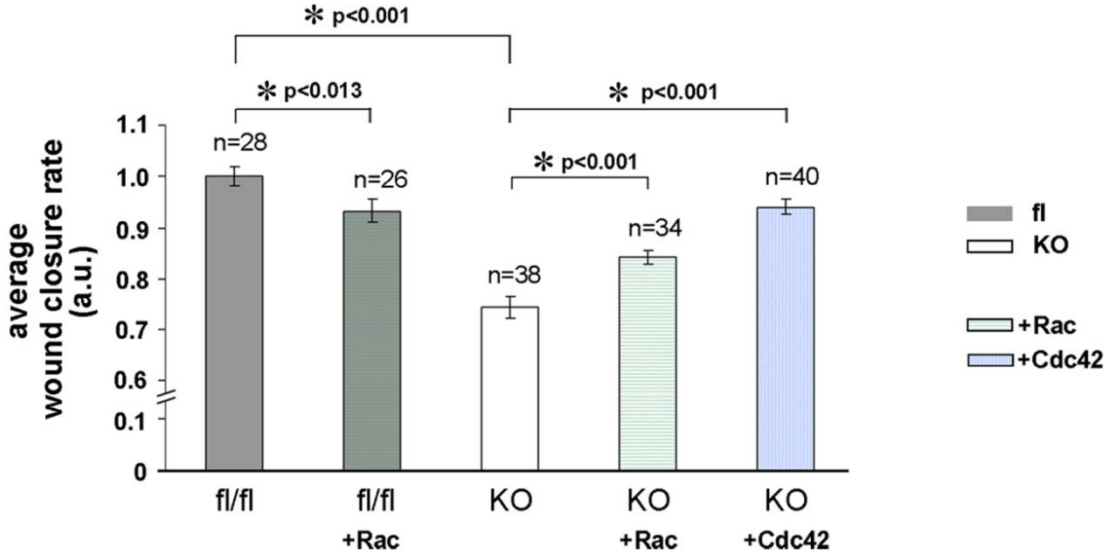

Figure 3-2: The wound closure rate of cortactin-deficient cells can be restored by expression of constitutively active Rho-GTPases.

Control (fl/fl) and cortactin KO cells were transfected with either EGFP, EGFP-Rac1 or EGFP-Cdc42, as indicated. One day after transfection, cells were FACS-sorted and seeded into 12-well plates. After two days a wound was scratched into the cell monolayer and wound closure was monitored using an automatic microscope. Average wound closure rates were calculated by dividing the wound area at the beginning of movies by the time cells needed for wound closure. Wound closure rates from control cells were normalized to 1. n corresponds to number of movies analyzed. Data are means and standard errors of means (error bars). Statistically significant differences are indicated with asterisks.

3.1.2 Analysis of α-actinin expression in control and cortactin KO cells

During the characterization of cortactin KO cells, an RNA array (Affymetrix, Santa Clara, USA) was carried out, which allowed the comparison between the transcription levels of genes in cortactin control and KO cells and was employed to detect genes that were up- or downregulated upon cortactin depletion. Analysis of the RNA array data revealed that the message of the actin bundling protein α-actinin, which is present in focal adhesions, stress fibers and the cell periphery, is reduced to between 25% and 50% in cortactin KO cells. The variability derives from several independent array positions that correspond to different complementary sequences of the α-actinin message. To examine, if the reduction of α-actinin is also detectable on protein level, quantitative western blots were performed.

3.1.2.1 α-actinin isoform 4 is also downregulated upon cortactin depletion at the protein level

Mammals express α-actinin in four different isoforms. Isoforms 2 and 3 are restricted to muscle cells, whereas in non-muscle cells α-actinin isoforms 1 and 4 are found, which localize primarily to focal adhesions, in a spotty fashion along stress fibers (Sjöblom, Salmazo, and Djinović-Carugo, 2008) and lamellipodia (Otey and Carpen, 2004). In the first approach to determine the protein level of α-actinin in control and cortactin KO cells a pan-antibody was used, which detects all isoforms. When western blots were performed, at least four bands between 90 and 120 kDa were visible representing different isoforms of α-actinin or cross reactions of the antibody, which complicated density measurements of the protein bands (data not shown). To circumvent this problem, an antibody solely recognizing α-actinin isoform 4 was applied, which detected only one band at the expected molecular weight of 100 kDa.

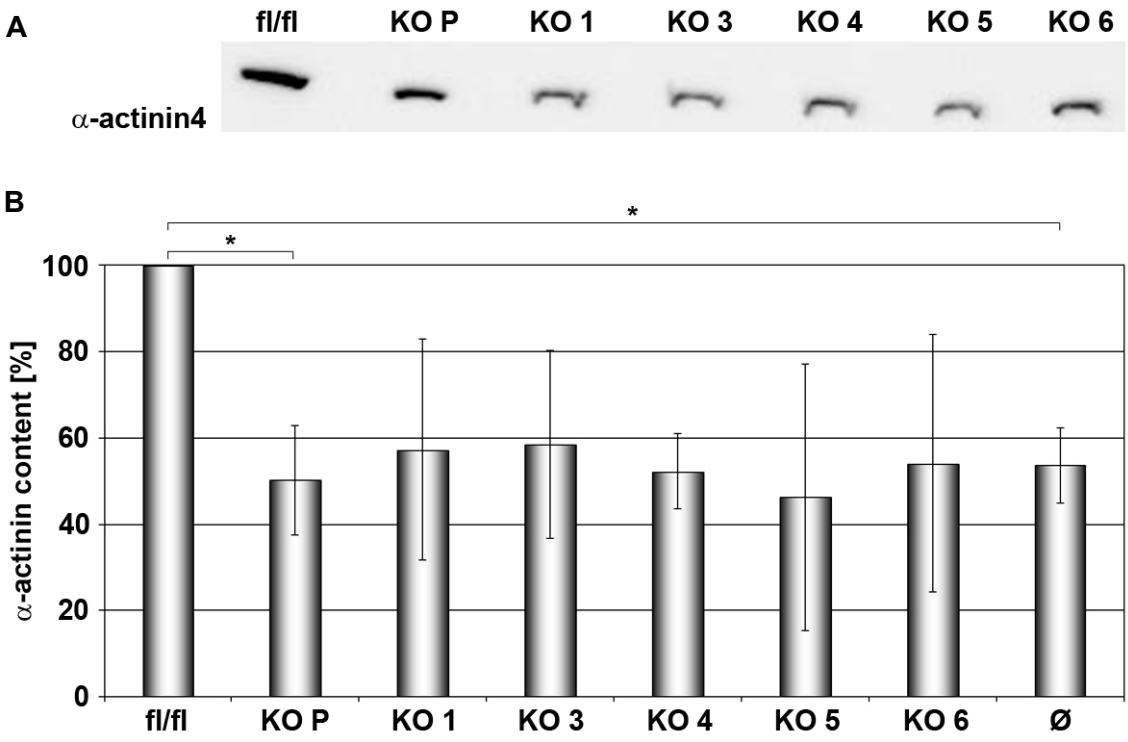

Figure 3-3: α-actinin4 protein level is reduced in cortactin-deficient cells.

(**A**) Exemplary western blot with SDS samples from control cells (fl/fl) and the pooled KO cell population (KO P), as well as the individual KO clones (KO 1, 3-6) probed with anti-α-actinin4 antibodies. (**B**) Five blots as in (A) were subjected to density measurements of α-actinin4 and vinculin. α-actinin levels of the control cells were normalized to 100%. Ø represents the arithmetic mean of all individual clones. All data are means and standard errors of means (error bars). Asterisks indicate statistically significant differences between fl/fl cells and both KO P and the mean of all individual clones (Ø).

The cortactin-deficient cells used in this thesis were a pooled population of five individual clones derived after Adenovirus Cre-induced gene disruption. For

determination of α-actinin protein levels, SDS samples of control cells and the pooled cortactin KO cells were used. Additionally, SDS samples from all five individual KO clones were used in western blotting to ensure that all KO clones showed comparable α-actinin protein levels (Figure 3-3). Bands from five western blots as in Figure 3-3 were subjected to density measurements and the analysis of western blots with samples harvested at different days revealed that the protein level of α-actinin4 was reduced to ~50% in the pooled cortactin KO cells. α-actinin levels in the individual cortactin KO clones varied between 45% and 60%, however, all clones were reduced in α-actinin4 protein levels and the average of all individual clones mirrored the value of the pooled population. These results confirmed the RNA array data concerning the downregulation of α-actinin to 50% upon depletion of cortactin, although no link between the absence of cortactin and reduced α-actinin levels could be established so far.

3.1.2.2 Subcellular localization of endogenous α-actinin4

The distribution of endogenous α-actinin4 in control and cortactin KO cells was elucidated in order to detect potential differences in the localization of the protein upon cortactin depletion. Immunofluorescence stainings with the anti-α-actinin4 antibody showed the same localization to focal adhesions and the cell front in both cell populations (Figure 3-4). In conclusion, although cortactin depletion clearly affected α-actinin expression levels, it did not apparently influence its subcellular positioning.

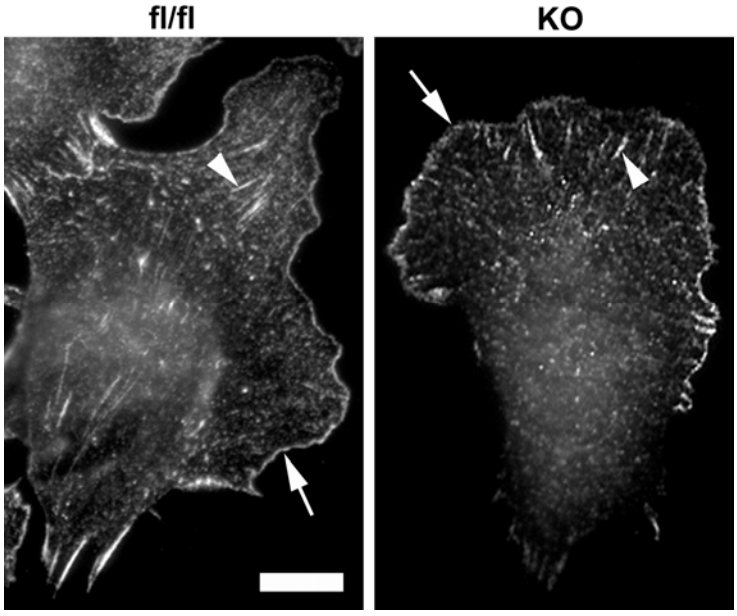

Figure 3-4: Localization of endogenous α-actinin4 in control and cortactin KO cells.

Control (fl/fl) and cortactin KO cells were seeded on fibronectin, fixed and stained with an anti-α-actinin4 antibody. In both cell lines the antibody labeled focal contacts (arrowheads) and lamellipodia (arrows). No differences in expression levels were discernable. Bar, 10 µm.

3.1.3 Invasion of *Listeria monocytogenes* is strongly impaired in cortactin KO cells

Cortactin has been implicated in host-pathogen interactions, such as EPEC pedestal formation (Cantarelli et al., 2002) and invasion by both *Shigella flexneri* (Bougneres et al., 2004) and *Listeria monocytogenes*. It localizes to attachment sites of the pathogens at the host cell surface and throughout the actin comet tails driving the movement of certain intracellular bacteria (Barroso et al., 2006), pointing to a function of cortactin in the formation and/or maintenance of these structures.

In earlier studies, the cortactin-deficient cells studied here were subjected to infection experiments with different pathogens such as enterohemorrhagic *Escherichia coli* (EHEC), enteropathogenic *Escherichia coli* (EPEC) and *S. flexneri* (experiments were performed by Tanja Bosse and Brigitte Denker, data not shown). Surprisingly, no changes could be identified in pedestal formation of EHEC and EPEC, or in invasion by and intracellular actin tail formation of *S. flexneri*, demonstrating that although cortactin is recruited to pathogen-induced actin rearrangements, it is dispensable for attachment, invasion and intracellular movement of those bacteria mentioned above (unpublished data).

For *Listeria* invasion experiments, which were carried out by Tanja Bosse, control and cortactin KO cells were seeded in 24-well plates and were infected on the next day with both *L. monocytogenes* WT and a mutant lacking both Internalin A and B (*L. m.* ΔInlA/B). *L. monocytogenes* employs interaction with the E-cadherin and c-Met transmembrane receptors to enter host cells mediated by bacterial InlA and B, respectively. Upon binding of both internalins to their receptors, cellular response are induced that lead to the uptake of the bacterium. Additionally, invasion can take place independently of InlA/B through so far unknown factors, currently referred to as “non-specific” uptake. InlA was shown to exclusively associate with human E-cadherin (Lecuit et al., 1999; Schubert et al., 2002), thus invasion of *L. monocytogenes* could only take place via InlB or the non-specific pathway in these cells, as they were of murine origin. As displayed in Figure 3-5, the non-specific uptake of *L. monocytogenes* measured by invasion of the InternalinA/B null mutant accounted for about 50% of total internalization in control cells and was only marginally lower in cortactin KO cells. Thus, the non-specific invasion path was strongly employed by the bacteria in both cell lines and did not require cortactin function. In contrast, invasion efficiency of WT *L. monocytogenes* was reduced to 50% upon cortactin deletion, which equals the values of non-specific bacterial uptake.

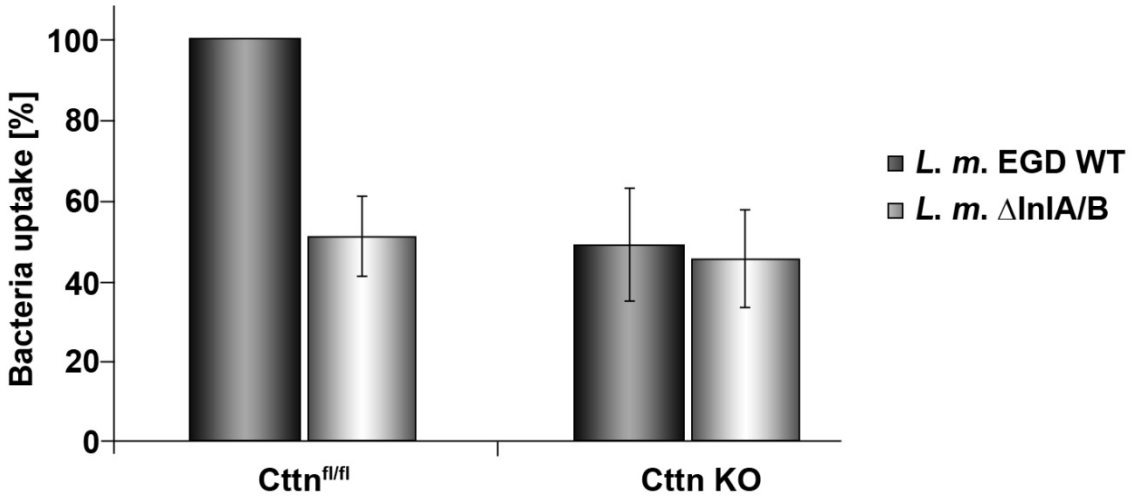

Figure 3-5: The specific invasion of *L. monocytogenes* is blocked in cortactin KO cells.

Uptake of *L. monocytogenes* EGD WT and ΔInlA/B mutant in control (Cttn$^{fl/fl}$) and Cttn KO cells as examined by a gentamicin protection assay, demonstrating that the specific invasion of *Listeria* is inhibited upon cortactin depletion. Bacteria uptake of WT bacteria in control cells was normalized to 100%. Data are means and standard errors of means (error bars) from at least three independent experiments. Data were kindly provided by Tanja Bosse.

Invasion experiments with *L. monocytogenes* were repeated using control and cortactin-deficient cells derived from Cttn$^{fl/fl}$ mice after Flpe recombination (see 2.1.20 and Figure 3-1), called control^{Flpe} and cortactin KO^{Flpe} cells, to verify that cortactin loss-of-function was indeed the cause for defective InlB-mediated invasion in the aforementioned experiment. To confirm that cortactin KO^{Flpe} cells did not express cortactin, western blotting was performed using cortactin antibodies.

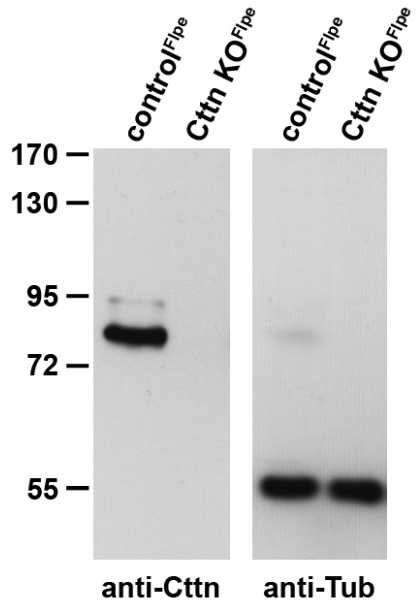

Figure 3-6: Cortactin is absent from Cttn KO^{Flpe} cells.

Western blotting of cell extracts from control^{Flpe} and cortactin KO^{Flpe} (Cttn KO^{Flpe}) cells with anti-cortactin (anti-Cttn) and anti-tubulin (anti-Tub) antibodies. Note that in control^{Flpe} cells a double band characteristic for cortactin is visible, whereas no band is visible in cortactin KO^{Flpe} cells. The tubulin blot confirms equal loading. Numbers correspond to protein size in kDa.

In control^{Flpe} cells, a characteristic double band corresponding to cortactin was visible, albeit in extracts from cortactin KO^{Flpe} cells no band was discernable. The same blot was stripped and incubated with anti-tubulin antibodies to confirm equal loading of control^{Flpe} and cortactin KO^{Flpe} cell extracts (Figure 3-6).

As shown in Figure 3-7, cortactin KO^{Flpe} cells showed the same reduction of WT *Listeria* uptake to about 50% in comparison to control^{Flpe} cells, and the non-specific invasion as measured with the InlA/B-deficient *Listeria* mutant accounted for half of the total bacterial uptake. In conclusion, the InlB-dependent invasion pathway was completely blocked in the absence of cortactin, which was in good agreement with previous studies using cortactin RNAi (Barroso et al., 2006).

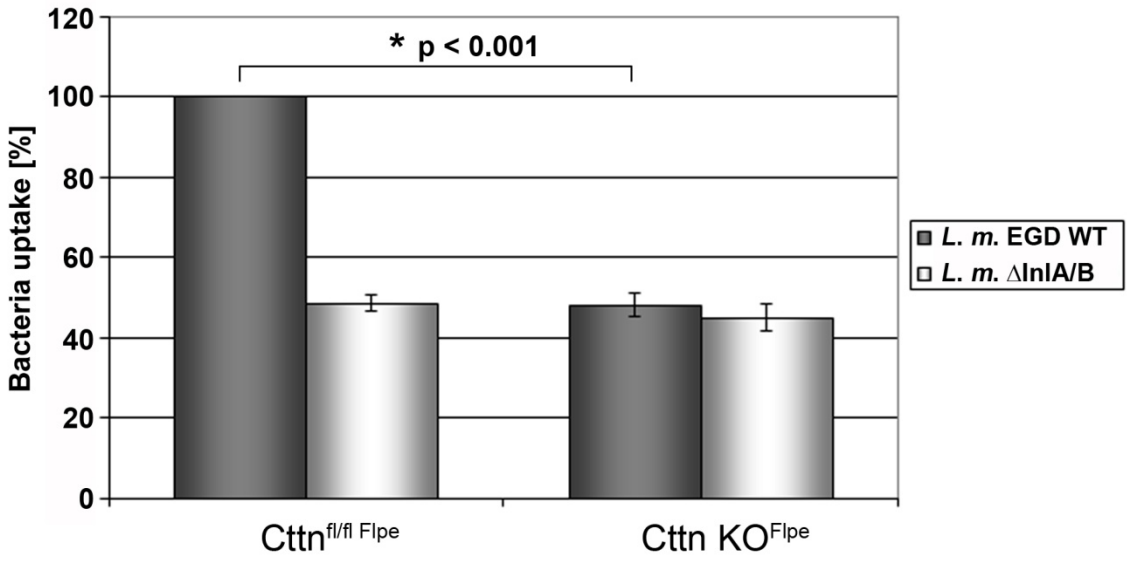

Figure 3-7: Recapitulation of dependence of InlB-mediated *Listeria* invasion on cortactin.

Listeria invasion experiments as in Figure 3-5 were repeated using control (Cttn$^{fl/fl\ Flpe}$) and cortactin KO^{Flpe} (Cttn KO^{Flpe}) cells, which confirmed the abolishment of InlB-mediated *Listeria* internalization upon cortactin knockout. WT bacteria uptake in contol^{Flpe} cells was normalized to 100%. Data are means and standard errors of means (error bars) from three independent experiments. Asterisk and corresponding p value indicates statistically significant differences between uptake of WT bacteria in control^{Flpe} and cortactin KO^{Flpe} cells.

3.1.4 Stimulation of the c-Met pathway is not affected upon cortactin depletion

So far, no link was established between InlB-mediated invasion employing c-Met receptor and cortactin. As outlined above, InlB binds to the transmembrane receptor c-Met, which induces a signaling cascade that induces local actin polymerization engulfing the bacterium and finally results in the uptake of the pathogen into the host cell. An important question was, whether the signaling cascade of c-Met was defective in cortactin KO cells leading to abolished InlB-dependent invasion. To answer this, stimulation experiments were performed using HGF, the mammalian ligand of c-Met

receptor, and purified, soluble InlB (kindly provided by Dr. Hartmut Niemann, University of Bielefeld), which is produced by *L. monocytogenes* to hijack the c-Met pathway during entry into the host cell. Stimulation of c-Met is known to induce dorsal ruffles (Buccione, Orth, and McNiven, 2004). Dorsal ruffles are actin-rich structures that form upon growth factor treatment with factors such as EGF and HGF, and are implicated in receptor internalization and macropinocytosis (see 1.1.2).

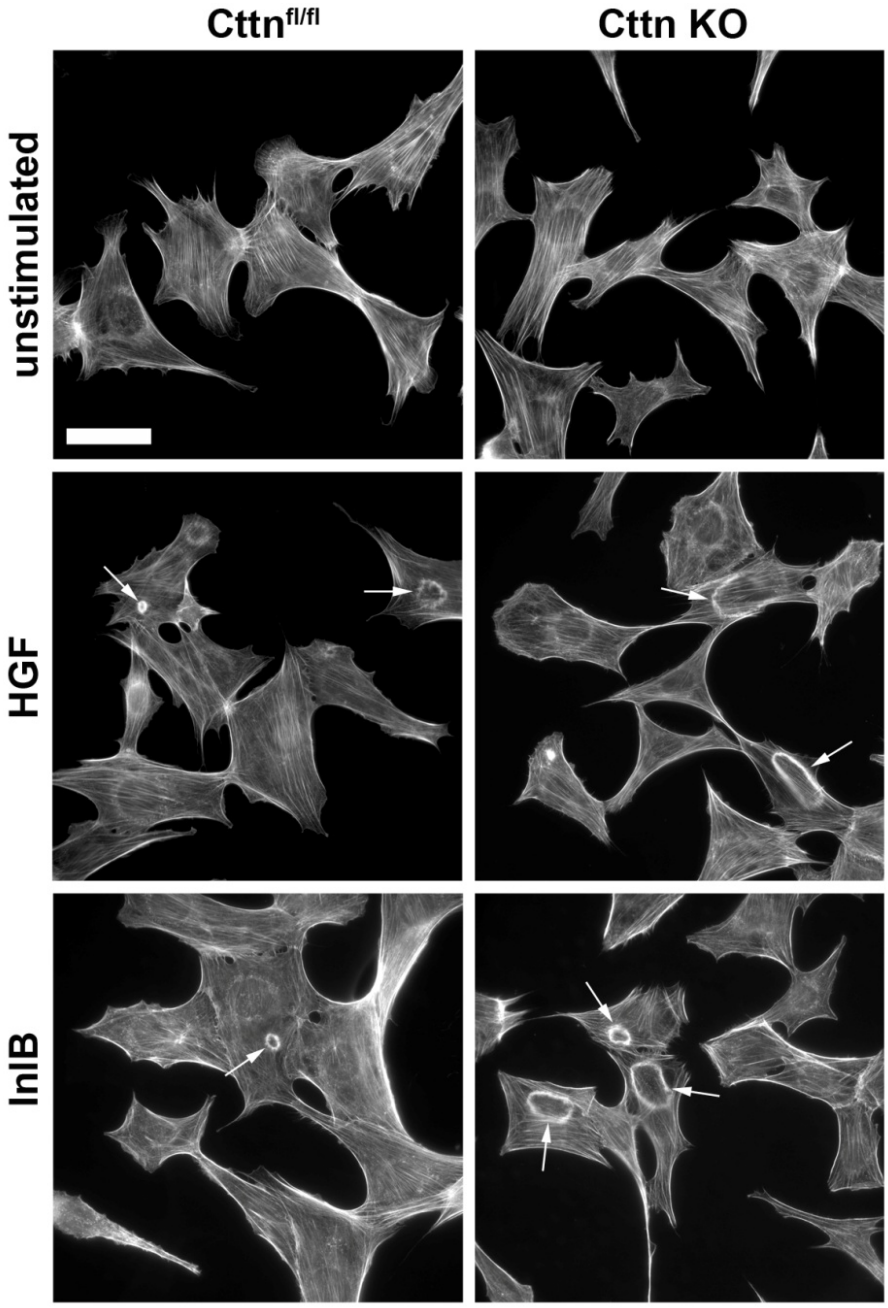

Figure 3-8: HGF and InlB stimulation is not impaired in cortactin KO cells.

Representative phalloidin stainings of the actin cytoskeleton of cells, which were starved with DMEM without serum overnight and subsequently treated for 7.5 min with DMEM alone (unstimulated) or with DMEM containing 20 ng/ml HGF or 55 ng/ml InlB, respectively. Dorsal ruffles as response to growth factor treatment are indicated with arrows. Bar, 50 µm.

The formation of dorsal ruffles is often used as readout for successful induction of signal transduction to actin reorganization by a given growth factor, as it is sensitive and easily detectable upon phalloidin staining of the actin cytoskeleton. Interestingly, cortactin KO cells showed a severe reduction in PDGF-stimulated dorsal ruffling, which indicated that loss of cortactin interfered with the PDGF signaling pathway (Lai et al., 2009). Thus, it was thinkable that the abrogated InlB-mediated infection of *Listeria* was due to defective c-Met signaling. Prior to the stimulation, cells were seeded onto glass coverslips coated with fibronectin, starved overnight and treated for 7.5 min with either DMEM, or DMEM supplemented with HGF or InlB. The same concentrations of HGF and InlB (20 ng/ml and 55 ng/ml, respectively) were used, which were optimal for other mouse MEF cells (Bosse et al., 2007). After fixation and staining with fluorescently-labeled phalloidin, cells were quantified regarding their ability to form dorsal ruffles. Representative immunofluorescence stainings with and without stimulation are shown in Figure 3-8. Both control and cortactin KO cells did not form dorsal ruffles after treatment with DMEM alone (Figure 3-9). This is due to the fact that the minimal medium did not contain any growth factors, which could induce actin rearrangements. Upon HGF stimulation, 17% of control cells displayed dorsal ruffles and only 8% could be stimulated with InlB. In cortactin KO cells, 23% of cells formed dorsal ruffles upon HGF stimulation, and the dorsal ruffle formation upon InlB treatment was even slightly enhanced with about 18% of KO cells displaying dorsal ruffles. These data strongly suggest that cortactin deficiency does not lead to a general defect in c-Met signaling.

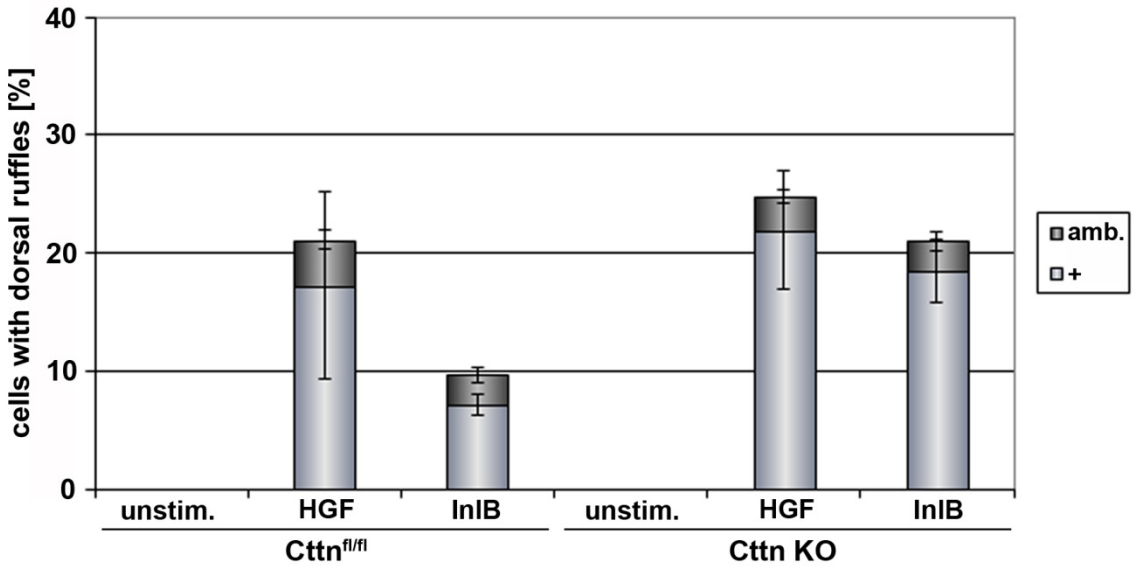

Figure 3-9: Quantification of cells forming dorsal ruffles in response to growth factor treatment.

Images as from Figure 3-8 were employed to quantify cells with dorsal ruffles (+) or with ambiguous phenotype (amb.) upon the indicated treatments. For each cell type and treatment, at least 100 cells were analyzed. Data are means and standard errors of means (error bars).

3.1.5 Mating statistics of cortactin and HS1/cortactin KO mice

In order to analyze cortactin deficiency in a higher organism, a conditional genetic KO of cortactin was generated in mice (21.1) by Frank Lai. Transgenic mice with targeted cortactin alleles were in the first approach crossed with mice expressing Cre recombinase to obtain mice carrying the deleted Neo allele (see Figure 3-1). In the second approach, mice with the targeted allele were first crossed with mice expressing Flpe recombinase to obtain the floxed allele. In a further round of mating the latter mice were crossed with Cre deleter mice, which generated mice carrying the deleted KO allele (Figure 3-1). All cortactin KO mouse lines were viable and fertile and did not display an obvious phenotype. Nevertheless, statistics concerning the genotypes and sexes of cortactin KO mice revealed some abnormalities. Matings of heterozygous animals carrying a WT and a deleted Neo allele displayed a small bias towards male offspring and the overall number of WT mice was increased as compared to the theoretical, expected number (Figure 3-10). In particular, the number of male KO mice was much lower than calculated. In contrast, heterozygous matings between mice harboring a WT and a deleted allele showed a drastic shift in direction of female offspring (Figure 3-11). From 307 mice, only 131 were male, which represented 43% instead of 50% of all mice born. Additionally, considerably more mice were born with heterozygous genotype, whereas both WT and KO mice were slightly underrepresented. Strikingly, there were much more females and much less males with heterozygous genotype than calculated. A X^2 test demonstrated that the probability for the latter deviation being due to chance was very low (see Table 9-1 and Table 9-2 in the Appendix).

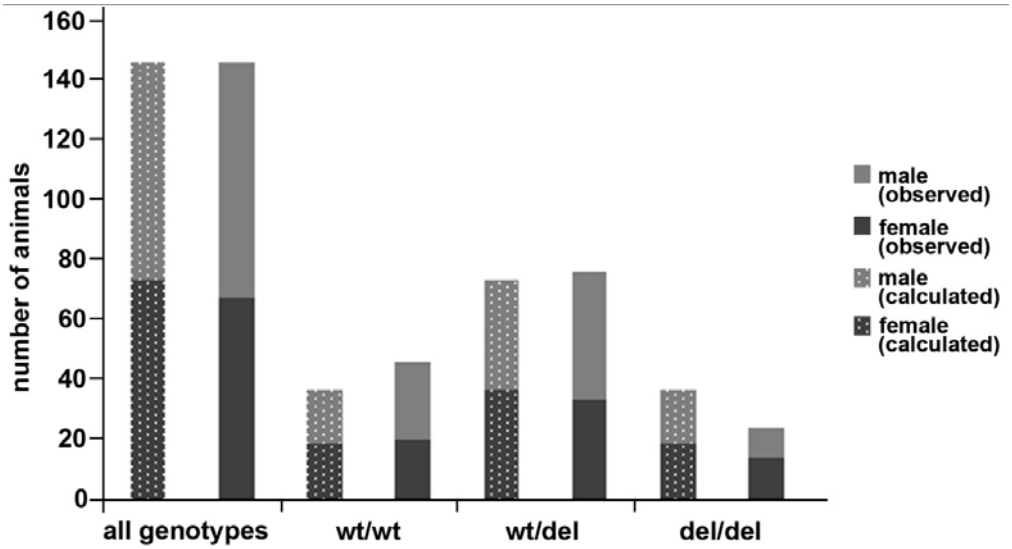

Figure 3-10: Distribution of genotypes and sexes of heterozygous crossings with mice carrying a WT and a cortactin deleted Neo allele.

Calculated and observed sexes and genotypes of 146 offspring derived from heterozygous crossings. (For exact numbers, see appendix.)

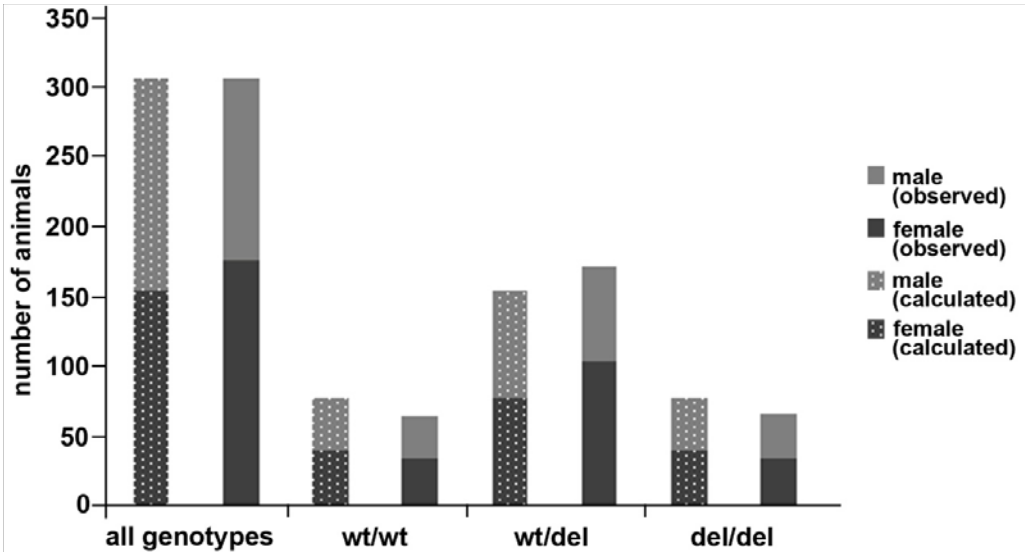

Figure 3-11: Distribution of genotypes and sexes of heterozygous crossings with mice carrying a WT and a deleted cortactin allele.

Calculated and observed sexes and genotypes of 307 offspring of heterozygous crossings. (For exact numbers, see appendix.)

Additionally, cortactin mice carrying the deleted Neo allele were crossed with $HS1^{del/del}$ mice in order to obtain animals deficient for both cortactin and HS1. Also these double-knockout mice were both viable and fertile and did not show apparent phenotypes. Crossings of $HS1^{del/del}Cttn^{wt/del}$ mice revealed no significant deviations from Mendelian ratios and expected distribution of sexes, only slightly more female mice were born than male (Figure 3-12 and Table 9-3).

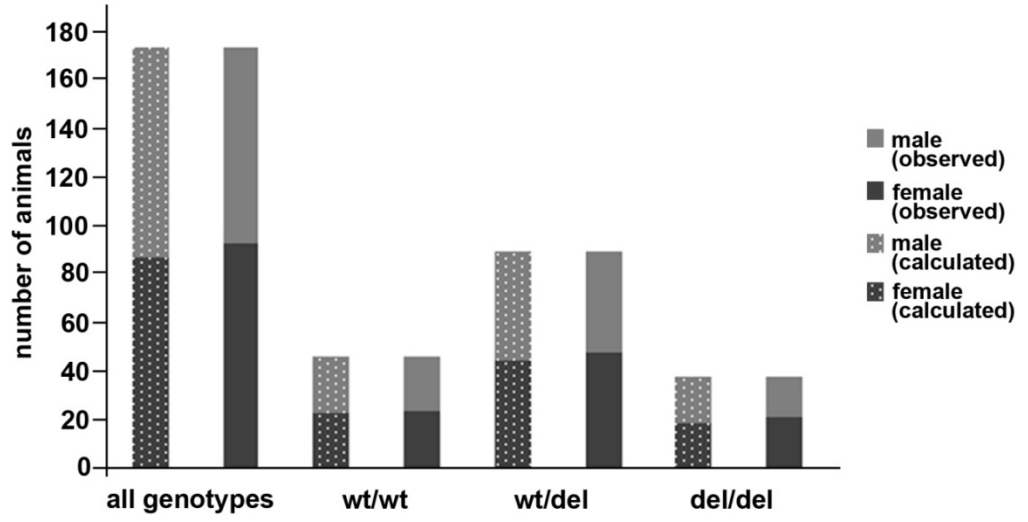

Figure 3-12: Distribution of genotypes and sexes of crossings with mice homozygous for HS1 deletion and heterozygous for the cortactin deleted Neo allele.

Calculated and observed sexes and genotypes of 174 offspring of crossings of $HS1^{del/del}Cttn^{wt/del}$ mice. (For exact numbers, see appendix.)

3.1.6 Analysis of cortactin- and HS1/cortactin-deficient primary macrophages

In several cell types like osteoclasts, smooth muscle cells and macrophages, a special actin-rich structure is assembled. When cells are plated on rigid surfaces like glass coverslips, so-called podosomes are formed on the ventral side of the cell that undergo rapid turnover. These structures support the adherence of cells on a substratum, but at the same time they allow fast migration, as the lifetime of podosomes is very short compared e.g. to focal contacts (see 1.1.5). The core of podosomes is built by a dense network of actin filaments, which is surrounded by a characteristic ring of proteins that are also part of the protein composition of focal contacts, such as vinculin, talin and zyxin. At variance to focal contacts, the Arp2/3 complex localizes to the actin rich core of podosomes. For this reason it is assumed that the Arp2/3 complex polymerizes the F-actin core. Support for this theory is given by the fact that also Arp2/3 activators like the class I NPF WASP and the class II NPF cortactin are present at the core of podosomes. Studies with WASP-deficient primary macrophages from transgenic mice revealed an essential role for this NPF in the formation of podosomes (Linder et al., 1999). Although cells were still able to adhere, no podosomes could be formed in the absence of WASP. In addition, RNAi studies indicated that cortactin is a major player in podosome formation, at least in osteoclasts and smooth muscle cells (Tehrani et al., 2006a; Webb, Eves, and Mak, 2006). Therefore, it was intriguing to ask, whether macrophages from cortactin-deficient mice or from mice lacking both cortactin and HS1, the hematopoietic homolog of cortactin, still displayed podosomes and if so, whether they were normal regarding their shape, protein composition and frequency of occurrence.

For these experiments, primary macrophages from control and cortactin KO mouse littermates from heterozygous crossings of mice carrying the deleted cortactin allele were isolated from the peritoneum, seeded on coverslips coated with fibronectin and stained for F-actin, vinculin and cortactin. In control cells, podosomes were visible as actin-rich dots surrounded by a ring composed of vinculin, and the actin cores co-localized with cortactin (Figure 3-13), as expected. Podosomes could also be seen in macrophages from cortactin KO mice, in spite of the complete loss of cortactin staining (Figure 3-13). When comparing the podosomes of macrophages with and without cortactin, no apparent differences were discernable regarding size and morphology in the conditions used here.

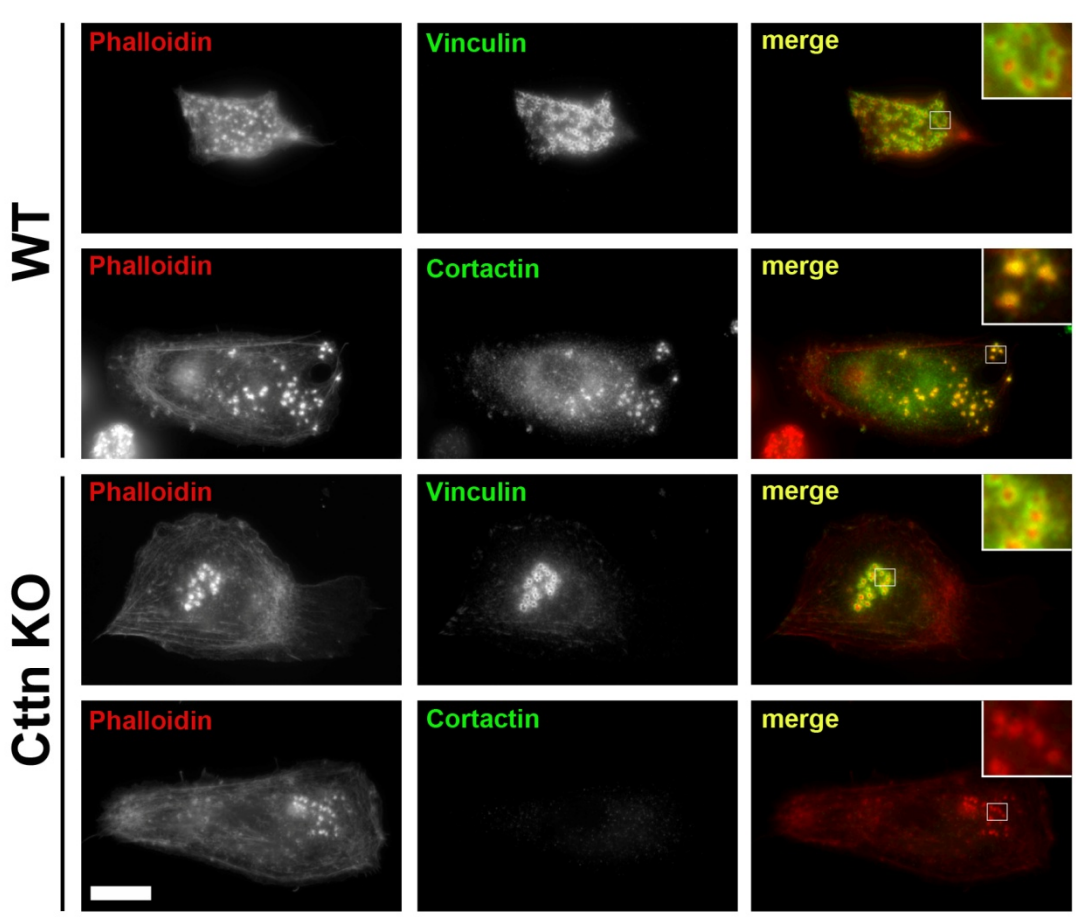

Figure 3-13: Organization of the actin cytoskeleton, and localization of vinculin and cortactin in control and cortactin KO macrophages.

Immunofluorescence stainings of peritoneal macrophages harvested from WT or cortactin KO littermates derived from heterozygous crossings of mice with the deleted cortactin allele. Both macrophage populations displayed podosomes, F-actin-rich dot-like structures (red in merge) characteristically surrounded by a ring of focal adhesion proteins like vinculin (green in merge). In WT macrophages cortactin (green in merge) co-localized with the F-actin-rich core of podosomes, whereas no cortactin staining is visible in cortactin KO macrophages. Boxed regions in merges are displayed as insets in higher magnification. Bar, 10 µm.

However, it was not clear whether the number of cells displaying podosomes was reduced in cortactin KO macrophages. To test this, macrophages from WT and KO mice were co-stained with phalloidin and vinculin and the number of cells displaying podosomes determined. Again, no significant difference in the number of cells with podosomes was discernible between cells with and without cortactin (Figure 3-14). In conclusion, cortactin is dispensable for podosome formation in peritoneal macrophages. Nevertheless, preliminary results from a collaboration with Christiane Wiesner and Stefan Linder (UKE Hamburg) revealed that although the podosome formation upon cortactin depletion was normal, gelatin degradation was drastically reduced in macrophages from cortactin KO mice (unpublished data). Matrix degradation assays have to be repeated to confirm this phenotype.

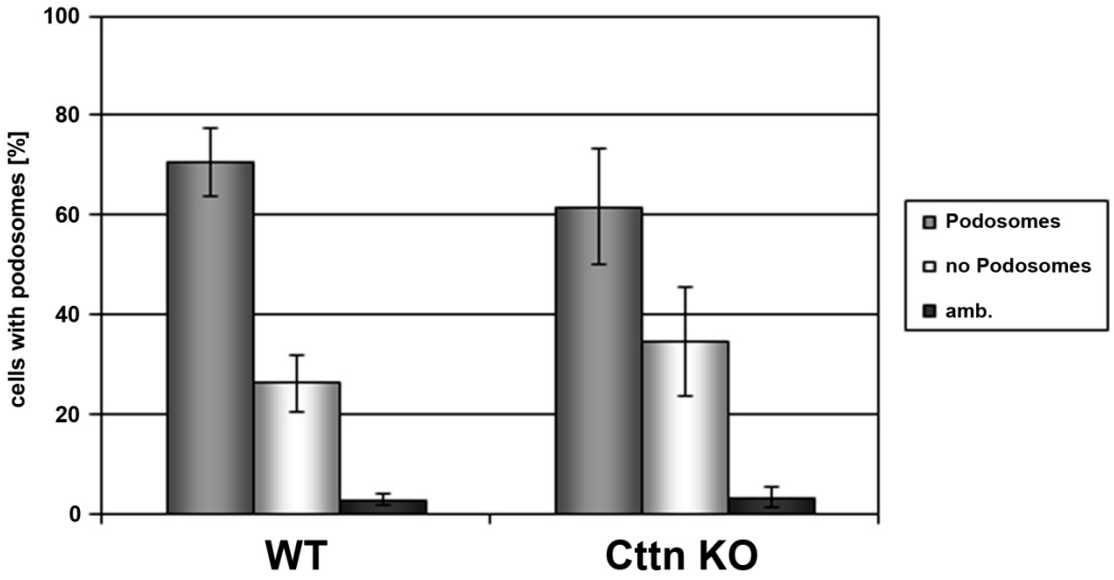

Figure 3-14: Quantification of frequency of WT and cortactin KO macrophages displaying podosomes.

Peritoneal macrophages from WT and cortactin KO mice were stained for F-actin with fluorescently-labeled phalloidin and vinculin. Cells were categorized into cells with podosomes ("Podosomes"), without podosomes ("no Podosomes") or with an ambiguous morphology ("amb."). At least 100 cells were counted for each condition and the experiment was performed in triplicate. Error bars correspond to standard errors of means.

To check the expression levels of HS1 in macrophages, western blot analysis with extracts from control and cortactin KO macrophages was performed (Figure 3-15). An extract of B16-F1 cells transiently expressing HS1-EGFP served as control that the antibody recognizes HS1. In the extract from fibroblast cells no HS1 band was detectable, because HS1 is only expressed in cells of the hematopoietic lineage.

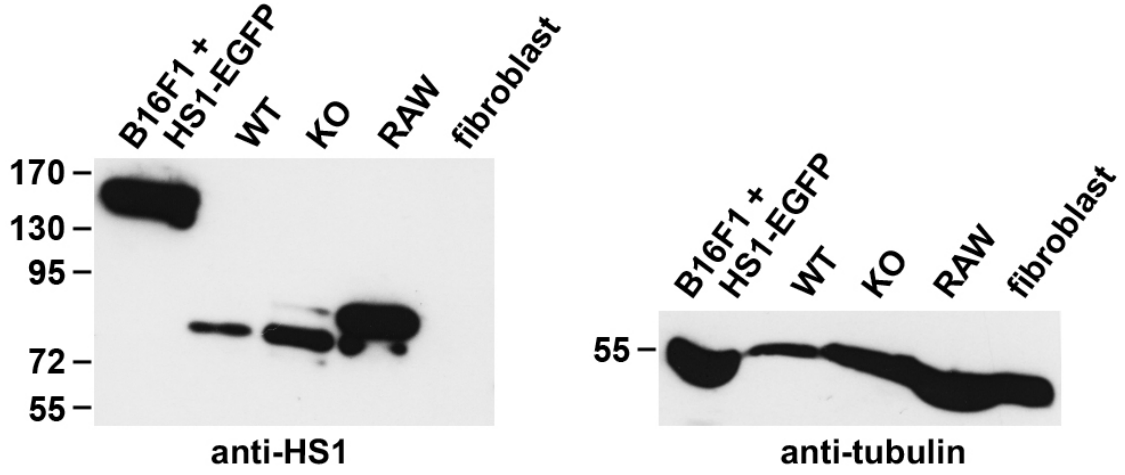

Figure 3-15: HS1 is expressed in cortactin WT and KO macrophages.

Western blot analysis of extracts from B16-F1 cells transfected with HS1-EGFP, macrophages from cortactin control (WT) and cortactin-depleted (KO) mice, Raw cells and fibroblasts with an anti-HS1 antibody (upper panel). The same blot was reprobed with an anti-tubulin antibody as loading control (lower panel). Numbers correspond to protein size in kDa.

In cortactin WT and KO macrophages as well as in the macrophage cell line Raw the antibody recognized one or two HS1 bands demonstrating that these cells express HS1. In analogy to cortactin (Huang et al., 1997), the two bands might correspond to different phosphorylation states of HS1. The HS1 band in cortactin KO macrophages is stronger compared to cortactin WT macrophages, but the protein concentration of the samples was not measured due to the low number of isolated cells, and the anti-α-tubulin blot indicates that more extract from KO macrophages was loaded (Figure 3-15). Thus, HS1 does not seem to be upregulated in cortactin-deficient macrophages in order to compensate the loss of cortactin.

In analogy to the experiments with cortactin-deficient macrophages, cells isolated from mice lacking both cortactin and its hematopoietic form, HS1, were examined in fluorescence stainings regarding the existence of podosomes. As shown in Figure 3-16, cells lacking both cortactin and HS1 were also able to form podosomes with an actin rich core and a surrounding vinculin ring.

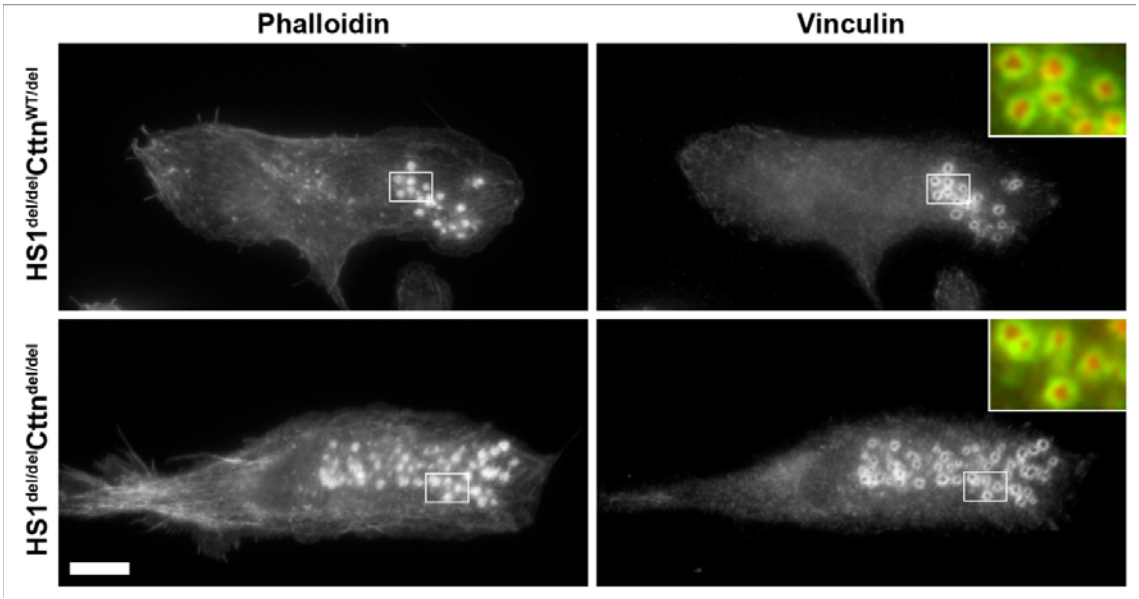

Figure 3-16: HS1/Cttn double KO macrophages are able to form podosomes on fibronectin.

Epifluorescence images of peritoneal macrophages from HS1$^{del/del}$Cortactin$^{WT/del}$ and HS1$^{del/del}$Cortactin$^{del/del}$ mice stained for F-actin with phalloidin and with an anti-vinculin antibody. The macrophages can form podosomes consisting of an F-actin core (red in merged insets) and a ring structure rich in vinculin (green in merged insets), as expected. Boxed regions are shown as merged inset in the right images. Bar, 10 µm.

The quantification of double KO macrophages displaying podosomes (Figure 3-17) revealed that about 85% of cells formed podosomes, irrespective of their genotype. So again no decrease in podosome formation frequency could be observed in double KO macrophages demonstrating that also the combined loss of cortactin and HS1 does not hinder cells to form podosomes.

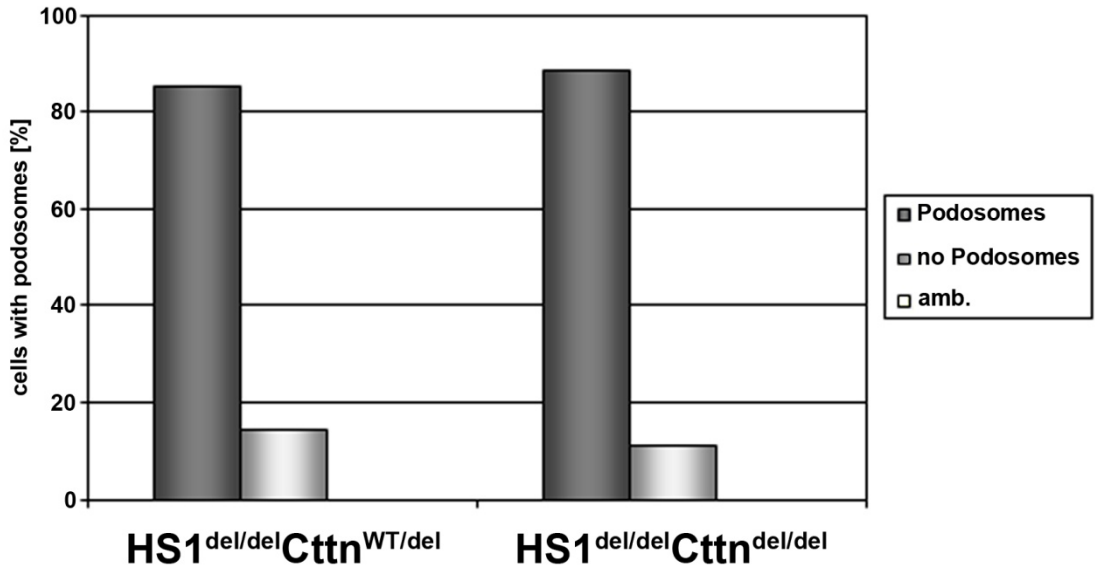

Figure 3-17: Depletion of both HS1 and cortactin does not alter the frequency of macrophages forming podosomes.

Macrophages from HS1$^{del/del}$Cttn$^{WT/del}$ and HS1$^{del/del}$Cttn$^{del/del}$ mice were stained for F-actin. Cells were classified as with podosomes ("Podosomes"), without podosomes ("no Podosomes") or with ambiguous phenotype (amb.). The data summarizes one experiment, in which at least 100 cells were analyzed.

3.2 Establishment of an *in vivo* actin nucleation assay

In the literature mainly *in vitro* assays are used in order to characterize a protein concerning its impact on actin nucleation. Cortactin only weakly activated the Arp2/3 complex in an *in vitro* actin polymerization assay (Uruno et al., 2001; Weaver et al., 2001), so the question occurred, if such a weak promotion of actin nucleation was in fact relevant in the cell. Literature searches reveal previous approaches to study NPFs *in vivo*. For example, actin polymerization was directed to organelles, such as mitochondria (Kessels and Qualmann, 2002; Pistor et al., 1994) or late endosomes in *Dictyostelium* (Schmauch et al., 2009). However, endosomes have an actin shell on their own, so it was difficult to distinguish between the contribution of endogenous and ectopic factors to actin assembly. Mitochondria, on the other hand, are highly dynamic structures and change their shape and size within seconds, so e.g. turnover experiments using live cell imaging was impossible on mitochondria.

Nevertheless, targeting the actin polymerization machinery to an ectopic place in the cell seemed to be a promising approach for an *in vivo* actin nucleation assay. Instead of mitochondria or endosomes, a cellular structure was needed that was relatively stable and also devoid of endogenous actin, such as microtubules. As a matter of fact, the plus tips of microtubules undergo rapid growth and shrinking as well as catastrophes, but the rest of the network, especially the minus ends, are stable and can be imaged for a long period of time.

3.2.1 Actin polymerization can be induced on microtubules by the VVCA-domain of N-WASP

The first construct that was tested, was obtained from Stefan Köstler from the laboratory of Vic Small, Vienna. In this construct (see Figure 3-18) the microtubule binding domain (MBD) of MAP4, a protein stabilizing and bundling microtubules, was cloned directly after the EGFP-tag of EGFP-VVCA (Lommel et al., 2004).

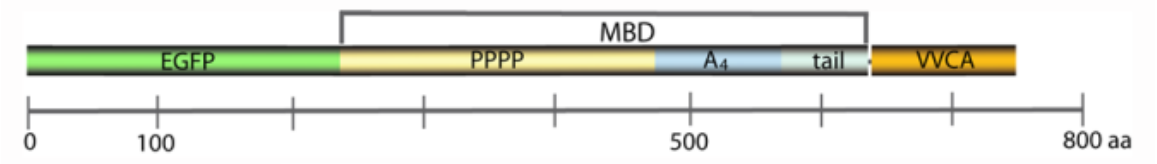

Figure 3-18: Domain structure of MBD-constructs.

MBD-constructs harbored an N-terminal fluorescent tag, in most cases EGFP, followed by the microtubule binding domain of MAP4 comprises a proline-rich domain (PPPP) and four A-domains (A_4), and a tail region required as linker between the MBD and the nucleator or NPF. At the C-terminus the protein of interest, exemplified here by VVCA, was located. The scale below the domain structure indicates the length of the domains in amino acids (aa).

The MBD consisted of a proline-rich domain and four so-called A-domains, both contributing to microtubule binding activity, followed by a tail region, which separated the MBD from the nucleator or NPF located at the C-terminus of the construct. The VVCA fragment is located at the C-terminus of N-WASP, and is a potent Arp2/3 complex activator (see 1.1.6.2), so the construct was well-suited to test the properties of ectopic actin nucleation on microtubules. In cells transfected with MBD-VVCA, the construct labeled the microtubule network proving that the affinity of MBD was high enough to target the construct to microtubules (Figure 3-19C). Fluorescently-labeled phalloidin bound strongly to structures co-localizing with MBD-VVCA (Figure 3-19A), which evidenced that the MBD-VVCA construct was able to induce the polymerization of actin filaments on microtubules. When a tagged subunit of the Arp2/3 complex, mCherry-p16B, was co-transfected with MBD-VVCA, it localized to microtubules as well (Figure 3-19B and Supplementary Video 1). This demonstrated that the Arp2/3 complex was recruited to microtubules through MBD-VVCA, and indicated that it was activated to effect actin filaments.

B16-F1 cells seeded on laminin frequently form lamellipodia, as laminin stimulates the activation of Rho-GTPases such as Rac and promotes actin reorganization leading to lamellipodia formation (Fujiwara, Gu, and Sekiguchi, 2004; Weston et al., 2007). In cells transfected with MBD-VVCA, only very rarely lamellipodia could be observed. Instead, most cells were not able to migrate and displayed a square shape (Figure 3-19 and Figure 3-23). The reason for the altered morphology was most likely due to the fact that MBD-VVCA sequestered the Arp2/3 complex by recruiting it to microtubules. As a

consequence, the cytoplasm lacked sufficient amounts of Arp2/3 complex molecules to be activated at the cell periphery, which is presumably required for the nucleation of actin filaments to build lamellipodia.

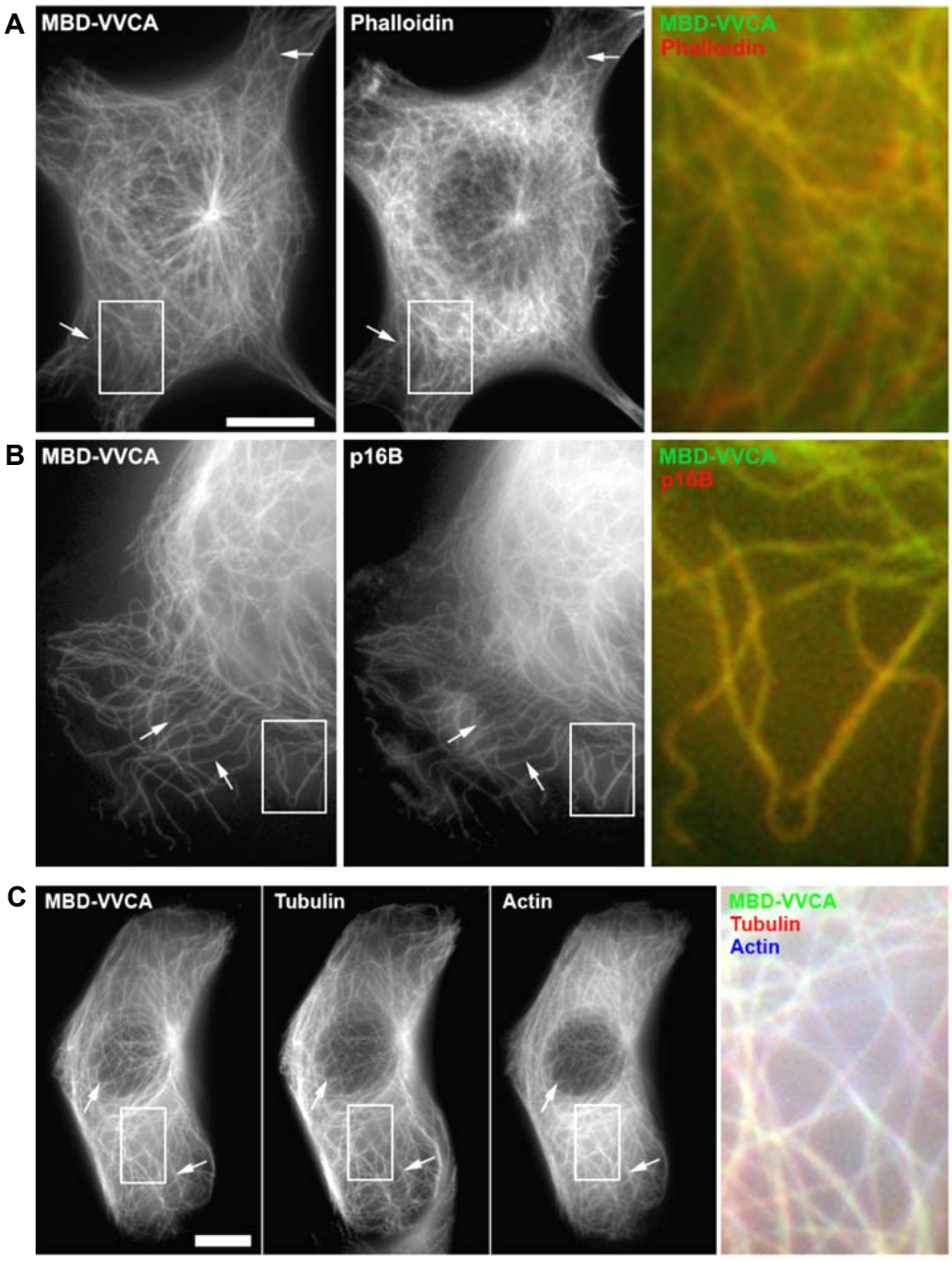

Figure 3-19: MBD-VVCA induces actin accumulation on microtubules by recruiting the Arp2/3 complex.

(**A**) Phalloidin staining of a B16-F1 cell transfected with MBD-VVCA showing co-localization of F-actin with the MBD-VVCA construct. Arrows point to individual microtubules strongly labeled with phalloidin. (**B**) Representative frame from a time-lapse movie of a cell co-transfected with MBD-VVCA and mCherry-p16B, the smallest subunit of the Arp2/3 complex. Arrows and merged image indicate co-localization of MBD-VVCA and p16B. (**C**) B16-F1 cell co-expressing EGFP-MBD-VVCA and EBFP-actin was fixed and the microtubule network was labeled using anti-α-tubulin antibodies. Arrows point to strong co-localizations of all three structures. Boxed insets are shown as merge on the right. Bars, 10 µm.

3.2.2 MBD alone as well as F-actin binding proteins cannot recruit actin to microtubules

An important control experiment was done by expressing an EGFP-MBD-construct lacking actin nucleators or nucleation promoting factors to exclude that actin or Arp2/3 complex recruitment could be already induced by the tagged MBD-domain alone. The MBD-construct accurately labeled the microtubule network, but neither actin nor p16B co-localized with the MBD-construct (Figure 3-20, Supplementary Videos 2 and 3). This demonstrated that the MBD was inert regarding actin nucleation and did not by itself mediate targeting of actin or the Arp2/3 complex to microtubules.

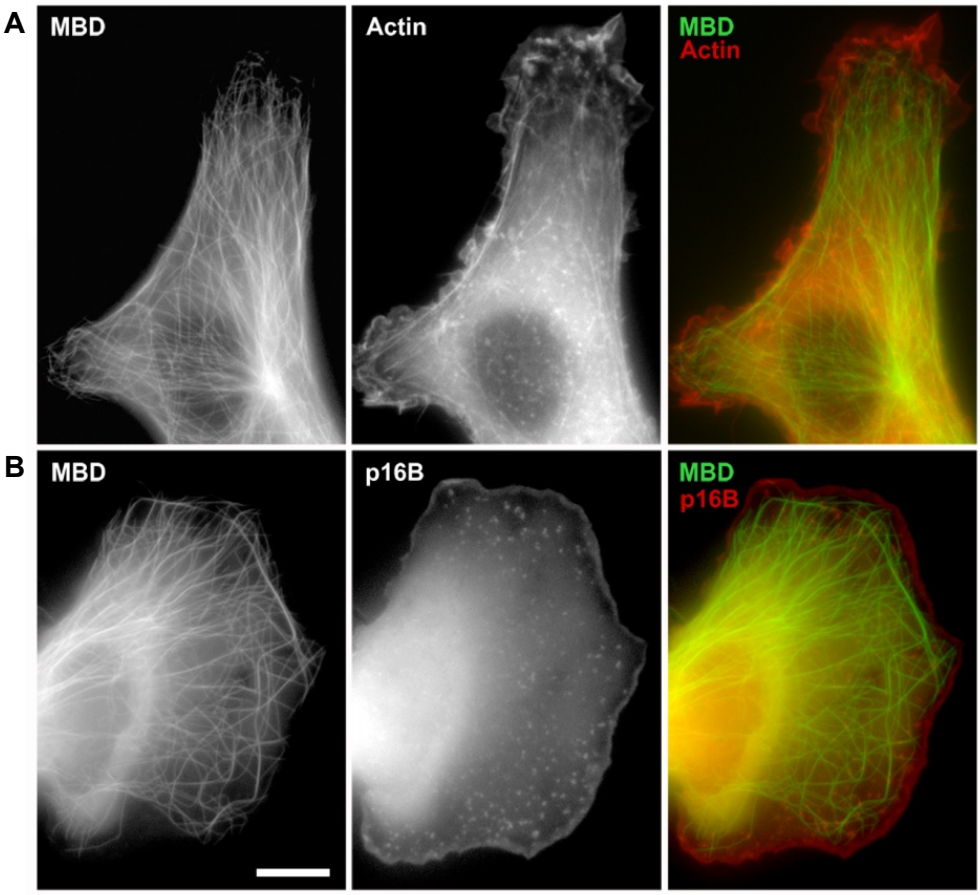

Figure 3-20: MBD does not recruit actin or the Arp2/3 complex to microtubules.

Epifluorescence images of cells transfected with EGFP-MBD and (**A**) mCherry-actin or (**B**) mCherry-p16B, respectively. EGFP-MBD localized strongly to microtubules, but neither actin nor Arp2/3 complex was discernable that co-localized with the MBD-construct on microtubules. Bar, 5 µm.

It could already be shown that microtubule targeting of an Arp2/3 activator led to actin filament accumulation on microtubules indicating that Arp2/3-mediated nucleation was the major mechanism of actin filament assembly. However, as another possibility, the recruitment of actin filaments rather than initiation of nucleation would also explain the actin accumulation on microtubules. To test this, the MBD was fused to fascin, an actin

bundling protein found in filopodia and microspikes (Jayo and Parsons, 2010), and the actin binding domain of α-actinin. Both constructs showed a dual localization when they were expressed in B16-F1 cells. The MBD directed both constructs to the microtubule network. Additionally, fascin coupled to MBD still bound to its natural localization site, microspikes embedded in the lamellipodium, and MBD-ABD labeled F-actin-rich structures like small ruffles and microspikes. Co-expression with mCherry-actin proved that although MBD-fascin and MBD-ABD were still able to bind filamentous actin, e.g. in microspikes no actin accumulation was apparent on microtubules (Figure 3-21). In conclusion, actin accumulation on microtubules could only be induced by nucleation and not by recruitment of actin filaments.

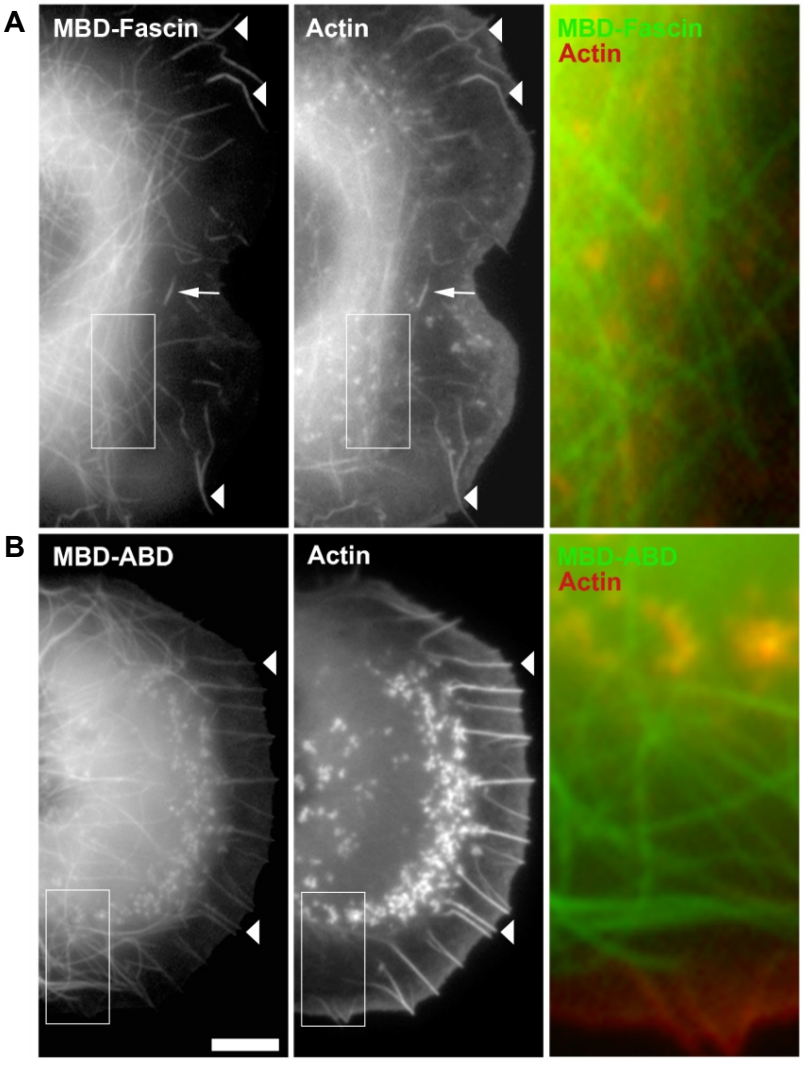

Figure 3-21: Actin binding domains do not induce actin accumulation on microtubules.

Epifluorescence images of B16-F1 cells expressing mCherry-actin and (**A**) MBD-fascin or (**B**) MBD-ABD (ABD: actin binding domain of α-actinin), respectively. Both constructs co-localize with microspikes in the lamellipodium (arrowheads). The arrow points to a former microspike that became integrated into the lamella as observed by live cell imaging. Merged images are magnifications of the boxed areas in the first two panels and show that no co-localization of microtubules with the actin cytoskeleton was detectable. Bar, 5 µm.

3.2.3 Analysis of the ultrastructure of actin induced by MBD-VVCA on microtubules

In order to visualize the ultrastructure of the actin accumulation on microtubules induced by MBD-VVCA, correlated light and electron tomography was performed by M. Vinzenz, M. Nemethova, S. Jacob and J.V. Small in Vienna. This technique allows first the detection of transfected, fluorescently-labeled proteins in a cell using epifluorescence microscopy, and after fixation the same cell is subjected to negative stain electron microscopy. A B16-F1 cell was transfected with MBD-VVCA and mCherry-actin and the co-localization of both proteins on microtubules was verified in the light microscope (Figure 3-22A, B). The cell was subsequently subjected to negative stain electron tomography. A composite image assembled from 30 slices confirmed the earlier findings with phalloidin stainings that the actin accumulations on microtubules induced by MBD-VVCA consisted of polymerized actin filaments. Over the complete length of a microtubule, short actin filaments were visible, which surrounded the microtubule (Figure 3-22D, arrowheads) in an unorganized fashion. For most actin filaments it was difficult to track, if they were directly associated with the microtubule, but single filaments polymerizing directly from the microtubule surface could be identified (Figure 3-22D, arrow), proving that actin filaments can in principle be nucleated on the microtubule surface. As control, an untransfected cell was subjected to electron tomography, in which microtubules were discernable as large tubular structures (Figure 3-22E). Actin filaments were loosely distributed in the section of the cell and randomly crossed or overlapped with microtubules but there was no clear correlation of actin filament and microtubule accumulation comparable to MBD-VVCA expressors.

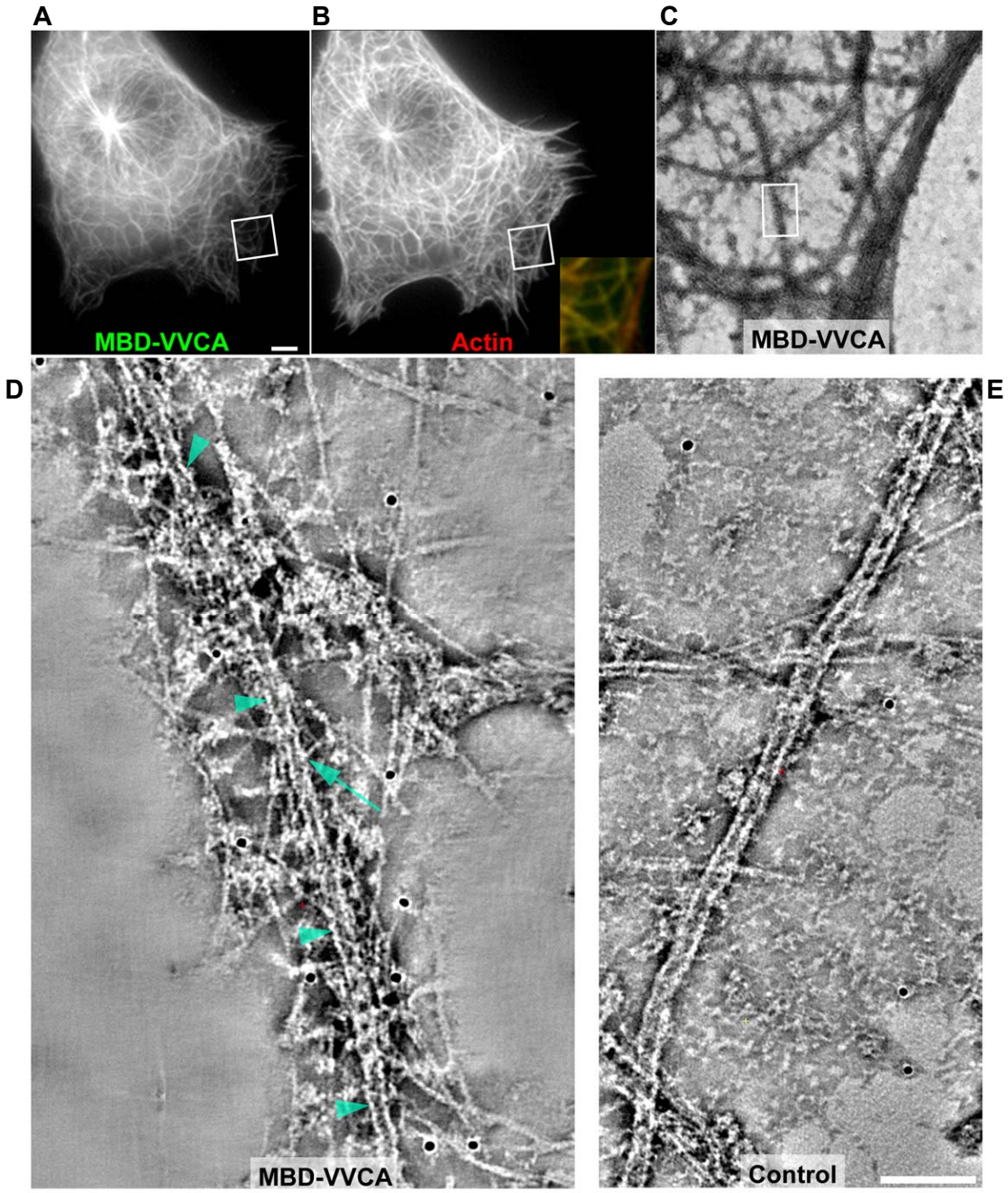

Figure 3-22: Actin filaments induced by MBD-VVCA form an unorganized cloud around microtubules.

(**A**-**D**) Correlated light microscopy and electron tomography. (**A**, **B**) Epifluorescence images of a B16-F1 cell transiently expressing MBD-VVCA (A) and mCherry-actin (B), respectively. Boxed regions are shown as merge in inset of (B) confirming co-localization of both constructs. Bar in (A) corresponds to 10 µm. (**C**) Electron micrograph of the merged inset shown in (B). (**D**) Composite image assembled from 30 slices (0.75 nm) of a tomogram of the region boxed in (C). Arrowheads mark a single microtubule, which is surrounded by various short actin filaments in an unorganized fashion. The arrow points to a filament directly attached to the microtubule. (**E**) Composite image assembled from 40 slices (0.75 nm) of a tomogram of an untransfected control cell displaying a microtubule, which is randomly crossed by actin filaments. Note that the density of actin filaments in (D) is significantly higher than in (E). Bar in (E) is valid for (D) and (E) and equals 100 nm. Electron microscopy was performed by M. Vinzenz, M. Nemethova, S. Jacob and J.V. Small in Vienna.

3.2.4 Dynamics of MBD-VVCA and actin

In addition to phalloidin stainings, it was also possible to detect the MBD-VVCA-induced actin accumulation on microtubules using fluorescent protein-tagged actin, which provided the possibility to analyze the dynamics of MBD-VVCA and actin on microtubules in living cells (Figure 3-23 and Supplementary Video).

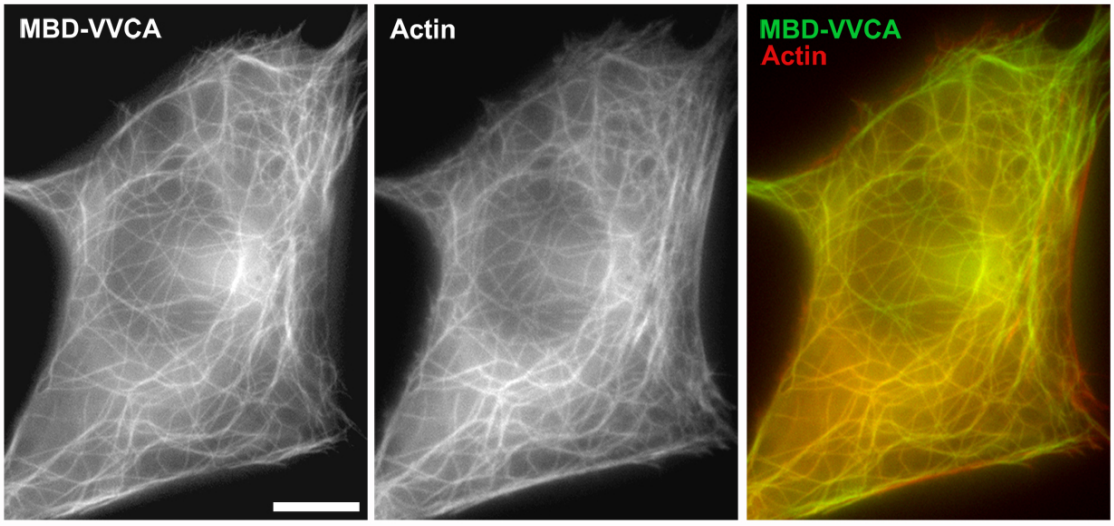

Figure 3-23: Actin nucleation induced by MBD-VVCA can be visualized with fluorescent protein-tagged actin

Epifluorescence images of time-lapse movies of a cell transfected with MBD-VVCA and mCherry-actin. The merged image on the right proved that mCherry-actin co-localized with MBD-VVCA. Bar, 10 µm.

Supplementary Video 4 served as source to detect growing and shrinking microtubules. Individual microtubules visualized with MBD-VVCA were tracked and analyzed regarding their co-localization with actin. An example for both a growing and a shrinking microtubule with associated actin is shown in Figure 3-24 and in Supplementary Videos 5 and 6. By comparing the corresponding frames from both fluorescence channels it became obvious that the actin filaments grew and shrank exactly at the speed of MBD-VVCA. This implied that actin filaments were nucleated instantaneously to accumulation of MBD-VVCA on the surface of microtubules, and they disassembled and depolymerized simultaneously with MBD-VVCA release from shrinking microtubules. So the existence of actin on microtubules is directly coupled to the presence of microtubules in these cells or more accurately, is dependent on MBD-VVCA accumulation on microtubules, which is virtually complete in these conditions.

One major advantage of targeting actin polymerization to microtubules was the stability of the majority of the microtubule network compared e.g. to organelles or endosomes. To define the turnover rate of MBD-VVCA and the associated actin filaments, FRAP experiments were carried out.

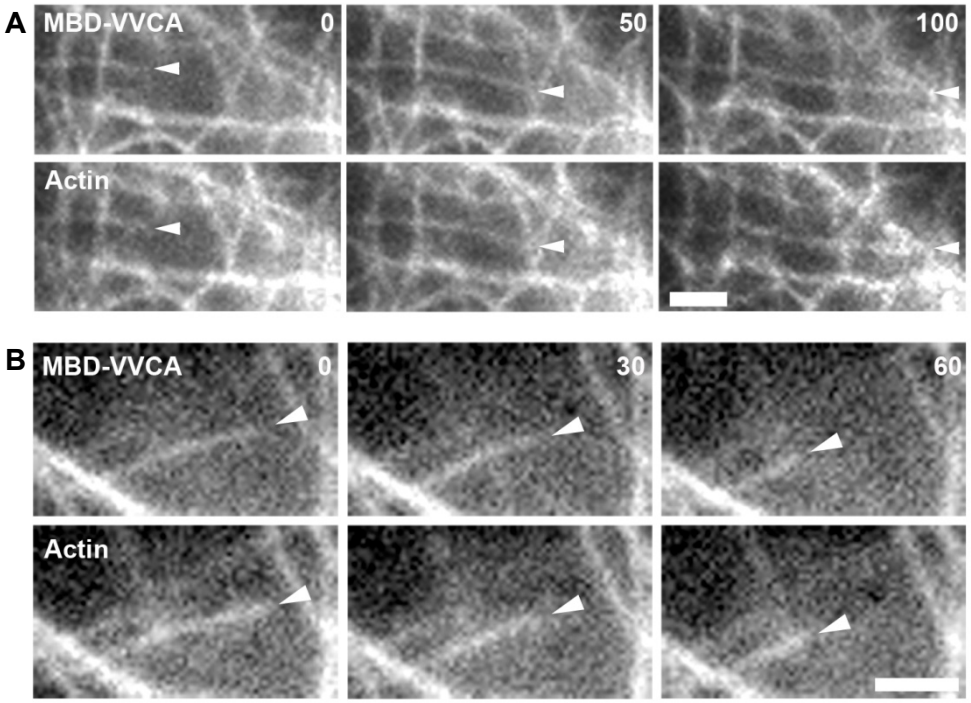

Figure 3-24: Actin filaments are instantly polymerized on growing and disassembled on shrinking microtubules.

Image sequences were taken from a time lapse movie of a cell transfected with MBD-VVCA and mCherry-actin. In (**A**) the arrowheads point to a growing microtubule, in (**B**) they indicate a shrinking microtubule. Time is in seconds; bars equal 2 µm.

Single microtubules of transfected B16-F1 cells were bleached with a 405 nm laser beam until the fluorescence was extinguished. The cell was further imaged for at least 180 s to allow the substitution of bleached and fluorescent MBD-VVCA molecules, which resulted in recovery of fluorescence on the microtubule. As depicted in the frames of a representative FRAP movie (Figure 3-25A), the microtubule was completely bleached in the circular region. After several seconds the molecules that were bound to the microtubule exchanged, and fluorescence nearly recovered after approximately 30 s. This effect could be also displayed in a diagram, in which the average fluorescence intensity, subtracted from background and acquisition photobleaching, was plotted over time. The time at half-maximal fluorescence recovery ($t_{1/2}$) is a measure of how fast molecules were exchanged. MBD-VVCA had a halftime of recovery of 7.7 s (Figure 3-25C), which was similar to the Arp2/3 complex activator WAVE in the lamellipodium (Lai et al., 2008). To determine the turnover of actin filaments polymerized on microtubules, mCherry-MBD-VVCA and EGFP-actin were co-transfected. EGFP-constructs were preferred as bleaching compounds in FRAP experiments, because the EGFP-tag was brighter and more stable during prolonged acquisition of cells. As shown in Figure 3-25B, mCherry-MBD-VVCA induced actin accumulation on microtubules as strongly as EGFP-MBD-VVCA. In analogy to the turnover measurements of MBD-VVCA also EGFP-actin that co-localized with MBD-

VVCA at microtubules (Figure 3-25B) was bleached and time-lapse movies were acquired. Calculation of the halftime of recovery (16 s) revealed that actin had a slower turnover rate (Figure 3-25D). So the turnover of MBD-VVCA is significantly higher than that of actin. One explanation for these differences could be that not every MBD-VVCA molecule binding to the microtubule necessarily succeeds in Arp2/3 complex activation and thus effecting actin assembly, which might lead to faster turnover rates observed for MBD-VVCA.

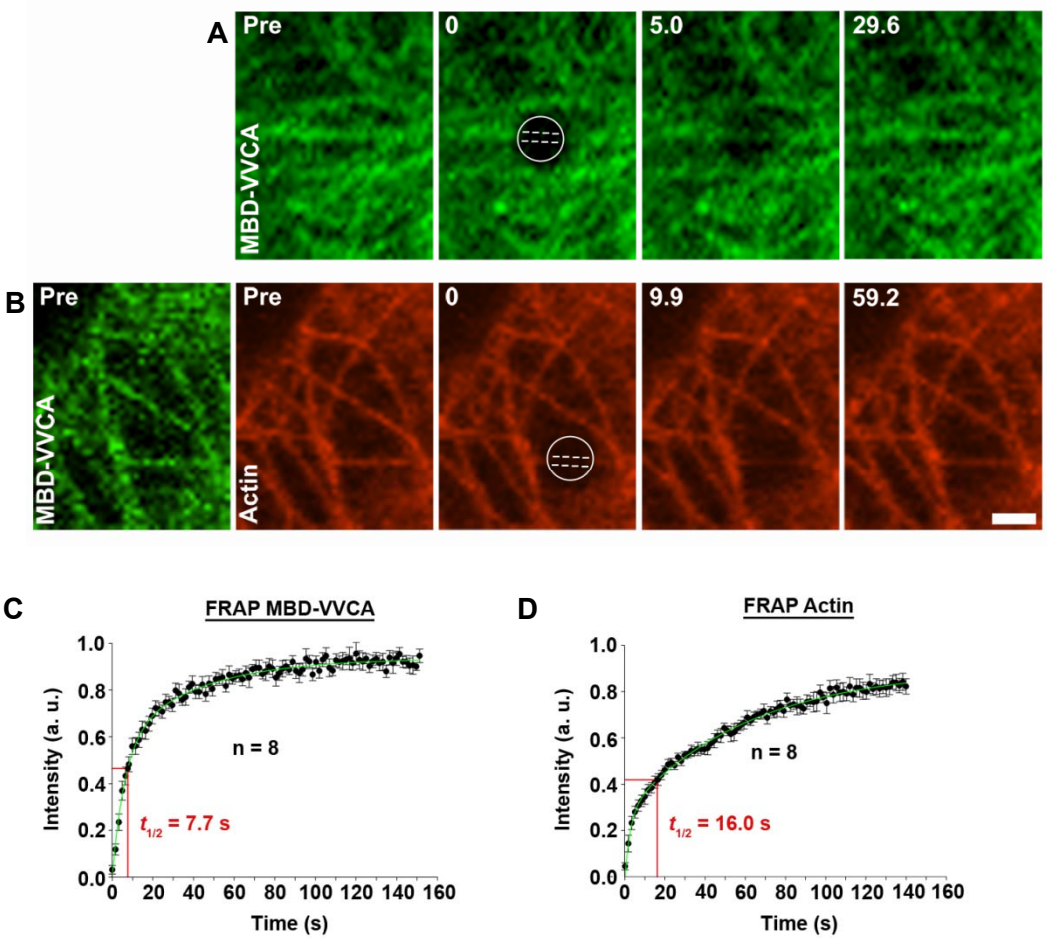

Figure 3-25: Turnover of MBD-VVCA and associated actin on microtubules.

(**A**, **B**) Frames from representative time-lapse movies of cells transfected with (A) EGFP-MBD-VVCA or (B) mCherry-MBD-VVCA and EGFP-actin, respectively. In (B) images are false-colored for clarity. Circles indicate the bleached areas and the broken lines the bleached microtubule. Time is in seconds; bar, 2 µm. (**C**, **D**) Fluorescence recovery curves derived from FRAP experiments as in (A, B). In (C) the fluorescence recovery of MBD-VVCA is plotted, in (D) the recovery curve of actin is depicted. $t_{1/2}$ values indicate the halftime of recovery and n corresponds to the number of movies analyzed.

3.2.5 Cortactin is not able to activate the Arp2/3 complex *in vivo*

The experiments with MBD-VVCA (see above) demonstrated that Arp2/3 complex activation via an NPF worked robustly in the MBD-assay. Next, the class II NPF cortactin was coupled to MBD instead of N-WASP-VVCA and thereby targeted to microtubules. The MBD-cortactin construct (MBD-Cttn) showed a dual specificity when

transfected into cells (Figure 3-26A and Supplementary Video 7). The MBD targeted the construct efficiently to microtubules, but it also localized to lamellipodia and microspikes mediated by cortactin. This fact already implied that the cortactin construct was functional and neither the EGFP-tag nor MBD affected protein function. However, in movies of cells expressing MBD-cortactin and actin, no overlap of both structures could be observed.

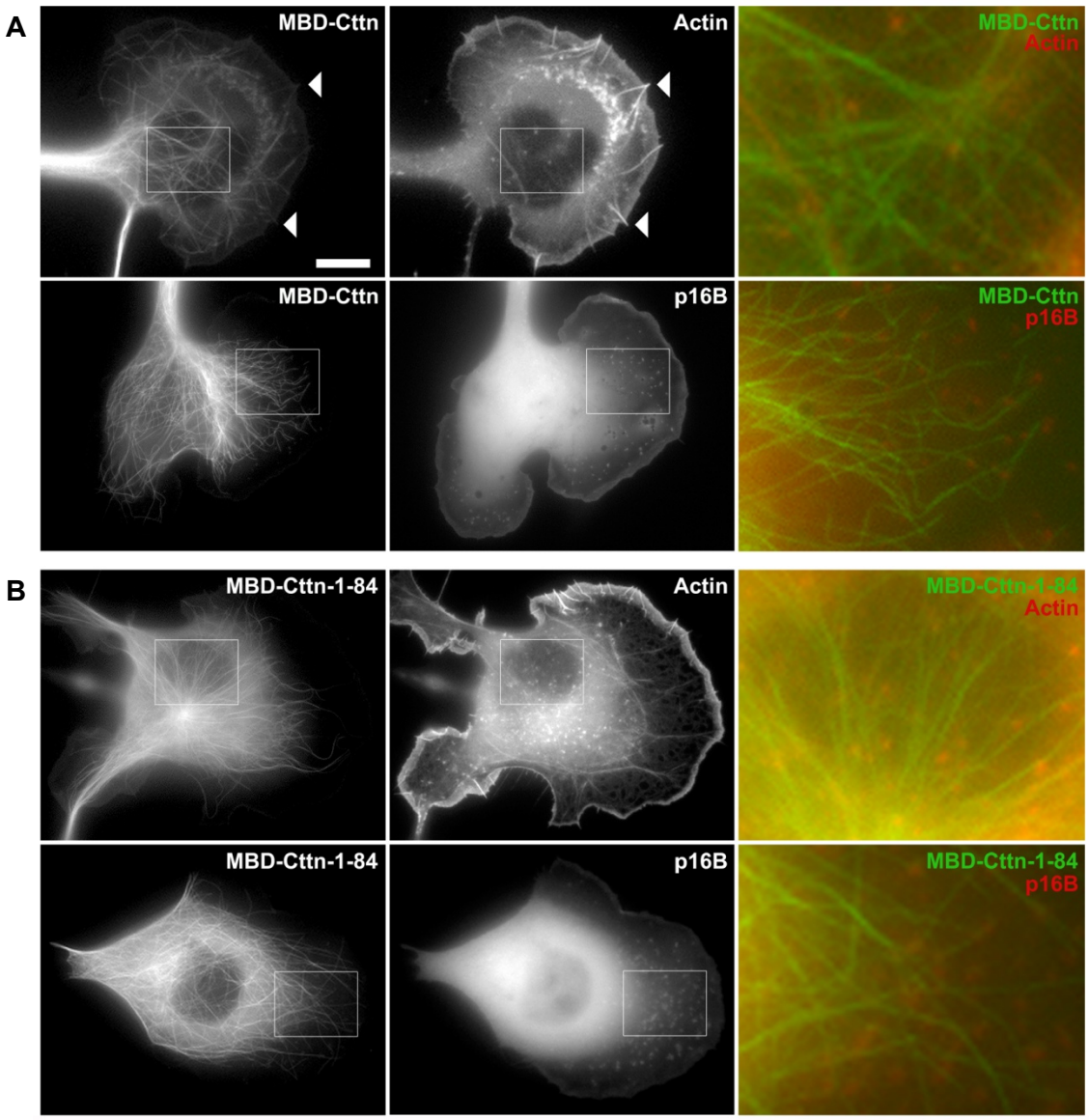

Figure 3-26: MBD-cortactin does not recruit or activate the Arp2/3 complex on microtubules.

Individual frames from representative movies of cells transfected with mCherry-actin or mCherry-p16B and (**A**) MBD-cortactin or (**B**) MBD-Cttn 1-84. Insets are shown as magnified merges in the right panel. Arrowheads point to microspikes co-localizing with cortactin. Bar, 10 µm.

Even more surprising, MBD-cortactin did not recruit the Arp2/3 complex to microtubules when it was co-transfected with mCherry-p16B (Figure 3-26A, Supplementary Video 8) in contrast to MBD-VVCA. To exclude the possibility that cortactin was not active on

microtubules due to missing regulatory factors, a second MBD-construct was cloned comprising only the NTA (aa 1-84), which is postulated to harbor the domain that binds to the Arp2/3 complex (Weaver et al., 2002; Weaver et al., 2001; Weed et al., 2000). However, again also this construct neither induced actin accumulation nor was able to recruit the Arp2/3 complex to microtubules (Figure 3-26B, Supplementary Videos 9 and 10). In conclusion with the experiments in the MBD-assay, cortactin did not show properties of an Arp2/3 complex activator *in vivo*, which together with the data derived from the genetic KO of cortactin (Lai et al., 2009 and chapter 23.1-3.1.4) strongly suggests that cortactin does not serve as an NPF in living cells.

3.2.6 Localization studies of cortactin constructs

As cortactin did not show any recruitment of the Arp2/3 complex to microtubules in the MBD-assay, localization studies with different cortactin constructs were employed to learn more about the domains that target cortactin to Arp2/3-rich structures such as lamellipodia or ruffles. Results from these studies could provide valuable information about domains mediating correct localization of cortactin and help to understand the function of cortactin *in vivo*.

For the localization studies of cortactin, three constructs were available. The first construct tested encoded EGFP-cortactin full-length. In agreement with previous studies (Weed et al., 2000), this construct localized to the lamellipodium and to ruffles on the ventral side of the cell (Figure 3-27 and Supplementary Video 11). Interestingly, cortactin full-length could be found in microspikes, which are embedded into the lamellipodium. A second construct consisted of the N-terminal acidic domain and the first 1.5 F-actin binding repeats (Cttn 1-146). This construct localized to the lamellipodium and to membrane ruffles similar to the full-length construct, but was not found in microspikes (Figure 3-27 and Supplementary Video 12), indicating that the domain that directs cortactin to microspikes had to be C-terminal of the cortactin 1-146 construct. The localization of cortactin 1-146 to the lamellipodium is in contradiction to published data from Weed et al. (Weed et al., 2000). The authors performed deletion studies of cortactin and concluded that the F-actin repeats no. 4 were essential for localization of cortactin to the cell periphery. Nevertheless, they did not test a 1-146 aa construct and used a different cell type in their study.

As outlined in chapter 1.1.6.3, cortactin binds to the Arp2/3 complex via the NTA and to F-actin with 6.5 F-actin binding repeats. To investigate whether Arp2/3-binding mediated the localization of cortactin to the cell periphery, a construct only comprising the Arp2/3 binding surface (cortactin 1-84) was transfected into B16-F1 cells. As displayed in Figure 3-27 and Supplementary Video 13, this construct was entirely

cytosolic and did neither localize to the lamellipodium nor to ruffles. This data indicate that the Arp2/3-binding domain of cortactin is not sufficient to mediate the localization of the protein to the cell periphery. The fact that full-length cortactin also accumulated in microspikes (white arrow in Figure 3-27), which are largely devoid of Arp2/3 complex (Svitkina and Borisy, 1999) adds to evidence indicating interactions with factors other than Arp2/3 to contribute to subcellular cortactin positioning. Thus, cortactin localization is not solely and perhaps not directly dictated by the presence of Arp2/3 complex, and whether its association with microspikes is exclusively determined by interactions with actin filaments remains to be established.

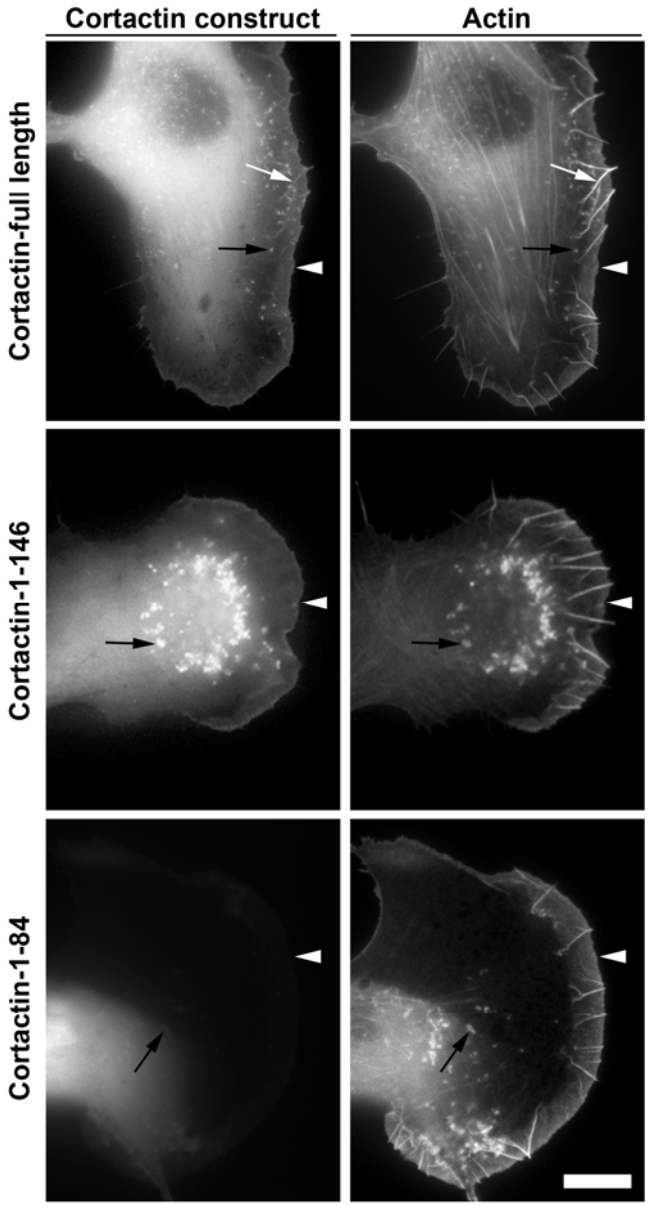

Figure 3-27: Localization of cortactin full length and truncated cortactin constructs.

Epifluorescence images of B16-F1 cells transfected with mCherry-actin and either EGFP-cortactin full-length, cortactin-1-146 or cortactin 1-84, as indicated. Arrowheads mark lamellipodia, the white arrow points to a microspike co-localizing with cortactin full-length, and the black arrows indicates ruffles or vesicles at the ventral side of the cells. Bar, 10 µm.

3.2.7 The nucleators Drf3ΔDAD and Spir-NT induce actin polymerization on microtubules when fused to MBD

Apart from the Arp2/3 complex, cells have developed other mechanisms for the nucleation of actin filaments. Formins stabilizes actin dimers and trimers with their FH2 domains and thereby trigger actin nucleation, whereas tandem G-actin-binding proteins bind three or four actin monomers and thereby generate actin nuclei that can spontaneously polymerize into filaments. These latter nucleators include leiomodin and Cobl with three and Spir with four actin binding domains (see 1.1.7 and 1.1.8 for details). Both the constitutively active formin Drf3ΔDAD and the N-terminal domain of Spir comprising the four WH2-domains and the KIND-domain were cloned into MBD-vectors and expressed in B16-F1 cells. As displayed in Figure 3-28A and B, MBD-Drf3ΔDAD and MBD-Spir-NT nucleated actin filament assemblies on microtubules. MBD-Spir-NT was a strong nucleator, comparable to MBD-VVCA, since virtually all transfected cells displayed a robust phalloidin staining on microtubules (not shown).

It was shown in *in vitro* assays that the last two WH2-domains of Spir (Spir-CD), which are connected with a so-called monomer binding linker (MBL), were sufficient for efficient actin nucleation (Zuchero et al., 2009). To test if these findings are also valid *in vivo*, an MBD-Spir-CD construct was cloned and transfected into B16-F1 cells. Indeed, MBD-Spir-CD induced actin accumulation on microtubules comparably strong to Spir-NT demonstrating that also in the living cell the last two WH2-domains of Spir are able to nucleate actin filaments (Figure 3-28C). In contrast, MBD-Drf3ΔDAD showed weak, yet clearly detectable actin nucleation efficiency, although *in vivo* studies identified the formin to be a potent nucleator (Block et al., 2008). An explanation for this discrepancy could be that in the MBD-assay, Drf3ΔDAD is potentially kept tightly bound to the microtubule surface, counteracting the processivity of the formin when driving actin filament elongation after nucleation. This activity of the formin would not be constrained in a comparable way in filopodia tips, where Drf3 usually drives actin polymerization. Notwithstanding this live cell imaging with cells that co-expressed mCherry-actin unambiguously demonstrated that MBD-Drf3ΔDAD and MBD-Spir-NT induced actin accumulation on microtubules (Supplementary Videos 14 and 15). To probe if the actin nucleation of Drf3ΔDAD and Spir-NT occurs independently of Arp2/3 complex, cells were transfected with the respective nucleator fused to MBD, and stained with an anti-p16A antibody.

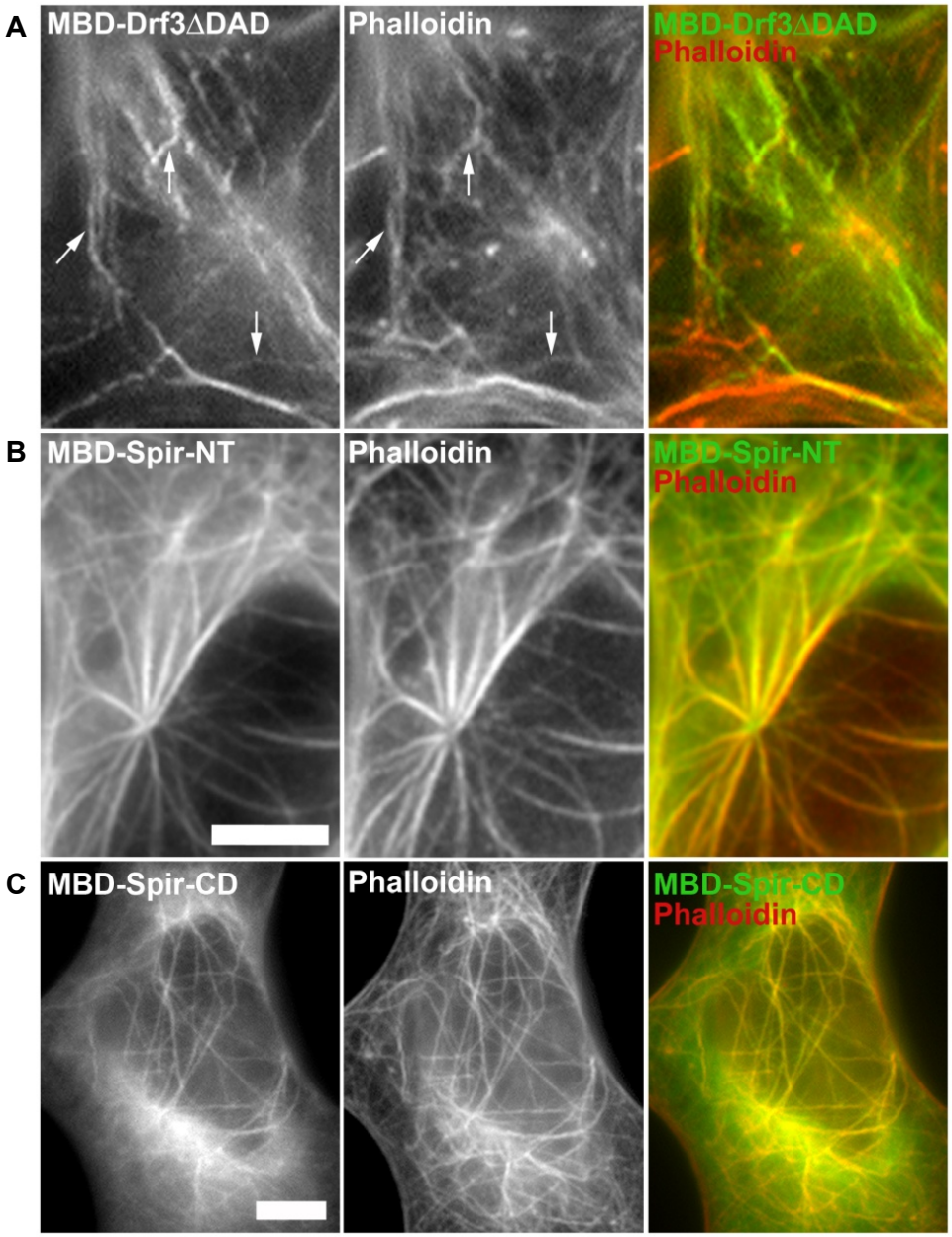

Figure 3-28: MBD-Drf3ΔDAD, MBD-Spir-NT and MBD-Spir-CD nucleate actin on microtubules.

Phalloidin stainings of cells transfected with (**A**) MBD-Drf3ΔDAD, (**B**) MBD-Spir-NT or (**C**) MBD-Spir-CD (CD: the last two WH2-domains of Spir including the MBL sequence), respectively. Arrows and merged images on the right indicate co-localization of F-actin and MBD-constructs. Bar, 5 µm.

As displayed in Figure 3-29, the Arp2/3 complex subunit p16A localized to the lamellipodium and dot-like structures in the lamella in an untransfected cell, but was completely absent from the microtubule-bound nucleators, which strongly indicated that the actin structures induced by both nucleators were assembled independently of the Arp2/3 complex.

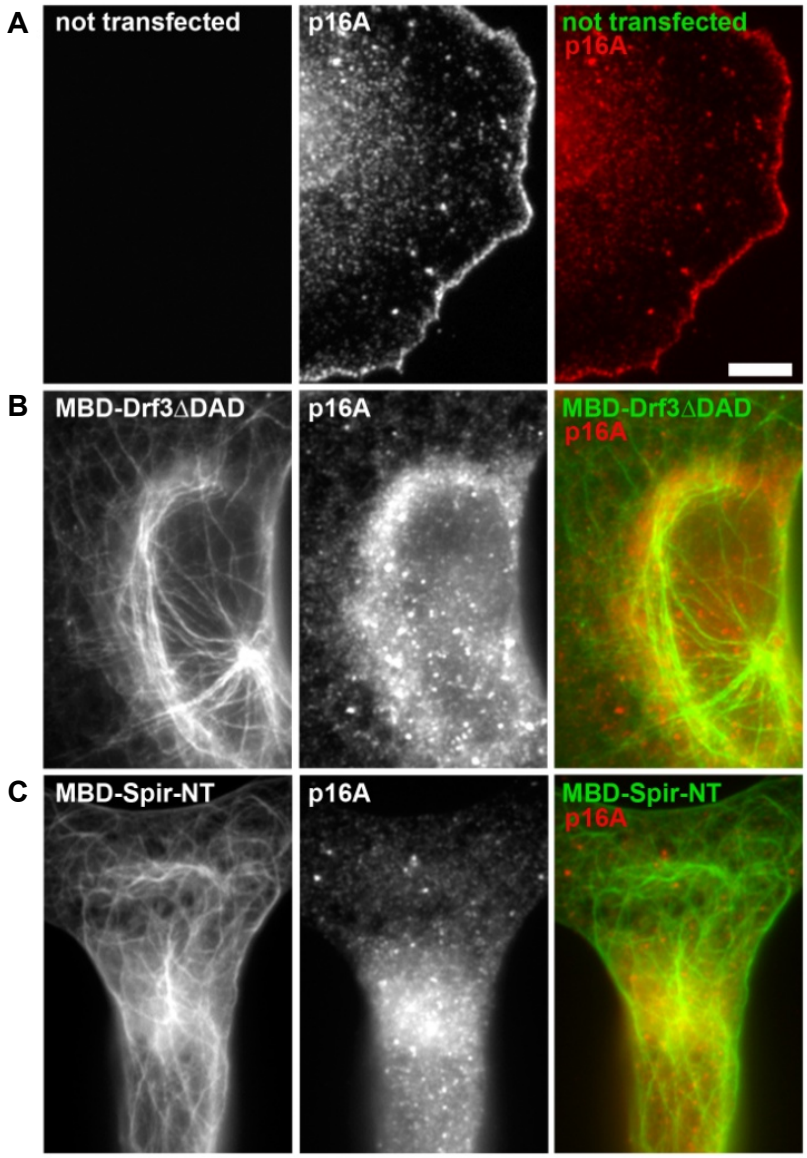

Figure 3-29: Drf3ΔDAD and Spir-NT nucleate actin independently of the Arp2/3 complex.

Epifluorescence images of an untransfected cell (**A**) and cells expressing MBD-Drf3ΔDAD (**B**) or MBD-Spir-NT (**C**), respectively, which were stained with an anti-p16A-antibody. The antibody labels the lamellipodium in the untransfected cell (A) and does not co-localize with the indicated MBD-constructs. Bar, 5 µm.

3.2.8 Actin nucleation by clustering of actin monomers

A shown in chapter 3.1.8, proteins or protein domains associating with actin filaments did not induce actin accumulation on microtubules. However, another MBD-construct with actin filament binding capacity was cloned comprising Lifeact, a peptide of 17 aa encoding the actin binding domain of Abp140, which is expressed in *S. cerevisiae* (Riedl et al., 2008). In biochemical assays, Lifeact binds both actin filaments and actin monomers, although the latter with 30-fold less affinity. The actin binding domain is conserved among close relatives of *S. cerevisiae* but absent from other organisms (Riedl et al., 2008). Nevertheless, structural features of Lifeact resemble those of thymosin β_4, a protein known to sequester G-actin and closely related to WH2-domains

(Carlier et al., 2007). Initially thought as a negative control to exclude that actin filament binding is sufficient to induce actin assembly on microtubules in case of fascin and the ABD of α-actinin, expression of MBD-Lifeact in B16-F1 cells led to actin filament accumulation on microtubules (Figure 3-30). This was verified both by phalloidin stainings (Figure 3-30) and live cell imaging of cells co-expressing mCherry-actin (not shown). As Lifeact has the ability to bind both actin filaments and actin monomers, it was impossible to determine, which of the actin binding properties of Lifeact triggered actin assembly on microtubules. However, previous experiments with F-actin binding proteins indicated, that filament recruitment is not sufficient to target actin accumulation to microtubules. Another explanation for Lifeact-induced actin assemblies was that MBD-Lifeact nucleated actin by recruiting actin monomers to the microtubule surface and thereby enhanced the local actin concentration, which allowed actin nucleus formation. To test if clustering of actin monomers on microtubules could in principle lead to actin polymerization, actin was fused to MBD thereby directly targeting actin to microtubules. Indeed, MBD-actin also induced actin assembly on microtubules (Figure 3-30), providing evidence that high concentration of actin can induce actin nucleation, suggesting that also Lifeact could nucleate actin filaments via monomer clustering.

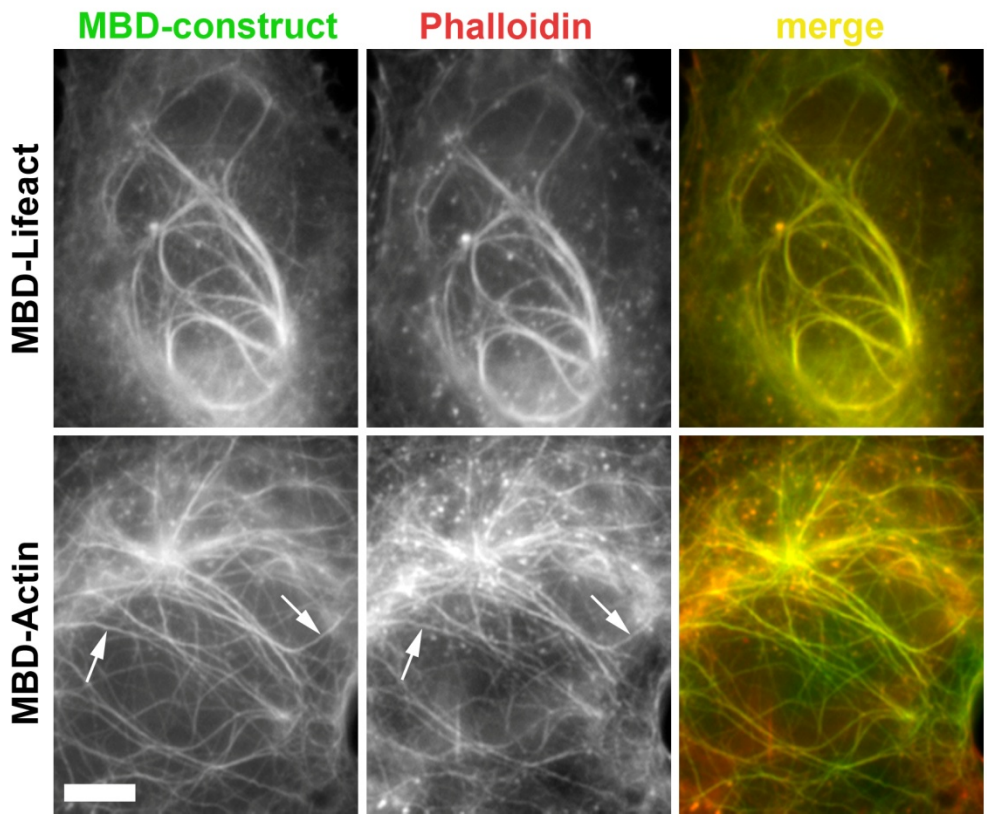

Figure 3-30: Actin polymerization can be induced by monomer clustering.

Phalloidin stainings of cells transfected with MBD-Lifeact (upper panel) or MBD-actin (lower panel). Arrows and merges show co-localization of both MBD-constructs with F-actin. Bar, 5 µm.

The possibility that actin monomer clustering by actin binding domains could nucleate actin filaments raised the question, whether actin polymerization on microtubules induced by MBD-VVCA as in Figure 3-19 was truly Arp2/3 complex-dependent or whether the two isolated WH2-domains of N-WASP that were shown to bind actin monomers *in vitro* (Chereau et al., 2005) nucleated actin on their own. When the two N-WASP WH2-domains (VV) fused to MBD were expressed in cells, no Arp2/3 complex recruitment occurred, as expected, as no Arp2/3-binding domain was present in the truncated N-WASP construct (Figure 3-31 and Supplementary Video 16).

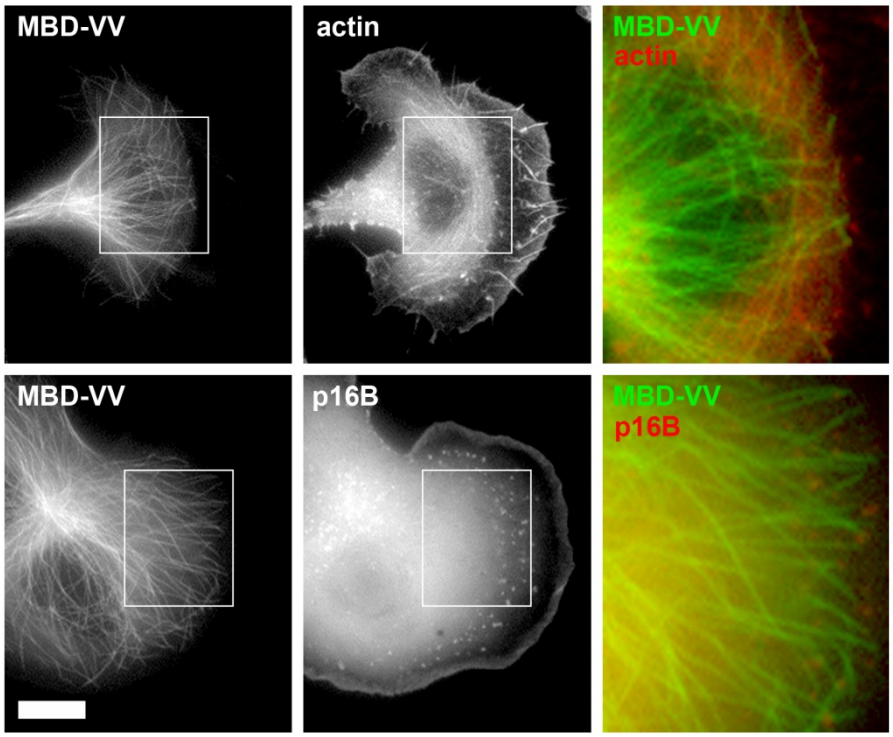

Figure 3-31: The two WH2-domains of N-WASP are unable to nucleate actin on microtubules.

Frames from time-lapse movies of cells transfected with MBD-VV (VV: the two WH2 domains of murine N-WASP) and actin (upper panel) or p16B (lower panel), respectively. The inset is shown in large on the right side. Bar, 10 µm.

Co-expression with mCherry-actin revealed that also no actin assemblies were visible on microtubules (Figure 3-31 and Supplementary Video 17), proving that MBD-VV was not able to nucleate actin, thus MBD-VVCA-induced actin polymerization seemed to be indeed dependent on Arp2/3 complex activation. On the other hand, actin monomer binding alone does not seem to be sufficient to induce actin polymerization on microtubules. Probably, a specific arrangement of actin binding domains is necessary to efficiently nucleate actin by monomer clustering. In comparison with the two WH2-domains that consist of 68 aa, Lifeact with its 17 aa presumably has the flexibility to bring three actin monomers in close contact leading to actin nuclei. The same effect

could be simulated by directly coupling actin to MBD, the only difference being the absence of the actin binding peptide Lifeact.

3.2.9 Minimal requirements of N-WASP-induced actin polymerization

For the examination of N-WASP-dependent actin nucleation, most commonly the VVCA-fragment is used as in this thesis, because it harbors both the WH2-domains thought to deliver actin monomers to the Arp2/3 complex, and the C- and A-domain, which bind to and activate the Arp2/3 complex. The A-domain contains a conserved tryptophan residue, which is considered to be essential for NPF function of N-WASP and WAVE and also in the case of cortactin (see 1.1.6.1). However, a recent study showed that although a higher concentration of Arp2/3 complex was needed, the VVC domain immobilized on artificial vesicles was able to induce actin polymerization and promoted vesicle movement indicating that the A-domain of N-WASP is not essential for reconstituted actin-based motility (Delatour et al., 2008). Still, VVC-induced actin filament arrays were two-fold less dense than those induced by N-WASP. The relevance of the A-domain *in vivo* remained unclear, so an MBD-VVC construct was generated lacking the A-domain. Figure 3-32A shows robust phalloidin staining on microtubules, demonstrating that actin filaments were still polymerized, even in the absence of the A-domain.

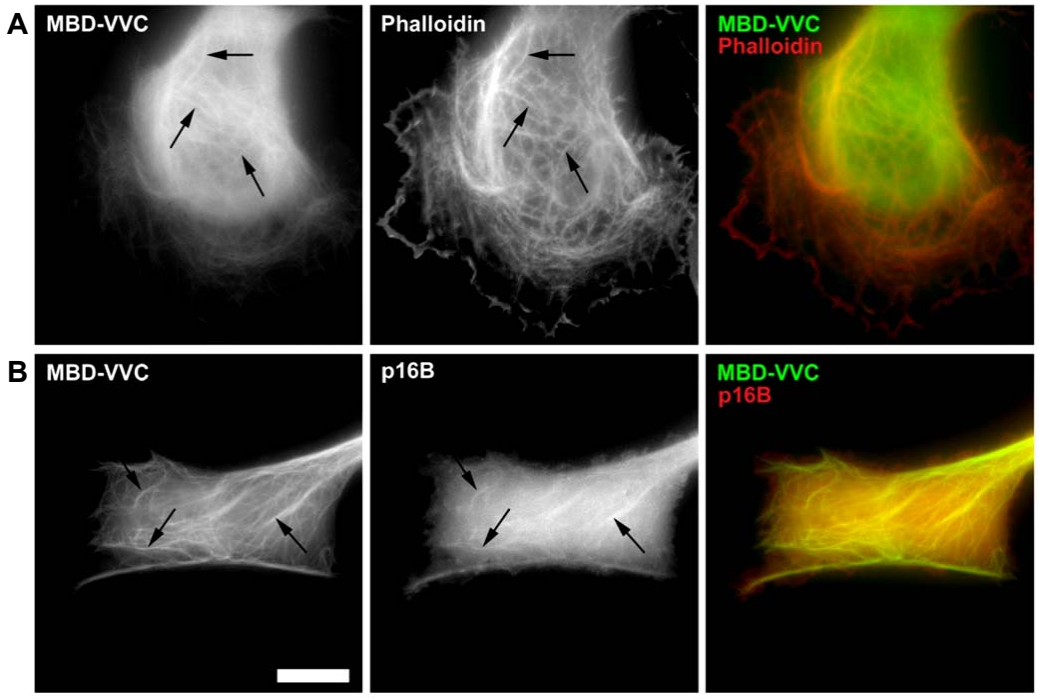

Figure 3-32: The N-WASP A-domain is dispensable for Arp2/3 activation.

(**A**) Phalloidin staining of a cell transfected with MBD-VVC. Arrows indicate co-localization of the MBD-construct and F-actin. (**B**) Individual frame from a time-lapse movie of a cell expressing MBD-VVC and p16B showing partial co-localization of both proteins (arrows). Merged images with MBD-VVC in green and the respective mCherry-construct in red are shown in the right panel. Bar, 10 µm.

When MBD-VVC was co-transfected with mCherry-p16B, a recruitment of the latter was observable, although the efficiency was strongly reduced compared to Arp2/3 complex recruitment by MBD-VVCA (Figure 3-32B). The differences in Arp2/3 complex recruitment and actin nucleation of MBD-VVCA as compared to MBD-VVC and MBD-VV were quantified by live cell imaging. Cells were transfected with the respective MBD-construct and either mCherry-actin or mCherry-p16B, and using epifluorescence microscopy the number of cells displaying co-localization of the constructs on microtubules was determined (Figure 3-33).

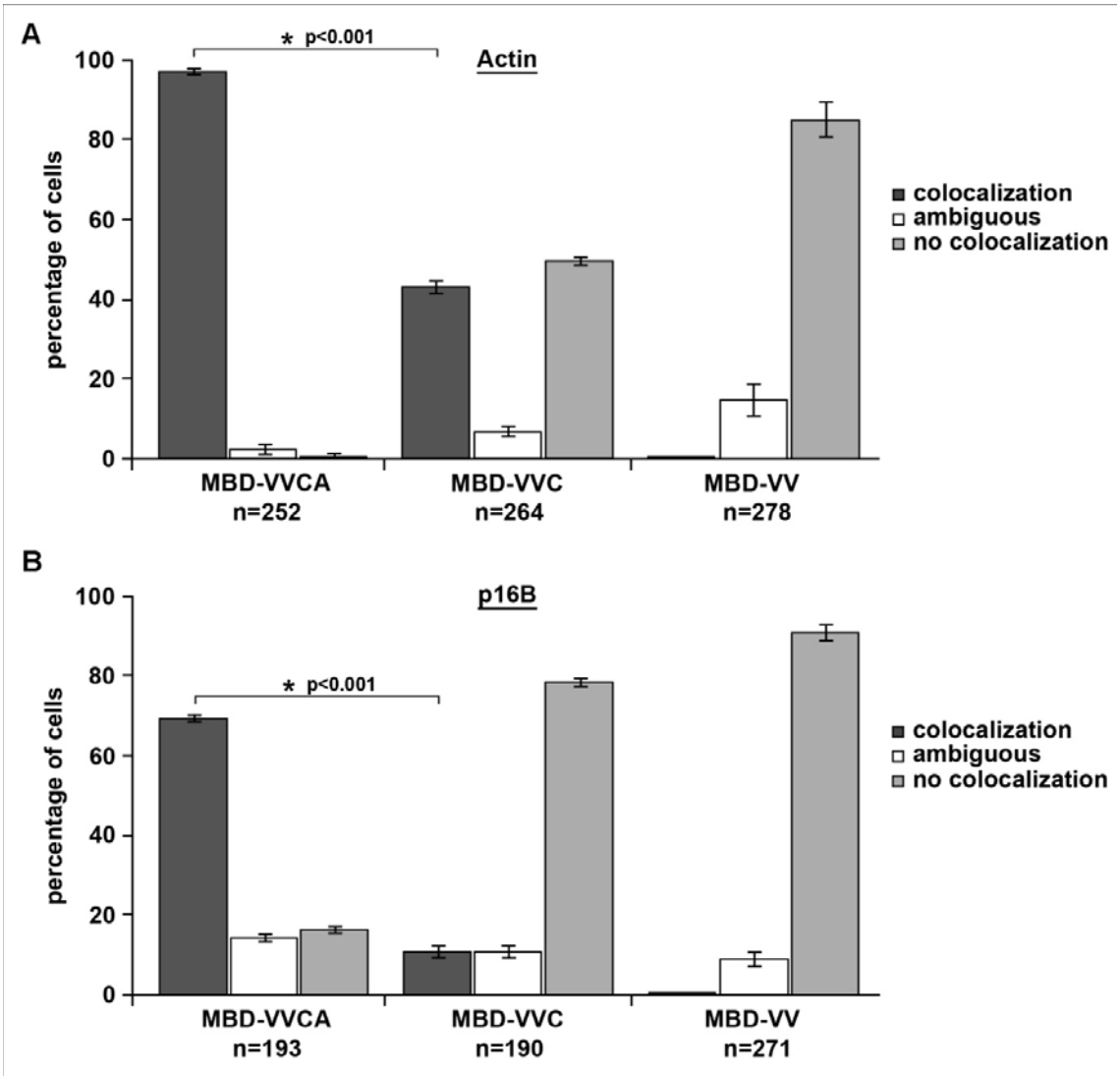

Figure 3-33: Quantification of actin assembly on and Arp2/3 recruitment to microtubules in cells expressing MBD-VVCA, MBD-VVC and MBD-VV.

Cells were transfected with the respective MBD-construct and either mCherry-actin or mCherry-p16B. Transfected cells were classified concerning the co-localization of MBD-constructs with (**A**) actin or (**B**) p16B. Categories were with co-localization, without co-localization and ambiguous, the latter mostly applying to cells that overexpressed both constructs. Data are means and standard errors of means (error bars). n corresponds to number of cells analyzed, and asterisks with corresponding p-values indicate differences to be statistically significant.

In almost all cells transfected with MBD-VVCA and actin, a co-localization on microtubules was visible, but in case of MBD-VVC this number was reduced to 43.2%. The recruitment of the Arp2/3 complex was clearly seen in 69.4% of cells expressing MBD-VVCA, but the construct lacking the A-domain recruited Arp2/3 complex to microtubules only in 10.7% of the cells. Strikingly, the number of cells with apparent Arp2/3 complex co-localization was lower with both constructs compared to the number of cells quantified for actin accumulation on microtubules. This might simply be due to reduced efficiency of Arp2/3 complex detection on microtubules, since neither actin nor Arp2/3 accumulation was detectable in the absence of an Arp2/3-binding domain (MBD-VV). The data unambiguously proved that the A-domain was not essential for the recruitment as well as the activation of Arp2/3 complex on microtubules. To verify that the A-domain was also non-essential in a more physiological *in vivo* process, reconstitution experiments of actin tail formation in N-WASP KO cells were performed. The formation of actin tails by *Shigella* is N-WASP-dependent, as this NPF is recruited to the *Shigella* surface to polymerize actin filaments that form the actin tail and propel the bacteria through the cell (see also 1.1.16). Accordingly, no actin tails are formed in cells lacking N-WASP, but EGFP-N-WASP constructs can reconstitute this phenotype (Lommel et al., 2001).

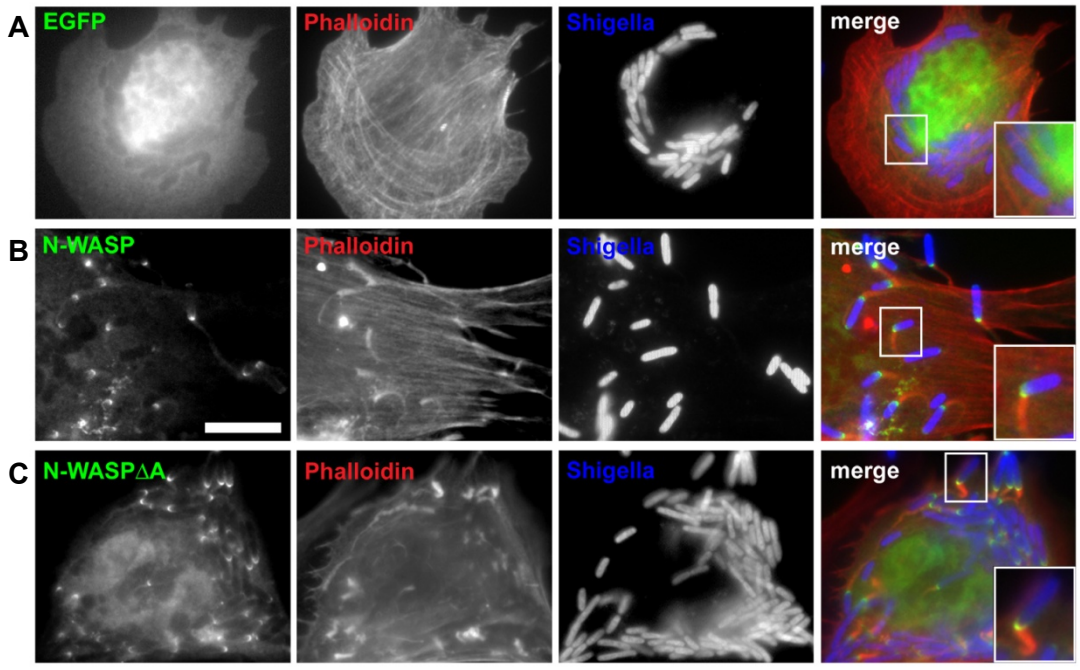

Figure 3-34: N-WASPΔA reconstitutes *Shigella*-induced actin tail formation in N-WASP-deficient cells.

Immunofluorescence and phalloidin stainings of N-WASP null cells expressing (**A**) EGFP, (**B**) N-WASP full-length or (**C**) N-WASPΔA infected with *Shigella flexneri*. The magnified insets in the right panel show individual bacteria with or without actin tails, depending on the construct transfected. Bar, 5 µm.

To test if the A-domain was also dispensable for actin tail formation, N-WASP-deficient cells were transfected with either EGFP, EGFP-N-WASP full-length or EGFP-N-WASPΔA and infected with *S. flexneri* followed by immunofluorescence staining of the bacteria and F-actin (Figure 3-34). In cells expressing EGFP, no actin tails could be observed, as expected. However, both N-WASP full-length and N-WASPΔA-expressing cells formed prominent actin tails, although the frequency was reduced in the latter. Nevertheless, N-WASPΔA clearly reconstituted the missing NPF, so the dispensability of the acidic domain was confirmed in the *Shigella* actin tail formation assay. These results provided evidence that the data obtained in the MBD-assay mirrored the *in vivo* mode of Arp2/3 activation by N-WASP for which the A-domain is helpful but not essential.

3.2.10 Applying the MBD-assay for co-localization studies

The MBD-assay could not only be used to elucidate whether a given factor led to actin nucleation, but also which proteins were recruited downstream of distinct actin nucleation machineries. For this kind of experiments, the MBD-construct of a nucleator or nucleation promoting factor was simply co-expressed with the protein tested for its co-localization with the actin assemblies induced. In principle, one example of these experiments already shown is the recruitment of the Arp2/3 complex by MBD-VVCA (see Figure 3-19).

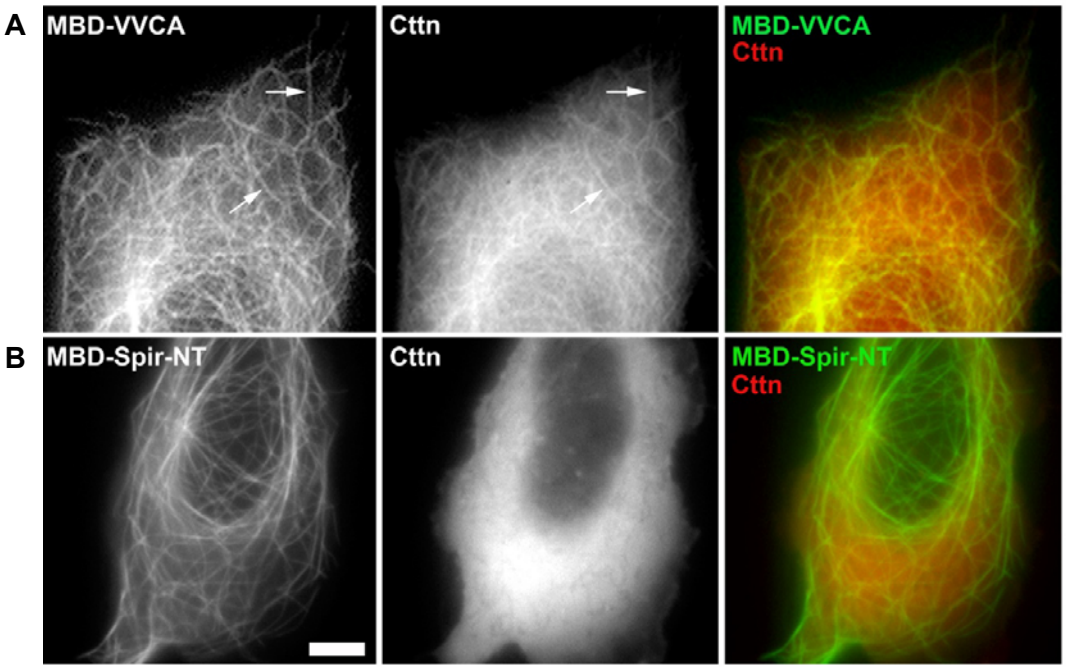

Figure 3-35: Cortactin is recruited to Arp2/3 complex-mediated but not Spir-induced actin structures.

Individual frames from time-lapse movies of cells co-expressing cortactin and (**A**) MBD-VVCA or (**B**) MBD-Spir-NT. In merged images on the right, yellow color indicates co-localization of both constructs. Arrows in (A) point to co-localization of MBD-VVCA and cortactin. Bar, 5 µm.

As displayed in 3.1.11, cortactin did not induce actin polymerization in the MBD-assay. Yet, EGFP-tagged as well as endogenous cortactin localizes to sites of active, Arp2/3-dependent actin nucleation, such as lamellipodia, dorsal ruffles, podosomes or actin comet tails induced by bacteria. This notion and *in vitro* experiments led to the assumption that cortactin can also drive in the activation of the Arp2/3 complex, which could neither be confirmed by analysis of cortactin-deficient MEFs nor by applying the MBD-assay. However, it was interesting to investigate whether cortactin was also present at Arp2/3-dependent actin polymerization sites induced by MBD-VVCA.

To test this, cells were transfected with mCherry-MBD-VVCA and EGFP-cortactin and subjected to fluorescence microscopy. As shown in Figure 3-35A, there was indeed a strong co-localization of MBD-VVCA and cortactin. So cortactin recruitment coincided with actin nucleation induced by the Arp2/3 complex on microtubules as in other *in vivo* processes, although its role was most likely not the activation of the nucleator. To test whether cortactin recruitment is specific for Arp2/3-dependent actin nucleation, a second and comparably strong nucleator, Spir-NT, was co-transfected with cortactin. In these cells, no overlap between the MBD-construct and cortactin was discernable as MBD-Spir-NT localized to microtubules and cortactin was diffusely distributed in the cytoplasm (Figure 3-35B) or localized to the cell periphery (not shown). Thus, the localization of cortactin to Arp2/3 complex-induced actin nucleation on microtubules appeared to be specific, as it did not occur with Spir.

Another protein previously implicated in the regulation of Arp2/3-dependent lamellipodia formation is capping protein. It localizes throughout the lamellipodium, and was found to be an essential lamellipodial component, as knockdown of capping protein completely abolishes lamellipodia, although the mechanism of capping protein function is still elusive (Mejillano et al., 2004). Capping protein is also required for Arp2/3-dependent reconstituted actin-based motility together with ADF/cofilin (Loisel et al., 1999). It is currently unknown, which factor determines capping protein localization to the lamellipodium, and how capping protein is able to distinguish between actin filaments nucleated by Arp2/3 complex and other nucleators. To test capping protein localization in cells with ectopic actin filament arrays nucleated by Arp2/3 or Spir-NT, respectively, capping protein was co-transfected with MBD-VVCA and MBD-Spir-NT. In almost all cells analyzed that were transfected with MBD-VVCA capping protein localized to the microtubule network (Figure 3-36).

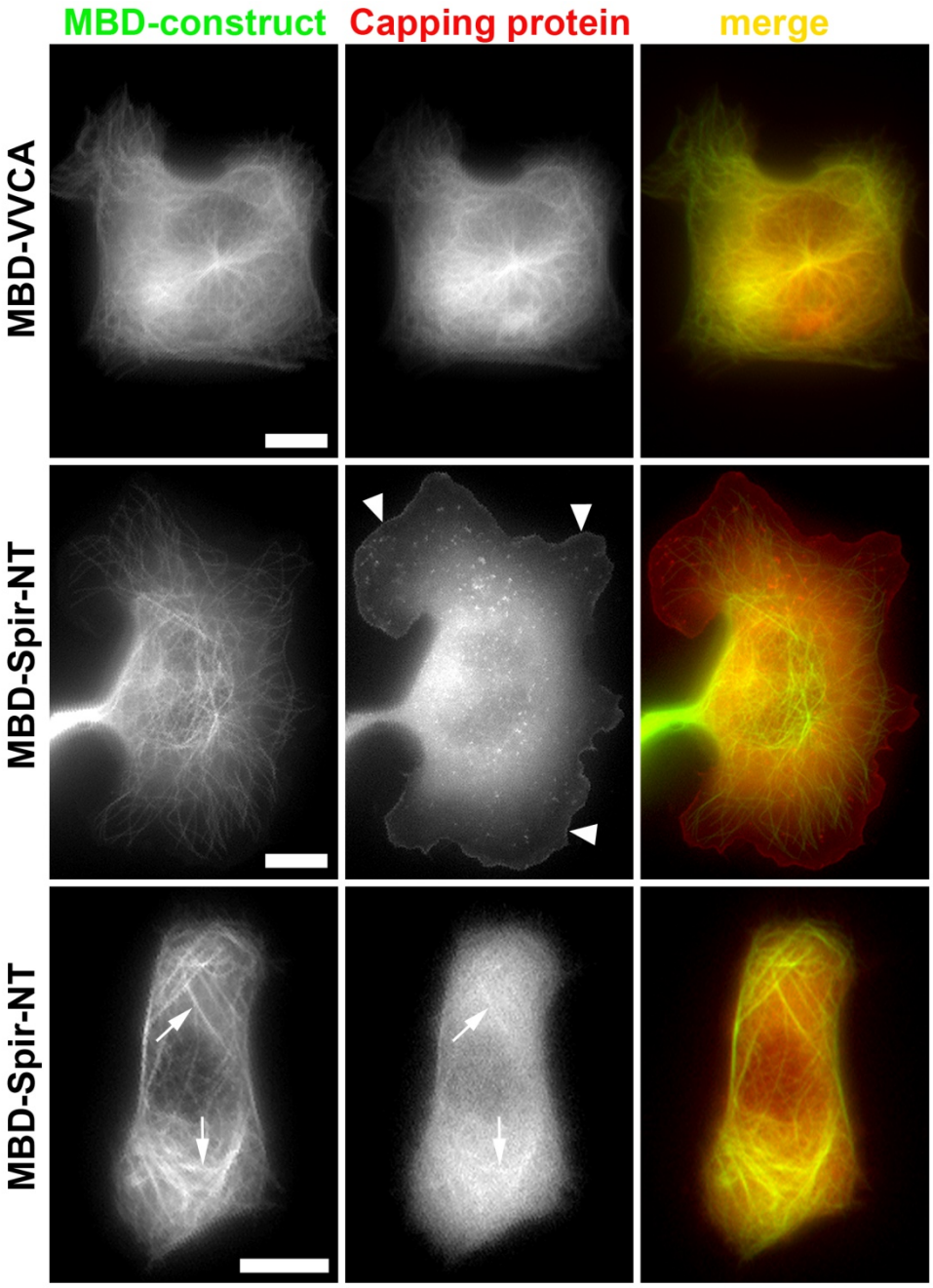

Figure 3-36: Capping protein is predominantly recruited to Arp2/3- and not Spir-NT-induced actin filament assemblies.

Representative epifluorescence images of B16-F1 cells expressing capping protein and MBD-VVCA (first panel) or MBD-Spir-NT (second and third panel). Arrowheads indicate lamellipodial localization of capping protein and arrows the weak co-localization of MBD-Spir-NT with capping protein. Bars, 10 µm.

This was also represented in the quantification, where more than 90% of the cells showed recruitment of capping protein (Figure 3-37). In contrast, in most cells transfected with MBD-Spir-NT capping protein did not localize to the MBD-construct but to lamellipodia, and even when a co-localization was visible (in 16% of cells, see Figure 3-37) the co-localization was significantly weaker compared to the average of cells observed, which were transfected with MBD-VVCA (Figure 3-36).

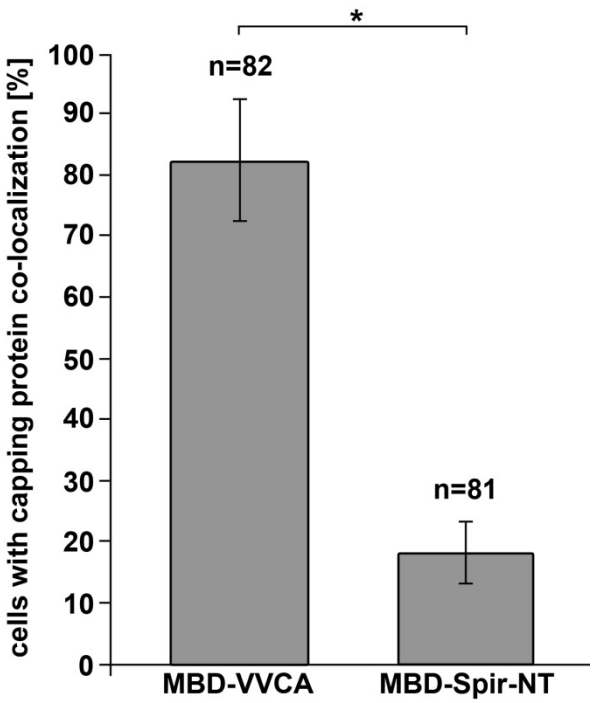

Figure 3-37: Quantification of capping protein co-localization in cells expressing MBD-VVCA or MBD-Spir-NT.

Cells expressing capping protein and either MBD-VVCA or MBD-Spir-NT (for representative images see Figure 3-36) were classified regarding the co-localization of the indicated MBD-constructs with capping protein. Data are means and standard errors of means (error bars). n corresponds to number of movies analyzed and asterisks indicate statistically significant differences with $p \leq 0.05$.

3.2.11 MBD-capping protein does not induce actin accumulation on microtubules

As displayed above, the Arp2/3 complex or factors co-recruited to Arp2/3-induced actin filament arrays seem to determine capping protein localization, as capping protein was specifically recruited to actin accumulations mediated by MBD-VVCA. In a following experiment it was tested, whether capping protein is able to target the Arp2/3 complex nucleation machinery to microtubules, or even nucleates actin on its own as was reported by Caldwell et al. in *in vitro* experiments (Caldwell et al., 1989). For this purpose, an MBD-capping protein-β2 construct was cloned. As capping protein is only active as heterodimer consisting of a β2 and α1 subunit, it was first tested, if the MBD-construct was able to recruit the isoform α1. So both MBD-capping protein-β2 and capping protein-α1 coupled with different fluorescent dyes were expressed in B16-F1 cells. As displayed in Figure 3-38A, MBD-capping protein β2 recruited capping protein α1 isoform, which suggested that the two capping protein subunits were able to associate in spite of the fluorescent protein tags and the MBD and were co-recruited as functional unit to the microtubule surface. However, when MBD-capping protein was co-transfected with mCherry-actin, no actin accumulation on microtubules was

discernable (Figure 3-38B). This indicates that capping protein does not determine the localization of Arp2/3-dependent actin polymerization, but rather binds to existing Arp2/3-induced actin arrays. Moreover, capping protein does not seem to nucleate actin filaments on its own *in vivo*.

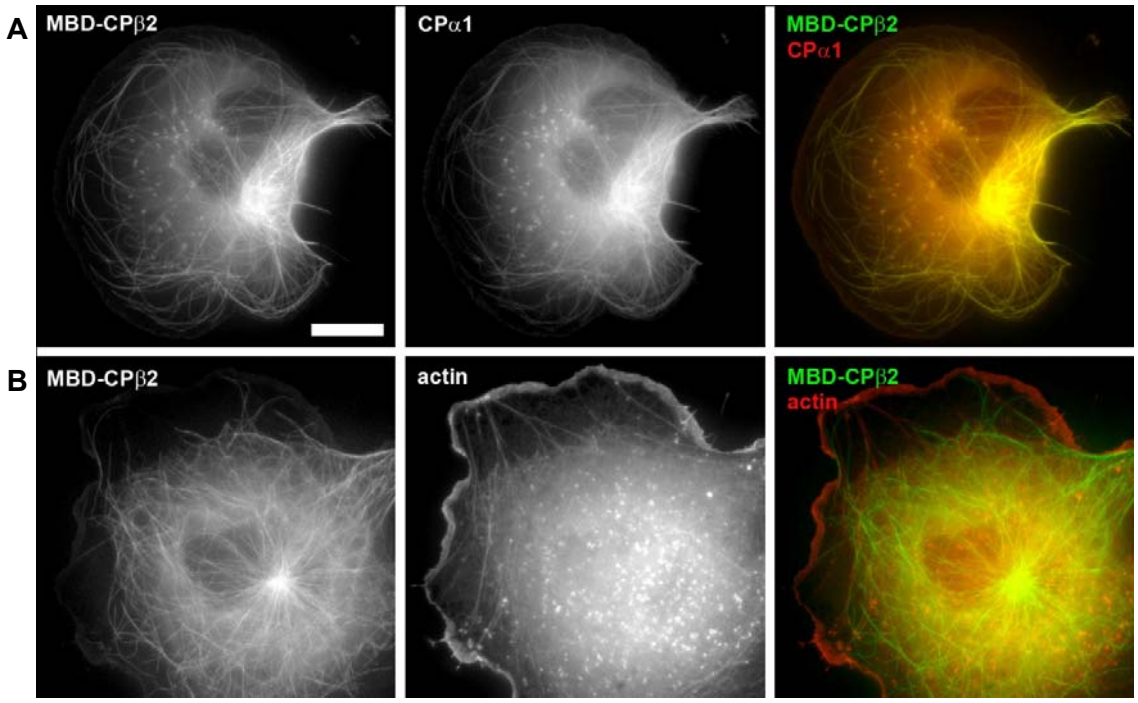

Figure 3-38: MBD-capping protein-β2 recruits capping protein-α1, but does not induce actin accumulation on microtubules.

Individual frames of time lapse movies from B16-F1 cells transfected with EGFP-MBD-CPβ2 and (**A**) mCherry-CPα1 or (**B**) mCherry-actin. Merged images on the right demonstrate that MBD-CPβ2 recruits CPα1, but it does not co-localize with actin. Bar, 10 µm.

In conclusion, the MBD-assay allows examining the nucleation or nucleation promoting activity of a given protein in the cytoplasm of the cell with a simple readout, namely the polymerization of actin filaments on microtubules. In the MBD-assay, N-WASP-VVCA induced actin polymerization through Arp2/3 complex activation, for which the A-domain was dispensable. Cortactin did not recruit or activate the Arp2/3 complex *in vivo* suggesting that it does not act as a NPF, which is in line with results obtained from cortactin-deficient cells. Altogether, the MBD-assay constitutes a versatile tool for the examination of the different nucleation machineries in the complex environment of the cytoplasm.

4 Discussion and Outlook

The actin cytoskeleton is key to various cellular processes, such as cell migration, endocytosis or cell adhesion. The property of the actin cytoskeleton to dynamically remodel upon intracellular or extracellular signals depends both on the tight regulation of actin polymerization in the cytoplasm and the constantly rising number of actin modulators. The actin-associated protein cortactin was identified to bind filamentous actin and the actin nucleator Arp2/3 complex. Cortactin localizes to sites of active Arp2/3-dependent actin assembly, which implicated a role for cortactin in the nucleation process (Weaver et al., 2002; Weaver et al., 2001; Weed et al., 2000). *In vitro* studies, dominant-negative approaches and knockdown experiments substantiated these findings and established cortactin as an NPF with essential roles in lamellipodia and podosome formation, endocytosis, host-pathogen interactions and cell-cell adhesions (Cosen-Binker and Kapus, 2006). However, some findings were challenging the role of cortactin as NPF. These included the fact that cortactin did not incorporate at the front of lamellipodia in FRAP experiments as the Arp2/3 complex and the NPF WAVE, but instead recovered throughout the whole lamellipodium (Lai et al., 2008) inconsistent with function of cortactin in Arp2/3 activation. Additionally, the work from Padrick et al. indicated that binding of cortactin to the Arp2/3 complex, previously considered to activate the nucleator, could serve an inhibitory rather than stimulatory role on Arp2/3 activation e.g. by WASP family proteins (Padrick et al., 2008). This is because dimerized class I NPFs such as N-WASP or WAVE that are able to hyperactivate the nucleator compete with cortactin for one additional binding site on the Arp2/3 complex.

The analysis of cells genetically depleted for cortactin allowed testing which processes are truly impaired upon loss of cortactin. The findings of Lai et al. confirmed that cortactin depletion inhibited PDGF-induced actin rearrangement and decreased migration speed as well as wound healing efficiency. However, no alteration in lamellipodial ultrastructure, Rac-induced lamellipodia formation or clathrin-mediated endocytosis was discernible (Lai et al., 2009). In the present thesis, cortactin loss-of-function was examined in more detail both at the cellular level and in cortactin and HS1/cortactin KO mice. Moreover, the relevance of cortactin-mediated Arp2/3 complex activation *in vivo* was determined using a novel actin polymerization assay operating in the cytoplasm of living cells.

4.1 Decreased wound healing rates in cortactin KO cells can be reconstituted with active Rho-GTPases

Several studies have reported that interference with cortactin function reduced migration and thus wound healing efficiency, which was often attributed to impaired lamellipodia formation or persistence (Bryce et al., 2005; Kelley et al., 2010; Kowalski et al., 2005; Zhu et al., 2010). Cortactin KO MEF cells also displayed impaired migration, as they were moving slower compared to control cells in random migration assays and needed more time to close an artificial wound in *in vitro* wound healing assays (Lai et al., 2009). The fact that lamellipodia formation *per se* was not affected, but the activity of the small Rho-GTPases Rac1 and Cdc42 was reduced in cortactin-depleted cells (Lai et al., 2009) led to the assumption that the migration defect might correlate with low Rho-GTPase levels. This connection could be confirmed in this thesis by overexpression of constitutively active Rac1 and Cdc42, which both enhanced the wound healing rate in cortactin KO cells, and Cdc42 overexpression reconstituted the migration defect to almost WT levels (Figure 3-2). Interestingly, Rac1 overexpression in control cells reduced the wound healing efficiency, which demonstrated that the amount of active Rac1 does not directly correlate with migration speed and Rac1 overexpression enhances motility only if Rac1 activity is low. Although cortactin deficiency does not abolish lamellipodia formation, the signaling pathway e.g. as induced by PDGF resulting in actin rearrangements is impaired in cortactin KO cells (Lai et al., 2009). Upon wounding a confluent layer of cells, a signaling cascade is activated in the cells facing the wound, which drives directed cell migration into the cell-free area until wound closure is complete. For effective migration, mesenchymal cells need to form lamellipodia, which is dependent on small Rho-GTPases. Rac1 is considered to be crucial for lamellipodia formation together with Arp2/3 and WAVE complex (Guo et al., 2006; Ridley et al., 1992; Steffen et al., 2004; Vidali et al., 2006), because it activates the WAVE complex and thereby induces actin polymerization in the lamellipodium driven by the Arp2/3 complex, which promotes cell migration. Cdc42 is also able to induce lamellipodia (Aspenström, Fransson, and Saras, 2004; Nobes and Hall, 1995), although it does not directly interact with the WAVE complex. Instead, Cdc42 was shown to activate Rac (Nobes and Hall, 1995), which in turn could promote lamellipodia formation and trigger efficient migration. In a recent study in which Cdc42 was downregulated using RNAi, the depletion of Cdc42 caused impaired cell migration, although the level of active Rac was unaltered, indicating that Cdc42 might promote motility also independent of Rac (Monypenny et al., 2009). Whatever the case, the wound healing defect in cortactin KO cells is probably due to impaired signaling in the

cells near the wound, which are unable to activate as much Rac1 and Cdc42 as control cells leading to lower wound closure rates.

Wound healing experiments as performed in this thesis together with Rho-GTPase activation assays would be an adequate approach for reconstitution experiments with mutated cortactin constructs to find out which domain in the cortactin protein is responsible for the promotion of Rho-GTPase activity. Given that cortactin does not directly alter the actin cytoskeleton, but loss of cortactin impairs the activation of Rho-GTPases, it is tempting to speculate that cortactin recruits a GEF to sites of active actin nucleation, where the latter may continuously refill the pool of GTP-loaded Rho-GTPases, which in turn drive the activity of NPFs and subsequently of the Arp2/3 complex. Indeed, cortactin was shown to bind to the Cdc42 GEF Fgd1 via its SH3 domain (Hou et al., 2003). In addition the interaction between the cortactin homolog HS1 and the GEF VAV1 was established, the latter being responsible for nucleotide exchange in both Rac and Cdc42 in the hematopoietic system. Both proteins were implicated in the formation of the immunological synapse and association between HS1 and VAV1 required tyrosine phosphorylation of HS1 and the SH2 domain of VAV1 (Gomez et al., 2006). VAV1 is restricted to the hematopoietic system, but the two isoforms VAV2 and VAV3 are expressed more ubiquitously (Schuebel et al., 1996; Trenkle et al., 2000). Recruitment of a GEF by cortactin is an attractive model, as it would explain the signaling defect and impaired wound healing detected in cortactin KO cells. In addition, it would explain why cortactin localizes to sites of active, Arp2/3-dependent actin nucleation irrespective of the activation of the complex. It is possible that cortactin is not the only protein targeting GEFs to e.g. the lamellipodium, which would explain the reduction and not abolishment of PDGF-induced actin rearrangement (Lai et al., 2009). Whether the signaling defect in cortactin KO cells regarding Rho-GTPase activity is truly linked to missing recruitment of Fgd1, VAV2/3 or a different GEF remains to be determined.

4.2 Reduction of α-actinin4 expression in cortactin KO cells

The use of an Affymetrix RNA array for the detection of genes with higher or lower transcription levels upon cortactin KO indicated that α-actinin mRNAs were reduced to 25-50%. To verify that lower transcription of α-actinin also results in lower amounts of protein, western blot analysis was performed using an antibody specific for the α-actinin isoform 4, one of the two isoforms expressed in non-muscle cells. Indeed, also at the protein level, α-actinin4 was reduced on average to 50% compared to control cells in both the pooled cortactin KO cell population and the five individual cortactin KO clones (Figure 3-3). Nevertheless, cortactin deficiency did not alter the subcellular

localization of α-actinin4, as examined by immunofluorescence stainings (Figure 3-4). To date, no direct link between cortactin and α-actinin is known. Reduced protein levels of α-actinin could be explained by an inhibitory effect of cortactin depletion on transcription, although a potential connection of cortactin to the nucleus and transcription remains elusive.

The fact that α-actinin is reduced in cortactin KO cells could explain the loss of focal adhesion disassembly upon PDGF treatment in cortactin KO cells (Lai et al., 2009). α-actinin has been reported to be redistributed prior to focal adhesion disassembly upon PDGF stimulation and PI3-kinase activation, as α-actinin bound to PIP_2 and PIP_3 in the plasma membrane, the latter of which is generated by PI3-kinase (Fraley et al., 2003; Greenwood et al., 2000). In cortactin KO cells, the PDGF-mediated disassembly of focal adhesions and stress fibers was abrogated (Lai et al., 2009). It is possible that on one hand the relocation of α-actinin serves as a trigger for focal adhesion disassembly. On the other hand, cortactin could regulate the activity of the PI3-kinase, for instance by enhancing the association of PI3-kinase with growth factor receptors such as the PDGF-receptor, which activates PI3-kinase (Cantley, 2002). If this was the case, the formation of PIP_2 and PIP_3 could be impaired upon cortactin depletion, which would explain both the lack of focal adhesion disassembly that is triggered by PIP_2 and PIP_3 formation (Greenwood et al., 2000), and reduced Rho-GTPase levels, as the PI3-kinase is a key molecule in the activation of Rac and Cdc42 (Kolsch, Charest, and Firtel, 2008). In future work, it will be beneficial to step by step dissect the PDGF response in cortactin KO cells to precisely determine which process in the sequence of events to activation of Rho-GTPases is defective upon loss of cortactin.

4.3 Cortactin is essential for InlB-mediated *Listeria* invasion

Loss of cortactin was also reported in the literature to influence the ability of pathogens to adhere to and infect host cells as well as to move in the cytoplasm of eukaryotic cells. Gentamicin protection assays in control and cortactin KO fibroblasts cells revealed that the specific invasion of *Listeria*, which is mediated by the bacterial factor InlB in murine tissue, was blocked in the absence of cortactin in two independently generated cell populations with different deleted cortactin alleles (Figure 3-5 and Figure 3-7). InlA-mediated bacterial entry was irrelevant in these cells, because InlA is only able to associate with human E-cadherin (Lecuit et al., 1999; Schubert et al., 2002). Non-specific uptake of bacteria as determined using an InlA/B-deficient *Listeria* strain accounted for 50% of total *Listeria* internalization and could occur, for instance, through the formation of macropinosomes. These special vesicles form e.g. upon closure of dorsal ruffles and contain extracellular fluid, which can also include bacteria (Kerr and

Teasdale, 2009). However, it is also possible that so far unknown bacterial factors drive internalization of *Listeria* in addition to InlA and B.

Regarding InlB-dependent *Listeria* invasion, it was shown that c-Met activation and downstream activation of Rac was crucial for infection efficiency (Bosse et al., 2007; Seveau et al., 2007). To investigate whether the signaling involved in *Listeria* invasion was impaired in cortactin-deficient cells, control and cortactin KO cells were treated either with the host cell ligand for c-Met, HGF, or with the bacterial ligand, InlB. The signaling cascade triggered by ligand-receptor binding leads to dorsal ruffle formation, which can be easily quantified using fluorescence microscopy. Dorsal ruffling has been emerged as a sensitive readout and was already used to detect and quantify the impairment of PDGF-induced actin rearrangements in cortactin KO cells (Lai et al., 2009). In contrast to PDGF treatment, cells lacking cortactin were able to form dorsal ruffles upon both HGF and InlB stimulation, at frequencies identical to control cells (Figure 3-9). Thus, defective c-Met signaling did not seem to be the reason for abolished InlB-dependent uptake of *Listeria* upon cortactin deletion. Interestingly, cortactin has not only been implicated in InlB-mediated *Listeria* entry, but was also shown to be crucial for infection through the InlA pathway. Knockdown of cortactin via RNAi resulted in reduced uptake of mutant *Listeria* lacking InlB, which was attributed to cortactin-mediated Arp2/3 complex activation, as overexpression of cortactin constructs sequestering or unable to bind the Arp2/3 complex inhibited *Listeria* internalization (Sousa et al., 2007). Of course it would have been intriguing to examine whether or not the InlA pathway was also affected in cells genetically depleted for cortactin, but as InlA does not interact with murine E-cadherin, it was impossible to verify these results in the cortactin KO cells used in this thesis.

In order to shed light onto the implications of cortactin in InlB-mediated *Listeria* invasion, again reconstitution experiments would be helpful. Through re-expression of cortactin constructs with either point mutations or deletion of whole domains in cortactin KO cells combined with *Listeria* infection experiments, domains involved in the internalization process could be identified and a mechanism for cortactin in the infection process could be established.

4.4 Analysis of cortactin- and HS1/cortactin-deficiency in mice

In general, the use of KO mice has important advantages compared to cellular studies. On one hand, the deletion of a gene in the whole organism allows examining its role in embryogenesis, brain and organ formation, and behavior all of which require functional cytoskeleton (Erck et al., 2005; Lommel et al., 2001; Rust et al., 2010). On the other

hand, KO mice can be used as source for organs or primary cells, which can be applied to *in vitro* experiments.

Mice lacking cortactin were viable, fertile and did not show obvious phenotypes in SPF animal housing. This demonstrated that cortactin was not essential during embryogenesis, although contradictory results were obtained using a gene trap approach instead of a conditional KO (Yu et al., 2010). Yu et al. reported that heterozygous matings did not produce KO pups and examination of fertilized oocytes revealed that no KO embryos in the two-cell stage could be observed. Thus, Yu et al. claimed that cortactin was essential for asymmetric division in oocytes. As cortactin KO mice were born mostly at Mendelian ratio (see below), a role for cortactin in embryonic cell division can be excluded, and the results from Yu et al. indicate a complication in the gene trap approach.

Heterozygous matings of two different mouse populations served as source to analyze the frequency of the different genotypes and sexes in the offspring. In both mouse lines, WT, heterozygous as well as homozygous pups from both sexes were born, but the frequencies differed from Mendelian ratios in some cases. Crossings of heterozygous mice harboring the deleted Neo allele produced more male than female offspring, but male KO mice were underrepresented (Figure 3-10). Interestingly, in heterozygous matings of mice carrying the deleted cortactin allele, more female pups were born, and especially heterozygous females were more frequent than calculated (Figure 3-11). These results demonstrate that although in principle all combinations of genotypes and sexes were generated, still the different allele composition of parental mice biased the frequency of certain combinations in the offspring. The reasons for these differences are unknown, but could be due to the different genetic background of the cell lines or the conditions in the animal husbandry.

In cortactin KO mice, the hematopoietic homolog of cortactin, HS1, was still present. In order to generate a knockout lacking both class II NPFs found in mammals, crossings between mice with the cortactin deleted Neo allele and HS1 KO mice were arranged by Frank Lai. The double KO was also fertile, viable and without apparent phenotype. However, HS1 KO mice were previously shown to be impaired in antibody production, immunoreceptor-induced proliferation of B and T cells (Taniuchi et al., 1995) and blood coagulation (Kahner et al., 2007). These defects were certainly also present in the double KO mice, but neither was the immune system challenged with pathogens nor were mice wounded, so none of these phenotypes were observed in our animal husbandry. Mating statistics of crossings of mice homozygous for HS1 KO and heterozygous for cortactin KO revealed that these mice were born as expected from Mendel's rules (Figure 3-12).

In the literature, cortactin was described as essential component in the formation of podosomes in cell types as various as osteoclasts, smooth muscle cells and v-Src-transformed fibroblasts. Osteoclasts depleted for cortactin neither formed podosomes nor sealing rings, and were defective in bone resorption (Tehrani et al., 2006a). Podosome formation was also reported to be abolished in smooth-muscle cells after cortactin knockdown (Zhou et al., 2006).

In the present study, peritoneal macrophages isolated from control mice and littermates deleted for cortactin or both cortactin and HS1, respectively, all displayed podosomes with unaltered morphology and typical protein composition (Figure 3-13 and Figure 3-16). The number of cells forming podosomes was also comparable in control and KO macrophages (Figure 3-14 and Figure 3-17). It could be excluded that HS1 was upregulated to compensate for the absence of cortactin, as western blot analysis detected equal amounts of HS1 in both control and cortactin KO macrophages (Figure 3-15). More importantly, also the double KO macrophages lacking both cortactin and HS1 were able to form podosomes. In conclusion, at least in macrophages, podosomes can be assembled in the absence of cortactin. Yet it remains to be answered whether macrophages are the only cell type forming podosomes independently of cortactin. To address this question, osteoclasts and smooth muscle cells from cortactin KO mice should be examined regarding the existence of podosomes, because the essential role for cortactin could be specific for these cell types. However, the impairment in podosome assembly obtained with RNAi-induced knockdown of cortactin could also have other reasons such as off-target effects, as this is one major disadvantage of silencing genes using RNAi (Jackson et al., 2003). Jackson et al. could demonstrate that direct silencing of non-targeted genes required as few as eleven contiguous nucleotides of identity to the siRNA, so misinterpretation from RNAi experiments can easily occur. Thus, the potential role for cortactin in podosome formation in osteoclasts and smooth-muscle cells should be re-evaluated.

Although podosome formation and recruitment of typical proteins in cortactin and HS1/cortactin KO macrophages was normal, nothing is known about the functionality of podosomes lacking cortactin and/or HS1. In order to cross endothelial barriers, macrophages recruit metalloproteases to podosomes, where they are secreted into the extracellular lumen and decompose the ECM (Linder, 2007). Preliminary results from a collaboration with Christiane Wiesner and Stefan Linder (UKE Hamburg), where macrophages from cortactin KO mice were subjected to matrix degradation assays revealed that upon cortactin depletion macrophages displayed a severe impairment in gelatin degradation (unpublished data). These experiments have to be repeated in the

future to verify whether or not cortactin may indeed play a role in the degradation process of the ECM mediated by podosomes.

4.5 *In vivo* versus *in vitro* actin polymerization assays

In order to investigate the impact of a protein on actin polymerization, mostly *in vitro* assays are employed. A common method is the so-called pyrene assay, in which the increase of fluorescence of pyrene-actin upon incorporation into an actin filament is utilized to measure actin polymerization rates (Cooper, Walker, and Pollard, 1983). Purified proteins of interest are mixed with actin and pyrene-labeled actin and fluorescence is measured over time, which allows assessing the ability of a protein to promote actin filament formation (Ismail et al., 2009; Marchand et al., 2001; Padrick et al., 2008; Zuchero et al., 2009). In case of testing NPFs, the Arp2/3 complex is added to the assay and enhancement in Arp2/3 complex-dependent actin nucleation is measured. The use of *in vitro* assays is highly useful and provides important information regarding the direct impact of a specific factor on actin polymerization. A major advantage is that a defined amount and composition of proteins can be assayed. Still, *in vitro* assays also have disadvantages, for instance, they are often carried out in non-physiological salt concentrations, which do not reflect the *in vivo* situation and can lead to irrelevant results. Additionally, when using defined protein mixtures important factors such as components essential for the activity of the protein of interest could be missing, with strong potential impact on the outcome of the experiment. Most importantly, although proteins in *in vitro* experiments can display a certain activity e.g. on actin polymerization, this activity is not necessarily relevant in living cells. Cellular functions of a protein are often determined using loss-of-function experiments, such as knockdown or knockout of a protein. Nevertheless, a handy tool to directly assay the actin polymerizing activity of a given factor *in vivo* was missing so far. There have been attempts to target the actin polymerization machinery to cellular organelles like mitochondria and endosomes (Kessels and Qualmann, 2002; Pistor et al., 1994; Schmauch et al., 2009). However, endosomes possess an actin shell, which makes it impossible to differentiate between the effects of endogenous and exogenous actin-binding factors. Mitochondria lack actin filaments, but are highly dynamic, which makes them unsuitable for live cell imaging and FRAP experiments. In this thesis, a novel approach was introduced, which is also based on protein recruitment to an ectopic site in the cell. Potential actin nucleators or NPFs were targeted to the microtubule network, which is relatively stable in interphase cells, apart from the highly dynamic plus ends (Etienne-Manneville, 2010). Whether an MBD-construct induced actin assembly on microtubules was explored by simple and straight forward microscopy. Employment of

the MBD-assay allowed the use of live cell imaging of actin polymerization at microtubules as well as turnover measurements using FRAP. As confirmed by EM tomography, control microtubules were largely devoid of actin filaments, so only coincidental overlaps between microtubules and actin filaments could be discerned (Figure 3-22E). Thus, no interference of endogenous actin regulators with microtubule-targeted nucleators or NPFs was expected. Of note, the novel microtubule-based actin polymerization assay was not developed to replace *in vitro* assays. Instead, it is established here as a tool to verify results obtained in *in vitro* experiments, and to test for their relevance *in vivo*.

4.6 Properties of N-WASP-VVCA-mediated actin nucleation *in vivo*

The characteristics of the *in vivo* actin polymerization assay were determined using a chimeric protein consisting of an EGFP-tag for the detection of the protein, the microtubule-binding domain (MBD) of MAP4, which mediated targeting to microtubules, and the VVCA domain of N-WASP. The N-WASP-VVCA was established as a potent Arp2/3 activating peptide (Yamaguchi et al., 2000) and was thus well-suited to assess the properties of the MBD-assay. MBD-VVCA was demonstrated to bind to microtubules with counterstaining of α-tubulin, recruit the Arp2/3 complex and mediate actin polymerization, as the actin accumulations on microtubules were positive for phalloidin staining and therefore contained actin filaments (Figure 3-19).

To prove that the actin assembly induced by MBD-VVCA was generated through nucleation via the Arp2/3 complex on microtubules, several control experiments were carried out. A construct only comprising the EGFP-tagged MBD was transfected into cells, which did not induce actin accumulation or Arp2/3 complex recruitment (Figure 3-20), showing that the VVCA was required to target the Arp2/3-dependent actin machinery to microtubules. Neither the F-actin-binding domains of α-actinin nor full-length fascin were able to recruit actin filaments to microtubules (Figure 3-21), so sole recruitment of actin filaments from the cytoplasm did not seem to suffice as mechanism of actin accumulation. In addition, an MBD-construct comprising only the two WH2 domains of N-WASP was tested concerning its ability to recruit actin filaments to microtubules, as they were recently shown to be capable of binding to actin filaments (Co et al., 2007). But also this construct did not mediate actin assembly on microtubules, and when analyzing 278 cells co-expressing MBD-VV not a single cell was identified with co-localization of the MBD-construct and actin filaments (Figure 3-31B and Figure 3-33). In conclusion, the induction of actin filament assembly on microtubules cannot be attributed to sole F-actin recruitment; instead it seems to be dependent on actin nucleation.

Cells co-transfected with MBD-VVCA and actin were used to determine the dynamics of actin assembly induced by MBD-VVCA. Video microscopy revealed that on growing microtubules association of MBD-VVCA and actin polymerization occurred synchronously (Figure 3-24A). These findings demonstrated that after MBD-VVCA binding to the microtubule, actin was nucleated instantaneously, so actin assembly was fast and its delay not resolvable with the microscope settings used. Similarly, on shrinking microtubules, MBD-VVCA and actin dissociated simultaneously (Figure 3-24B), which showed that MBD-VVCA-induced actin accumulation needed the physical interaction with the MBD-construct and the microtubule.

To learn more about the dynamics of MBD-VVCA and associated actin on microtubules, FRAP experiments were performed. This method is well-suited to detect how molecules are incorporated into a given structure and allows drawing conclusions concerning the stability and the turnover of a given structure. Recently, a comprehensive study on the dynamics of the actin network in the lamellipodium was published, in which the turnover of actin itself as well as actin-associated proteins was determined in FRAP experiments (Lai et al., 2008). The halftime of recovery of MBD-VVCA was 7.7 s (Figure 3-25), which is in the same range as the Arp2/3 complex NPF WAVE at the lamellipodium tip (Lai et al., 2008). The residency time of NPFs both in lamellipodia and on microtubules could be essential for effective nucleation by the Arp2/3 complex, although this would have to be verified in additional experiments, in which the interaction time with the microtubule surface is engineered to be shortened or enhanced. The turnover of actin filaments on microtubules was significantly slower than that of MBD-VVCA (Figure 3-25), again reminiscent of the actin turnover in lamellipodia (Lai et al., 2008). The delay in actin filament recovery on microtubules was probably caused by the fact that not every MBD-VVCA molecule was able to recruit and activate the Arp2/3 complex on microtubules. The FRAP experiments demonstrated that microtubules were stable enough for assaying turnover of nucleators or NPFs and associated actin filaments.

The ultrastructure of actin filaments nucleated by Arp2/3 complex on microtubules was explored by correlative light and electron tomography. This method was used to first detect microtubules decorated with MBD-VVCA and associated actin filaments using fluorescence microscopy. Subsequently, the same cell was fixed and subjected to electron tomography, where a region with prominent microtubules as identified in the fluorescence microscope was selected. Through comparison of both images, a microtubule with MBD-VVCA and actin association could be relocated and analyzed in the electron microscope. In the tomogram shown in Figure 3-22, a microtubule is visible that is associated with a high number of small filaments arranged in an

unorganized fashion, whereas in the control cell, only small numbers of actin filaments randomly crossed the microtubule. These findings on one hand confirmed that the actin accumulations on microtubules contained filamentous actin, and on the other hand demonstrated that actin filaments induced by MBD-VVCA were apparently not assembled into regular structures e.g. by actin bundling proteins. In future experiments, it would be interesting to investigate whether the different actin nucleators executing their distinct actin nucleation mechanisms all form similar actin filament arrays or whether each nucleator induces a unique actin filament pattern on microtubules. Moreover, in-depth analysis of filaments induced by MBD-VVCA could answer the question if the Arp2/3 complex nucleates branched actin filaments in the cytoplasm or not. Recent publications using negative stain electron microscopy and cryo-electron tomography challenged the widely accepted opinion that the lamellipodium consists of a dendritic actin filament network (Koestler et al., 2008; Urban et al., 2010). Nevertheless, potential, transiently formed actin branches at the proximity of the plasma membrane could not be examined so far, as the membrane is extracted during sample preparation, which could lead to a loss of newly nucleated filaments associated with the membrane. This problem is not expected to occur using the MBD-assay, as the actin filaments are nucleated on the microtubule surface far away from membranes.

In the course of my experiments, a construct lacking the acidic domain of VVCA was cloned. Surprisingly, this construct was still able to induce Arp2/3-dependent actin assembly on microtubules (Figure 3-32 and Figure 3-33). It had been demonstrated in independent studies that the acidic domain in the VCA module is essential for Arp2/3 complex activation (Kelly et al., 2006; Marchand et al., 2001). Special importance was attributed to the tryptophan residue on position 500 within the acidic domain, as mutation of this residue abolished Arp2/3 binding (Marchand et al., 2001). One *in vitro* study had previously shown that VVC could activate Arp2/3 on artificial vesicles, although higher concentrations of Arp2/3 were needed (Delatour et al., 2008). Moreover, microinjection of GST-bound WASP-VC in macrophages induced actin clumps (Hüfner et al., 2001), although this activity was subsequently attributed to an artifact caused by GST-mediated dimerization (Kelly et al., 2006). Thus, no direct evidence was provided that Arp2/3 activation could take place without the acidic domain *in vivo*. In the present study, I also explored *Shigella* actin tail formation, which is known to essentially require N-WASP (Lommel et al., 2001), and thus constitutes a physiologically relevant system to study N-WASP function *in vivo*. In N-WASP KO cells, *Shigella* could form actin comet tails upon reconstitution not only with full-length N-WASP, as expected, but also using an N-WASP construct lacking the acidic domain (Figure 3-34). These data undoubtedly confirmed that the acidic domain was not

essential for Arp2/3 complex recruitment and activation *in vivo*. Nevertheless, the MBD-VVC construct was impaired both in Arp2/3 complex recruitment and in inducing actin polymerization, as determined by quantification of cells co-expressing actin or p16B with the respective MBD-construct (Figure 3-33). In the case of MBD-VVCA, almost every cell displayed actin accumulation on microtubules and in two-thirds of cells Arp2/3 complex association was detectable. In contrast, only half of the cells transfected with MBD-VVC accumulated actin on microtubules, and clear Arp2/3 complex accumulation was seen in as few as 10% of the cells. The MBD-assay also confirmed that the central domain is essential for Arp2/3 complex recruitment and activation *in vivo*, as the construct comprising only the two WH2 domains of N-WASP neither induced actin assembly on microtubules nor recruited the Arp2/3 complex. However, the acidic domain is not essential for the induction of actin assembly *in vivo*, although both the recruitment of and actin polymerization by Arp2/3 are more efficient with the complete VVCA-module. Strikingly, the amount of cells with MBD-construct and actin co-localization exceeded the number of cells with co-localization of MBD-construct and p16B, which is probably due to reduced efficiency of p16B detection on microtubules. The possibility that Arp2/3-independent actin polymerization might occur could be formally excluded, since abolished Arp2/3 recruitment observed with MBD-VV coincided with a complete block of actin assembly.

4.7 Cortactin: inactive as NPF but still a determinant of Arp2/3-mediated actin nucleation *in vivo*

As outlined above, the results from various experiments did not argue for the widely accepted view that cortactin acts as Arp2/3 complex activator *in vivo*. Thus, it was intriguing to test how cortactin behaved in the MBD-assay. Two constructs were cloned: full-length cortactin and the isolated NTA-domain harboring the Arp2/3-binding domain coupled to MBD. Surprisingly, both constructs were unable to recruit the Arp2/3 complex to microtubules, indicating that the binding affinity *in vivo* for the Arp2/3 complex does not suffice to target the Arp2/3 complex to microtubules (Figure 3-26A). In line with these findings, no actin polymerization was induced by the two MBD-cortactin-constructs (Figure 3-26B). In summary, the lack of Arp2/3 complex recruitment of MBD-cortactin contradicted the view that it acts as Arp2/3 activator *in vivo*. Nevertheless, by using the MBD-assay, it could be confirmed that cortactin is apparently involved in Arp2/3 complex-dependent processes, as cortactin was specifically co-recruited to actin filaments nucleated by VVCA and Arp2/3 complex (Figure 3-35). Thus, in spite of the inability of cortactin to activate Arp2/3 and consistent with numerous cellular studies, which detected cortactin in Arp2/3 complex-rich

structures (Ammer and Weed, 2008), cortactin localized to MBD-VVCA-induced actin networks downstream of their formation. However, the precise role of cortactin in Arp2/3-dependent actin polymerization remains elusive.

An interesting result also in the context of cortactin was that the A-domain of N-WASP was dispensable for activation of the Arp2/3 complex (see 3.1.15). The A-domain including its conserved tryptophan residue is the only common feature between class I and class II NPFs concerning Arp2/3 activation. The MBD-assay as well as reconstitution of *Shigella* actin tail formation suggests that the essential unit for induction of Arp2/3-dependent actin nucleation is the VVC-domain, which is absent in cortactin and thus might explain the inability of cortactin to activate the Arp2/3 complex *in vivo*. However, the efficiency of actin polymerization as well as recruitment of Arp2/3 was enhanced using the complete VVCA domain, which suggests that A-domain-mediated Arp2/3 complex interaction might increase the efficiency for nucleation. In case of class I NPFs, this could thus effect productive Arp2/3 activation, whereas in case of cortactin the A-domain might solely determine the localization of cortactin to Arp2/3-dependent actin polymerization, or even counteracts the efficient activation observed for class I NPF-dimers (Padrick et al., 2008). This hypothesis awaits confirmation in future experiments.

To get more information about the domains of cortactin mediating its correct localization in the cell, localization studies were performed using different cortactin constructs. As expected, the full length cortactin construct localized to lamellipodia and membrane ruffles. In contrast to the Arp2/3 complex, it also labeled microspikes, which indicated that the Arp2/3 complex was not the only determinant for cortactin localization. Another striking result was obtained by using truncated cortactin constructs. The NTA, which was shown to bind the Arp2/3 complex *in vitro* (Weed et al., 2000), was not able to target the construct to lamellipodia. This finding is consistent with previous studies, in which myc-tagged constructs were used (Weed et al., 2000). In the study of Weed et al., the minimal construct that localized to the cell cortex comprised the NTA and F-actin repeats 1 to 4, whereas the fourth repeat was claimed to be most important for F-actin binding. However, the EGFP-cortactin 1-146 construct targeted to lamellipodia in B16-F1 cells, so either the localization of cortactin to the cell periphery depends on the NTA and much less of the actin binding repeats (only N-terminal 1.5 repeats present), or the sequence responsible for cortactin localization to lamellipodia is encoded by aa residues 85 to 146. Interestingly, EGFP-cortactin 1-146 was not found in microspikes, which indicated that the association with the latter was mediated by more C-terminal parts of the protein. To unambiguously map the domains required for lamellipodia and microspike localization of cortactin, systematical deletion

studies are needed. However, the results obtained in this thesis already demonstrate that binding to the Arp2/3 complex via the NTA alone is not sufficient for localizing cortactin to the lamellipodium, and that further N-terminal sequence stretches (perhaps including the first 1.5 actin binding repeats) were needed additionally to the NTA to target cortactin to the cell periphery. Nevertheless, also the C-terminal part of cortactin seems to contribute to subcellular localization, as the association with microspikes was only detectable using the full-length construct. As an example for further experiments, it would be worthwhile to test a construct lacking the NTA in order to re-evaluate the importance of Arp2/3 binding for correct localization, both concerning the localization to the cell periphery and also to MBD-VVCA-induced actin assembly.

4.8 Actin nucleation on microtubules by Spir and Drf3ΔDAD

As outlined in the introduction, additional mechanisms of actin nucleators exist, which differ from mimicking an actin dimer as established for the Arp2/3 complex. I have tested therefore whether actin nucleation by Spir or formins can also drive actin assembly in the MBD-assay. As expected, both actin nucleators induced actin polymerization on microtubules (Figure 3-28), albeit the potency to induce actin accumulation differed significantly. Spir, which has so far been classified as a moderately potent actin nucleator (Quinlan et al., 2005), strongly induced actin polymerization on microtubules, and as with MBD-VVCA, nearly all transfected cells displayed actin accumulation on microtubules (data not shown). In contrast, the powerful actin nucleator Drf3ΔDAD (Li and Higgs, 2005) nucleated only few actin filaments on microtubules and cells displaying actin on microtubules were infrequent. These conflicting results could have very simple explanations. Concerning Spir, it was previously shown that the nucleator cooperates with the formin2 (Pechlivanis, Samol, and Kerkhoff, 2009). Thus, the strong actin nucleation activity of Spir *in vivo* could be due to co-recruitment of formin2 promoting actin assembly. However, the two isolated Spir WH2 domains including the monomer-binding linker were also able to potently nucleate actin (Figure 3-28C), and this construct lacked the formin-interaction domain. Thus, my findings suggest that the conditions used in the *in vitro* assay do not precisely reflect the situation in the cytoplasm, for instance concerning salt concentrations or pH, and potential Spir activators present in the cytoplasm could have been missing *in vitro*. The weak actin nucleation activity of Drf3ΔDAD possibly had different reasons. For formin-mediated actin nucleation, the formation of a homodimer by actin binding to the two FH2 domains is a crucial step, as exemplified by mDia1 and Bni1 (Moseley et al., 2004). The dimerization of the MBD-constructs could be complicated on microtubules due to sterical constraints that hinder the formation of the active formin unit. Another

explanation could be that targeting of the formin to the surface of microtubules might interfere with its processivity, thus decelerating formin-mediated actin polymerization. Additional formins could be tested to distinguish between these possibilities.

A recent publication demonstrated that the DAD domain of mDia1 contributed to actin nucleation by binding G-actin (Gould et al., 2011), which could provide an additional explanation for low actin nucleation activity of MBD-Drf3ΔDAD. Thus, future efforts should include the comparison of the actin assembly activities of formins or formin fragments harboring and lacking the DAD domain, also in the context of the MBD-assay. In addition, point mutations in the DAD or DID domain could serve to mediate the relief of autoinhibition to generate constitutively active formins.

4.9 Actin nucleation by monomer clustering

Another surprising result was obtained by the fusion of MBD to Lifeact, an F-actin binding sequence derived from the yeast protein Abp140. Initially considered as potential negative control together with fascin and the ABD of α-actinin, MBD-Lifeact to our surprise accumulated actin filaments on microtubules (Figure 3-30A). The other F-actin-binding proteins appeared unable to induce actin accumulation on microtubules (see above), so it was unlikely that Lifeact would recruit F-actin to microtubules. *In vitro*, Lifeact was previously shown to bind both F- and G-actin, although the latter with significantly lower affinity (Riedl et al., 2008). However, this actin monomer binding activity might constitute the decisive difference to fascin or the ABD of α-actinin, which were unable to drive actin accumulation. This was thinkable, as Lifeact was probably crowded on the microtubule surface, and high concentration of actin monomers in close proximity to each other could induce efficient actin nucleus formation. Evidence supporting this theory was provided by a following experiment, in which the MBD was fused to actin. This experimental setup allowed to ask directly if concentrating actin monomers by clustering on microtubules was sufficient to trigger actin nucleation. And indeed, MBD-actin induced actin filaments on microtubules (Figure 3-30B) and thus supported the hypothesis that the actin filaments assembled by Lifeact likely originate from nucleation rather than F-actin recruitment. Nevertheless, the ability of a construct to solely bind G-actin was not necessarily sufficient to nucleate actin on microtubules, as the two WH2-domains of N-WASP did not induce actin polymerization (Figure 3-31B). At first sight, this result opposed the idea that Lifeact can nucleate actin. However, effective nucleus formation might require a certain orientation and proximity of actin monomers to one another. This might be stochastically achieved by sequestering actin monomers by a peptide sequence as short as the 17 aa Lifeact. Although actin nucleation by clustering actin monomers is simple and apparently

feasible, this mechanism does not seem to be employed by cells. This is probably due to the fact that actin nucleation has to be highly regulated and only induced locally and in a temporally precise fashion for proper formation of functional actin filament arrays. The addition of a regulatory domain to an actin clustering sequence would most likely abolish its function regarding actin nucleation, which accounts for the much more elaborate actin nucleation mechanisms present in eukaryotic cells. It would be interesting to test, whether fusions of MBD with single WH2 domains e.g. derived from N-WASP, as well as other G-actin binding domains are also able to nucleate actin filaments or if Lifeact has unique features mediating actin nucleation on microtubules.

4.10 Involvement of capping protein in Arp2/3-dependent actin structures

A very interesting protein regulating the actin cytoskeleton is capping protein. It is enriched at the lamellipodium tip and RNAi experiments depleting capping protein indicated that it is crucial for lamellipodia formation (Mejillano et al., 2004). Additionally, capping protein belongs to the essential components of reconstituted Arp2/3-dependent actin-based motility (Loisel et al., 1999). The major biochemical activity of capping protein is the binding to barbed ends, which terminates actin polymerization, but at the same time protects the filaments from disassembly (Cooper and Sept, 2008). *In vitro*, capping protein was also reported to be capable of actin nucleation (Caldwell et al., 1989), although the capping activity predominated (Cooper and Sept, 2008). A more recent study defined capping protein as a co-factor of Arp2/3 complex-dependent actin assembly, at least *in vitro* (Akin and Mullins, 2008). The ability of capping protein to nucleate actin filaments *in vivo* or to recruit the Arp2/3-dependent actin machinery to microtubules was examined in the MBD assay. MBD-capping protein β2 recruited the α1 isoform to microtubules, which indicated that the functional heterodimeric unit could be formed (Figure 3-38). Still, no actin filaments were assembled by MBD-capping protein, so the actin nucleation activity did not seem to be existing *in vivo*. Additionally, capping protein does not seem to be able to recruit activated Arp2/3 complex to microtubules.

The localization of capping protein *in vivo* is largely restricted to the lamellipodium tip and possibly other Arp2/3-dependent structures, although the latter less established. It is entirely unclear how accumulation of capping protein in the lamellipodium tip is determined, and if Arp2/3 complex constitutes a determinant of capping protein localization or not. The MBD-assay offered the opportunity to test capping protein association with ectopic actin arrays nucleated by Arp2/3 complex or, in comparison, Spir-NT. In most cells transfected with MBD-VVCA, capping protein localized to the

microtubule network, as expected. In contrast, co-localization between Spir-NT-induced actin filaments and capping protein could only be observed in 18% of transfected cells, and the co-localization was not as strong as compared to MBD-VVCA (Figure 3-37 and Figure 3-36). Both the Arp2/3 complex and Spir-NT generate actin filaments with free barbed ends and actin nucleation by both proteins on microtubule surfaces was comparable strong. These data indicated that capping protein localization is probably not solely determined by the number of free barbed ends to which the protein binds, as expected, but that additional factors may regulate capping protein accumulation in Arp2/3-dependent actin arrays. The nature of these proteins remains mostly unclear. Another protein prone to be analyzed in recruitment studies using the MBD-assay is cofilin. As capping protein, cofilin is essential for reconstituted actin-based motility (Loisel et al., 1999). Using *in vitro* assays, cofilin was found to be able to both depolymerize and sever actin filaments (Bamburg, Harris, and Weeds, 1980; Ichetovkin, Grant, and Condeelis, 2002; Maciver, Zot, and Pollard, 1991). Different models have emerged to explain how cofilin triggers actin polymerization. On one hand, cofilin-mediated actin filament depolymerization could enhance the concentration of actin monomers that can be newly incorporated into actin filaments (Carlier et al., 1997). The severing activity, on the other hand, was suggested to increase the number of free barbed ends ready for polymerization (Ichetovkin, Grant, and Condeelis, 2002). *In vivo*, cofilin was postulated to directly promote actin polymerization by generation of free barbed ends and to induce protrusion (Ghosh et al., 2004). However, knockdown of cofilin decreased lamellipodia width and actin turnover was reduced in lamellipodia (Hotulainen et al., 2005), which was attributed to delayed depolymerization and turnover in the absence of cofilin. These findings were supported by FRAP analysis of cofilin in lamellipodia, as it localizes to the entire lamellipodium and turned over rapidly throughout the structure. This behavior was inconsistent with promoting actin nucleation at the tip (Lai et al., 2008). In order to unequivocally exclude a role for cofilin in actin filament nucleation, it would be interesting to probe its effects upon MBD-mediated clustering on the microtubule surface. Furthermore, co-expression e.g. with MBD-VVCA with or without downregulation of cofilin by RNAi would allow the examination of its potential to promote Arp2/3-dependent actin assembly, as proposed (Oser and Condeelis, 2009).

4.11 Concluding remarks

The MBD-assay has emerged as a versatile tool for the investigation of actin polymerization *in vivo*. During the characterization of the assay, it could be demonstrated that actin accumulation on microtubules seems only to occur through

actin nucleation, yet the applicability of the assay is not limited to test potential actin nucleators. Ectopic targeting of different actin nucleation machineries to microtubules allows the comparison concerning the ultrastructure of the resulting actin filament arrays as well as the detection of proteins that are co-recruited to different nucleators, which could help to dissect the underlying mechanisms. As displayed in the EM tomogram, the actin filaments polymerized on microtubules were not arranged into a well ordered structure such as the lamellipodium. This indicates that the activity is restricted perhaps to actin nucleation and polymerization, which is ideally suited to directly assay the impact of a given factor to specific actin assembly mechanisms. For example, it is now possible to induce ectopic actin filament arrays using distinct actin nucleators in cells depleted for a given protein via RNAi or a knockout approach to compare its relevance in different nucleation mechanisms. One example for such a study might be capping protein, which has been shown to be crucial for lamellipodia formation; yet it is still unclear if capping protein directly influences actin nucleation mediated by Arp2/3 complex in this structure. As loss of capping protein might abrogate lamellipodia formation not exclusively due to loss of Arp2/3 complex function, our MBD-assay as gain-of-function approach can now be used to ask whether or not capping protein is essential for MBD-VVCA-induced nucleation and thus Arp2/3-dependent actin assembly. Using the MBD-assay, the function of cortactin in Arp2/3 activation could be assayed for the first time *in vivo*. Not entirely unexpected, cortactin did not act as NPF and neither induced actin accumulation nor recruited the Arp2/3 complex. However, cortactin co-recruitment to Arp2/3 complex-induced actin filaments confirmed its potential role as a modulator of Arp2/3-dependent actin assembly. In spite of extensive research on cortactin in the past ten years, we are only beginning to understand the function of cortactin in the living cell, thus future studies will have to aim particularly at defining the role of cortactin in regulating Rho-GTPase activity, InlB-mediated uptake of *Listeria* and the precise function in Arp2/3-dependent actin nucleation.

5 Summary

Actin polymerization is a fundamental cellular process driving as diverse functions as cell migration, endocytosis, intracellular transport, cell division and adhesion. To fulfill its various tasks in the cell, the assembly and disassembly of actin filaments has to be highly regulated allowing only temporary and local formation of actin filament arrays that result, for instance, in directed movement of a cell. Cortactin was identified as Arp2/3 complex activating protein that stabilizes actin branches in dendritic actin filament networks. Particularly the characterization of cortactin KO cells has challenged this role in Arp2/3 activation, as lamellipodia formation as well as endocytosis was normal in the absence of cortactin. In this thesis, the implications of cortactin in migration, podosome formation and on Arp2/3 complex activation were determined. The observed migration defect in cortactin-deficient cells could be restored by overexpression of constitutively active Rac1 and Cdc42, whose activities were decreased in cortactin KO cells. This suggested that cortactin might promote cell migration by contributing to the activation of Rho-GTPases. Cortactin was also found to be essential in InlB-mediated uptake of *Listeria*, which did not result from defective signaling of InlB to induce actin rearrangements, but must be due to other, so far undefined reasons. Moreover, I established that macrophages from cortactin KO mice as well as mice deficient in both cortactin and HS1 were able to form podosomes, confirming the lack of an essential function of cortactin in Arp2/3-dependent actin assembly.

In a second project, the ability of cortactin to directly activate the Arp2/3 complex was tested *in vivo*. For this purpose, a microtubule-based actin polymerization assay was established targeting actin nucleators or NPFs to microtubules. The characterization of the N-WASP-VVCA domain coupled to the MBD of MAP4 showed that actin polymerization was induced on microtubules and depended on the presence of the Arp2/3 complex. MBD-VVCA-mediated actin filaments were short and unorganized on the microtubule surface, and the actin polymerization induced was instantaneous and continuous. Interestingly, cortactin fused to MBD did not induce actin filament assembly on nor recruit the Arp2/3 complex to microtubules, in line with accumulating evidence questioning an essential role for cortactin in Arp2/3 activation. However, cortactin was secondarily recruited downstream of Arp2/3-dependent actin assembly demonstrating its intimate connection to the Arp2/3 complex. By using the MBD-assay, it was possible to recapitulate all known actin polymerization mechanisms including Spir- and formin-mediated nucleation *in vivo*. It could further be demonstrated that the A-domain of N-WASP is not essential for, albeit helpful in Arp2/3 complex activation.

6 Abbreviations

aa	amino acids
ABD	actin binding domain
Abi	Abelson interactor
Abp	actin binding protein
ActA	actin assembly-inducing protein
ADF	actin depolymerizing factor
A-domain	acidic domain
ADP	adenosine diphosphate
Arp	actin-related protein
ATP	adenosine triphosphate
bp	base pairs
CaM	calmodulin
Cdc42	cell division control protein 42 homolog
C-domain	central domain
CH	calponin homology
Cobl	Cordonbleu
Cre	cyclization recombination
CRIB	Cdc42/Rac interactive-binding
C-terminal	carboxyl-terminal
DAD	diaphanous autoregulatory domain
del	deleted
DID	diaphanous inhibitory domain
DMEM	Dulbecco’s modified Eagle's medium
DNA	desoxyribonucleic acid
Drf	diaphanous-related formin
ECM	extracellular matrix
EGF	epidermal growth factor
EGFP	enhanced green fluorescent protein
EHEC	enterohemorrhagic *Escherichia coli*
EM	electron microscopy
Ena	Enabled
EPEC	enteropathogenic *Escherichia coli*
ER	endoplasmic reticulum
ERK	extracellular-signal-regulated kinases

ES cells	embryonic stem cells
EVH1	ena/VASP homology
FACS	fluorescence-activated cell sorting
F-actin	filamentous actin
FAK	focal adhesion kinase
FCS	fetal calf serum
FGD1	faciogenital dysplasia 1 protein
FH	formin homology
fl	floxed
Flpe	Flippase
FRAP	fluorescence recovery after photobleaching
frt	flip-recombinase targets
G-actin	globular actin
GAP	GTPase-activating protein
GBD	GTPase binding domain
GDI	guanine nucleotide dissociation inhibitors
GDP	guanosine diphosphate
GEF	guanine nucleotide exchange factor
GTP	guanosine triphosphate
HGF	hepatocyte growth factor
HS1	hematopoietic specific 1
IcsA	intracellular spread protein A
InlA/B	Internalin A and B
IRSp53	insulin receptor tyrosine kinase substrate p53
JMY	junction-mediating and regulatory protein
KIND	kinase non-catalytic C-lobe domain
KO	knockout
loxP	locus of X-over P1
MAP	microtubule-associated protein
MBD	microtubule binding domain
MBL	monomer-binding linker
mDia	murine diaphanous
MEF	mouse embryonic fibroblast
MEKK	MAP kinase kinase kinase
Mena	mouse Enabled
Nap	Nck associated protein
NPF	nucleation promoting factor
NTA	N-terminal acidic domain

N-terminal	amino-terminal
N-WASP	neuronal Wiskott-Aldrich syndrome protein
PAK	p21 activated kinase
PBS	phosphate buffered saline
PCR	polymerase chain reaction
PDGF	platelet-derived growth factor
P_i	phosphate
PI3-kinase	Phosphatidylinositol 3-kinases
PIP_2	phosphatidylinositol 4,5-bisphosphate
PKC	protein kinase C
PKD	protein kinase D
PRD	proline-rich domain
PVDF	polyvinylidene fluoride
Rac	Ras-related C3 botulinum toxin substrate
Rho	Ras homolog gene family member
Rif	Rho in filopodia
RNA	ribonucleic acid
RNAi	RNA interference
rpm	rounds per minute
RPMI	Roswell Park Memorial Institute medium
Scar	suppressor of cAR
SDS-PAGE	sodium dodecyl sulfate polyacrylamide gel electrophoresis
SH	Src homology
SHD	Src homology domain
SPF	specific pathogen free
Sra	specifically Rac associated protein
TBS-T	Tris buffered saline Tween
TIRF	total internal reflection microscopy
TOCA	transducer of Cdc42-dependent actin assembly
VASP	vasodilator-stimulated phosphoprotein
V-domain	verprolin homology domain
v-Src	viral-sarcoma
WASH	Wiskott-Aldrich syndrome protein and Scar homolog
WAVE	Wiskott-Aldrich syndrome verprolin homologue protein
WH2	WASP homology 2
WHAMM	WASP homolog associated with actin, membranes and microtubules
WIP	WASP interacting protein
WT	wildtype

7 Acknowledgements

Zum Schluss möchte ich mich bei einigen Menschen bedanken, ohne die diese Doktorarbeit nicht möglich gewesen wäre.

Mein größter Dank geht an Prof. Dr. Klemens Rottner, der durch seine fachliche Kompetenz, viele inspirierende Gespräche, nie endende aufmunternde Worte und eine perfekte Mischung aus Unterstützung und geförderter Selbständigkeit maßgeblich zum Gelingen meiner Doktorarbeit beigetragen hat.

Ganz herzlich danke ich außerdem Prof. Dr. Martin Korte und Prof. Dr. Ralf-R. Mendel für die Übernahme des Referats bzw. des Prüfungsvorsitzes.

Ein großer Dank geht an Frank Lai, dessen Projekt ich übernehmen durfte, für die Einarbeitung und fortwährende Unterstützung bezüglich des Cortactin-Projekts, und an Stefan Köstler, der die Idee für den MBD-Assay in unsere Arbeitsgruppe gebracht und mir bei der Charakterisierung mit Rat und Tat zur Seite gestanden hat. Theresia Stradal danke ich für die anregenden Diskussionen und für die Versorgung mit Konstrukten und Antikörpern aus ihrer Arbeitsgruppe.

Vielen Dank auch an Victor Small, Sonja Jakob, Maria Nemethova und Marlene Vinzenz aus Wien für die elektronenmikroskopischen Aufnahmen. Tanja Bosse danke ich für die unpublizierten *Listerien*-Daten. Eugen Kerkhoff, Steffen Backert und Jan Faix möchte ich für die Bereitstellung teilweise unpublizierter Konstrukte danken.

Des Weiteren geht ein Riesendankeschön an alle Mitglieder der Arbeitsgruppen CYD, SIM und ZB am HZI für die hervorragende Zusammenarbeit und produktive Arbeitsatmosphäre. Im Besonderen möchte ich Kathrin Ladwein danken für die Vermittlung der Doktorandenstelle, die Einarbeitung im Labor und für die schöne Zeit seit dem Studium. Brigitte, Frank, Gosia, Jan, Jenny, Kathrin, Marcin, Markus und Marco danke ich für ihre unablässige Hilfsbereitschaft, lustige Zellkultur-Sessions und die vielen Aktivitäten außerhalb des Labors. Bei Jenny möchte ich mich außerdem für die vielen aufbauenden Gespräche, während ich diese Arbeit geschrieben habe, bedanken. Danke auch an meine neuen Bonner Kollegen Anika und Gerd, für den schnellen Start im neuen Labor und die tolle Stimmung von Anfang an.

Meiner Familie danke für die große moralische Unterstützung nicht nur während der letzten dreieinhalb Jahre und dafür, dass sie immer an mich geglaubt haben.

Ein ganz besonderes Dankeschön geht an Christoph, der mir sowohl bei wissenschaftlichen Fragen als auch im Alltag stets zur Seite steht und mir durch seine liebevolle Art und großes Verständnis unglaublich viel Kraft gegeben hat.

8 References

Abercrombie, M. (1980). The Croonian Lecture, 1978: The Crawling Movement of Metazoan Cells. *Proceedings of the Royal Society of London. Series B. Biological Sciences* **207**(1167)**,** 129-147.

Ahern-Djamali, S. M., Bachmann, C., Hua, P., Reddy, S. K., Kastenmeier, A. S., Walter, U., and Hoffmann, F. M. (1999). Identification of profilin and src homology 3 domains as binding partners for Drosophila Enabled. *Proceedings of the National Academy of Sciences of the United States of America* **96**(9)**,** 4977-4982.

Ahuja, R., Pinyol, R., Reichenbach, N., Custer, L., Klingensmith, J., Kessels, M. M., and Qualmann, B. (2007). Cordon-Bleu Is an Actin Nucleation Factor and Controls Neuronal Morphology. *Cell* **131**(2)**,** 337-350.

Akin, O., and Mullins, R. D. (2008). Capping Protein Increases the Rate of Actin-Based Motility by Promoting Filament Nucleation by the Arp2/3 Complex. *Cell* **133**(5)**,** 841-851.

Albiges-Rizo, C., Destaing, O., Fourcade, B., Planus, E., and Block, M. R. (2009). Actin machinery and mechanosensitivity in invadopodia, podosomes and focal adhesions. *J Cell Sci* **122**(17)**,** 3037-3049.

Ammer, A. G., and Weed, S. A. (2008). Cortactin branches out: Roles in regulating protrusive actin dynamics. *Cell Motility and the Cytoskeleton* **65**(9)**,** 687-707.

Andrianantoandro, E., and Pollard, T. D. (2006). Mechanism of Actin Filament Turnover by Severing and Nucleation at Different Concentrations of ADF/Cofilin. *Molecular Cell* **24**(1)**,** 13-23.

Araki, N., Hatae, T., Yamada, T., and Hirohashi, S. (2000). Actinin-4 is preferentially involved in circular ruffling and macropinocytosis in mouse macrophages: analysis by fluorescence ratio imaging. *J Cell Sci* **113**(18)**,** 3329-3340.

Arber, S., Barbayannis, F. A., Hanser, H., Schneider, C., Stanyon, C. A., Bernard, O., and Caroni, P. (1998). Regulation of actin dynamics through phosphorylation of cofilin by LIM-kinase. *Nature* **393**(6687)**,** 805-809.

Ardern, H., Sandilands, E., Machesky, L. M., Timpson, P., Frame, M. C., and Brunton, V. G. (2006). Src-dependent phosphorylation of Scar1 promotes its association with the Arp2/3 complex. *Cell Motility and the Cytoskeleton* **63**(1)**,** 6-13.

Aspenström, P., Fransson, A., and Saras, J. (2004). Rho-GTPases have diverse effects on the organization of the actin filament system. *Biochem. J.* **377**(2)**,** 327-337.

Auinger, S., and Small, J. V. (2008). Correlated light and electron microscopy of the cytoskeleton. *Methods Cell Biol* **88,** 257-72.

Baird, D., Feng, Q., and Cerione, R. A. (2005). The Cool-2/[alpha]-Pix Protein Mediates a Cdc42-Rac Signaling Cascade. *Current Biology* **15**(1)**,** 1-10.

Bamburg, J. R., Harris, H. E., and Weeds, A. G. (1980). Partial purification and characterization of an actin depolymerizing factor from brain. *FEBS Letters* **121**(1)**,** 178-182.

Bardelli, A., Ponzetto, C., and Comoglio, P. M. (1994). Identification of functional domains in the hepatocyte growth factor and its receptor by molecular engineering. *Journal of Biotechnology* **37**(2)**,** 109-122.

Barroso, C., Rodenbusch, S. E., Welch, M. D., and Drubin, D. G. (2006). A role for cortactin in Listeria monocytogenes invasion of NIH 3T3 cells, but not in its intracellular motility. *Cell Motility and the Cytoskeleton* **63**(4)**,** 231-243.

Barzik, M., Kotova, T. I., Higgs, H. N., Hazelwood, L., Hanein, D., Gertler, F. B., and Schafer, D. A. (2005). Ena/VASP Proteins Enhance Actin Polymerization in the Presence of Barbed End Capping Proteins. *Journal of Biological Chemistry* **280**(31)**,** 28653-28662.

Bear, J. E., and Gertler, F. B. (2009). Ena/VASP: towards resolving a pointed controversy at the barbed end. *J Cell Sci* **122**(12)**,** 1947-1953.

Bear, J. E., Svitkina, T. M., Krause, M., Schafer, D. A., Loureiro, J. J., Strasser, G. A., Maly, I. V., Chaga, O. Y., Cooper, J. A., Borisy, G. G., and Gertler, F. B. (2002). Antagonism between Ena/VASP Proteins and Actin Filament Capping Regulates Fibroblast Motility. *Cell* **109**(4)**,** 509-521.

Benesch, S., Lommel, S., Steffen, A., Stradal, T. E. B., Scaplehorn, N., Way, M., Wehland, J., and Rottner, K. (2002). Phosphatidylinositol 4,5-Biphosphate (PIP2)-induced Vesicle Movement Depends on N-WASP and Involves Nck, WIP, and Grb2. *Journal of Biological Chemistry* **277**(40)**,** 37771-37776.

Benesch, S., Polo, S., Lai, F. P. L., Anderson, K. I., Stradal, T. E. B., Wehland, J., and Rottner, K. (2005). N-WASP deficiency impairs EGF internalization and actin assembly at clathrin-coated pits. *J Cell Sci* **118**(14)**,** 3103-3115.

Bernardini, M. L., Mounier, J., d'Hauteville, H., Coquis-Rondon, M., and Sansonetti, P. J. (1989). Identification of icsA, a plasmid locus of Shigella flexneri that governs bacterial intra- and intercellular spread through interaction with F-actin. *Proceedings of the National Academy of Sciences of the United States of America* **86**(10)**,** 3867-3871.

Bernstein, B. W., and Bamburg, J. R. (2010). ADF/Cofilin: a functional node in cell biology. *Trends in Cell Biology* **20**(4)**,** 187-195.

Bierne, H., Gouin, E., Roux, P., Caroni, P., Yin, H. L., and Cossart, P. (2001). A role for cofilin and LIM kinase in Listeria-induced phagocytosis. *The Journal of Cell Biology* **155**(1)**,** 101-112.

Billadeau, D. D., Nolz, J. C., and Gomez, T. S. (2007). Regulation of T-cell activation by the cytoskeleton. *Nat Rev Immunol* **7**(2)**,** 131-143.

Blain, E. J. (2009). Involvement of the cytoskeletal elements in articular cartilage homeostasis and pathology. *International Journal of Experimental Pathology* **90**(1)**,** 1-15.

Blanchard, A., Ohanian, V., and Critchley, D. (1989). The structure and function of alpha-actinin. *Journal of Muscle Research and Cell Motility* **10**(4)**,** 280-289.

Blanchoin, L., Amann, K. J., Higgs, H. N., Marchand, J.-B., Kaiser, D. A., and Pollard, T. D. (2000). Direct observation of dendritic actin filament networks nucleated by Arp2/3 complex and WASP/Scar proteins. *Nature* **404**(6781)**,** 1007-1011.

Block, J., Stradal, T. E. B., HÄNisch, J., Geffers, R., KÖStler, S. A., Urban, E., Small, J. V., Rottner, K., and Faix, J. (2008). Filopodia formation induced by active mDia2/Drf3. *Journal of Microscopy* **231**(3)**,** 506-517.

Bosse, T., Ehinger, J., Czuchra, A., Benesch, S., Steffen, A., Wu, X., Schloen, K., Niemann, H. H., Scita, G., Stradal, T. E. B., Brakebusch, C., and Rottner, K. (2007). Cdc42 and Phosphoinositide 3-Kinase Drive Rac-Mediated Actin Polymerization Downstream of c-Met in Distinct and Common Pathways. *Mol. Cell. Biol.* **27**(19)**,** 6615-6628.

Bottcher, R. T., Wiesner, S., Braun, A., Wimmer, R., Berna, A., Elad, N., Medalia, O., Pfeifer, A., Aszodi, A., Costell, M., and Fassler, R. (2009). Profilin 1 is required for abscission during late cytokinesis of chondrocytes. *EMBO J* **28**(8)**,** 1157-1169.

Bougneres, L., Girardin, S. E., Weed, S. A., Karginov, A. V., Olivo-Marin, J. C., Parsons, J. T., Sansonetti, P. J., and Van Nhieu, G. T. (2004). Cortactin and Crk cooperate to trigger actin polymerization during Shigella invasion of epithelial cells. *J Cell Biol* **166**(2)**,** 225-35.

Bouhamdan, M., Yan, H.-D., Yan, X.-H., Bannon, M. J., and Andrade, R. (2006). Brain-Specific Regulator of G-Protein Signaling 9-2 Selectively Interacts with {alpha}-Actinin-2 to Regulate Calcium-Dependent Inactivation of NMDA Receptors. *J. Neurosci.* **26**(9)**,** 2522-2530.

Boztug, K., Schmidt, M., Schwarzer, A., Banerjee, P. P., Díez, I. A., Dewey, R. A., Böhm, M., Nowrouzi, A., Ball, C. R., Glimm, H., Naundorf, S., Kühlcke, K., Blasczyk, R., Kondratenko, I., Maródi, L., Orange, J. S., von Kalle, C., and Klein, C. (2010). Stem-Cell Gene Therapy for the Wiskott–Aldrich Syndrome. *New England Journal of Medicine* **363**(20)**,** 1918-1927.

Braun, L., Ghebrehiwet, B., and Cossart, P. (2000). gC1q-R/p32, a C1q-binding protein, is a receptor for the InlB invasion protein of Listeria monocytogenes. *EMBO J* **19**(7)**,** 1458-1466.

Breitsprecher, D., Kiesewetter, A. K., Linkner, J., Urbanke, C., Resch, G. P., Small, J. V., and Faix, J. (2008). Clustering of VASP actively drives processive, WH2 domain-mediated actin filament elongation. *EMBO J* **27**(22)**,** 2943-2954.

Bryce, N. S., Clark, E. S., Leysath, J. M. L., Currie, J. D., Webb, D. J., and Weaver, A. M. (2005). Cortactin Promotes Cell Motility by Enhancing Lamellipodial Persistence. *Current Biology* **15**(14)**,** 1276-1285.

Bryce, N. S., Schevzov, G., Ferguson, V., Percival, J. M., Lin, J. J.-C., Matsumura, F., Bamburg, J. R., Jeffrey, P. L., Hardeman, E. C., Gunning, P., and Weinberger, R. P. (2003). Specification of Actin Filament Function and Molecular Composition by Tropomyosin Isoforms. *Mol. Biol. Cell* **14**(3)**,** 1002-1016.

Buccione, R., Orth, J. D., and McNiven, M. A. (2004). Foot and mouth: podosomes, invadopodia and circular dorsal ruffles. *Nat Rev Mol Cell Biol* **5**(8)**,** 647-657.

Buck, M., Xu, W., and Rosen, M. K. (2004). A Two-State Allosteric Model for Autoinhibition Rationalizes WASP Signal Integration and Targeting. *Journal of Molecular Biology* **338**(2)**,** 271-285.

Bugyi, B., and Carlier, M.-F. (2010). Control of Actin Filament Treadmilling in Cell Motility. *Annual Review of Biophysics* **39**(1)**,** 449-470.

Cabello, N., Remelli, R., Canela, L., Soriguera, A., Mallol, J., Canela, E. I., Robbins, M. J., Lluis, C., Franco, R., McIlhinney, R. A. J., and Ciruela, F. (2007). Actin-binding Protein α-Actinin-1 Interacts with the Metabotropic Glutamate Receptor Type 5b and Modulates the Cell Surface Expression and Function of the Receptor. *Journal of Biological Chemistry* **282**(16)**,** 12143-12153.

Cai, J.-h., Zhao, R., Zhu, J.-w., Jin, X.-l., Wan, F.-j., Liu, K., Ji, X.-p., Zhu, Y.-b., and Zhu, Z.-g. (2010). Expression of Cortactin Correlates with a Poor Prognosis in Patients with Stages II–III Colorectal Adenocarcinoma. *Journal of Gastrointestinal Surgery* **14**(8)**,** 1248-1257.

Caldwell, J. E., Heiss, S. G., Mermall, V., and Cooper, J. A. (1989). Effects of CapZ, an actin-capping protein of muscle, on the polymerization of actin. *Biochemistry* **28**(21)**,** 8506-8514.

Campellone, K. G., Webb, N. J., Znameroski, E. A., and Welch, M. D. (2008). WHAMM Is an Arp2/3 Complex Activator That Binds Microtubules and Functions in ER to Golgi Transport. *Cell* **134**(1)**,** 148-161.

Campellone, K. G., and Welch, M. D. (2010). A nucleator arms race: cellular control of actin assembly. *Nat Rev Mol Cell Biol* **11**(4)**,** 237-251.

Cantarelli, V. V., Kodama, T., Nijstad, N., Abolghait, S. K., Iida, T., and Honda, T. (2006). Cortactin is essential for F-actin assembly in enteropathogenic Escherichia coli (EPEC)- and enterohaemorrhagic E. coli (EHEC)-induced pedestals and the α-helical region is involved in the localization of cortactin to bacterial attachment sites. *Cellular Microbiology* **8**(5)**,** 769-780.

Cantarelli, V. V., Takahashi, A., Yanagihara, I., Akeda, Y., Imura, K., Kodama, T., Kono, G., Sato, Y., Iida, T., and Honda, T. (2002). Cortactin Is Necessary for F-Actin Accumulation in Pedestal Structures Induced by Enteropathogenic Escherichia coli Infection. *Infect. Immun.* **70**(4)**,** 2206-2209.

Cantley, L. C. (2002). The Phosphoinositide 3-Kinase Pathway. *Science* **296**(5573)**,** 1655-1657.

Cao, H., Chen, J., Krueger, E. W., and McNiven, M. A. (2010). Src-Mediated Phosphorylation of Dynamin and Cortactin Regulates the "Constitutive" Endocytosis of Transferrin. *Mol. Cell. Biol.* **30**(3)**,** 781-792.

Carlier, M.-F., Hertzog, M., Didry, D., Renault, L., Cantrelle, F.-X., Van Heijenoort, C., Knossow, M., and Guittet, E. (2007). Structure, Function, and Evolution of the β-Thymosin/WH2 (WASP-Homology2) Actin-Binding Module. *Annals of the New York Academy of Sciences* **1112**(1)**,** 67-75.

Carlier, M.-F., Laurent, V., Santolini, J., Melki, R., Didry, D., Xia, G.-X., Hong, Y., Chua, N.-H., and Pantaloni, D. (1997). Actin Depolymerizing Factor (ADF/Cofilin) Enhances the Rate of Filament Turnover: Implication in Actin-based Motility. *The Journal of Cell Biology* **136**(6)**,** 1307-1322.

Carlier, M.-F., and Pantaloni, D. (1997). Control of actin dynamics in cell motility. *Journal of Molecular Biology* **269**(4)**,** 459-467.

Carlson, L., Nyström, L. E., Lindberg, U., Kannan, K. K., H., C.-D., and Lövgren, S. (1976). Crystallization of a non-muscle actin. *Journal of Molecular Biology* **105**(3)**,** 353-366.

Carlsson, A. E. (2010). Actin Dynamics: From Nanoscale to Microscale. *Annual Review of Biophysics* **39**(1)**,** 91-110.

Chen, L., Wang, Z.-W., Zhu, J.-w., and Zhan, X. (2006). Roles of Cortactin, an Actin Polymerization Mediator, in Cell Endocytosis. *Acta Biochimica et Biophysica Sinica* **38**(2)**,** 95-103.

Chen, Z., Borek, D., Padrick, S. B., Gomez, T. S., Metlagel, Z., Ismail, A. M., Umetani, J., Billadeau, D. D., Otwinowski, Z., and Rosen, M. K. (2010). Structure and control of the actin regulatory WAVE complex. *Nature* **468**(7323)**,** 533-538.

Chereau, D., Kerff, F., Graceffa, P., Grabarek, Z., Langsetmo, K., and Dominguez, R. (2005). Actin-bound structures of Wiskott–Aldrich syndrome protein (WASP)-homology domain 2 and the implications for filament assembly. *Proceedings of the National Academy of Sciences of the United States of America* **102**(46)**,** 16644-16649.

Chinkers, M., McKanna, J. A., and Cohen, S. (1979). Rapid induction of morphological changes in human carcinoma cells A-431 by epidermal growth factors. *The Journal of Cell Biology* **83**(1)**,** 260-265.

Christerson, L. B., Vanderbilt, C. A., and Cobb, M. H. (1999). MEKK1 interacts with α-actinin and localizes to stress fibers and focal adhesions. *Cell Motility and the Cytoskeleton* **43**(3)**,** 186-198.

Chrzanowska-Wodnicka, M., and Burridge, K. (1996). Rho-stimulated contractility drives the formation of stress fibers and focal adhesions. *The Journal of Cell Biology* **133**(6)**,** 1403-1415.

Co, C., Wong, D. T., Gierke, S., Chang, V., and Taunton, J. (2007). Mechanism of Actin Network Attachment to Moving Membranes: Barbed End Capture by N-WASP WH2 Domains. *Cell* **128**(5)**,** 901-913.

Cooper, J. A. (1987). Effects of cytochalasin and phalloidin on actin. *The Journal of Cell Biology* **105**(4)**,** 1473-1478.

Cooper, J. A., and Sept, D. (2008). New Insights into Mechanism and Regulation of Actin Capping Protein. *In* "International Review of Cell and Molecular Biology" (W. J. Kwang, Ed.), Vol. Volume 267, pp. 183-206. Academic Press.

Cooper, J. A., Walker, S. B., and Pollard, T. D. (1983). Pyrene actin: documentation of the validity of a sensitive assay for actin polymerization. *Journal of Muscle Research and Cell Motility* **4**(2)**,** 253-262.

Cosen-Binker, L. I., and Kapus, A. (2006). Cortactin: The Gray Eminence of the Cytoskeleton. *Physiology* **21**(5)**,** 352-361.

Coutts, A. S., Weston, L., and La Thangue, N. B. (2009). A transcription co-factor integrates cell adhesion and motility with the p53 response. *Proceedings of the National Academy of Sciences* **106**(47)**,** 19872-19877.

Craig, A. W., Zirngibl, R., Williams, K., Cole, L. A., and Greer, P. A. (2001). Mice devoid of fer protein-tyrosine kinase activity are viable and fertile but display reduced cortactin phosphorylation. *Mol Cell Biol* **21**(2)**,** 603-13.

Cramer, L. P., Siebert, M., and Mitchison, T. J. (1997). Identification of Novel Graded Polarity Actin Filament Bundles in Locomoting Heart Fibroblasts: Implications for the Generation of Motile Force. *The Journal of Cell Biology* **136**(6)**,** 1287-1305.

Crostella, L., Lidder, S., Williams, R., and Skouteris, G. G. (2001). Hepatocyte Growth Factor/scatter factor-induces phosphorylation of cortactin in A431 cells in a Src kinase-independent manner. *Oncogene* **20**(28)**,** 3735-45.

Croucher, D. R., Rickwood, D., Tactacan, C. M., Musgrove, E. A., and Daly, R. J. (2010). Cortactin Modulates RhoA Activation and Expression of Cip/Kip Cyclin-Dependent Kinase Inhibitors To Promote Cell Cycle Progression in 11q13-Amplified Head and Neck Squamous Cell Carcinoma Cells. *Mol. Cell. Biol.* **30**(21)**,** 5057-5070.

Cuevas, B. D., Abell, A. N., Witowsky, J. A., Yujiri, T., Johnson, N. L., Kesavan, K., Ware, M., Jones, P. L., Weed, S. A., DeBiasi, R. L., Oka, Y., Tyler, K. L., and Johnson, G. L. (2003). MEKK1 regulates calpain-dependent proteolysis of focal adhesion proteins for rear-end detachment of migrating fibroblasts. *EMBO J* **22**(13)**,** 3346-3355.

Dabiri, G. A., Sanger, J. M., Portnoy, D. A., and Southwick, F. S. (1990). Listeria monocytogenes moves rapidly through the host-cell cytoplasm by inducing directional actin assembly. *Proceedings of the National Academy of Sciences of the United States of America* **87**(16)**,** 6068-6072.

Danson, C. M., Pocha, S. M., Bloomberg, G. B., and Cory, G. O. (2007). Phosphorylation of WAVE2 by MAP kinases regulates persistent cell migration and polarity. *J Cell Sci* **120**(23)**,** 4144-4154.

Davis, C. J., Meighan, P. C., Taishi, P., Krueger, J. M., Harding, J. W., and Wright, J. W. (2006). REM sleep deprivation attenuates actin-binding protein cortactin: A link between sleep and hippocampal plasticity. *Neuroscience Letters* **400**(3)**,** 191-196.

Dayel, M. J., and Mullins, R. D. (2004). Activation of Arp2/3 Complex: Addition of the First Subunit of the New Filament by a WASP Protein Triggers Rapid ATP Hydrolysis on Arp2. *PLoS Biol* **2**(4)**,** e91.

De Arcangelis, A., Georges-Labouesse, E., and Adams, J. C. (2004). Expression of fascin-1, the gene encoding the actin-bundling protein fascin-1, during mouse embryogenesis. *Gene Expression Patterns* **4**(6)**,** 637-643.

de la Fuente, M. A., Sasahara, Y., Calamito, M., Antón, I. M., Elkhal, A., Gallego, M. D., Suresh, K., Siminovitch, K., Ochs, H. D., Anderson, K. C., Rosen, F. S., Geha, R. S., and Ramesh, N. (2007). WIP is a chaperone for Wiskott–Aldrich syndrome protein (WASP). *Proceedings of the National Academy of Sciences* **104**(3)**,** 926-931.

Delatour, V., Helfer, E., Didry, D., Lê, K. H. D., Gaucher, J.-F., Carlier, M.-F., and Romet-Lemonne, G. (2008). Arp2/3 Controls the Motile Behavior of N-WASP-Functionalized GUVs and Modulates N-WASP Surface Distribution by Mediating Transient Links with Actin Filaments. *Biophysical Journal* **94**(12)**,** 4890-4905.

Derivery, E., Sousa, C., Gautier, J. J., Lombard, B., Loew, D., and Gautreau, A. (2009). The Arp2/3 Activator WASH Controls the Fission of Endosomes through a Large Multiprotein Complex. *Developmental Cell* **17**(5)**,** 712-723.

DerMardirossian, C., and Bokoch, G. M. (2005). GDIs: central regulatory molecules in Rho-GTPase activation. *Trends in Cell Biology* **15**(7)**,** 356-363.

DerMardirossian, C., Schnelzer, A., and Bokoch, G. M. (2004). Phosphorylation of RhoGDI by Pak1 Mediates Dissociation of Rac GTPase. *Molecular Cell* **15**(1)**,** 117-127.

Destaing, O., Saltel, F., Geminard, J.-C., Jurdic, P., and Bard, F. (2003). Podosomes Display Actin Turnover and Dynamic Self-Organization in Osteoclasts Expressing Actin-Green Fluorescent Protein. *Mol. Biol. Cell* **14**(2)**,** 407-416.

Dharmawardhane, S., Sanders, L. C., Martin, S. S., Daniels, R. H., and Bokoch, G. M. (1997). Localization of p21-Activated Kinase 1 (PAK1) to Pinocytic Vesicles and Cortical Actin Structures in Stimulated Cells. *The Journal of Cell Biology* **138**(6)**,** 1265-1278.

Disanza, A., Steffen, A., Hertzog, M., Frittoli, E., Rottner, K., and Scita, G. (2005). Actin polymerization machinery: the finish line of signaling networks, the starting point of cellular movement. *Cellular and Molecular Life Sciences* **62**(9)**,** 955-970.

Domann, E., Wehland, J., Rohde, M., Pistor, S., Hartl, M., Goebel, W., Leimeister-Wachter, M., Wuenscher, M., and Chakraborty, T. (1992). A novel bacterial virulence gene in Listeria monocytogenes required for host cell microfilament interaction with homology to the proline-rich region of vinculin. *The EMBO journal* **11**(5)**,** 1981-90.

Dominguez, R. (2009). Actin filament nucleation and elongation factors – structure-function relationships. *Critical Review in Biochemistry and Molecular Biology* **44**(6)**,** 351-366.

Dowrick, P., Kenworthy, P., McCann, B., and Warn, R. (1993). "Circular ruffle formation and closure lead to macropinocytosis in hepatocyte growth factor/scatter factor-treated cells." 61.

Ducka, A. M., Joel, P., Popowicz, G. M., Trybus, K. M., Schleicher, M., Noegel, A. A., Huber, R., Holak, T. A., and Sitar, T. (2010). Structures of actin-bound Wiskott-

Aldrich syndrome protein homology 2 (WH2) domains of Spire and the implication for filament nucleation. *Proceedings of the National Academy of Sciences* **107**(26)**,** 11757-11762.

Dudek, S. M., Birukov, K. G., Zhan, X., and Garcia, J. G. N. (2002). Novel interaction of cortactin with endothelial cell myosin light chain kinase. *Biochemical and Biophysical Research Communications* **298**(4)**,** 511-519.

Duleh, S. N., and Welch, M. D. (2010). WASH and the Arp2/3 complex regulate endosome shape and trafficking. *Cytoskeleton* **67**(3)**,** 193-206.

Duncan, M. C., Cope, M. J. T. V., Goode, B. L., Wendland, B., and Drubin, D. G. (2001). Yeast Eps15-like endocytic protein, Pan1p, activates the Arp2/3 complex. *Nat Cell Biol* **3**(7)**,** 687-690.

Eden, S., Rohatgi, R., Podtelejnikov, A. V., Mann, M., and Kirschner, M. W. (2002). Mechanism of regulation of WAVE1-induced actin nucleation by Rac1 and Nck. *Nature* **418**(6899)**,** 790-793.

Edlund, M., Lotano, M. A., and Otey, C. A. (2001). Dynamics of α-actinin in focal adhesions and stress fibers visualized with α-actinin-green fluorescent protein. *Cell Motility and the Cytoskeleton* **48**(3)**,** 190-200.

Egerton, M., Moritz, R. L., Druker, B., Kelso, A., and Simpson, R. J. (1996). Identification of the 70kD Heat Shock Cognate Protein (Hsc70) and [alpha]-Actinin-1 as Novel Phosphotyrosine-Containing Proteins in T Lymphocytes. *Biochemical and Biophysical Research Communications* **224**(3)**,** 666-674.

Egile, C., Loisel, T. P., Laurent, V., Li, R., Pantaloni, D., Sansonetti, P. J., and Carlier, M.-F. (1999). Activation of the Cdc42 Effector N-Wasp by the Shigella flexneri Icsa Protein Promotes Actin Nucleation by Arp2/3 Complex and Bacterial Actin-Based Motility. *The Journal of Cell Biology* **146**(6)**,** 1319-1332.

Eiseler, T., Hausser, A., De Kimpe, L., Van Lint, J., and Pfizenmaier, K. (2010). Protein Kinase D Controls Actin Polymerization and Cell Motility through Phosphorylation of Cortactin. *Journal of Biological Chemistry* **285**(24)**,** 18672-18683.

Ellenbroek, S., and Collard, J. (2007). Rho-GTPases: functions and association with cancer. *Clinical and Experimental Metastasis* **24**(8)**,** 657-672.

Erck, C., Peris, L., Andrieux, A., Meissirel, C., Gruber, A. D., Vernet, M., Schweitzer, A., Saoudi, Y., Pointu, H., Bosc, C., Salin, P. A., Job, D., and Wehland, J. (2005). A vital role of tubulin-tyrosine-ligase for neuronal organization. *Proceedings of the National Academy of Sciences of the United States of America* **102**(22)**,** 7853-7858.

Etienne-Manneville, S. (2010). From signaling pathways to microtubule dynamics: the key players. *Current Opinion in Cell Biology* **22**(1)**,** 104-111.

Evans, S. S., Schleider, D. M., Bowman, L. A., Francis, M. L., Kansas, G. S., and Black, J. D. (1999). Dynamic Association of L-Selectin with the Lymphocyte Cytoskeletal Matrix. *The Journal of Immunology* **162**(6)**,** 3615-3624.

Faix, J., Breitsprecher, D., Stradal, T. E. B., and Rottner, K. (2009). Filopodia: Complex models for simple rods. *The International Journal of Biochemistry & Cell Biology* **41**(8-9)**,** 1656-1664.

Faix, J., and Rottner, K. (2006). The making of filopodia. *Current Opinion in Cell Biology* **18**(1)**,** 18-25.

Firat-Karalar, E. N., and Welch, M. D. (2011). New mechanisms and functions of actin nucleation. *Current Opinion in Cell Biology* **23**(1)**,** 4-13.

Fraley, T. S., Tran, T. C., Corgan, A. M., Nash, C. A., Hao, J., Critchley, D. R., and Greenwood, J. A. (2003). Phosphoinositide Binding Inhibits α-Actinin Bundling Activity. *Journal of Biological Chemistry* **278**(26)**,** 24039-24045.

Fujiwara, H., Gu, J., and Sekiguchi, K. (2004). Rac regulates integrin-mediated endothelial cell adhesion and migration on laminin-8. *Experimental Cell Research* **292**(1)**,** 67-77.

Furman, C., Sieminski, A. L., Kwiatkowski, A. V., Rubinson, D. A., Vasile, E., Bronson, R. T., Fässler, R., and Gertler, F. B. (2007). Ena/VASP is required for endothelial barrier function in vivo. *The Journal of Cell Biology* **179**(4)**,** 761-775.

Gad, A. K. B., and Aspenström, P. (2010). Rif proteins take to the RhoD: Rho-GTPases at the crossroads of actin dynamics and membrane trafficking. *Cellular Signalling* **22**(2)**,** 183-189.

Gandhi, M., Achard, V., Blanchoin, L., and Goode, B. L. (2009). Coronin Switches Roles in Actin Disassembly Depending on the Nucleotide State of Actin. *Molecular Cell* **34**(3)**,** 364-374.

Gardel, M. L., Schneider, I. C., Aratyn-Schaus, Yvonne, and Waterman, C. M. (2010). Mechanical Integration of Actin and Adhesion Dynamics in Cell Migration. *Annual Review of Cell and Developmental Biology* **26**(1)**,** 315-333.

Gautreau, A., Ho, H.-y. H., Li, J., Steen, H., Gygi, S. P., and Kirschner, M. W. (2004). Purification and architecture of the ubiquitous Wave complex. *Proceedings of the National Academy of Sciences of the United States of America* **101**(13)**,** 4379-4383.

Ghosh, M., Song, X., Mouneimne, G., Sidani, M., Lawrence, D. S., and Condeelis, J. S. (2004). Cofilin Promotes Actin Polymerization and Defines the Direction of Cell Motility. *Science* **304**(5671)**,** 743-746.

Giannone, G., Dubin-Thaler, B. J., Rossier, O., Cai, Y., Chaga, O., Jiang, G., Beaver, W., Döbereiner, H.-G., Freund, Y., Borisy, G., and Sheetz, M. P. (2007). Lamellipodial Actin Mechanically Links Myosin Activity with Adhesion-Site Formation. *Cell* **128**(3)**,** 561-575.

Gimona, M., and Buccione, R. (2006). Adhesions that mediate invasion. *The International Journal of Biochemistry & Cell Biology* **38**(11)**,** 1875-1892.

Gimona, M., Djinovic-Carugo, K., Kranewitter, W. J., and Winder, S. J. (2002). Functional plasticity of CH domains. *FEBS Letters* **513**(1)**,** 98-106.

Goldberg, M. B. (2001). Actin-Based Motility of Intracellular Microbial Pathogens. *Microbiol. Mol. Biol. Rev.* **65**(4)**,** 595-626.

Goldberg, M. B., and Theriot, J. A. (1995). Shigella flexneri surface protein IcsA is sufficient to direct actin-based motility. *Proceedings of the National Academy of Sciences of the United States of America* **92**(14)**,** 6572-6576.

Goldberg, M. B., Theriot, J. A., and Sansonetti, P. J. (1994). Regulation of surface presentation of IcsA, a Shigella protein essential to intracellular movement and spread, is growth phase dependent. *Infect. Immun.* **62**(12)**,** 5664-5668.

Goley, E. D., Rodenbusch, S. E., Martin, A. C., and Welch, M. D. (2004). Critical Conformational Changes in the Arp2/3 Complex Are Induced by Nucleotide and Nucleation Promoting Factor. *Molecular Cell* **16**(2)**,** 269-279.

Gomez, T. S., and Billadeau, D. D. (2009). A FAM21-Containing WASH Complex Regulates Retromer-Dependent Sorting. *Developmental Cell* **17**(5)**,** 699-711.

Gomez, T. S., McCarney, S. D., Carrizosa, E., Labno, C. M., Comiskey, E. O., Nolz, J. C., Zhu, P., Freedman, B. D., Clark, M. R., Rawlings, D. J., Billadeau, D. D., and

Burkhardt, J. K. (2006). HS1 Functions as an Essential Actin-Regulatory Adaptor Protein at the Immune Synapse. *Immunity* **24**(6)**,** 741-752.

Goode, B. L., Rodal, A. A., Barnes, G., and Drubin, D. G. (2001). Activation of the Arp2/3 Complex by the Actin Filament Binding Protein Abp1p. *The Journal of Cell Biology* **153**(3)**,** 627-634.

Gould, C. J., Maiti, S., Michelot, A., Graziano, B. R., Blanchoin, L., and Goode, B. L. (2011). The Formin DAD Domain Plays Dual Roles in Autoinhibition and Actin Nucleation. *Current Biology* **21**(5)**,** 384-390.

Gournier, H., Goley, E. D., Niederstrasser, H., Trinh, T., and Welch, M. D. (2001). Reconstitution of Human Arp2/3 Complex Reveals Critical Roles of Individual Subunits in Complex Structure and Activity. *Molecular Cell* **8**(5)**,** 1041-1052.

Grassart, A., Meas-Yedid, V., Dufour, A., Olivo-Marin, J.-C., Dautry-Varsat, A., and Sauvonnet, N. (2010). Pak1 Phosphorylation Enhances Cortactin–N-WASP Interaction in Clathrin-Caveolin-Independent Endocytosis. *Traffic* **11**(8)**,** 1079-1091.

Gray, N. W., Kruchten, A. E., Chen, J., and McNiven, M. A. (2005). A dynamin-3 spliced variant modulates the actin/cortactin-dependent morphogenesis of dendritic spines. *J Cell Sci* **118**(6)**,** 1279-1290.

Greenwood, J. A., Theibert, A. B., Prestwich, G. D., and Murphy-Ullrich, J. E. (2000). Restructuring of Focal Adhesion Plaques by Pi 3-Kinase. *The Journal of Cell Biology* **150**(3)**,** 627-642.

Guo, F., Debidda, M., Yang, L., Williams, D. A., and Zheng, Y. (2006). Genetic Deletion of Rac1 GTPase Reveals Its Critical Role in Actin Stress Fiber Formation and Focal Adhesion Complex Assembly. *Journal of Biological Chemistry* **281**(27)**,** 18652-18659.

Gurniak, C. B., Perlas, E., and Witke, W. (2005). The actin depolymerizing factor n-cofilin is essential for neural tube morphogenesis and neural crest cell migration. *Developmental Biology* **278**(1)**,** 231-241.

Haffner, C., Jarchau, T., Reinhard, M., Hoppe, J., Lohmann, S., and Walter, U. (1995). Molecular cloning, structural analysis and functional expression of the proline-rich focal adhesion and microfilament-associated protein VASP. *EMBO J* **14,** 19-27.

Hänisch, J., Ehinger, J., Ladwein, M., Rohde, M., Derivery, E., Bosse, T., Steffen, A., Bumann, D., Misselwitz, B., Hardt, W.-D., Gautreau, A., Stradal, T. E. B., and Rottner, K. (2010). Molecular dissection of Salmonella-induced membrane ruffling versus invasion. *Cellular Microbiology* **12**(1)**,** 84-98.

Hansen, S. D., and Mullins, R. D. (2010). VASP is a processive actin polymerase that requires monomeric actin for barbed end association. *The Journal of Cell Biology* **191**(3)**,** 571-584.

Harris, E. S., Li, F., and Higgs, H. N. (2004). The Mouse Formin, FRLα, Slows Actin Filament Barbed End Elongation, Competes with Capping Protein, Accelerates Polymerization from Monomers, and Severs Filaments. *Journal of Biological Chemistry* **279**(19)**,** 20076-20087.

Hashimoto, Y., Parsons, M., and Adams, J. C. (2007). Dual Actin-bundling and Protein Kinase C-binding Activities of Fascin Regulate Carcinoma Cell Migration Downstream of Rac and Contribute to Metastasis. *Mol. Biol. Cell* **18**(11)**,** 4591-4602.

Hashimoto, Y., Skacel, M., and Adams, J. C. (2005). Roles of fascin in human carcinoma motility and signaling: Prospects for a novel biomarker? *The International Journal of Biochemistry & Cell Biology* **37**(9)**,** 1787-1804.

Herrmann, H., Bar, H., Kreplak, L., Strelkov, S. V., and Aebi, U. (2007). Intermediate filaments: from cell architecture to nanomechanics. *Nat Rev Mol Cell Biol* **8**(7)**,** 562-573.

Herrmann, H., Strelkov, S. V., Burkhard, P., and Aebi, U. (2009). Intermediate filaments: primary determinants of cell architecture and plasticity. *The Journal of Clinical Investigation* **119**(7)**,** 1772-1783.

Higgs, H. N., and Pollard, T. D. (1999). Regulation of Actin Polymerization by Arp2/3 Complex and WASp/Scar Proteins. *Journal of Biological Chemistry* **274**(46)**,** 32531-32534.

Higgs, H. N., and Pollard, T. D. (2000). Activation by Cdc42 and Pip2 of Wiskott-Aldrich Syndrome Protein (Wasp) Stimulates Actin Nucleation by Arp2/3 Complex. *The Journal of Cell Biology* **150**(6)**,** 1311-1320.

Ho, H.-Y. H., Rohatgi, R., Lebensohn, A. M., Le, M., Li, J., Gygi, S. P., and Kirschner, M. W. (2004). Toca-1 Mediates Cdc42-Dependent Actin Nucleation by Activating the N-WASP-WIP Complex. *Cell* **118**(2)**,** 203-216.

Hoffman, G. R., Nassar, N., and Cerione, R. A. (2000). Structure of the Rho Family GTP-Binding Protein Cdc42 in Complex with the Multifunctional Regulator RhoGDI. *Cell* **100**(3)**,** 345-356.

Horwitz, A., Duggan, K., Buck, C., Beckerle, M. C., and Burridge, K. (1986). Interaction of plasma membrane fibronectin receptor with talin[mdash]a transmembrane linkage. *Nature* **320**(6062)**,** 531-533.

Hotulainen, P., Paunola, E., Vartiainen, M. K., and Lappalainen, P. (2005). Actin-depolymerizing Factor and Cofilin-1 Play Overlapping Roles in Promoting Rapid F-Actin Depolymerization in Mammalian Nonmuscle Cells. *Mol. Biol. Cell* **16**(2)**,** 649-664.

Hou, P., Estrada, L., Kinley, A. W., Parsons, J. T., Vojtek, A. B., and Gorski, J. L. (2003). Fgd1, the Cdc42 GEF responsible for Faciogenital Dysplasia, directly interacts with cortactin and mAbp1 to modulate cell shape. *Human Molecular Genetics* **12**(16)**,** 1981-1993.

Huang, C., Liu, J., Haudenschild, C. C., and Zhan, X. (1998). The role of tyrosine phosphorylation of cortactin in the locomotion of endothelial cells. *J Biol Chem* **273**(40)**,** 25770-6.

Huang, C., Ni, Y., Wang, T., Gao, Y., Haudenschild, C. C., and Zhan, X. (1997). Down-regulation of the Filamentous Actin Cross-linking Activity of Cortactin by Src-mediated Tyrosine Phosphorylation. *Journal of Biological Chemistry* **272**(21)**,** 13911-13915.

Hüfner, K., Higgs, H. N., Pollard, T. D., Jacobi, C., Aepfelbacher, M., and Linder, S. (2001). The Verprolin-like Central (VC) Region of Wiskott-Aldrich Syndrome Protein Induces Arp2/3 Complex-dependent Actin Nucleation. *Journal of Biological Chemistry* **276**(38)**,** 35761-35767.

Humphries, J. D., Wang, P., Streuli, C., Geiger, B., Humphries, M. J., and Ballestrem, C. (2007). Vinculin controls focal adhesion formation by direct interactions with talin and actin. *J Cell Biol* **179**(5)**,** 1043-57.

Ichetovkin, I., Grant, W., and Condeelis, J. (2002). Cofilin Produces Newly Polymerized Actin Filaments that Are Preferred for Dendritic Nucleation by the Arp2/3 Complex. *Current Biology* **12**(1)**,** 79-84.

Iki, J., Inoue, A., Bito, H., and Okabe, S. (2005). Bi-directional regulation of postsynaptic cortactin distribution by BDNF and NMDA receptor activity. *European Journal of Neuroscience* **22**(12)**,** 2985-2994.

Innocenti, M., Gerboth, S., Rottner, K., Lai, F. P. L., Hertzog, M., Stradal, T. E. B., Frittoli, E., Didry, D., Polo, S., Disanza, A., Benesch, S., Fiore, P. P. D., Carlier, M.-F., and Scita, G. (2005). Abi1 regulates the activity of N-WASP and WAVE in distinct actin-based processes. *Nat Cell Biol* **7**(10)**,** 969-976.

Innocenti, M., Zucconi, A., Disanza, A., Frittoli, E., Areces, L. B., Steffen, A., Stradal, T. E. B., Fiore, P. P. D., Carlier, M.-F., and Scita, G. (2004). Abi1 is essential for the formation and activation of a WAVE2 signalling complex. *Nat Cell Biol* **6**(4)**,** 319-327.

Ireton, K., Payrastre, B., Chap, H., Ogawa, W., Sakaue, H., Kasuga, M., and Cossart, P. (1996). A Role for Phosphoinositide 3-Kinase in Bacterial Invasion. *Science* **274**(5288)**,** 780-782.

Isaac, B. M., Ishihara, D., Nusblat, L. M., Gevrey, J.-C., Dovas, A., Condeelis, J., and Cox, D. (2010). N-WASP has the ability to compensate for the loss of WASP in macrophage podosome formation and chemotaxis. *Experimental Cell Research* **316**(20)**,** 3406-3416.

Ismail, A. M., Padrick, S. B., Chen, B., Umetani, J., and Rosen, M. K. (2009). The WAVE regulatory complex is inhibited. *Nat Struct Mol Biol* **16**(5)**,** 561-563.

Izaguirre, G., Aguirre, L., Hu, Y.-P., Lee, H. Y., Schlaepfer, D. D., Aneskievich, B. J., and Haimovich, B. (2001). The Cytoskeletal/Non-muscle Isoform of α-Actinin Is Phosphorylated on Its Actin-binding Domain by the Focal Adhesion Kinase. *Journal of Biological Chemistry* **276**(31)**,** 28676-28685.

Jackson, A. L., Bartz, S. R., Schelter, J., Kobayashi, S. V., Burchard, J., Mao, M., Li, B., Cavet, G., and Linsley, P. S. (2003). Expression profiling reveals off-target gene regulation by RNAi. *Nat Biotech* **21**(6)**,** 635-637.

Jay, P., Pham, P., Wong, S., and Elson, E. (1995). A mechanical function of myosin II in cell motility. *J Cell Sci* **108**(1)**,** 387-393.

Jayo, A., and Parsons, M. (2010). Fascin: A key regulator of cytoskeletal dynamics. *The International Journal of Biochemistry & Cell Biology* **42**(10)**,** 1614-1617.

Jenzora, A., Behrendt, B., Small, J. V., Wehland, J., and Stradal, T. E. B. (2005). PREL1 provides a link from Ras signalling to the actin cytoskeleton via Ena/VASP proteins. *FEBS Letters* **579**(2)**,** 455-463.

Kahner, B. N., Dorsam, R. T., Mada, S. R., Kim, S., Stalker, T. J., Brass, L. F., Daniel, J. L., Kitamura, D., and Kunapuli, S. P. (2007). Hematopoietic lineage cell specific protein 1 (HS1) is a functionally important signaling molecule in platelet activation. *Blood* **110**(7)**,** 2449-2456.

Kelleher, J. F., Atkinson, S. J., and Pollard, T. D. (1995). Sequences, structural models, and cellular localization of the actin-related proteins Arp2 and Arp3 from Acanthamoeba. *The Journal of Cell Biology* **131**(2)**,** 385-397.

Kelley, L. C., Hayes, K. E., Ammer, A. G., Martin, K. H., and Weed, S. A. (2010). Cortactin Phosphorylated by ERK1/2 Localizes to Sites of Dynamic Actin Regulation and Is Required for Carcinoma Lamellipodia Persistence. *PLoS ONE* **5**(11)**,** e13847.

Kelly, A. E., Kranitz, H., Dötsch, V., and Mullins, R. D. (2006). Actin Binding to the Central Domain of WASP/Scar Proteins Plays a Critical Role in the Activation of the Arp2/3 Complex. *Journal of Biological Chemistry* **281**(15)**,** 10589-10597.

Kempiak, S. J., Yamaguchi, H., Sarmiento, C., Sidani, M., Ghosh, M., Eddy, R. J., DesMarais, V., Way, M., Condeelis, J., and Segall, J. E. (2005). A Neural Wiskott-Aldrich Syndrome Protein-mediated Pathway for Localized Activation of Actin

Polymerization That Is Regulated by Cortactin. *Journal of Biological Chemistry* **280**(7)**,** 5836-5842.

Kerkhoff, E., Simpson, J. C., Leberfinger, C. B., Otto, I. M., Doerks, T., Bork, P., Rapp, U. R., Raabe, T., and Pepperkok, R. (2001). The Spir actin organizers are involved in vesicle transport processes. *Current Biology* **11**(24)**,** 1963-1968.

Kerr, M. C., and Teasdale, R. D. (2009). Defining Macropinocytosis. *Traffic* **10**(4)**,** 364-371.

Kessels, M. M., and Qualmann, B. (2002). Syndapins integrate N-WASP in receptor-mediated endocytosis. *EMBO J* **21**(22)**,** 6083-94.

Kikuchi, S., Honda, K., Tsuda, H., Hiraoka, N., Imoto, I., Kosuge, T., Umaki, T., Onozato, K., Shitashige, M., Yamaguchi, U., Ono, M., Tsuchida, A., Aoki, T., Inazawa, J., Hirohashi, S., and Yamada, T. (2008). Expression and Gene Amplification of Actinin-4 in Invasive Ductal Carcinoma of the Pancreas. *Clinical Cancer Research* **14**(17)**,** 5348-5356.

Kim, K., Hou, P., Gorski, J. L., and Cooper, J. A. (2004). Effect of Fgd1 on Cortactin in Arp2/3 Complex-Mediated Actin Assembly†. *Biochemistry* **43**(9)**,** 2422-2427.

Kinley, A. W., Weed, S. A., Weaver, A. M., Karginov, A. V., Bissonette, E., Cooper, J. A., and Parsons, J. T. (2003). Cortactin Interacts with WIP in Regulating Arp2/3 Activation and Membrane Protrusion. *Current Biology* **13**(5)**,** 384-393.

Kitamura, D., Kaneko, H., Miyagoe, Y., Ariyasu, T., and Watanabe, T. (1989). Isolation and characterization of a novel human gene expressed specifically in the cells of hematopoietic lineage. *Nucleic Acids Res* **17**(22)**,** 9367-79.

Kobayashi, K., Kuroda, S., Fukata, M., Nakamura, T., Nagase, T., Nomura, N., Matsuura, Y., Yoshida-Kubomura, N., Iwamatsu, A., and Kaibuchi, K. (1998). p140Sra-1 (Specifically Rac1-associated Protein) Is a Novel Specific Target for Rac1 Small GTPase. *Journal of Biological Chemistry* **273**(1)**,** 291-295.

Kocks, C., Gouin, E., Tabouret, M., Berche, P., Ohayon, H., and Cossart, P. (1992). L. monocytogenes-induced actin assembly requires the actA gene product, a surface protein. *Cell* **68**(3)**,** 521-531.

Koestler, S. A., Auinger, S., Vinzenz, M., Rottner, K., and Small, J. V. (2008). Differentially oriented populations of actin filaments generated in lamellipodia collaborate in pushing and pausing at the cell front. *Nat Cell Biol* **10**(3)**,** 306-313.

Kolsch, V., Charest, P. G., and Firtel, R. A. (2008). The regulation of cell motility and chemotaxis by phospholipid signaling. *J Cell Sci* **121**(5)**,** 551-559.

Kovar, D. R., Harris, E. S., Mahaffy, R., Higgs, H. N., and Pollard, T. D. (2006). Control of the Assembly of ATP- and ADP-Actin by Formins and Profilin. *Cell* **124**(2)**,** 423-435.

Kowalski, J. R., Egile, C., Gil, S., Snapper, S. B., Li, R., and Thomas, S. M. (2005). Cortactin regulates cell migration through activation of N-WASP. *J Cell Sci* **118**(1)**,** 79-87.

Krause, M., Leslie, J. D., Stewart, M., Lafuente, E. M., Valderrama, F., Jagannathan, R., Strasser, G. A., Rubinson, D. A., Liu, H., Way, M., Yaffe, M. B., Boussiotis, V. A., and Gertler, F. B. (2004). Lamellipodin, an Ena/VASP Ligand, Is Implicated in the Regulation of Lamellipodial Dynamics. *Developmental Cell* **7**(4)**,** 571-583.

Krueger, E. W., Orth, J. D., Cao, H., and McNiven, M. A. (2003). A Dynamin-Cortactin-Arp2/3 Complex Mediates Actin Reorganization in Growth Factor-stimulated Cells. *Mol. Biol. Cell* **14**(3)**,** 1085-1096.

Kunda, P., Craig, G., Dominguez, V., and Baum, B. (2003). Abi, Sra1, and Kette Control the Stability and Localization of SCAR/WAVE to Regulate the Formation of Actin-Based Protrusions. *Current Biology* **13**(21)**,** 1867-1875.

Kurisu, S., and Takenawa, T. (2009). The WASP and WAVE family proteins. *Genome Biology* **10**(6)**,** 226.

Kurklinsky, S., Chen, J., and McNiven, M. A. (2011). Growth cone morphology and spreading are regulated by a dynamin-cortactin complex at point contacts in hippocampal neurons. *Journal of Neurochemistry***,** no-no.

Kwiatkowski, A. V., Rubinson, D. A., Dent, E. W., Edward van Veen, J., Leslie, J. D., Zhang, J., Mebane, L. M., Philippar, U., Pinheiro, E. M., Burds, A. A., Bronson, R. T., Mori, S., Fässler, R., and Gertler, F. B. (2007). Ena/VASP Is Required for Neuritogenesis in the Developing Cortex. *Neuron* **56**(3)**,** 441-455.

Ladwein, M., and Rottner, K. (2008). On the Rho'd: The regulation of membrane protrusions by Rho-GTPases. *FEBS Letters* **582**(14)**,** 2066-2074.

Laemmli, U. K. (1970). Cleavage of structural proteins during the assembly of the head of bacteriophage T4. *Nature* **227**(5259)**,** 680-5.

Lai, F. P., Szczodrak, M., Block, J., Faix, J., Breitsprecher, D., Mannherz, H. G., Stradal, T. E., Dunn, G. A., Small, J. V., and Rottner, K. (2008). Arp2/3 complex interactions and actin network turnover in lamellipodia. *EMBO J* **27**(7)**,** 982-92.

Lai, F. P., Szczodrak, M., Oelkers, J. M., Ladwein, M., Acconcia, F., Benesch, S., Auinger, S., Faix, J., Small, J. V., Polo, S., Stradal, T. E., and Rottner, K. (2009). Cortactin promotes migration and platelet-derived growth factor-induced actin reorganization by signaling to Rho-GTPases. *Mol Biol Cell* **20**(14)**,** 3209-23.

Lammers, M., Rose, R., Scrima, A., and Wittinghofer, A. (2005). The regulation of mDia1 by autoinhibition and its release by Rho[bull]GTP. *EMBO J* **24**(23)**,** 4176-4187.

Lang Hrtska, S. C., Kemp, M. M., Muñoz, E. M., Azizad, O., Banerjee, M., Raposo, C., Kumaran, J., Ghosh, P., and Linhardt, R. J. (2007). Investigation of the Mechanism of Binding between Internalin B and Heparin Using Surface Plasmon Resonance. *Biochemistry* **46**(10)**,** 2697-2706.

Lanzetti, L., Palamidessi, A., Areces, L., Scita, G., and Di Fiore, P. P. (2004). Rab5 is a signalling GTPase involved in actin remodelling by receptor tyrosine kinases. *Nature* **429**(6989)**,** 309-314.

Lassing, I., and Lindberg, U. (1988). Specificity of the interaction between phosphatidylinositol 4,5-bisphosphate and the profilin:actin complex. *Journal of Cellular Biochemistry* **37**(3)**,** 255-267.

Le Clainche, C., and Carlier, M.-F. (2001). "Actin-Based Motility Assay." Current Protocols in Cell Biology John Wiley & Sons, Inc.

Le Clainche, C., Pantaloni, D., and Carlier, M.-F. (2003). ATP hydrolysis on actin-related protein 2/3 complex causes debranching of dendritic actin arrays. *Proceedings of the National Academy of Sciences of the United States of America* **100**(11)**,** 6337-6342.

LeClaire, L. L., Baumgartner, M., Iwasa, J. H., Mullins, R. D., and Barber, D. L. (2008). Phosphorylation of the Arp2/3 complex is necessary to nucleate actin filaments. *The Journal of Cell Biology* **182**(4)**,** 647-654.

Lecuit, M., Dramsi, S., Gottardi, C., Fedor-Chaiken, M., Gumbiner, B., and Cossart, P. (1999). A single amino acid in E-cadherin responsible for host specificity towards the human pathogen Listeria monocytogenes. *EMBO J* **18**(14)**,** 3956-3963.

Lee, S. H. (2005). Interaction of nonreceptor tyrosine-kinase Fer and p120 catenin is involved in neuronal polarization. *Mol Cells* **20**(2)**,** 256-62.

Li, A., Dawson, J. C., Forero-Vargas, M., Spence, H. J., Yu, X., König, I., Anderson, K., and Machesky, L. M. (2010). The Actin-Bundling Protein Fascin Stabilizes Actin in Invadopodia and Potentiates Protrusive Invasion. *Current Biology* **20**(4)**,** 339-345.

Li, F., and Higgs, H. N. (2005). Dissecting Requirements for Auto-inhibition of Actin Nucleation by the Formin, mDia1. *Journal of Biological Chemistry* **280**(8)**,** 6986-6992.

Linder, S. (2007). The matrix corroded: podosomes and invadopodia in extracellular matrix degradation. *Trends in Cell Biology* **17**(3)**,** 107-117.

Linder, S., Nelson, D., Weiss, M., and Aepfelbacher, M. (1999). Wiskott-Aldrich syndrome protein regulates podosomes in primary human macrophages. *Proceedings of the National Academy of Sciences of the United States of America* **96**(17)**,** 9648-9653.

Loisel, T. P., Boujemaa, R., Pantaloni, D., and Carlier, M.-F. (1999). Reconstitution of actin-based motility of Listeria and Shigella using pure proteins. *Nature* **401**(6753)**,** 613-616.

Lommel, S., Benesch, S., Rohde, M., Wehland, J., and Rottner, K. (2004). Enterohaemorrhagic and enteropathogenic Escherichia coli use different mechanisms for actin pedestal formation that converge on N-WASP. *Cell Microbiol* **6**(3)**,** 243-54.

Lommel, S., Benesch, S., Rottner, K., Franz, T., Wehland, J., and Kuhn, R. (2001). Actin pedestal formation by enteropathogenic Escherichia coli and intracellular motility of Shigella flexneri are abolished in N-WASP-defective cells. *EMBO Rep* **2**(9)**,** 850-7.

Luther, P. (2009). The vertebrate muscle Z-disc: sarcomere anchor for structure and signalling. *Journal of Muscle Research and Cell Motility* **30**(5)**,** 171-185.

Lynch, D. K., Winata, S. C., Lyons, R. J., Hughes, W. E., Lehrbach, G. M., Wasinger, V., Corthals, G., Cordwell, S., and Daly, R. J. (2003). A Cortactin-CD2-associated Protein (CD2AP) Complex Provides a Novel Link between Epidermal Growth Factor Receptor Endocytosis and the Actin Cytoskeleton. *Journal of Biological Chemistry* **278**(24)**,** 21805-21813.

Machesky, L. M., Atkinson, S. J., Ampe, C., Vandekerckhove, J., and Pollard, T. D. (1994). Purification of a cortical complex containing two unconventional actins from Acanthamoeba by affinity chromatography on profilin-agarose. *The Journal of Cell Biology* **127**(1)**,** 107-115.

Machesky, L. M., Mullins, R. D., Higgs, H. N., Kaiser, D. A., Blanchoin, L., May, R. C., Hall, M. E., and Pollard, T. D. (1999). Scar, a WASp-related protein, activates nucleation of actin filaments by the Arp2/3 complex. *Proceedings of the National Academy of Sciences of the United States of America* **96**(7)**,** 3739-3744.

Maciver, S. K., Zot, H. G., and Pollard, T. D. (1991). Characterization of actin filament severing by actophorin from Acanthamoeba castellanii. *The Journal of Cell Biology* **115**(6)**,** 1611-1620.

Madhavan, R., Gong, Z. L., Ma, J. J., Chan, A. W. S., and Peng, H. B. (2009). The Function of Cortactin in the Clustering of Acetylcholine Receptors at the Vertebrate Neuromuscular Junction. *PLoS ONE* **4**(12)**,** e8478.

Mammoto, A., Sasaki, T., Asakura, T., Hotta, I., Imamura, H., Takahashi, K., Matsuura, Y., Shirao, T., and Takai, Y. (1998). Interactions of Drebrin and Gephyrin with Profilin. *Biochemical and Biophysical Research Communications* **243**(1)**,** 86-89.

Marchand, J.-B., Kaiser, D. A., Pollard, T. D., and Higgs, H. N. (2001). Interaction of WASP/Scar proteins with actin and vertebrate Arp2/3 complex. *Nat Cell Biol* **3**(1)**,** 76-82.

Martin, A. C., Welch, M. D., and Drubin, D. G. (2006). Arp2/3 ATP hydrolysis-catalysed branch dissociation is critical for endocytic force generation. *Nat Cell Biol* **8**(8)**,** 826-833.

Martinez-Quiles, N., Ho, H.-Y. H., Kirschner, M. W., Ramesh, N., and Geha, R. S. (2004). Erk/Src Phosphorylation of Cortactin Acts as a Switch On-Switch Off Mechanism That Controls Its Ability To Activate N-WASP. *Mol. Cell. Biol.* **24**(12)**,** 5269-5280.

Martinez-Quiles, N., Rohatgi, R., Anton, I. M., Medina, M., Saville, S. P., Miki, H., Yamaguchi, H., Takenawa, T., Hartwig, J. H., Geha, R. S., and Ramesh, N. (2001). WIP regulates N-WASP-mediated actin polymerization and filopodium formation. *Nat Cell Biol* **3**(5)**,** 484-491.

Mattila, P. K., and Lappalainen, P. (2008). Filopodia: molecular architecture and cellular functions. *Nat Rev Mol Cell Biol* **9**(6)**,** 446-454.

McNiven, M. A., Kim, L., Krueger, E. W., Orth, J. D., Cao, H., and Wong, T. W. (2000). Regulated Interactions between Dynamin and the Actin-Binding Protein Cortactin Modulate Cell Shape. *The Journal of Cell Biology* **151**(1)**,** 187-198.

Meighan, S. E., Meighan, P. C., Choudhury, P., Davis, C. J., Olson, M. L., Zornes, P. A., Wright, J. W., and Harding, J. W. (2006). Effects of extracellular matrix-degrading proteases matrix metalloproteinases 3 and 9 on spatial learning and synaptic plasticity. *Journal of Neurochemistry* **96**(5)**,** 1227-1241.

Mejillano, M. R., Kojima, S.-i., Applewhite, D. A., Gertler, F. B., Svitkina, T. M., and Borisy, G. G. (2004). Lamellipodial Versus Filopodial Mode of the Actin Nanomachinery: Pivotal Role of the Filament Barbed End. *Cell* **118**(3)**,** 363-373.

Mellstrom, K. (1983). The effect of platelet-derived growth factor on morphology and motility of human glial cells. *J. Muscle Res. Cell Motil.* **4,** 589-609.

Mengaud, J., Ohayon, H., Gounon, P., Mège, R.-M., and Cossart, P. (1996). E-Cadherin Is the Receptor for Internalin, a Surface Protein Required for Entry of L. monocytogenes into Epithelial Cells. *Cell* **84**(6)**,** 923-932.

Menzies, A. S., Aszodi, A., Williams, S. E., Pfeifer, A., Wehman, A. M., Goh, K. L., Mason, C. A., Fassler, R., and Gertler, F. B. (2004). Mena and Vasodilator-Stimulated Phosphoprotein Are Required for Multiple Actin-Dependent Processes That Shape the Vertebrate Nervous System. *J. Neurosci.* **24**(37)**,** 8029-8038.

Michaelsen, K., Murk, K., Zagrebelsky, M., Dreznjak, A., Jockusch, B. M., Rothkegel, M., and Korte, M. (2010). Fine-tuning of neuronal architecture requires two profilin isoforms. *Proceedings of the National Academy of Sciences* **107**(36)**,** 15780-15785.

Miki, H., Yamaguchi, H., Suetsugu, S., and Takenawa, T. (2000). IRSp53 is an essential intermediate between Rac and WAVE in the regulation of membrane ruffling. *Nature* **408**(6813)**,** 732-735.

Mizutani, K., Miki, H., He, H., Maruta, H., and Takenawa, T. (2002). Essential Role of Neural Wiskott-Aldrich Syndrome Protein in Podosome Formation and Degradation of Extracellular Matrix in src-transformed Fibroblasts. *Cancer Research* **62**(3)**,** 669-674.

Mockrin, S. C., and Korn, E. D. (1980). Acanthamoeba profilin interacts with G-actin to increase the rate of exchange of actin-bound adenosine 5'-triphosphate. *Biochemistry* **19**(23)**,** 5359-5362.

Montanez, E., Ussar, S., Schifferer, M., Bösl, M., Zent, R., Moser, M., and Fässler, R. (2008). Kindlin-2 controls bidirectional signaling of integrins. *Genes & Development* **22**(10)**,** 1325-1330.

Monypenny, J., Zicha, D., Higashida, C., Oceguera-Yanez, F., Narumiya, S., and Watanabe, N. (2009). Cdc42 and Rac Family GTPases Regulate Mode and Speed but Not Direction of Primary Fibroblast Migration during Platelet-Derived Growth Factor-Dependent Chemotaxis. *Mol. Cell. Biol.* **29**(10)**,** 2730-2747.

Moody, J. D., Grange, J., Ascione, M. P. A., Boothe, D., Bushnell, E., and Hansen, M. D. H. (2009). A zyxin head-tail interaction regulates zyxin-VASP complex formation. *Biochemical and Biophysical Research Communications* **378**(3)**,** 625-628.

Mooren, O. L., Kotova, T. I., Moore, A. J., and Schafer, D. A. (2009). Dynamin2 GTPase and Cortactin Remodel Actin Filaments. *Journal of Biological Chemistry* **284**(36)**,** 23995-24005.

Moseley, J. B., Sagot, I., Manning, A. L., Xu, Y., Eck, M. J., Pellman, D., and Goode, B. L. (2004). A Conserved Mechanism for Bni1- and mDia1-induced Actin Assembly and Dual Regulation of Bni1 by Bud6 and Profilin. *Mol. Biol. Cell* **15**(2)**,** 896-907.

Mullins, R. D., Heuser, J. A., and Pollard, T. D. (1998). The interaction of Arp2/3 complex with actin: Nucleation, high affinity pointed end capping, and formation of branching networks of filaments. *Proceedings of the National Academy of Sciences of the United States of America* **95**(11)**,** 6181-6186.

Nagata-Ohashi, K., Ohta, Y., Goto, K., Chiba, S., Mori, R., Nishita, M., Ohashi, K., Kousaka, K., Iwamatsu, A., Niwa, R., Uemura, T., and Mizuno, K. (2004). A pathway of neuregulin-induced activation of cofilin-phosphatase Slingshot and cofilin in lamellipodia. *The Journal of Cell Biology* **165**(4)**,** 465-471.

Nicholson-Dykstra, S. M., and Higgs, H. N. (2008). Arp2 depletion inhibits sheet-like protrusions but not linear protrusions of fibroblasts and lymphocytes. *Cell Motility and the Cytoskeleton* **65**(11)**,** 904-922.

Niebuhr, K., Ebel, F., Frank, R., Reinhard, M., Domann, E., Carl, U. D., Walter, U., Gertler, F. B., Wehland, J., and Chakraborty, T. (1997). A novel proline-rich motif present in ActA of Listeria monocytogenes and cytoskeletal proteins is the ligand for the EVH1 domain, a protein module present in the Ena/VASP family. *EMBO J* **16**(17)**,** 5433-5444.

Niemann, H. H., Jäger, V., Butler, P. J. G., van den Heuvel, J., Schmidt, S., Ferraris, D., Gherardi, E., and Heinz, D. W. (2007). Structure of the Human Receptor Tyrosine Kinase Met in Complex with the Listeria Invasion Protein InlB. *Cell* **130**(2)**,** 235-246.

Nishimura, T., Yamaguchi, T., Kato, K., Yoshizawa, M., Nabeshima, Y.-i., Ohno, S., Hoshino, M., and Kaibuchi, K. (2005). PAR-6-PAR-3 mediates Cdc42-induced Rac activation through the Rac GEFs STEF/Tiam1. *Nat Cell Biol* **7**(3)**,** 270-277.

Nobes, C. D., and Hall, A. (1995). Rho, Rac, and Cdc42 GTPases regulate the assembly of multimolecular focal complexes associated with actin stress fibers, lamellipodia, and filopodia. *Cell* **81**(1)**,** 53-62.

Ohta, Y., Hartwig, J. H., and Stossel, T. P. (2006). FilGAP, a Rho- and ROCK-regulated GAP for Rac binds filamin A to control actin remodelling. *Nat Cell Biol* **8**(8)**,** 803-814.

Orth, J. D., Krueger, E. W., and McNiven, M. A. (2003). A dynamin-cortactin-N-WASp complex mediates the sequestration and macropinocytic internalization of the EGF-receptor via dorsal ruffles/waves. *Mol. Biol. Cell* **14**(Suppl. 1)**,** A465.

Oser, M., and Condeelis, J. (2009). The cofilin activity cycle in lamellipodia and invadopodia. *Journal of Cellular Biochemistry* **108**(6)**,** 1252-1262.

Oser, M., Mader, C. C., Gil-Henn, H., Magalhaes, M., Bravo-Cordero, J. J., Koleske, A. J., and Condeelis, J. (2010). Specific tyrosine phosphorylation sites on cortactin regulate Nck1-dependent actin polymerization in invadopodia. *J Cell Sci* **123**(21)**,** 3662-3673.

Oser, M., Yamaguchi, H., Mader, C. C., Bravo-Cordero, J. J., Arias, M., Chen, X., DesMarais, V., van Rheenen, J., Koleske, A. J., and Condeelis, J. (2009). Cortactin regulates cofilin and N-WASp activities to control the stages of invadopodium assembly and maturation. *The Journal of Cell Biology* **186**(4)**,** 571-587.

Otey, C. A., and Carpen, O. (2004). α-actinin revisited: A fresh look at an old player. *Cell Motility and the Cytoskeleton* **58**(2)**,** 104-111.

Padrick, S. B., Cheng, H.-C., Ismail, A. M., Panchal, S. C., Doolittle, L. K., Kim, S., Skehan, B. M., Umetani, J., Brautigam, C. A., Leong, J. M., and Rosen, M. K. (2008). Hierarchical Regulation of WASP/WAVE Proteins. *Molecular Cell* **32**(3)**,** 426-438.

Padrick, S. B., and Rosen, M. K. (2010). Physical Mechanisms of Signal Integration by WASP Family Proteins. *Annual Review of Biochemistry* **79**(1)**,** 707-735.

Panchal, S. C., Kaiser, D. A., Torres, E., Pollard, T. D., and Rosen, M. K. (2003). A conserved amphipathic helix in WASP/Scar proteins is essential for activation of Arp2/3 complex. *Nat Struct Mol Biol* **10**(8)**,** 591-598.

Pantaloni, D., Clainche, C. L., and Carlier, M.-F. (2001). Mechanism of Actin-Based Motility. *Science* **292**(5521)**,** 1502-1506.

Pasic, L., Kotova, T., and Schafer, D. A. (2008). Ena/VASP Proteins Capture Actin Filament Barbed Ends. *Journal of Biological Chemistry* **283**(15)**,** 9814-9819.

Patel, A. S., Schechter, G. L., Wasilenko, W. J., and Somers, K. D. (1998). Overexpression of EMS1/cortactin in NIH3T3 fibroblasts causes increased cell motility and invasion in vitro. *Oncogene* **16**(25)**,** 3227-32.

Paterson, H. F., Self, A. J., Garrett, M. D., Just, I., Aktories, K., and Hall, A. (1990). Microinjection of recombinant p21rho induces rapid changes in cell morphology. *The Journal of Cell Biology* **111**(3)**,** 1001-1007.

Paul, A., and Pollard, T. (2008). The Role of the FH1 Domain and Profilin in Formin-Mediated Actin-Filament Elongation and Nucleation. *Current Biology* **18**(1)**,** 9-19.

Paul, A. S., and Pollard, T. D. (2009). Energetic Requirements for Processive Elongation of Actin Filaments by FH1FH2-formins. *Journal of Biological Chemistry* **284**(18)**,** 12533-12540.

Pavalko, F. M., and Burridge, K. (1991). Disruption of the actin cytoskeleton after microinjection of proteolytic fragments of alpha-actinin. *The Journal of Cell Biology* **114**(3)**,** 481-491.

Pechlivanis, M., Samol, A., and Kerkhoff, E. (2009). Identification of a Short Spir Interaction Sequence at the C-terminal End of Formin Subgroup Proteins. *Journal of Biological Chemistry* **284**(37)**,** 25324-25333.

Pellegrin, S., and Mellor, H. (2005). The Rho Family GTPase Rif Induces Filopodia through mDia2. *Current Biology* **15**(2)**,** 129-133.

Peng, J., Wallar, B. J., Flanders, A., Swiatek, P. J., and Alberts, A. S. (2003). Disruption of the Diaphanous-Related Formin Drf1 Gene Encoding mDia1 Reveals a Role for Drf3 as an Effector for Cdc42. *Current Biology* **13**(7)**,** 534-545.

Pistor, S., Chakraborty, T., Niebuhr, K., Domann, E., and Wehland, J. (1994). The ActA protein of Listeria monocytogenes acts as a nucleator inducing reorganization of the actin cytoskeleton. *EMBO J* **13**(4)**,** 758-63.

Pizarro-Cerdá, J., Bonazzi, M., and Cossart, P. (2010). Clathrin-mediated endocytosis: What works for small, also works for big. *BioEssays* **32**(6)**,** 496-504.

Pizarro-Cerdá, J., and Cossart, P. (2006). Bacterial Adhesion and Entry into Host Cells. *Cell* **124**(4)**,** 715-727.

Pollard, T. D. (2007). Regulation of Actin Filament Assembly by Arp2/3 Complex and Formins. *Annual Review of Biophysics and Biomolecular Structure* **36**(1)**,** 451-477.

Pollard, T. D., Blanchoin, L., and Mullins, R. D. (2000). MOLECULAR MECHANISMS CONTROLLING ACTIN FILAMENT DYNAMICS IN NONMUSCLE CELLS. *Annual Review of Biophysics and Biomolecular Structure* **29**(1)**,** 545-576.

Pollard, T. D., and Borisy, G. G. (2003). Cellular Motility Driven by Assembly and Disassembly of Actin Filaments. *Cell* **112**(4)**,** 453-465.

Pollard, T. D., and Cooper, J. A. (1984). Quantitative analysis of the effect of Acanthamoeba profilin on actin filament nucleation and elongation. *Biochemistry* **23**(26)**,** 6631-6641.

Pollitt, A. Y., and Insall, R. H. (2009). WASP and SCAR/WAVE proteins: the drivers of actin assembly. *J Cell Sci* **122**(15)**,** 2575-2578.

Qualmann, B., and Kessels, M. M. (2009). New players in actin polymerization - WH2-domain-containing actin nucleators. *Trends in Cell Biology* **19**(6)**,** 276-285.

Quinlan, M. E., Heuser, J. E., Kerkhoff, E., and Dyche Mullins, R. (2005). Drosophila Spire is an actin nucleation factor. *Nature* **433**(7024)**,** 382-388.

Quintavalle, M., Elia, L., Condorelli, G., and Courtneidge, S. A. (2010). MicroRNA control of podosome formation in vascular smooth muscle cells in vivo and in vitro. *The Journal of Cell Biology* **189**(1)**,** 13-22.

Rabut, G., and Ellenberg, J. (2005). "Photobleaching Techniques to Study Mobility and Molecular Dynamics of Proteins in Live Cells: FRAP, iFRAP, and FLIP. ." Live Cell Imaging, A Laboratory Manual. (R. D. a. S. In Goldman, D.L. (eds.), Ed.) Cold Spring Harbor Laboratory Press, New York.

Ravanelli, A. M., and Klingensmith, J. (2011). The actin nucleator Cordon-bleu is required for development of motile cilia in zebrafish. *Developmental Biology* **350**(1)**,** 101-111.

Ridley, A. J. (2006). Rho-GTPases and actin dynamics in membrane protrusions and vesicle trafficking. *Trends in Cell Biology* **16**(10)**,** 522-529.

Ridley, A. J., Paterson, H. F., Johnston, C. L., Diekmann, D., and Hall, A. (1992). The small GTP-binding protein rac regulates growth factor-induced membrane ruffling. *Cell* **70**(3)**,** 401-410.

Riedl, J., Crevenna, A. H., Kessenbrock, K., Yu, J. H., Neukirchen, D., Bista, M., Bradke, F., Jenne, D., Holak, T. A., Werb, Z., Sixt, M., and Wedlich-Soldner, R. (2008). Lifeact: a versatile marker to visualize F-actin. *Nat Methods* **5**(7)**,** 605-7.

Rohatgi, R., Ho, H.-y. H., and Kirschner, M. W. (2000). Mechanism of N-Wasp Activation by Cdc42 and Phosphatidylinositol 4,5-Bisphosphate. *The Journal of Cell Biology* **150**(6)**,** 1299-1310.

Romero, S., Le Clainche, C., Didry, D., Egile, C., Pantaloni, D., and Carlier, M.-F. (2004). Formin Is a Processive Motor that Requires Profilin to Accelerate Actin Assembly and Associated ATP Hydrolysis. *Cell* **119**(3)**,** 419-429.

Rosales-Nieves, A. E., Johndrow, J. E., Keller, L. C., Magie, C. R., Pinto-Santini, D. M., and Parkhurst, S. M. (2006). Coordination of microtubule and microfilament dynamics by Drosophila Rho1, Spire and Cappuccino. *Nat Cell Biol* **8**(4)**,** 367-376.

Rose, R., Weyand, M., Lammers, M., Ishizaki, T., Ahmadian, M. R., and Wittinghofer, A. (2005). Structural and mechanistic insights into the interaction between Rho and mammalian Dia. *Nature* **435**(7041)**,** 513-518.

Rottner, K., Hall, A., and Small, J. V. (1999). Interplay between Rac and Rho in the control of substrate contact dynamics. *Current Biology* **9**(12)**,** 640-648, S1.

Rottner, K., Hänisch, J., and Campellone, K. G. (2010). WASH, WHAMM and JMY: regulation of Arp2/3 complex and beyond. *Trends in Cell Biology* **20**(11)**,** 650-661.

Rouiller, I., Xu, X.-P., Amann, K. J., Egile, C., Nickell, S., Nicastro, D., Li, R., Pollard, T. D., Volkmann, N., and Hanein, D. (2008). The structural basis of actin filament branching by the Arp2/3 complex. *The Journal of Cell Biology* **180**(5)**,** 887-895.

Rust, M. B., Gurniak, C. B., Renner, M., Vara, H., Morando, L., Gorlich, A., Sassoe-Pognetto, M., Banchaabouchi, M. A., Giustetto, M., Triller, A., Choquet, D., and Witke, W. (2010). Learning, AMPA receptor mobility and synaptic plasticity depend on n-cofilin-mediated actin dynamics. *EMBO J* **29**(11)**,** 1889-1902.

Samarin, S., Romero, S., Kocks, C., Didry, D., Pantaloni, D., and Carlier, M.-F. (2003). How VASP enhances actin-based motility. *The Journal of Cell Biology* **163**(1)**,** 131-142.

Sansonetti, P. J., Ryter, A., Clerc, P., Maurelli, A. T., and Mounier, J. (1986). Multiplication of Shigella flexneri within HeLa cells: lysis of the phagocytic vacuole and plasmid-mediated contact hemolysis. *Infect. Immun.* **51**(2)**,** 461-469.

Sauvonnet, N., Dujeancourt, A., and Dautry-Varsat, A. (2005). Cortactin and dynamin are required for the clathrin-independent endocytosis of γc cytokine receptor. *The Journal of Cell Biology* **168**(1)**,** 155-163.

Schirenbeck, A., Arasada, R., Bretschneider, T., Stradal, T. E. B., Schleicher, M., and Faix, J. (2006). The bundling activity of vasodilator-stimulated phosphoprotein is required for filopodium formation. *Proceedings of the National Academy of Sciences* **103**(20)**,** 7694-7699.

Schirenbeck, A., Bretschneider, T., Arasada, R., Schleicher, M., and Faix, J. (2005). The Diaphanous-related formin dDia2 is required for the formation and maintenance of filopodia. *Nat Cell Biol* **7**(6)**,** 619-625.

Schmauch, C., Claussner, S., Zoltzer, H., and Maniak, M. (2009). Targeting the actin-binding protein VASP to late endosomes induces the formation of giant actin aggregates. *Eur J Cell Biol* **88**(7)**,** 385-96.

Schubert, W.-D., Urbanke, C., Ziehm, T., Beier, V., Machner, M. P., Domann, E., Wehland, J., Chakraborty, T., and Heinz, D. W. (2002). Structure of Internalin, a Major Invasion Protein of Listeria monocytogenes, in Complex with Its Human Receptor E-Cadherin. *Cell* **111**(6)**,** 825-836.

Schuebel, K., Bustelo, X., Nielsen, D., Song, B., Barbacid, M., Goldman, D., and Lee, I. (1996). Isolation and characterization of murine vav2, a member of the vav family of proto-oncogenes. *Oncogene* **13**(2)**,** 363-371.

Schutt, C. E., Myslik, J. C., Rozycki, M. D., Goonesekere, N. C. W., and Lindberg, U. (1993). The structure of crystalline profilin-[beta]-actin. *Nature* **365**(6449)**,** 810-816.

Schuuring, E., van Damme, H., Schuuring-Scholtes, E., Verhoeven, E., Michalides, R., Geelen, E., de Boer, C., Brok, H., van Buuren, V., and Kluin, P. (1998). Characterization of the EMS1 gene and its product, human Cortactin. *Cell Adhesion and Communication* **6,** 185-209.

Selbach, M., and Backert, S. (2005). Cortactin: an Achilles' heel of the actin cytoskeleton targeted by pathogens. *Trends in Microbiology* **13**(4)**,** 181-189.

Selbach, M., Moese, S., Hurwitz, R., Hauck, C. R., Meyer, T. F., and Backert, S. (2003). The Helicobacter pylori CagA protein induces cortactin dephosphorylation and actin rearrangement by c-Src inactivation. *EMBO J* **22**(3)**,** 515-528.

Seveau, S., Tham, T. N., Payrastre, B., Hoppe, A. D., Swanson, J. A., and Cossart, P. (2007). A FRET analysis to unravel the role of cholesterol in Rac1 and PI 3-kinase activation in the InlB/Met signalling pathway. *Cellular Microbiology* **9**(3)**,** 790-803.

Shen, Y., Naujokas, M., Park, M., and Ireton, K. (2000). InlB-Dependent Internalization of Listeria Is Mediated by the Met Receptor Tyrosine Kinase. *Cell* **103**(3)**,** 501-510.

Sidani, M., Wessels, D., Mouneimne, G., Ghosh, M., Goswami, S., Sarmiento, C., Wang, W., Kuhl, S., El-Sibai, M., Backer, J. M., Eddy, R., Soll, D., and Condeelis, J. (2007). Cofilin determines the migration behavior and turning frequency of metastatic cancer cells. *The Journal of Cell Biology* **179**(4)**,** 777-791.

Sjöblom, B., Salmazo, A., and Djinović-Carugo, K. (2008). α-Actinin structure and regulation. *Cellular and Molecular Life Sciences* **65**(17)**,** 2688-2701.

Small, J. V., Isenberg, G., and Celis, J. E. (1978). Polarity of actin at the leading edge of cultured cells. *Nature* **272**(5654)**,** 638-639.

Small, J. V., Rottner, K., Kaverina, I., and Anderson, K. I. (1998). Assembling an actin cytoskeleton for cell attachment and movement. *Biochimica et Biophysica Acta (BBA) - Molecular Cell Research* **1404**(3)**,** 271-281.

Small, J. V., Stradal, T., Vignal, E., and Rottner, K. (2002). The lamellipodium: where motility begins. *Trends in Cell Biology* **12**(3)**,** 112-120.

Snapper, S. B., Takeshima, F., Anton, I., Liu, C.-H., Thomas, S. M., Nguyen, D., Dudley, D., Fraser, H., Purich, D., Lopez-Ilasaca, M., Klein, C., Davidson, L., Bronson, R., Mulligan, R. C., Southwick, F., Geha, R., Goldberg, M. B., Rosen, F. S., Hartwig, J. H., and Alt, F. W. (2001). N-WASP deficiency reveals distinct pathways for cell surface projections and microbial actin-based motility. *Nat Cell Biol* **3**(10)**,** 897-904.

Sousa, S., Cabanes, D., Archambaud, C., Colland, F., Lemichez, E., Popoff, M., Boisson-Dupuis, S., Gouin, E., Lecuit, M., Legrain, P., and Cossart, P. (2005). ARHGAP10 is necessary for [alpha]-catenin recruitment at adherens junctions and for Listeria invasion. *Nat Cell Biol* **7**(10)**,** 954-960.

Sousa, S., Cabanes, D., Bougnères, L., Lecuit, M., Sansonetti, P., Tran-Van-Nhieu, G., and Cossart, P. (2007). Src, cortactin and Arp2/3 complex are required for E-cadherin-mediated internalization of Listeria into cells. *Cellular Microbiology* **9**(11)**,** 2629-2643.

Sousa, S., Cabanes, D., El-Amraoui, A., Petit, C., Lecuit, M., and Cossart, P. (2004). Unconventional myosin VIIa and vezatin, two proteins crucial for Listeria entry into epithelial cells. *J Cell Sci* **117**(10)**,** 2121-2130.

Steffen, A., Faix, J., Resch, G. P., Linkner, J., Wehland, J., Small, J. V., Rottner, K., and Stradal, T. E. B. (2006). Filopodia Formation in the Absence of Functional WAVE- and Arp2/3-Complexes. *Mol. Biol. Cell* **17**(6)**,** 2581-2591.

Steffen, A., Rottner, K., Ehinger, J., Innocenti, M., Scita, G., Wehland, J., and Stradal, T. E. B. (2004). Sra-1 and Nap1 link Rac to actin assembly driving lamellipodia formation. *EMBO J* **23**(4)**,** 749-759.

Stradal, T. E. B., and Scita, G. (2006). Protein complexes regulating Arp2/3-mediated actin assembly. *Current Opinion in Cell Biology* **18**(1)**,** 4-10.

Stuart, J. R., Gonzalez, F. H., Kawai, H., and Yuan, Z.-M. (2006). c-Abl Interacts with the WAVE2 Signaling Complex to Induce Membrane Ruffling and Cell Spreading. *Journal of Biological Chemistry* **281**(42)**,** 31290-31297.

Suetsugu, S., Yamazaki, D., Kurisu, S., and Takenawa, T. (2003). Differential Roles of WAVE1 and WAVE2 in Dorsal and Peripheral Ruffle Formation for Fibroblast Cell Migration. *Developmental Cell* **5**(4)**,** 595-609.

Suzuki, T., Miki, H., Takenawa, T., and Sasakawa, C. (1998). Neural Wiskott-Aldrich syndrome protein is implicated in the actin-based motility of Shigella flexneri. *EMBO J* **17**(10)**,** 2767-2776.

Svitkina, T. M., and Borisy, G. G. (1999). Arp2/3 Complex and Actin Depolymerizing Factor/Cofilin in Dendritic Organization and Treadmilling of Actin Filament Array in Lamellipodia. *The Journal of Cell Biology* **145**(5)**,** 1009-1026.

Svitkina, T. M., Bulanova, E. A., Chaga, O. Y., Vignjevic, D. M., Kojima, S.-i., Vasiliev, J. M., and Borisy, G. G. (2003). Mechanism of filopodia initiation by reorganization of a dendritic network. *The Journal of Cell Biology* **160**(3)**,** 409-421.

Tahirovic, S., Hellal, F., Neukirchen, D., Hindges, R., Garvalov, B. K., Flynn, K. C., Stradal, T. E., Chrostek-Grashoff, A., Brakebusch, C., and Bradke, F. (2010). Rac1 Regulates Neuronal Polarization through the WAVE Complex. *J. Neurosci.* **30**(20)**,** 6930-6943.

Tanaka, S., Kunii, M., Harada, A., and Okabe, S. (2009). Generation of cortactin floxed mice and cellular analysis of motility in fibroblasts. *Genesis* **47**(9)**,** 638-646.

Taniuchi, I., Kitamura, D., Maekawa, Y., Fukuda, T., Kishi, H., and Watanabe, T. (1995). Antigen-receptor induced clonal expansion and deletion of lymphocytes are impaired in mice lacking HS1 protein, a substrate of the antigen-receptor-coupled tyrosine kinases. *EMBO J* **14**(15)**,** 3664-78.

Tehrani, S., Faccio, R., Chandrasekar, I., Ross, F. P., and Cooper, J. A. (2006a). Cortactin Has an Essential and Specific Role in Osteoclast Actin Assembly. *Mol. Biol. Cell* **17**(7)**,** 2882-2895.

Tehrani, S., Faccio, R., Chandrasekar, I., Ross, F. P., and Cooper, J. A. (2006b). Cortactin has an essential and specific role in osteoclast actin assembly. *Mol Biol Cell* **17**(7)**,** 2882-95.

Tomasevic, N., Jia, Z., Russell, A., Fujii, T., Hartman, J. J., Clancy, S., Wang, M., Beraud, C., Wood, K. W., and Sakowicz, R. (2007). Differential Regulation of WASP and N-WASP by Cdc42, Rac1, Nck, and PI(4,5)P2. *Biochemistry* **46**(11)**,** 3494-3502.

Trenkle, T., McClelland, M., Adlkofer, K., and Welsh, J. (2000). Major transcript variants of VAV3, a new member of the VAV family of guanine nucleotide exchange factors. *Gene* **245**(1)**,** 139-149.

Tubb, B., Mulholland, D. J., Vogl, W., Lan, Z.-J., Niederberger, C., Cooney, A., and Bryan, J. (2002). Testis Fascin (FSCN3): A Novel Paralog of the Actin-Bundling Protein Fascin Expressed Specifically in the Elongate Spermatid Head. *Experimental Cell Research* **275**(1)**,** 92-109.

Turner, C. E., Glenney, J. R., and Burridge, K. (1990). Paxillin: a new vinculin-binding protein present in focal adhesions. *The Journal of Cell Biology* **111**(3)**,** 1059-1068.

Urban, E., Jacob, S., Nemethova, M., Resch, G. P., and Small, J. V. (2010). Electron tomography reveals unbranched networks of actin filaments in lamellipodia. *Nat Cell Biol* **12**(5)**,** 429-435.

Uruno, T., Liu, J., Li, Y., Smith, N., and Zhan, X. (2003). Sequential Interaction of Actin-related Proteins 2 and 3 (Arp2/3) Complex with Neural Wiscott-Aldrich Syndrome

Protein (N-WASP) and Cortactin during Branched Actin Filament Network Formation. *Journal of Biological Chemistry* **278**(28)**,** 26086-26093.

Uruno, T., Liu, J., Zhang, P., Fan, Y.-x., Egile, C., Li, R., Mueller, S. C., and Zhan, X. (2001). Activation of Arp2/3 complex-mediated actin polymerization by cortactin. *Nat Cell Biol* **3**(3)**,** 259-266.

van Leeuwen, F. N., van Delft, S., Kain, H. E., van der Kammen, R. A., and Collard, J. G. (1999). Rac regulates phosphorylation of the myosin-II heavy chain, actinomyosin disassembly and cell spreading. *Nat Cell Biol* **1**(4)**,** 242-248.

van Rossum, A., Gibcus, J., van der Wal, J., and Schuuring, E. (2005a). Cortactin overexpression results in sustained epidermal growth factor receptor signaling by preventing ligand-induced receptor degradation in human carcinoma cells. *Breast Cancer Research* **7**(6)**,** 235 - 237.

van Rossum, A., Schuuring-Scholtes, E., Seggelen, V., Kluin, P., and Schuuring, E. (2005b). Comparative genome analysis of cortactin and HS1: the significance of the F-actin binding repeat domain. *BMC Genomics* **6**(1)**,** 15.

van Rossum, A. G. S. H., Moolenaar, W. H., and Schuuring, E. (2006). Cortactin affects cell migration by regulating intercellular adhesion and cell spreading. *Experimental Cell Research* **312**(9)**,** 1658-1670.

Vavylonis, D., Kovar, D. R., O'Shaughnessy, B., and Pollard, T. D. (2006). Model of Formin-Associated Actin Filament Elongation. *Molecular Cell* **21**(4)**,** 455-466.

Veiga, E., and Cossart, P. (2005). Listeria hijacks the clathrin-dependent endocytic machinery to invade mammalian cells. *Nat Cell Biol* **7**(9)**,** 894-900.

Vidali, L., Chen, F., Cicchetti, G., Ohta, Y., and Kwiatkowski, D. J. (2006). Rac1-null Mouse Embryonic Fibroblasts Are Motile and Respond to Platelet-derived Growth Factor. *Mol. Biol. Cell* **17**(5)**,** 2377-2390.

Vignjevic, D., Kojima, S.-i., Aratyn, Y., Danciu, O., Svitkina, T., and Borisy, G. G. (2006). Role of fascin in filopodial protrusion. *The Journal of Cell Biology* **174**(6)**,** 863-875.

Virel, A., and Backman, L. (2007). A Comparative and Phylogenetic Analysis of the α-Actinin Rod Domain. *Molecular Biology and Evolution* **24**(10)**,** 2254-2265.

Wada, Y., Abe, T., Takeshita, T., Sato, H., Yanashima, K., and Tamai, M. (2001). Mutation of Human Retinal Fascin Gene (FSCN2) Causes Autosomal Dominant Retinitis Pigmentosa. *Investigative Ophthalmology & Visual Science* **42**(10)**,** 2395-2400.

Wang, Y. L. (1985). Exchange of actin subunits at the leading edge of living fibroblasts: possible role of treadmilling. *The Journal of Cell Biology* **101**(2)**,** 597-602.

Watanabe, N., Madaule, P., Reid, T., Ishizaki, T., Watanabe, G., Kakizuka, A., Saito, Y., Nakao, K., Jockusch, B. M., and Narumiya, S. (1997). p140mDia, a mammalian homolog of Drosophila diaphanous,is a target protein for Rho small GTPase and is a ligand for profilin. *EMBO J* **16**(11)**,** 3044-3056.

Weaver, A. M. (2008). Cortactin in tumor invasiveness. *Cancer Letters* **265**(2)**,** 157-166.

Weaver, A. M., Heuser, J. E., Karginov, A. V., Lee, W.-l., Parsons, J. T., and Cooper, J. A. (2002). Interaction of Cortactin and N-WASp with Arp2/3 Complex. *Current Biology* **12**(15)**,** 1270-1278.

Weaver, A. M., Karginov, A. V., Kinley, A. W., Weed, S. A., Li, Y., Parsons, J. T., and Cooper, J. A. (2001). Cortactin promotes and stabilizes Arp2/3-induced actin filament network formation. *Current Biology* **11**(5)**,** 370-374.

Webb, B. A., Eves, R., and Mak, A. S. (2006). Cortactin regulates podosome formation: Roles of the protein interaction domains. *Experimental Cell Research* **312**(6)**,** 760-769.

Webb, B. A., Zhou, S., Eves, R., Shen, L., Jia, L., and Mak, A. S. (2006). Phosphorylation of cortactin by p21-activated kinase. *Archives of Biochemistry and Biophysics* **456**(2)**,** 183-193.

Weed, S., Du, Y., and Parsons, J. (1998). Translocation of cortactin to the cell periphery is mediated by the small GTPase Rac1. *J Cell Sci* **111**(16)**,** 2433-2443.

Weed, S. A., Karginov, A. V., Schafer, D. A., Weaver, A. M., Kinley, A. W., Cooper, J. A., and Parsons, J. T. (2000). Cortactin Localization to Sites of Actin Assembly in Lamellipodia Requires Interactions with F-Actin and the Arp2/3 Complex. *The Journal of Cell Biology* **151**(1)**,** 29-40.

Welch, M. D., Iwamatsu, A., and Mitchison, T. J. (1997). Actin polymerization is induced by Arp 2/3 protein complex at the surface of Listeria monocytogenes. *Nature* **385**(6613)**,** 265-269.

Welch, M. D., Rosenblatt, J., Skoble, J., Portnoy, D. A., and Mitchison, T. J. (1998). Interaction of Human Arp2/3 Complex and the Listeria monocytogenes ActA Protein in Actin Filament Nucleation. *Science* **281**(5373)**,** 105-108.

Weston, C. A., Teressa, G., Weeks, B. S., and Prives, J. (2007). Agrin and laminin induce acetylcholine receptor clustering by convergent, Rho-GTPase-dependent signaling pathways. *J Cell Sci* **120**(5)**,** 868-875.

Wiesner, C., Faix, J., Himmel, M., Bentzien, F., and Linder, S. (2010). KIF5B and KIF3A/KIF3B kinesins drive MT1-MMP surface exposure, CD44 shedding, and extracellular matrix degradation in primary macrophages. *Blood* **116**(9)**,** 1559-1569.

Wiesner, S., Legate, K. R., and Fässler, R. (2005). Integrin-actin interactions. *Cellular and Molecular Life Sciences* **62**(10)**,** 1081-1099.

Wildenberg, G. A., Dohn, M. R., Carnahan, R. H., Davis, M. A., Lobdell, N. A., Settleman, J., and Reynolds, A. B. (2006). p120-Catenin and p190RhoGAP Regulate Cell-Cell Adhesion by Coordinating Antagonism between Rac and Rho. *Cell* **127**(5)**,** 1027-1039.

Witke, W., Hofmann, A., Köppel, B., Schleicher, M., and Noegel, A. A. (1993). The Ca(2+)-binding domains in non-muscle type alpha-actinin: biochemical and genetic analysis. *The Journal of Cell Biology* **121**(3)**,** 599-606.

Witke, W., Sutherland, J. D., Sharpe, A., Arai, M., and Kwiatkowski, D. J. (2001). Profilin I is essential for cell survival and cell division in early mouse development. *Proceedings of the National Academy of Sciences of the United States of America* **98**(7)**,** 3832-3836.

Wu, H., and Parsons, J. T. (1993). Cortactin, an 80/85-kilodalton pp60src substrate, is a filamentous actin-binding protein enriched in the cell cortex. *The Journal of Cell Biology* **120**(6)**,** 1417-1426.

Wu, H., Reynolds, A. B., Kanner, S. B., Vines, R. R., and Parsons, J. T. (1991). Identification and characterization of a novel cytoskeleton-associated pp60src substrate. *Mol. Cell. Biol.* **11**(10)**,** 5113-5124.

Xu, Y., Moseley, J. B., Sagot, I., Poy, F., Pellman, D., Goode, B. L., and Eck, M. J. (2004). Crystal Structures of a Formin Homology-2 Domain Reveal a Tethered Dimer Architecture. *Cell* **116**(5)**,** 711-723.

Yamaguchi, H., Miki, H., Suetsugu, S., Ma, L., Kirschner, M. W., and Takenawa, T. (2000). Two tandem verprolin homology domains are necessary for a strong

activation of Arp2/3 complex-induced actin polymerization and induction of microspike formation by N-WASP. *Proceedings of the National Academy of Sciences of the United States of America* **97**(23)**,** 12631-12636.

Yamakita, Y., Ono, S., Matsumura, F., and Yamashiro, S. (1996). Phosphorylation of Human Fascin Inhibits Its Actin Binding and Bundling Activities. *Journal of Biological Chemistry* **271**(21)**,** 12632-12638.

Yamamoto, S., Tsuda, H., Honda, K., Onozato, K., Takano, M., Tamai, S., Imoto, I., Inazawa, J., Yamada, T., and Matsubara, O. (2009). Actinin-4 gene amplification in ovarian cancer: a candidate oncogene associated with poor patient prognosis and tumor chemoresistance. *Mod Pathol* **22**(4)**,** 499-507.

Yamashita, A., Maeda, K., and Maeda, Y. (2003). Crystal structure of CapZ: structural basis for actin filament barbed end capping. *EMBO J* **22**(7)**,** 1529-1538.

Yu, D., Zhang, H., Blanpied, T. A., Smith, E., and Zhan, X. (2010). Cortactin is implicated in murine zygotic development. *Experimental Cell Research* **316**(5)**,** 848-858.

Yu, T. W., Hao, J. C., Lim, W., Tessier-Lavigne, M., and Bargmann, C. I. (2002). Shared receptors in axon guidance: SAX-3/Robo signals via UNC-34/Enabled and a Netrin-independent UNC-40/DCC function. *Nat Neurosci* **5**(11)**,** 1147-1154.

Zaidel-Bar, R., Ballestrem, C., Kam, Z., and Geiger, B. (2003). Early molecular events in the assembly of matrix adhesions at the leading edge of migrating cells. *J Cell Sci* **116**(22)**,** 4605-4613.

Zalevsky, J., Lempert, L., Kranitz, H., and Mullins, R. D. (2001). Different WASP family proteins stimulate different Arp2/3 complex-dependent actin-nucleating activities. *Current Biology* **11**(24)**,** 1903-1913.

Zhou, S., Webb, B. A., Eves, R., and Mak, A. S. (2006). Effects of tyrosine phosphorylation of cortactin on podosome formation in A7r5 vascular smooth muscle cells. *American Journal of Physiology - Cell Physiology* **290**(2)**,** C463-C471.

Zhu, J., Zhou, K., Hao, J.-J., Liu, J., Smith, N., and Zhan, X. (2005). Regulation of cortactin/dynamin interaction by actin polymerization during the fission of clathrin-coated pits. *J Cell Sci* **118**(4)**,** 807-817.

Zhu, T., Mancini, J. A., Sapieha, P. S., Yang, C., Joyal, J.-S., Honore, J.-C., Leduc, M., Zaniolo, K., Hardy, P., Shao, Z., Fan, L., Hou, X., Rivard, G.-E., and Chemtob, S. (2010). Cortactin activation by FVIIa/tissue factor and PAR2 promotes endothelial cell migration. *American Journal of Physiology - Regulatory, Integrative and Comparative Physiology*.

Zuchero, J. B., Coutts, A. S., Quinlan, M. E., Thangue, N. B. L., and Mullins, R. D. (2009). p53-cofactor JMY is a multifunctional actin nucleation factor. *Nat Cell Biol* **11**(4)**,** 451-459.

9 Appendix

9.1 Supplementary video legends

Video 1: MBD-VVCA recruits the subunit p16B of the Arp2/3 complex to microtubules.

Video 2: MBD alone does not induce actin accumulation on microtubules.

Video 3: The Arp2/3 complex is not recruited to the isolated MBD on microtubules.

Video 4: MBD-VVCA induces actin accumulations on microtubules.

Video 5: Actin is instantaneously polymerized on a growing microtubule coated with MBD-VVCA.

Video 6: Actin filaments are rapidly disassembled from a shrinking microtubule decorated with MBD-VVCA.

Video 7: MBD-cortactin is not able to induce actin polymerization on microtubules.

Video 8: MBD-cortactin does not recruit the Arp2/3 complex to microtubules.

Video 9: MBD-tagged cortactin 1-84 is not able to trigger actin nucleation on microtubules.

Video 10: MBD-cortactin 1-84 does not recruit the Arp2/3 complex to microtubules.

Video 11: B16-F1 cell moving on laminin and expressing EGFP-tagged, full-length cortactin and mCherry-actin.

Video 12: B16-F1 cell co-transfected with EGFP-cortactin 1-146 and mCherry-actin.

Video 13: Migrating B16-F1 cell expressing EGFP-cortactin 1-84 and mCherry-actin.

Video 14: MBD-Drf3ΔDAD polymerizes actin on microtubules.

Video 15: MBD-Spir-NT nucleates actin filaments on microtubules.

Video 16: MBD-VV does not assemble actin filaments on microtubules.

Video 17: MBD-VV is not able to recruit the Arp2/3 complex to microtubules.

Table 9-1: Distribution of genotypes and sexes of heterozygous crossings of mice carrying the cortactin deleted Neo allele and corresponding probabilities for the observed numbers

Genotypes and sexes of heterozygous matings		Expected (theoretical)	Observed (actual)	Probability (χ^2)
Total				
	Female	73	67	0.321
	Male	73	79	0.321
Wildtype (wt/wt)		36.5	46	0.032
	Female	23	20	0.376
	Male	23	26	0.376
Heterozygous (wt/del)		73	76	0.032
	Female	38	33	0.251
	Male	38	43	0.251
Homozygous (del/del)		36.5	24	0.032
	Female	12	14	0.414
	Male	12	10	0.414

Table 9-2: Distribution of genotypes and sexes of heterozygous crossings of mice carrying the cortactin deleted allele and corresponding probabilities for the observed numbers

Genotypes and sexes of heterozygous matings		Expected (theoretical)	Observed (actual)	Probability (χ^2)
Total				
	Female	153.5	176	0.010
	Male	153.5	131	0.010
Wildtype (wt/wt)		76.75	70	0.099
	Female	35	33	0.363
	Male	35	30	0.363
Heterozygous (wt/del)		153.5	172	0.099
	Female	86	103	0.010
	Male	86	69	0.010
Homozygous (del/del)		76.75	65	0.099
	Female	32.5	33	0.901
	Male	32.5	32	0.901

Table 9-3: Distribution of genotypes and sexes of crossings of $HS1^{del/del}/Cttn^{WT/del}$ and corresponding probabilities for the observed numbers

Genotypes and sexes of heterozygous matings		Expected (theoretical)	Observed (actual)	Probability (χ^2)
Total				
	Female	87	93	0.363
	Male	87	81	0.363
Wildtype (wt/wt)		43.5	46	0.624
	Female	23	24	0.768
	Male	23	22	0.768
Heterozygous (wt/del)		87	90	0.624
	Female	45	48	0.527
	Male	45	42	0.527
Homozygous (del/del)		43.5	38	0.624
	Female	19	21	0.516
	Male	19	17	0.516

9.2 List of figures

9.3 List of tables